Food and Agriculture Organization
of the United Nations

Handbook on remote sensing for agricultural statistics

Publication prepared in the framework of the Global Strategy to improve Agricultural and Rural Statistics

Handbook on remote sensing for agricultural statistics

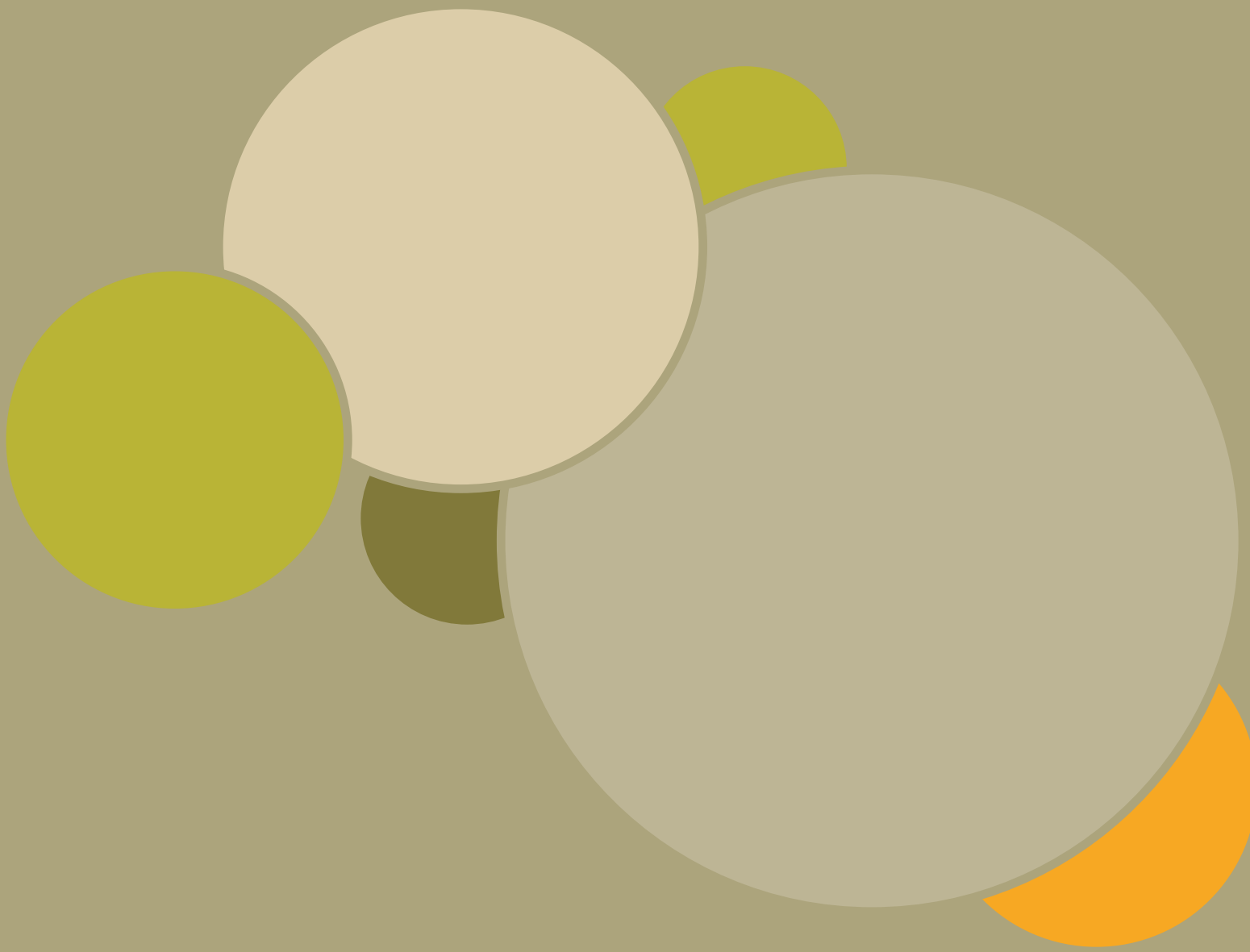

Contents

Acronyms

AAFC	Agriculture and Agri-Food Canada
ACI	Annual Crop Inventory (Canada)
AMIS	Agricultural Market Information System (FAO)
ASF	Area Sampling Frame
ASI	Agroclimatic Information System
ASIA-RiCE	Asian Rice Crop Estimation & Monitoring
ASIS	Agriculture Stress Index System (FAO)
CAPE	Crop Acreage and Production Estimation program (India)
CAS	Chinese Academy of Science (China)
CDL	Crop Data Layer
CHIRPS	Climate Hazards Group Infrared Precipitation with Station data
CLC	CORINE Land Cover
COTS	Commercial-off-the-Shelf Software
CV	Coefficient of Variation
DEM	Digital Elevation Model
DT	Decision Tree Classifier
EA	Enumeration Area
EEA	European Environment Agency
ENSO	El Niño-Southern Oscillation
EO	Earth Observation
ESA	European Space Agency
ETA	Actual EvapoTranspiration
EU	European Union
EWS	Early Warning System
FAO	Food and Agriculture Organization of the United Nations
FAS	Foreign Agriculture Service (USDA)
FASAL	Forecasting Agricultural Output using Space, Agrometeorology and Land-based observations (India)
fPAR	Fraction of Photosynthetic Active Radiation
FRA	Forest Resources Assessment (FAO)
FSA	Farm Service Agency (USDA)
GEE	Google Earth Engine
GEOGLAM	Group on Earth Observations GLobal Agricultural Monitoring
GFW	Global Forest Watch project
GIS	Geographical Information System
GLCN	Global Land Cover Network
GNSS	Global Navigation Satellite System
GPS	Global Positioning System
GPU	Graphics Processing Unit
GRD	Ground Range Detected level-1 SAR
GSD	Ground Sampling Distance
IIASA	International Institute for Applied Systems Analysis (Vienna)
JECAM	Joint Experiment for Crop Assessment and Monitoring network
JRC	Joint Research Centre (EU)
KML	Keyhole Markup Language file format

LACIE	Large Area Crop Inventory Experiment
LAI	Leaf Area Index
LCCS	Land Cover Classification System
LCML	Land Cover Meta-Language
LSF	List Sampling Frame
MARS	Monitoring Agriculture with Remote Sensing (EU)
ML	Maximum Likelihood classification
MMU	Minimum Mapping Unit
MSF	Master Sampling Frame
NASA	National Aeronautics and Space Administration (USA)
NASS	National Agriculture Statistical Service (USDA)
NCFC	Mahalanobis National Crop Forecast Centre (India)
NDVI	Normalized Difference Vegetation Index
NIR	Near-InfraRed
NOAA	National Oceanic and Atmospheric Administration (USA)
OA	Overall Accuracy (of classification)
OSM	Open Street Map
PA	Producer Accuracy
PPS	Probability Proportional to Size (sampling)
PSU	Primary Sampling Unit
RADI	Institute of Remote Sensing and Digital Earth (China)
REDD+	Reduction of Emissions from Deforestation and forest Degradation
RF	Random Forest Classifier
RMSE	Root Mean Square Error
RWP	Rain Water Productivity
SAE	Small Area Estimation
SAR	Synthetic Aperture Radar
SIGMA	Stimulating Innovation for Global Monitoring of Agriculture activity
S1tbx	Sentinel-1 toolbox
SNAP	Sentinel Application Platform
SRTM	Shuttle Radar Topography Mission
SSU	Secondary Sampling Unit
SVM	Support Vector Machine Classifier
SWIR	Short-Wavelength Infrared
TOA	Top-of-Atmosphere Reflectance
TOC	Top-of-Canopy Reflectance
UA	User Accuracy
UAV	Unmanned Aerial Vehicle
UNEP	United Nations Environment Program
UNFCCC	United Nations Framework Convention on Climate Change
USDA	U.S. Department of Agriculture (United States of America)
USGS	U.S. Geological Survey (United States of America)
VHR	Very High Resolution (imagery)
WCA 2020	World Program for the Census of Agriculture 2020
WMS	Web Map Service
XML	Extensible Markup Language

Tables and figures

TABLES

Chapter 1

Chapter 2

Chapter 4

Chapter 5

Chapter 7

Chapter 8

Chapter 9

Annex

FIGURES

Chapter 1

Chapter 2

Chapter 3

Chapter 4

Chapter 5

Chapter 6

Chapter 7

Chapter 8

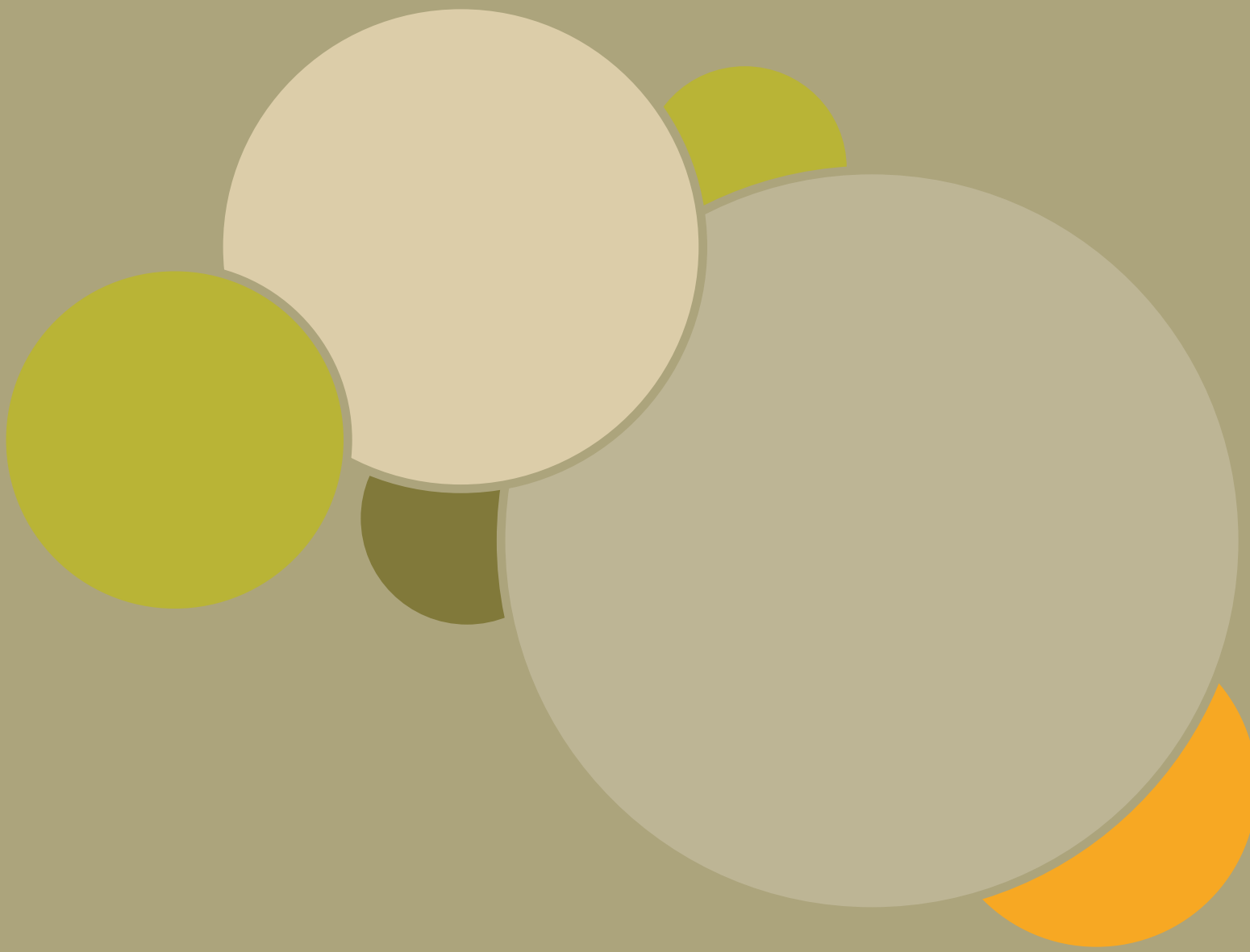

Recommended citations

HANDBOOK:

Global Strategy to improve Agricultural and Rural Statistics (GSARS). 2017. *Handbook on Remote Sensing for Agricultural Statistics*. GSARS Handbook: Rome.

INDIVIDUAL CHAPTERS:

Lemoine, G. 2017. Data access and data analysis software. In: J. Delincé (ed.), *Handbook on Remote Sensing for Agricultural Statistics* (Chapter 1). Handbook of the Global Strategy to improve Agricultural and Rural Statistics (GSARS): Rome.

Defourny, P. 2017. Land cover mapping and monitoring. In: J. Delincé (ed.), *Handbook on Remote Sensing for Agricultural Statistics* (Chapter 2). Handbook of the Global Strategy to improve Agricultural and Rural Statistics (GSARS): Rome.

Gallego, J. 2017. Use of remote sensing for the design of sampling frames. In: J. Delincé (ed.), *Handbook on Remote Sensing for Agricultural Statistics* (Chapter 3). Handbook of the Global Strategy to improve Agricultural and Rural Statistics (GSARS): Rome.

Davidson, A.M., Fisette, T., Mcnairn, H. & Daneshfar, B. 2017. Detailed crop mapping using remote sensing data (Crop Data Layers). In: J. Delincé (ed.), *Handbook on Remote Sensing for Agricultural Statistics* (Chapter 4). Handbook of the Global Strategy to improve Agricultural and Rural Statistics (GSARS): Rome.

Ray, S. & Neetu. 2017. Crop area estimation with Remote Sensing. In: J. Delincé (ed.), *Handbook on Remote Sensing for Agricultural Statistics* (Chapter 5). Handbook of the Global Strategy to improve Agricultural and Rural Statistics (GSARS): Rome.

Rojas, O. 2017. Early Warning Systems and crop yield estimation. In: J. Delincé (ed.), *Handbook on Remote Sensing for Agricultural Statistics* (Chapter 6). Handbook of the Global Strategy to improve Agricultural and Rural Statistics (GSARS): Rome.

Achard, F., Malheiros de Oliveira, Y.M. & Mollicone, D. 2017. Monitoring forest cover and deforestation. In: J. Delincé (ed.), *Handbook on Remote Sensing for Agricultural Statistics* (Chapter 7). Handbook of the Global Strategy to improve Agricultural and Rural Statistics (GSARS): Rome.

Latham, J. 2017. Organization, resources and competences for adopting remote sensing in agricultural statistics. In: J. Delincé (ed.), *Handbook on Remote Sensing for Agricultural Statistics* (Chapter 8). Handbook of the Global Strategy to improve Agricultural and Rural Statistics (GSARS): Rome.

Delincé, J. 2017. The cost-effectiveness of remote sensing in agricultural statistics. In: J. Delincé (ed.), *Handbook on Remote Sensing for Agricultural Statistics* (Chapter 9). Handbook of the Global Strategy to improve Agricultural and Rural Statistics (GSARS): Rome.

Acknowledgments

This Handbook on Remote Sensing for Agricultural Statistics was prepared by a core team of senior international experts in the field of remote sensing with extensive knowledge and several decades of experience in various regions of the world. Jacques Delincé, Consultant of the Global Strategy Office, coordinated the team's work. The authors' affiliations are as follows:

Frederic Achard, Javier Gallego, Guido Lemoine: Joint Research Centre, European Commission, Ispra, Italy

Pierre Defourny: Université Catholique de Louvain-la-Neuve, Belgium

Andrew Davidson, Thierry Fisette, Heather McNairn and Bahram Daneshfar: Agriculture and Agri-Food Canada, Ottawa, Ontario

Jacques Delincé, Danilo Mollicone and John Latham: FAO, Rome, Italy

Shibendu Ray and Neetu: Mahalanobis National Crop Forecasting Center, New Delhi, India

Oscar Rojas: FAO-SLM, Panama.

The Handbook was reviewed by an expert working group that met in Rome on 24 November 2016. Our particular gratitude goes to its participants – Giulia Conchedda (FAO, Italy), Carlos di Bella (INTA, Argentina), Nasreen Khan (IRRI, Philippines), Andries Potgieter (Queensland University, Australia) and Pierre Sibiri Traore (ICRISAT, Mali) – for their constructive and detailed comments, which influenced the final revision of the Handbook.

This publication was prepared with the support of the Trust Fund of the Global Strategy, funded by the UK's Department for International Development (DfID) and the Bill & Melinda Gates Foundation (BMGF); and with the financial and technical support of the World Bank and the Joint Research Center of the European Union.

Overview

Jacques Delincé

The purpose of this handbook on *Remote Sensing for Agricultural Statistics* is to provide guidelines on the use of remote sensing in the context of agricultural statistics. Since the mid-1970s, remote sensing has been considered a promising technique for improving agricultural statistics. Various applications of remote sensing have taken place on all continents and today, several approaches may be considered mature enough to contribute to the sustainability of agricultural statistics. In the context of the Global Strategy to improve Agricultural and Rural Statistics (hereafter, GSARS or Global Strategy; see World Bank, 2011), remote sensing has been identified as a prime contributor to the localization and geocoding of the sampling units, a point of reference for Master Sampling Frames (MSFs), a methodological improvement in design and estimation terms, as a way to achieve sustainability and as a core data set for indicators linked to land uses and covers.

The Research component of the Global Strategy to improve Agricultural and Rural Statistics identified the use of remote sensing as one of its themes of activity. This led to the issue of five publications on remote sensing:

- *Developing More Efficient and Accurate Methods for Using Remote Sensing (2014)*
- *Technical Report on Improving the Use of GPS, GIS and Remote Sensing in Setting Up Master Sampling Frames (2014)*
- *Spatial Disaggregation and Small-Area Estimation Methods for Agricultural Surveys: Solutions and Perspectives (2015)*
- *Technical Report on Cost-Effectiveness of using Remote Sensing for Agricultural Statistics in Developing and Emerging Economies (2015)*
- *Information on Land in the Context of Agricultural Statistics (2016)*

In its 2009 handbook titled *Geospatial Infrastructure in Support of Census Activities*, the Statistics Division of the United Nations began to recommend the use of satellite and aerial imagery for the planning, execution and dissemination of census activities. In 2010, the Global Earth Observation System of Systems (GEOSS) Community of Practice published best practices for crop area estimation with remote sensing. Since 2014, on a monthly basis, the Agricultural Market Information System (AMIS) initiative based within the Food and Agriculture Organization of the United Nations (FAO) has been publishing the Group on Earth Observations GLobal Agricultural Monitoring (GEOGLAM) Remote Sensing analyses, aiming to provide real-time monitoring of areas and production for the major traded commodities.

The literature provides various publications dealing with the use of remote sensing in official statistics (FAO, 2015); however, the vast majority of publications focus on specific technical problems without exploring how to start integrating remote sensing into the process of compiling official statistics.

This handbook seeks to enable interested readers to comprehend whether remote sensing can meet their needs, and if its adoption can improve timeliness, coverage, precision and/or costs in a sustainable manner.

In line with the three GSARS pillars (World Bank, 2011), the current priorities of agricultural statistical services should be (1) establishing a master frame to foster the integration of agricultural statistics within the national statistical system; (2) improving the coverage, bias and precision of the estimates of the core indicators; and (3) selecting practices that are sustainable in terms of cost-efficiency, flexibility and accessibility. The technical advances in the digital management of information, global positioning and open access to remote sensing offer important opportunities to meet these priorities and indeed inspired the drafting and publication of this handbook.

The structure of the handbook reflects the diversity and complexity of the domain of agricultural statistics, as well as of the technicalities of remote sensing:

- An agricultural statistical information system is composed of several layers, each corresponding to different core statistical topics and societal needs. Remote sensing can be particularly efficient in improving Global Strategy core items linked to crop areas, yields and productions. Its role is highly versatile, potentially ranging from optimization of sampling design to the facilitation of the the fieldwork of enumerators, quality assurance and even data production. Societal needs can be separated into two components: (1) the production forecasts from early season to pre-harvest time, for food security monitoring and (2) classical agricultural statistics, of which the continuity and consistency over time will allow policy-makers to plan and evaluate agricultural policy and its positive effect on total factor productivity, farmer income and rural development.
- The techniques associated with remote sensing raise issues pertaining to the sensors (optical or radar), image resolution (30 cm to 5 m) and revisiting time (one hour to 16 days); to (non-)open access and the (generally prohibitive) associated prices; and to the software and hardware available for image analysis (open-source or commercial software, local or cloud computing). This aspect will require managers to identify the time, resources and staff competences required to move from experimentation to operational activities.

Chapter 1 describes the data sets relevant to the integration of remote sensing within agricultural statistics. First, the remote sensing data sources themselves will be addressed. The role of reference data and ancillary data layers, and their use in stratification and aggregation, will also be discussed. A key issue arising recently in data access is the general trend towards open access. Thus, while the major commercial remote sensing missions will be listed for reference, attention will be paid to open-access sources for a number of reasons: (1) to create wider awareness on data sets that are available under free and open licenses; (2) to provide a thorough understanding of how these data can be assessed; and (3) to discuss how open data can be used to optimize the acquisition – i.e. minimize the costs – of commercial data. Remote sensing data, from both open and commercial sources, usually requires post-processing for follow-up use in statistical analyses. The use of open-source software for image processing and geospatial analysis is another important development that accelerates the broader adoption of remote sensing data. The use of open-source software is discussed, and a listing of commercial software alternatives is provided. The chapter concludes with a discussion of the more recent trend to move data analytics into cloud computing environments.

Chapter 2 deals with land cover mapping. It first introduces the concept of land cover and then reviews some key elements of land cover mapping. Existing land cover maps are discussed systematically, based on a set of well-defined criteria. While land cover map supporting stratification always refers to previous years, recent experiences of map production throughout the ongoing season will also be explored. Today, land surface can be described in several ways, thanks to the unprecedented development of information technology and observation capabilities, ranging from Unmanned Aerial Vehicles (UAVs) to in-orbit Earth Observation (EO) platforms. Satellite remote sensing is an undisputed source of land information for a vast range of users at all geographical scales. Due to the increasing gap between remote sensing producers and map users, which is very much supported by spatial data infrastructure making a great deal of geographic information widely available, it is important to understand the different concepts and constraints underlying land cover mapping. This becomes even more critical when considering the use of a land cover map to support stratification at the sampling design level in the context of agricultural statistics. Indeed, maps derived from remote sensing that show, for instance, crop intensity classes, may significantly reduce sampling variances or, simply, reduce ground sampling effort and its associated costs. A land cover map can highlight the non-agricultural strata which should not be sampled or those strata which could be sampled differently. The efficiency of stratification is obviously related to the relevance of the land cover map selected for the stratification.

Chapter 3 focuses upon the use of remote sensing at design level in list and area frames. In the context of censuses, surveys or registers, satellite imagery can be of great support when defining or optimizing the design options. The imagery may be of primary importance when reference maps are absent or obsolete, as they enable a clear delimitation of the Enumeration Area (EA), the counting of dwellings and the planning of the workload. With reference to surveys, stratification on classified imagery will lead to a reduced sampling variance and a variation of sampling fraction (or of the probability proportional to size – PPS) that is proportional to agricultural intensity. Particular attention is paid to the creation of list frames, starting with the point area frame. With regard to area frames, if, in stratification, the strata should be as different as possible, in two-stage sampling, the Primary Sampling Units (PSUs) should be as similar as possible. In both scenarios, the imagery is of great help. The chapter reviews practical examples in developing and developed countries, thus illustrating the type of efficiency and homogeneity that can be achieved. Recommendations are given on segment size optimization in function of field pattern complexity.

The overarching goal of **Chapter 4** is to provide an overview of remote-sensing-based approaches for detailed (field-level) annual crop mapping at national scale. First, an overview of the existing approaches based on remote sensing used for cropland mapping is presented. This includes a brief overview of supervised image classification and pixel- versus object-based classification. Second, the various types of satellite data, ground data and secondary data used for detailed crop mapping are discussed. Third, the operational implementation of a national crop mapping program is demonstrated with specific reference to Canada's Annual Crop Inventory. Finally, the main challenges and opportunities for crop type mapping at national scales in the future are outlined. The past decade has borne witness to several attempts to articulate the spatially explicit requirements of remote sensing data to map cropping systems, and, particularly, where, when and how frequently, over which spectral range, and at what spatial resolution, data are needed. Elucidating the best data and methodologies for crop mapping remains a high priority on the international research agenda. Indeed, several international efforts have been made to achieve a convergence of approaches and develop monitoring and reporting protocols and best practices for a variety of global agricultural systems (e.g. the GEOGLAM initiative, which includes the Joint Experiment of Crop Assessment and Monitoring (JECAM), the Asian Rice Crop Estimation and Monitoring initiative (Asia-RiCE), the Stimulating Innovation for Global Monitoring of Agriculture activity (SIGMA), and contributions from the Sentinel-2 for Agriculture system (Sen2-Agri)).

Chapter 5 deals with crop area estimation using remote sensing. The chapter introduces the history of crop area estimation, reviewing the evolution from the use of conventional methods to the use of satellite data, with the attendant challenges and complexities. The major initial crop area estimation programmes using satellite data, such as LACIE and AgRISTARS, are discussed. The various approaches to crop area estimation, such as the Area Sampling Frame (ASF), pixel counting, and regression or calibration estimators are described with examples. Details of current major programmes for use of remote sensing in crop area estimation are provided under three categories: national (USDA-NASS's CDL and India's FASAL); regional (the European Commission's MARS); and global (USDA's FAS, China's CropWatch and GEOGLAM).The concluding section deals with the major issues and limitations in remote-sensing-based estimates and the way forward.

Chapter 6 reviews the fundamental concepts relating to Early Warning Systems (EWSs) and crop yield forecasting, to better address the climatic risks that bear an impact on food security. System-based dissemination of timely alerts and specifications of the probability of hazard occurrence are fundamental components of early warning information; systematic linkages to early action options and possibilities would go a long way towards saving lives and livelihoods. Forecasting crop yields and aggregate production is of significant importance in early warning systems that seek to assess the food supply and demand situation of a given country or region. Accurate analyses of market conditions, and identifications of the surplus and deficit areas in a country or region will contribute greatly to design appropriate policy responses to mitigate food security problems. Robust and accurate agricultural statistics are also crucial to achieve such important objectives. In this context, information derived from remote sensing plays a vital part in improving the production of agricultural statistics because it is capable of introducing independent verifying mechanisms, particularly when area frame or multiple frame sample designs are used. Remotely sensed data and information can be introduced at both design and estimator levels.

Chapter 7 deals with the estimation of forest cover and deforestation from global to national scales using Earth Observation technology. Considering the specificities of forestry statistics (permanence of the stands from year to year, plot sizes far exceeding pixel sizes, long-term management, availability of management registers in non-natural forests), a special chapter is dedicated to forest resources and deforestation. The main approaches to the use of remote sensing for forest cover assessment and evolution are reviewed, with particular focus on specificities and results as shown in the recent literature. After reviewing the background information on the use of remote sensing for monitoring forest cover, the Remote Sensing Survey of FAO's Global Forest Resources Assessment is described, as well as other examples of remote sensing surveys used for forestry statistics. Finally, the complementarity between estimates of changes occurring in forests and agriculture is analysed.

Chapter 8 presents fundamental requirements and criteria for an organization that is beginning to use geospatial analysis and, in particular, remote sensing for producing agricultural statistics. It also elucidates the need for resources and the competences necessary for application of remote sensing systems in the contexts of agricultural data collection and training needs. Furthermore, consideration is given to the human resources required in the multidisciplinary team, its qualifications, size and to the budget required.

Examples of collaboration between statistical services and mapping agencies are also provided, as well as explanations on the importance of close interaction with stakeholders.

The necessary budgets and business plans are presented.

Finally, **Chapter 9** explains how to evaluate the cost-efficiency of remote sensing. Examples are given of past and recent uses, showing why and where clear cases of cost-efficiency exist. Based on the current trend for free and open access to satellite imagery, agricultural complexity may soon be expected to become manageable with the images' increasing information content (spectral, spatial or textural).

1

Chapter 1

Data access and data analysis software

1.1 INTRODUCTION

This chapter describes the data sets that are relevant for the integration of remote sensing for agricultural statistics. First, the remote sensing data sources themselves will be considered. However, the role of reference data and ancillary data layers and their use in stratification and aggregation will also be discussed. A key issue in recent data access is the general trend towards open access. Thus, while the major commercial remote sensing missions are listed for reference, the emphasis will be on open-access sources for a number of reasons: (1) to create wider awareness on data sets that are available under free and open licenses; (2) to promote understanding on how these data can be accessed; and (3) to discuss how open data can be used to optimize acquisition – that is minimize the associated costs – of commercial data. Remote sensing data, both from open or commercial sources, usually require preprocessing for follow-up use in statistical analysis. The use of open-source software for image processing and geospatial analysis is another important development that will accelerate the take-up of remote sensing data. The use of open-source software will be discussed, and a listing of commercial software alternatives will be provided. The chapter will conclude with a discussion of the more recent trend to move data analytics into cloud computing environments.

1.2. RELEVANT SENSORS AND DATA SETS

Remote sensing data for use in agricultural statistics can be sourced from a wide range of sensors. Traditionally, the key sources were satellite sensors and airborne instruments. The latter are typically used to create large ortho-imagery coverages with a high level of spatial detail (that is, at a resolution higher than 1 m) for topographic mapping, or in the generation of land tenure or rural cadastres. The production of aerial ortho-imagery has experienced the rapid adoption of digital technology, which enables the improvement and acceleration of ortho-image production from stereo-flights. For large coverages, it remains a cost-effective alternative to high-resolution satellite imagery. In the United States of America and in many European countries, aerial ortho-imagery coverages are usually accessible under open licenses or are integrated as "background layers" in popular geoviewers (such as Google Earth, Google Maps or Bing Maps) or Geographical Information Systems (or GIS; for example, ArcMap and Quantum GIS). These layers can be used to assist manual digitization, such as in delineating agricultural parcel boundaries or infrastructure. Open access to the actual image tiles facilitates more sophisticated uses, such as the automatic ortho-correction of other image data sets.

Airborne instruments are also used in specialized surveying applications, for example together with hyper-spectral sensors for detailed spectral signature analysis, Light Detection And Ranging (LIDAR) in terrain modelling, or advanced Synthetic Aperture Radar (SAR) or other electromagnetic sensing techniques. Airborne platforms have the obvious advantages of being easy to configure and deployable on demand. This is even more evident with the increasing use of Unmanned Aerial Vehicles[1] (UAVs), which combine versatility with lightweight sensor deployment for specific and very-high-resolution (VHR) data collection. However, the use of UAVs is more difficult to scale to large area coverage. Safety regulations (for instance, line-of-sight operation by a certified operator or maximum flight altitudes) may be too restrictive to use these platforms beyond specialized high-value applications, such as in precision agriculture. The following sections concentrate on spaceborne remote sensing options. However, when designing agricultural statistical surveys, an essential first step is to compile an inventory of the available airborne ortho-imagery sets and airborne and UAV data collection capacities in the region of interest that can be used to set up the survey.

The growing availability of Earth Observation (EO) satellite sensors makes it increasingly difficult to identify the optimal availability with respect to the design of agricultural statistical surveys. This chapter will focus on satellite sensors that have demonstrated potential in land use and land cover classification, parcel delineation and crop characterization. The European Space Agency (ESA) has created a useful categorization of the sensor data sets available as so-called Copernicus contributing missions[2]. Sensors are classified into mission groups, which are specified by mission type and spatial resolution. The (adapted) mission groups are shown in table 1, together with the typology of resolution terms used and examples of currently operational missions[3]. The description column lists each mission category's advantages and disadvantages for use in agricultural statistics.

In terms of sensor characteristics, a first subdivision may be operated on the basis of whether the sensor operates (1) in the visible and infrared spectral domain (multispectral) or (2) in the microwave spectrum (SAR). This distinction determines whether imagery can be acquired independent of solar illumination and cloud cover. Multispectral sensors measure the reflected sunlight, and as such obviously depend on there being sufficient incident solar illumination and absence of cloud cover. This is important not only for instantaneous acquisitions but also for the creation of consistent time series, for example to compare data over several crop seasons. SARs measure the backscattered radiation from a microwave pulse emitted by the SAR itself, thus independently of solar illumination. For lower frequencies (C- and L-band), SARs are usually insensitive to atmospheric conditions, except in case of

1 An equivalent term often used is Remote Piloted Airborne Systems (RPAS).
2 https://spacedata.copernicus.eu/web/cscda/data-offer/mission-groups.
3 A full and up-to-date overview of operational satellite sensors is available found at: https://directory.eoportal.org/web/eoportal/satellite-missions and http://database.eohandbook.com/database/missiontable.aspx.

intensive rain events. Thus, one of the SAR's strengths is its capacity to ensure consistency in the acquisition of time series for use in crop delineation and area measurement. This is especially true for the Sentinel-1A and -1B instruments, which combine a spatial resolution of 10 m with a revisit frequency of six days.

The second subdivision in sensor groups depends upon spatial resolution. The ESA denomination relies upon the practical < 4 m, 4–10 m, 10–30 m, 30–300 m and > 300 m resolution ranges to group families of sensors. In addition to the difference in resolution, the 10–30 m range also demarcates the division between sensor data that is (predominantly) available under free and open licenses and those categories (<10 m) that fall within the commercial realm.

TABLE 1. CLASSIFICATION OF SATELLITE SENSOR CATEGORIES, BASED ON THE EUROPEAN SPACE AGENCY (ESA) NOMENCLATURE USED IN THE COPERNICUS PROGRAMME.

Mission group	Resolution	Examples	Utility in context of agricultural statistics
SAR	High, 4–30 m	Sentinel-1 Radarsat-2 ALOS-PALSAR 2 RISAT	6- to 24-day revisit, C-band (S1, R2) and L-band (ALOS). All weather, day and night imaging, including interferometry. Free (S1) and fee-based (R2, ALOS, RISAT). Contribute to crop delineation and identification (< 20 m resolution).
	Very high, 1–4 m	TerraSAR-X CosmoSkyMed Radarsat-2 (fine mode)	Multiple sensors, variable revisit (up to daily frequency). High-resolution but small swath. X-band (TSX, CSM) is less suitable for crop identification. All can acquire both high- and lower-resolution imagery, exclusively. Fee-based, expensive.
Multispectral	High, 4–30 m	Landsat, Sentinel-2 ASTER SPOT 6/7 RapidEye CBERS IRS LISS DMC	Free and open access to 10–30 m (Landsat, S2, ASTER), with large swath and including Short-Wave Infrared (SWIR) channels. 5- to 16-day revisit or better (e.g. RapidEye). SPOT combines 6 m multispectral with 1.5 m panchromatic. Suitable for crop delineation, crop type identification and area estimates (4–10 m resolution), regional crop occurrence and status (4–30 m).
	Very high, 0.3–4 m	WorldView-3 Pleiades PlanetLabs SkySAT DMC-III	Highest resolution (0.3 m WV-3), variable number of spectral bands, in visual and near-infrared (NIR) and SWIR range. Entry of new suppliers (e.g. PlanetLabs, SkySAT) is driving down (currently steep) prices. Suitable for parcel measurement (< 1 m resolution).
	Medium, 30–300 m	Proba-V Sentinel-3 MODIS VIIRS	1–3 days revisit over large swath (> 500 km). Including thermal channels (MODIS, VIIRS, S3). Composites for periodic trend analysis over large areas. Parcel detail typically lost. Useful for typification of large production areas and seasonal trends, for stratification. Free and open access except Proba-V (100 m resolution).
	Low, > 300 m	MODIS AVHRR	Mix of orbiting (MODIS) and geostationary (METOP-2 AVHRR). Mostly > 1 km resolution. Daily to 15-minute revisit. For radiation budgets, meteorological information.

The spatial resolution of a sensor determines, to a large extent, whether it can be useful in the context of agricultural statistics. Key factors are the nominal size of the production units (crop parcels and grazing areas) and the mappable landscape features (tree cover, mixed crops and eligible land use elements) that play a role in statistical estimation. As a rule, it is easier to acquire high-resolution imagery over small areas, in terms of both the sensor's technical capacity to acquire timely imagery and the lower attendant costs. For most VHR sensors, a 10 x 10 km^2 frame is a typical "unit of acquisition"; however, more versatile instruments, such as WorldView and Pleiades, are capable of acquiring a number of adjacent frames in a single orbit path (depending on cloud cover). Lower-resolution sensors acquire much larger areas (or swaths) per orbit. The swath of Sentinel-2A, for example, is 285 km wide; for this swath, the satellite collects four spectral channels at a 10-m resolution, six at a 20-m resolution and three at a 60-m resolution (for atmospheric correction). Thus, subsequent frames along the given orbit path can cover a significant proportion of a national territory. Low-resolution sensors have an even larger swath, for example, up to 2 100 km for MODIS; however, such imagery naturally cannot capture detailed landscape features for delineation of production areas.

Radiometric resolution gives rise to another subdivision in sensor categories. For multispectral instruments, the number of spectral bands and the spectral bandwidth are important parameters. The spectral bands determine which parts of the radiative spectrum are registered in the imagery, while the bandwidth sets the specificity of the spectral range for which the radiance is measured. For detailed crop characterization, it is generally preferable to have many bands (and therefore hyperspectral sensors) with narrow bandwidths. However, sensor design and satellite data link transfer rates pose important constraints upon the actual feasibility of acquisition. Many of the (very-) high-resolution instruments (SPOT 6/7, Pleiades and SkySAT) tend to combine lower-resolution multispectral channels in the visible and NIR range with a higher-resolution panchromatic channel to allow for upsampling in a "pansharpening" step during preprocessing. NIR imagery is essential to distinguish vegetation cover from bare soil. NIR reflectance is typically highest for fully closed crop canopies.

WorldView-3 currently produces the most detailed satellite imagery, with a panchromatic band having a resolution of 31 cm, four spectral bands in the visible and NIR (at 1.24 m), eight spectral bands in the SWIR band (at 3.7 m), and 12 additional channels (at 30 m) for atmospheric correction and cloud, snow and ice detection. In the high-resolution domain, special attention is given to spectral compatibility between sensors (such as Landsat and Sentinel 2), to facilitate imagery calibration and comparison. At the same time, Sentinel-2 complements Landsat-8 with additional channels in the so-called red-edge domain (the 570–720 nm spectral range) and an additional SWIR band. The red-edge domain is the spectral region that is highly sensitive to the reflectance of chlorophyll in plant tissue. Thus, it can be used to characterize partial canopy coverage and can contribute to the distinction of crop types. The often-cited Normalized Difference Vegetation Index (NDVI) is the normalized difference between the reflectance in the NIR band (top of the red-edge range) and red spectral bands (start of the red-edge range). Sentinel-2 is the first sensor to enable a full analysis of the red-edge spectral range.

SWIR bands are particularly useful when characterizing bare and partially covered soil, canopy senescence and stress conditions. Together with bands in the visible range, it can distinguish soil type due to reflectance differences in the mineral composition and carbon content. Landsat-8 is unique in its acquisition of Thermal Infrared (TIR) band imagery at a high resolution (90 m, resampled to 30 m).

For SARs, the subdivisions in spatial resolution regimes are equivalent to those in the multispectral domain. The term "spatial resolution" actually has a different meaning when referred to SARs; however, exploring this distinction in detail goes beyond the scope of this handbook. Radiometrically, SARs are characterized by the frequency at which they operate and the polarizations at which they can transmit and receive microwave pulses. Satellite SARs work in either the X-band (9.6 GHz, TerraSAR-X, CosmoSkyMed), the C-band (5.6 GHz, Sentinel-1, Radarsat-2) or the L-band (3.0 Ghz, ALOS-PALSAR-2). These frequencies correspond to wavelengths of 3.2, 5.8 and 10.2 cm, respectively. As a rule, the longer the SAR wavelength, the deeper the signal penetrates into vegetation canopies

(or dry soil surface) and, as a result, the more information can be inferred from the backscattered signal. Thus, there is generally a preference for the L-band in crop applications. However, the wide availability of frequent (C-band) Sentinel-1 data under the full, free and open Copernicus license makes it the current preferred SAR data set. SARs emit coherent microwave pulses, for which both the transmitted and received polarization plane can be measured, in terms of both intensity and phase. Fully polarimetric measurements provide more information on backscattering behavior (such as that of crops); however, their availability often requires a trade-off with the achievable resolution. Sentinel-1 generally provides polarized intensity measurements over land surfaces as a combination of vertically transmitted-vertically received (VV) co-polarized and vertical-horizontal (VH) cross-polarized channels. Interferometry refers to the technique of combining the coherent measurements of two distinct SAR acquisitions from the same sensor. Interferometric coherence has some potential to contribute to land use delineation; however, its use in the context of agricultural mapping is still rather limited. Interferometric SAR (InSAR) processing has been a specialist topic until recently. However, it may gain further relevance with the increasing availability of Sentinel-1 data – especially with both Sentinel-1A and Sentinel-1B in orbit – and related open-source software modules (see Section 2.2).

For all sensors, the temporal resolution relates to the time density with which repetitive coverages can be combined (stacked) to form a multitemporal composition. This resolution is closely related to the satellites' orbit configuration and the possibility to steer and point the sensor along and across the orbit path. Sensors having a very high spatial resolution are capable of acquiring imagery from neighboring orbits, achieving up to daily revisit, and even capturing multiple acquisitions along the orbit (such as WorldView and SkySAT), thus forming a video-like sequence (which however is not particularly useful for agricultural statistics). Fixed-view sensors (as, for example, Landsat and Sentinel-2) have a revisit frequency that is fully determined by the sensors' orbits (for example, 16 and 12 days, respectively). Orbits are typically chosen to ensure seamless coverage of the sensor swath at the Equator. This causes swaths to overlap on the sides, especially towards higher northern and lower southern latitudes, thus effectively leading to a higher revisit in those overlaps. The operation of identical sensors in a constellation of phased orbits (Sentinel-1, Sentinel-2, RapidEye and CosmoSkyMed) is another way to increase temporal resolution. For SAR sensors, the temporal resolution can be further increased by combining acquisitions from ascending and descending orbit passes, due to the active nature of those sensors.

The categories of low-resolution instruments are of less direct interest to agricultural area statistics. However, they generally contribute to wide-area, multiannual phenological trend analysis (see chapter 6). Further categories of sensors that are not listed in table 1 include passive radiometry missions, ocean sensors and atmospheric sounders. The benefits of these sensors to agricultural statistics are more indirect, for instance, as inputs to global circulation models that feed weather forecast models for agrometeorological yield modelling. As such, they are beyond the scope of this chapter, but may be referred to in other parts of this handbook.

It must be noted that the current analysis is limited to state-of-the-art sensors, that is, those currently available for operational use either under free and open licenses (Landsat, Sentinel and ASTER) or commercial licenses. Many other systems exist that are either non-operational (for example, research and development missions) or that are not widely and easily available (such as sensors from national programmes). In addition, there is a common risk of overestimating the potential of "the next solution in Earth Observation", often to the detriment of the uptake of existing capabilities. However, the general trend towards "more and better" technology in this domain is evident. The miniaturization and decreasing costs of digital space components are already stimulating the market entry of new industrial actors (Planet, TerraBella and UrTheCast) and prompting existing players to consider large constellations of small satellite sensors with VHR and daily revisit capacities. In the high- and medium-resolution range, it is hoped that the increasing number of national programmes (such as China's space programme, Canada's new Radarsat constellation and Argentina's SAOCOM will adopt free and open licensing and thus add to global monitoring capacities.

1.2.1. Cost factors relating to commercial imagery

A practical limitation upon the use of commercial satellite imagery relates to the associated costs. Several factors determine the total cost of data use. It is to be noted that, for most sensors, data use is licensed: the customer does not become the owner of the data, but rather pays for the right to use the data and derive information therefrom. The type of license itself can determine the costs to a considerable degree. For instance, single-use license is generally the cheapest, but data sharing may be restricted to a single user or a pre-identified group of users. Multiple-user licenses may distinguish between use within the organization only and wider sharing among (groups of) external users, with corresponding price increases.

It is also crucial to understand whether works derived from data analytics – such as classification results and digitized features – fall under license restrictions. Until recently, this was the case with most sensors. However, a recent and somewhat alarming trend is to introduce "viral" licenses, which are licenses that propagate to derived works, especially for the most advanced technological sensors (WorldView and Pleiades).

Other factors that determine price per unit area are whether the data can be sourced from existing archives or must be acquired upon request, and whether the acquisition is to be performed urgently and within a limited timeframe. Archive imagery is obviously the most affordable, especially for sensors for which the "shelf-life" is shortest when several providers are active in the resolution domain. Good planning avoids the need for urgent data acquisitions, which are typically the most expensive. Other factors in determining price are (1) the required technical quality of the imagery in terms of spatial and spectral resolution; (2) limitations in view angle range; (3) preprocessing requirements; and (4) the total coverage required. For the latter, it is typically relevant to ascertain whether areas must be acquired as contiguous coverage or as single units (for example, for a frame sample). It should also be noted that for several scene-based sensors, a minimum unit area size may apply.

An example of a public price list for a heterogeneous set of VHR sensors is given by e-geos[4], which provides a good overview of the factors discussed above and their effect on the estimated prices. Although prices per km^2 range from US$ 0.01 to US$ 145 (four orders of magnitude!) for Rapideye NextMap World 30 and WorldView 3 "Select Plus Tasking", respectively, only a fuller understanding of all relevant technical requirements and applicable conditions can enable the calculation of a more realistic price estimate for a planned activity.

In general, for projects that require VHR (< 4 m) satellite imagery, it is best to provide several suppliers with the full acquisition scenario and technical requirements and then "shop around" for the best offer, as this may make it possible to obtain significant discounts on list prices and special conditions that are beneficial to data sharing. For such acquisition scenarios, the feasibility studies are typically done free of charge as part of the satellite operators' customer services. Most sensor operators publish their archive holdings through web search interfaces, and there have been efforts to harmonize access to common information[5]. Independent data brokers and resellers offer (fee-based) services to assist in the selection of the "best economical" data acquisition offers. The 1–4 m resolution segment is becoming increasingly crowded on the supply side, which should lead to better customer services and greater discounting. For large contiguous coverages, digital airborne sensor operators should also be considered, especially since data ownership is typically implied and the cost/quality benefits may exceed those of satellite operators. ArcGIS World Imagery[6] contains an overview of the VHR imagery available, which is a mix of regularly updated satellite and airborne data sets sourced for different areas of the world.

4 http://www.e-geos.it/products/pdf/prices.pdf.
5 https://earth.esa.int/hma/.
6 http://www.arcgis.com/home/item.html?id=10df2279f9684e4a9f6a7f08febac2a9.

1.2.2. Free and open access

The introduction of the full, free and open license for the Sentinel sensor data of the European Union (EU) Copernicus programme is a vital complement to the United States of America's efforts to open up EO data sets from government sensors, such as MODIS and – in particular – Landsat missions. This shift towards open access to public satellite data resources has been emboldened recently, with the opening up of the Japanese/US ASTER sensor data. While the main motivation behind this trend is to establish a shared knowledge base for global environmental monitoring, open access does have a considerable impact on a wide range of potential applications in agricultural statistics. As discussed above, Sentinel-1 and -2 provide a basis to create crop-specific information at map scales of 1:25 000 to 1:50 000 as a support to statistical survey design studies. Thus, activities in this domain should consider Sentinel data as a common basis.

Similar to commercial service providers, open-access sensor operators provide web search interfaces[7] that enable searching archives for acquired imagery and orbit characteristics to understand revisit capabilities. A key difference between open-access operators and commercial equivalents is that in the case of open access, the archive search will provide a download link to the full-resolution product.

Graphical web search interfaces are convenient for occasional searches and downloads. For larger and recurring requests, it is often easier to run selections and downloads via scripts. Well-designed search interfaces expose the underlying protocols as a set of application programming interface (API) calls[8] that can be configured to specific selections in time, space and for specific mission metadata tags, and can then be run as scheduled batch scripts. This is particularly useful for bulky data sets, such as those of Landsat, Sentinel-2 and Sentinel-1 Ground Range Detected level-1 SAR (GRD), which may take up to 1 Gb per scene, and Sentinel-1 SLC (up to 8 Gb/scene). Sample Python scripts may be found on the Internet[9] or are available upon request to this author.

A side effect of full, free and open access is that third parties integrate access to these data in their cloud storage and processing infrastructures. For instance, Google[10] and Amazon[11] both download Sentinel-2 imagery from the ESA-hosted data access points and then make them available both for free access by all users and for use in their respective cloud computing infrastructures. The EU's Copernicus programme, together with ESA, plans to introduce alternative European data hosting and computing infrastructures in the near future. Cloud computing is further discussed in the last section of this chapter.

7 https://scihub.copernicus.eu/dhus/#/home (for Copernicus Sentinel-1 and -2) and http://earthexplorer.usgs.gov/ (for Landsat and ASTER, among others).
8 See, for example, https://scihub.copernicus.eu/userguide/5APIsAndBatchScripting.
9 http://www.cesbio.ups-tlse.fr/multitemp/?p=3121 (Landsat) and http://www.cesbio.ups-tlse.fr/multitemp/?p=6419 (Sentinel-2).
10 https://cloud.google.com/storage/docs/public-datasets/sentinel-2.
11 http://sentinel-pds.s3-website.eu-central-1.amazonaws.com/.

1.3. IMAGE PROCESSING AND PREPARING FOR DATA ANALYTICS

Depending on the sensor type and data processing levels, supplied satellite (or airborne) imagery may require preprocessing steps to prepare them for use in subsequent data analytics. Recently, this process has been dubbed the creation of "analysis-ready data". In this handbook, the top-level requirements will be discussed and linked to existing software solutions that implement the required functionality. For a more detailed understanding of the technical issues involved in each step, readers will be referred to relevant literature.

At a minimum, supplied satellite imagery can be expected to satisfy a number of basic technical requisites, such as consistent registration between different bands in multiband data, radiometric scaling and quantization that optimizes for the dynamic range of the sensor over the scene of interest (in other words, absence of excessive saturation or range compression) and appropriate bit-depth of the data type (such as byte, (un)signed integer and float). Furthermore, image data should be accompanied by metadata that describes image projection, (approximate) geolocation, processing levels and parameters that can be used to translate image band values into the physical measurements to which they refer, such as reflectance or radiance in multispectral imagery or backscattering intensity in SAR. Additional metadata usually provides information on sensor platform attitude (orbit position and viewing configuration at time of acquisition), extraneous environmental parameters (solar illumination), calibration parameters, and occasionally statistical estimates derived from image analysis at processing time (such as cloud cover and missing data estimates). It is good practice to control the presence of these prerequisites upon receiving the data, as suppliers will normally repair defects free of charge.

The most common preprocessing steps for multispectral imagery are orthocorrection and atmospheric correction. The need for orthocorrection depends on the processing level of the supplied imagery, and may include sensor-specific correction and terrain correction. The latter requires the use of an external digital elevation model (DEM) to georeference the imagery into a consistent map reference. Terrain correction is essential to correct imagery that has been acquired with off-nadir (oblique) view angles. Atmospheric correction is necessary to correct for atmospheric effects to derive Bottom-Of-Atmosphere (BOA, or the equivalent Top-Of-Canopy – TOC) reflectance from the Top-Of-Atmosphere (TOA) reflectance imagery that is typically supplied. BOA (or TOC) reflectance provide time-consistent values of the "true" reflectance of the pixel elements making up the raster imagery. For data sets that combine multispectral bands with a higher-resolution panchromatic band, pansharpening can be applied to create an upsampled "pseudo"-high-resolution multispectral image.

For SAR imagery, the equivalent steps are geocoding and calibration. Calibration converts SAR image band intensity values to backscattering coefficients. Due to the side-looking nature of SAR and the specificity of SAR image formation in azimuth and range directions, a dedicated geocoding must be applied to compensate for terrain effects (in this case too, an external DEM is required). Depending on the intended use, further processing involving multilooking and speckle filtering may be required.

The steps outlined above result in calibrated and georeferenced imagery that is ready for further treatment. In technical terms, preprocessing converts supplied imagery from 1A ("raw") or 1B (system-corrected 1A) levels to georeferenced (1C) and calibrated (2A) levels. In some cases, suppliers may be asked to provide Level 2A, usually for a fee. Otherwise, dedicated software must be used with the appropriate ancillary data (for example, a suitable DEM) to execute these steps. Depending on the intended use, further processing steps may be required, such as mosaicking of single scenes into large coverages, time compositing, classification, segmentation, etc. For these steps too, suitable software is required.

In recent years, a major trend in image processing has been the increased availability of open source software. These range from the relevant Python, Java and C++ libraries for generic image handling, to specific remote

sensing toolkits (for example, the Orfeo ToolBox[12]) and, most recently, the Sentinel-specific toolboxes. These are complemented with interactive geospatial visualization and analysis software (such as GRASS[13] and QGIS) and raster database solutions (PostgreSQL/Postgis[14]), which extend to the support of spatial web server solutions (GeoServer[15], MapServer). A basic yet highly versatile library supporting most of these solutions is the Geospatial Data Abstraction Library (GDAL[16]), which builds on lower-level libraries such as PROJ.4 and GEOS. Their equivalents in the Commercial-of-the-Shelf (COTS) domain are, among others[17], Excelis ENVI/IDL, ERDAS Imagine, PCI, and MapInfo and ESRI-ArcGIS.

The choice between open-source and COTS software may depend on several factors that determine the "cost of ownership", which goes beyond mere purchase and maintenance costs and may include an evaluation of the existing knowledge base, training needs, and other considerations. The balance has dramatically shifted towards open-source solutions, however, particularly because these are far more successful in integrating the latest developments (such as integration into parallel computing frameworks and use of dedicated hardware components such as Graphics Processing Units – GPUs), including those in the field of open-access satellite and reference data sets. The most widely adopted open-source software benefits from the exponential growth of a user base that excels in terms of collaborative efforts to design and implement cutting-edge solutions. Indeed, the development of COTS software is now mostly concerned with catching up on open-source solutions. In this regard, it may be interesting to note that well over 50 different image and vector data formats exist, most of which have a proprietary (rather than a logical) heritage – a fact that is all the more remarkable if compared to the mere three (DOC, PDF and ODT) formats available in the far larger user domain of word processing.

1.3.1. An example of processing

For the Sentinel satellites, ESA supports the development of the so-called Sentinel Application Platform (SNAP[18]), which provides a common architecture for Sentinel-specific processing functionalities. The SNAP software, which is Java-based, runs on all types of operating systems. It also supports a wide range of standard processing features (such as band arithmetic, vector-image analysis, reprojection, and import/export of multiple formats) which can be used either in an interactive mode or at predefined processing graphs on the command line and in batch. The Sentinel-1 toolbox (s1tbx) has been instrumental in the growing uptake of Sentinel-1 SAR imagery among the user community; SARs have traditionally been considered technically difficult to use, also because essential processing routines were only available as proprietary solutions.

The toolboxes are also excellent educational tools. Although ESA promotes SNAP as open-source software, some functionalities (such as Sentinel-2's sen2cor atmospheric correction module) remain in fact closed code. When combined with automated data selection and download, the toolboxes can be chained to process Sentinel-1 and Sentinel-2 (as well as Sentinel-3) on demand as required, in a stand-alone fashion (figure 1). This functional model can be further expanded into thematic application areas, as occurs for example in the Sen2Agri[19] project, the aim of which is to release a full processing chain for the use of Sentinel-2 in crop mask production, crop type classification and Leaf Area Index (LAI) extraction for large regions. Its use has already been successfully demonstrated in countrywide tests in the Czech Republic and Ukraine.

12 https://www.orfeo-toolbox.org/.
13 http://grass.osgeo.org/.
14 http://www.postgis.net/.
15 http://www.mapserver.org/, http://geoserver.org/.
16 http://www.gdal.org/.
17 See http://www.un-spider.org/links-and-resources/gis-rs-software.
18 http://step.esa.int/main/toolboxes/snap/.
19 http://www.esa-sen2agri.org/SitePages/Home.aspx.

The brief example[20] seen below demonstrates a workflow that searches for the Sentinel-1 GRD data frames that intersect a location near Kura, Nigeria for the four preceding months. This query will return a set of records formatted as XML, which are then saved to the file entitled `s1.xml`.

```
wget "https://{USER}:{PASSWORD}@scihub.copernicus.
eu/apihub/search?q=productType:GRD \
AND footprint:\"Intersects(11.769, 8.422)\" \
AND beginPosition:[NOW-4MONTHS TO NOW]&rows=100" -O s1.xml
```

A valid username and password are required to access scihub, and can be obtained after registration. The records are grouped as a feed, the number of entries of which correspond to the individual records for each image that meet the selection criteria. Each record has a set of metadata elements that describe format, date of acquisition and ingestion, file size, footprint, etc. The two most relevant metadata elements are the `link` element, to obtain the `href` attribute that provides the download link, and the `str` element with the `filename` attribute, which provides a unique filename for the downloaded file. XML is best read in a parser[21], which can extract the elements and attributes of interest, for example to set up a download script.

```
<?xml version="1.0" encoding="utf-8"?>
<feed xmlns:opensearch="http://a9.com/-/spec/opensearch/1.1/"
xmlns="http://www.w3.org/2005/Atom">
<title>Sentinels Scientific Data Hub search results for: productType:GRD AND
footprint:"Intersects(11.769, 8.422)" AND beginPosition:[NOW-4MONTHS TO NOW]</title>
<subtitle>Displaying 9 results. Request done in 0.177 seconds.</subtitle>
<updated>2016-11-08T14:22:56.407Z</updated>
<author>
<name>Sentinels Scientific Data Hub</name>
</author>
<id>https://scihub.copernicus.eu/apihub/search?q=productType:GRD AND
footprint:"Intersects(11.769, 8.422)" AND beginPosition:[NOW-4MONTHS TO NOW]</id>
<opensearch:totalResults>9</opensearch:totalResults>
<opensearch:startIndex>0</opensearch:startIndex>
<opensearch:itemsPerPage>100</opensearch:itemsPerPage>
...
<entry>
<title>S1A_IW_GRDH_1SDV_20161027T173813_20161027T173838_013679_015EF5_8838</title>
<link href="https://scihub.copernicus.eu/apihub/odata/v1/
Products('aa979434-a766-480d-a269-ba1a6b2b708a')/$value"/>
...
<summary>Date: 2016-10-27T17:38:13.561Z, Instrument: SAR-C SAR,
Mode: VV VH, Satellite: Sentinel-1, Size: 1.58 GB</summary>
...
<str name="filename">S1A_IW_
GRDH_1SDV_20161027T173813_20161027T173838_013679_015EF5_8838.SAFE</str>
<str name="gmlfootprint">&lt;gml:Polygon srsName="http://www.opengis.net/
gml/srs/epsg.xml#4326" xmlns:gml="http://www.opengis.net/gml"&gt;
   &lt;gml:outerBoundaryIs&gt;
```

20 This example assumes that a Linux platform is used. Equivalent commands are available for other operating systems.
21 Such as the lxml parser for Python, available at http:/lxml.de.

```
      &lt;gml:LinearRing&gt;
         &lt;gml:coordinates&gt;11.997962,7.224397 12.441014,9.497738
10.932872,9.795840 10.485979,7.535322 11.997962,7.224397&lt;/gml:coordinates&gt;
      &lt;/gml:LinearRing&gt;
   &lt;/gml:outerBoundaryIs&gt;
&lt;/gml:Polygon&gt;</str>
...
</entry>
<entry>
</entry>
...
<entry>
...
</feed>
```

Using the `href` and `filename` attributes, images can be downloaded as follows:

```
wget "https://{USER}:{PASSWORD}@scihub.copernicus.eu/apihub/odata/v1/
Products('aa979434-a766-480d-a269-ba1a6b2b708a')/\$value" -O S1A_IW_
GRDH_1SDV_20161027T173813_20161027T173838_013679_015EF5_8838.zip
```

This operation may be performed for each file in the time series.

The Sentinel-1 GRD file contain uncalibrated backscattering intensities organized in the range-azimuth geometry of the SAR. To convert this to georeferenced calibrated backscattering coefficients, the S1tbx software can be used to set up a processing chain. A convenient feature of the s1tbx is the concept of graphs, which enable the graphical drawing of a sequence of processing steps as a workflow (for an example, see figure 1). The graph can then be saved as an XML file and applied in a batch process to any other image in the time series, using parameter substitution.

```
/home/user/snap/bin/gpt /home/user/S1A/10m_Calibrated_Geocoded.xml \
-Pin_file=S1A_IW_GRDH_1SDV_20161027T173813_20161027T173838_013679_015EF5_8838.zip \
-Pout_file=S1A_IW_GRDH_1SDV_20161027T173813_20161027T173838_013679_015EF5_8838.tif
```

FIGURE 1. SAR PROCESSING WORKFLOW GRAPH IN S1TBX, TO GENERATE GEOCODED CALIBRATED BACKSCATTERING COEFFICIENTS FROM SENTINEL-1 GRD DATA SETS.

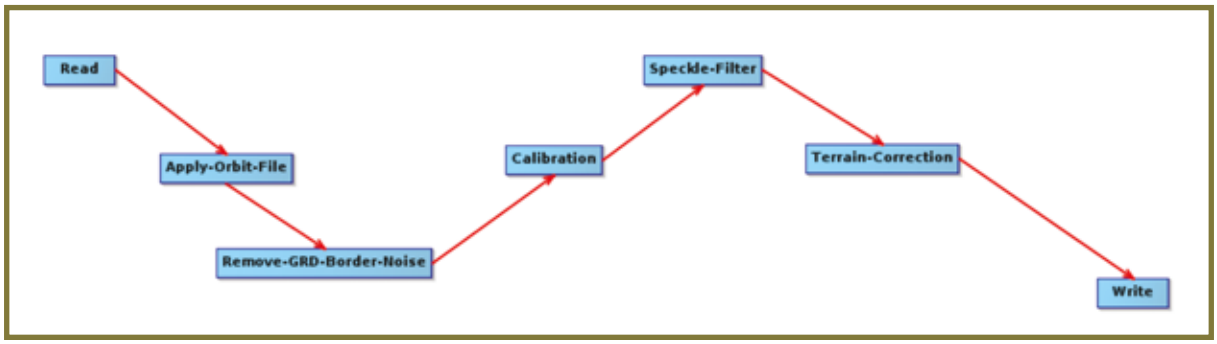

By integrating the Sentinel catalogue search, XML parsing and the scripting of an automated workflow into a single workflow, it is easy to set up batch procedures such as crontab jobs, which download and prepare data sets for an area of interest in the same tact as the revisit cycle. Figure 2 illustrates a stack of geocoded images for our selection, integrated into a QGIS session.

FIGURE 2. A GEOCODED SENTINEL-1 BACKSCATTERING COEFFICIENT COMPOSITE USING ASCENDING IMAGES (RELATIVE ORBIT 132, VV POLARIZATION) FROM 27 JULY, 9 SEPTEMBER AND 23 OCTOBER 2016 OVER AN AGRICULTURAL AREA NEAR KURA, NIGERIA.

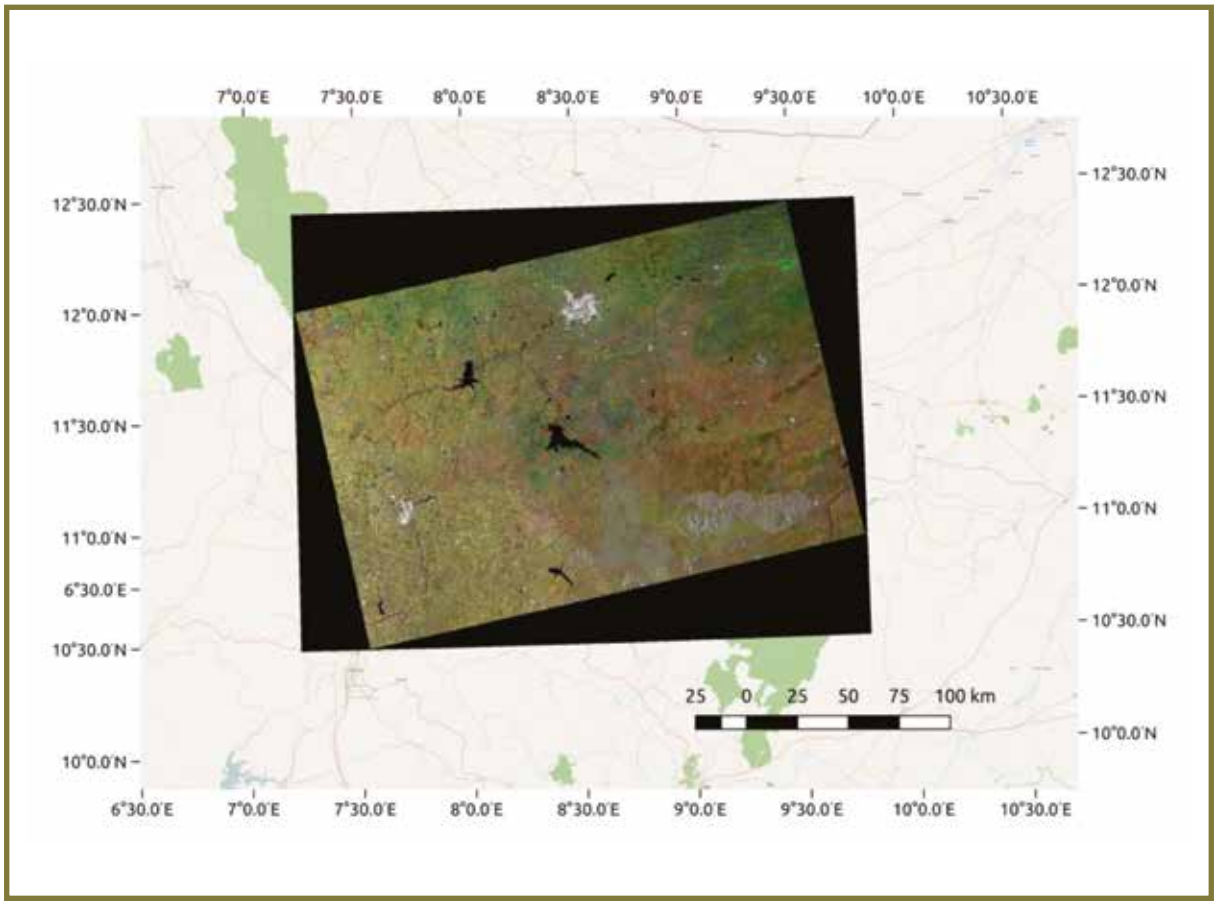

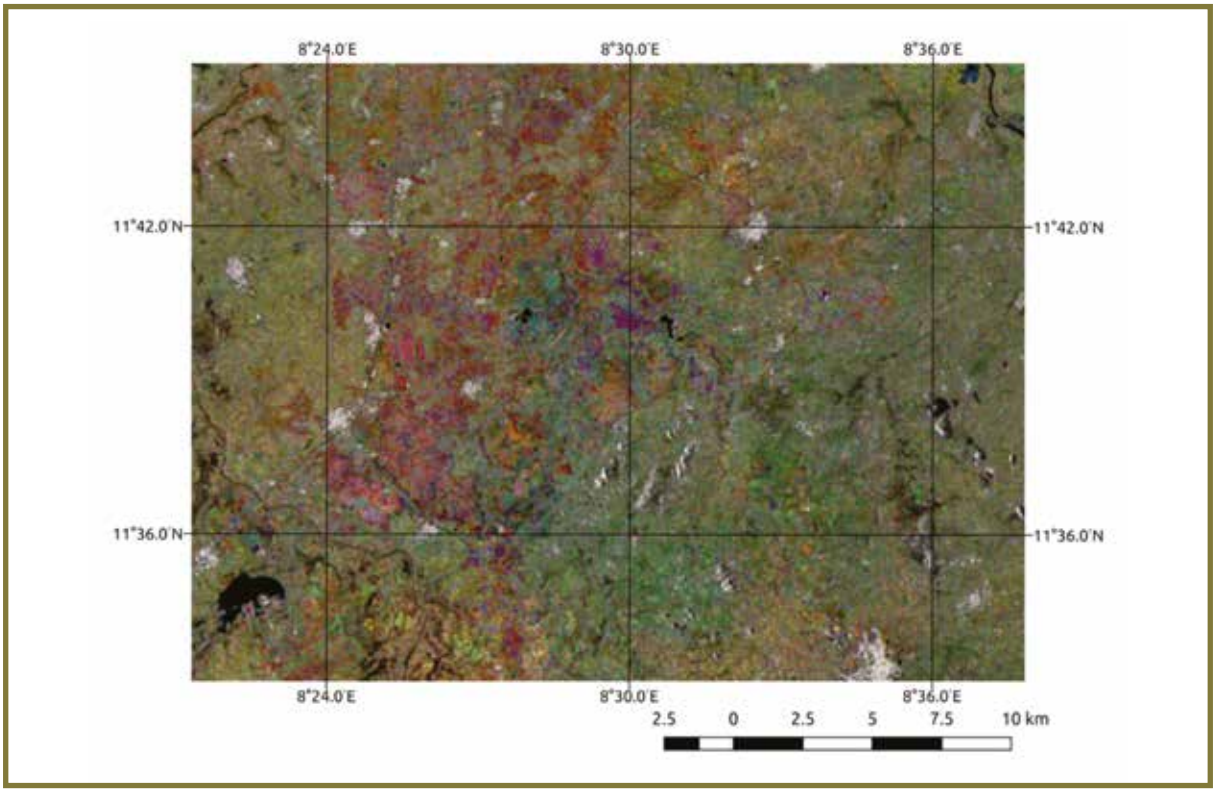

The reddish and orange colours outline agricultural areas subject to seasonal variation in the backscattering signature. Sentinel-1 data is under the copyright of the Copernicus programme, 2016.

1.4. REFERENCE DATA

The integration of satellite imagery into the context of agricultural statistical analysis requires access to a number of essential reference data layers. These layers are fundamental at the early stage, when survey design and data selection are being considered (for example, when deciding upon stratification of the sample, planning of logistics for ground survey execution, procurement of imagery with the required resolution and quality, verification and validation of image derived indicators, data aggregation to administrative units, etc.). A non-exhaustive list of relevant base layers is provided in table 2[22].

22 For further details on land monitoring applications, see European Environment Agency, 2013, Note on in-situ data requirements: Update of D2.1 – Report on In-situ data requirements, GMES in-situ coordination (GISC) Publication. Available at: http://gisc.pbe.eea.europa.eu/deliverables/d2.1.pdf/download/en/1/D2.1.pdf?action=view (pp. 121 ff.)

TABLE 2. RELEVANT REFERENCE DATA LAYERS FOR PREPARATION OF AGRICULTURAL SURVEYS AND RELATED EO ANALYSIS.

Reference set	Minimum scale	Comments
DEM	1:100 000 country wide	For stratification, image correction. Open access to global sets at 30 m (1 arcsec) from SRTM, ALOS-PRISM, ASTER. For use with VHR imagery, larger scales (>1:25 000) are recommended.
Digital topography	1:100 000 country wide, 1:25 000 for survey areas	For survey design, stratification, image registration. Linkage to food logistics (transport and storage), and relevant agricultural production factors (access to water, irrigation infrastructure).
Land use/Land cover	1:100 000	Stratification and survey design. Environmental factors (land conversion, biodiversity, grass- or rangeland).
Soil map	1:100 000	Land suitability, production factors, regionally specific production patterns, erosion and salinity risks.
Land registry	1:10 000	Land parcel identification, land tenure, stratification, support to image classification, survey design, statistical extrapolation and aggregation.
Administrative boundaries	1:50 000	Survey design and statistical aggregation.

Aside from data sets such as the global DEMs, the availability of these layers is highly heterogeneous in terms of both quality and licensing conditions, or even non-existent, depending on the country or region. Where the scales required are unavailable, extracts from smaller-scale global or regional data sets may provide initial estimates; however, additional efforts may be required to generate relevant scale maps, especially for important agricultural production zones. Actual satellite and airborne imagery may serve as an alternative source to derive reference layers, such as digital topography, land use/land cover; however, these require a great deal of resources at the preparation stage.

OpenStreetMap[23] (OSM) is an open-data initiative aiming to produce a digital map of the world through voluntary contributions, using local knowledge, GPS tracks and donated source data. Attributed digital feature data can be extracted from the OSM by region or feature type and then integrated in geospatial analysis software. The open-source QGIS[24] software is particularly useful for OSM analysis, as it provides simple interfaces to extract, change and upload digitized features.

QGIS has the added advantage of being a versatile tool to integrate imagery and feature data sets and build sophisticated geospatial analytical workflows.

23 https://www.openstreetmap.org.
24 http://www.qgis.org/en/site/.

1.5. CLOUD COMPUTING

A recent trend, often hailed as the "new Big Data paradigm", is to move large data storage and processing towards cloud solutions. Cloud solution providers provide the hardware infrastructure necessary to run data processing algorithms in parallel against large data sets. A key advantage lies in the fact that, because the data holdings and processing units are logically close to each other and the data structures and parallelization can be highly optimized for the tasks at hand, the overall data analytics can be considerably faster and, therefore, scaled to much larger data selections or be increasingly complex in terms of computer resource use. Another important advantage is that cloud solution users do not require the hardware solutions required for large data processing themselves. In fact, the client platforms that access cloud solutions can remain simple (such as ordinary laptops) and, because the need to download large amounts of data is greatly reduced, there is no need to scale up the Internet bandwidth used. Thus, cloud computing is a viable alternative in less developed countries, where the maintenance of dedicated hardware and software infrastructure may be difficult.

Some of the drawbacks of cloud solutions relate to the fact that users are no longer in full control of the workflow, and that reference and ancillary data and algorithms must be cohosted on the cloud infrastructure, which in turn may lead to issues pertaining to licensing, intellectual property rights, and cost issues (relating for example to cloud storage and computing capacity). These factors must be considered against the scale of the planned activities, the cost of maintaining existing infrastructure and investing in the necessary upgrades, additional expertise and training, etc.

To appreciate the capacities of cloud computing services and compare them with a stand-alone processing solution, let us consider a median-sized country, such as the Republic of Korea (the territorial area of which covers approximately 95 000 km^2). Full coverage requires 20 Sentinel-2 tiles (10 Gb per orbit), 13 Landsat-8 scenes (13 Gb per orbit) and 16 Sentinel-1 frames (8 descending, 8 ascending, 16 Gb per orbit[25]). Assuming full operational coverage from Sentinel-1A and Sentinel-1B (61 orbits per year) and Sentinel-2A and Sentinel-2B (73 orbits per year), the total amount of Level 1A/1C input data is 10*73 (S2) + 13*22 (L8) + 16*61 (S1) = 1 992 Gb (approximately 2 Tb) per year. After preprocessing (geocoding, calibration, removing cloud cover in optical data, masking sea surface), a data volume in the order of 1 Tb would feed into a country-wide statistical analysis. While this is still a manageable amount of data for a stand-alone operational workflow, a non-trivial effort and relatively robust platform would be required to systematically download, store and process such information in a timely manner.

A prime cloud computing solution in the geospatial use domain is Google Earth Engine[26] (GEE). GEE provides registered users[27] with access to most free and open-access data catalogues, including full-resolution MODIS, Landsat, Sentinel-1 and Sentinel-2 data, which are stored in Google's cloud storage infrastructure. Other open-access raster data resources, such as SRTM DEM at resolutions of 1 and 3 arcsecs, gridded rainfall estimates (using Climate Hazards Group Infrared Precipitation with Station data (CHIRPS)), atmosphere modelling outputs of the Global Forecasting System, and global land cover or thematic classification outputs are also available as catalogues. Raster data is typically available in the format as originally provided by the source (for example, the United States of America's National Oceanic and Atmospheric Administration – NOAA – or U.S. Geological Survey – USGS – or the European Union's Copernicus programme). Such data may include further processed versions, such as Landsat surface reflectance, MODIS indices, and spatial and temporal composites. Sentinel-1 data is included as geocoded calibrated backscattering coefficients after processing the GRD formatted originals with the Sentinel-1 toolbox, which prepares the data for use in analysis. GEE also facilitates integration of feature data sets; however, it has only a limited number of rather coarse global sets (for example country borders). However, a GEE user can upload (and download) raster and feature sets as private or shareable assets.

25 Approximately 96 Gb per orbit, should interferometric processing be required.
26 https://earthengine.google.com/.
27 GEE is free for non-commercial use.

A key feature of GEE is the possibility to integrate access to global data sets with programmable processing logic that is made available as a library of routines. Core libraries cover standard raster and feature processing tasks (such as filters, geometric operators, classifiers and statistical aggregation) that work across arbitrary numbers of image bands, time series combinations, multi-sensor compositions, etc. Matrix libraries provide functionalities for regression analysis, eigen analysis and (auto)correlation. Users can combine data selections and library functions in scripts that define pertinent workflows that can result in a raster output such as a classification result, or that can be reduced to a tabular format, such as spatial statistical aggregates. Scripting can be done in a browser interface (using JavaScript) or via the Python API. A critical advantage of this approach is that scripts, rather than downloads, can be shared among users, as it is generally more resource-efficient to rerun the script than to exchange large data volume renderings. GEE can also serve as the back-end to more elaborate (web) solutions, such as FAO's "Collect Earth"[28], which aims to the systematic collection and analysis of validation data in the contexts of land use and land use change, including agricultural land use.

1.6. CASE STUDY

To illustrate the overall concept of remote sensing data integration with reference data to support agricultural statistics, an ideal scenario will now be described, in which open access is available to essential data sets of a quality that matches, and even exceeds, overall requirements.

In the Netherlands, the Government strongly supports open access to the public data infrastructure, both in a legislative sense and in terms of the implementation of suitable technology platforms. The public map support service[29] facilitates public authorities in publishing their data holdings in a number of open formats. These data sets feed into the national geo-register, which, besides providing access to the data itself, supports a number of search, viewing and processing solutions, for example through web services protocols.

The thematic data sets include, among others, digital topography at a scale of 1:10 000, a LIDAR-derived DEM at 0.5 m spacing, (annual) ortho-imagery at 0.25 m resolution, soil information layers, and large amounts of thematically specific layers, including those relating to agricultural production. Agricultural land use is delineated in a parcel reference layer, which is part of the Integrated Administration and Control System supporting the European Common Agricultural Policy measures. Farmers register their land use annually on the basis of the parcel reference system. Both the parcels reference system and the annual land use layers are available (at a scale of 1:10 000) in the national geo-register[30]. The anonymized annual land use declarations are normally available in final form towards the end of the year (December), well after the end of the growing season (October YYYY-1 to October YYYY).

Therefore, while detailed crop statistics can be derived directly from the declaration data, the data sets constitute excellent reference material to validate post hoc the potential of remote sensing data mixes in deriving accurate crop estimates at various stages of the (preceding) growing season. Furthermore, the excellent quality of the reference data makes it possible to test various sampling approaches for collecting in-season crop reference information, for instance, as frame or point samples, in the context of "along-the-road" surveys, with or without the support of actual remote sensing data. Indeed, the example of the Netherlands can serve as a suitable training suite for a number of operational geostatistical experiments.

28 http://www.openforis.org/tools/collect-earth.html.
29 https://www.pdok.nl/.
30 Search for AAN (parcel register) and BRP (annual land use declarations), respectively.

FIGURE 3. OVERVIEW MAP OF THE HOLLANDS KROON (THE NETHERLANDS) MUNICIPALITY, OVERLAID WITH SENTINEL-2 IMAGE OF 5 JULY 2016 (BAND COMBINATION B8-B11-B4).

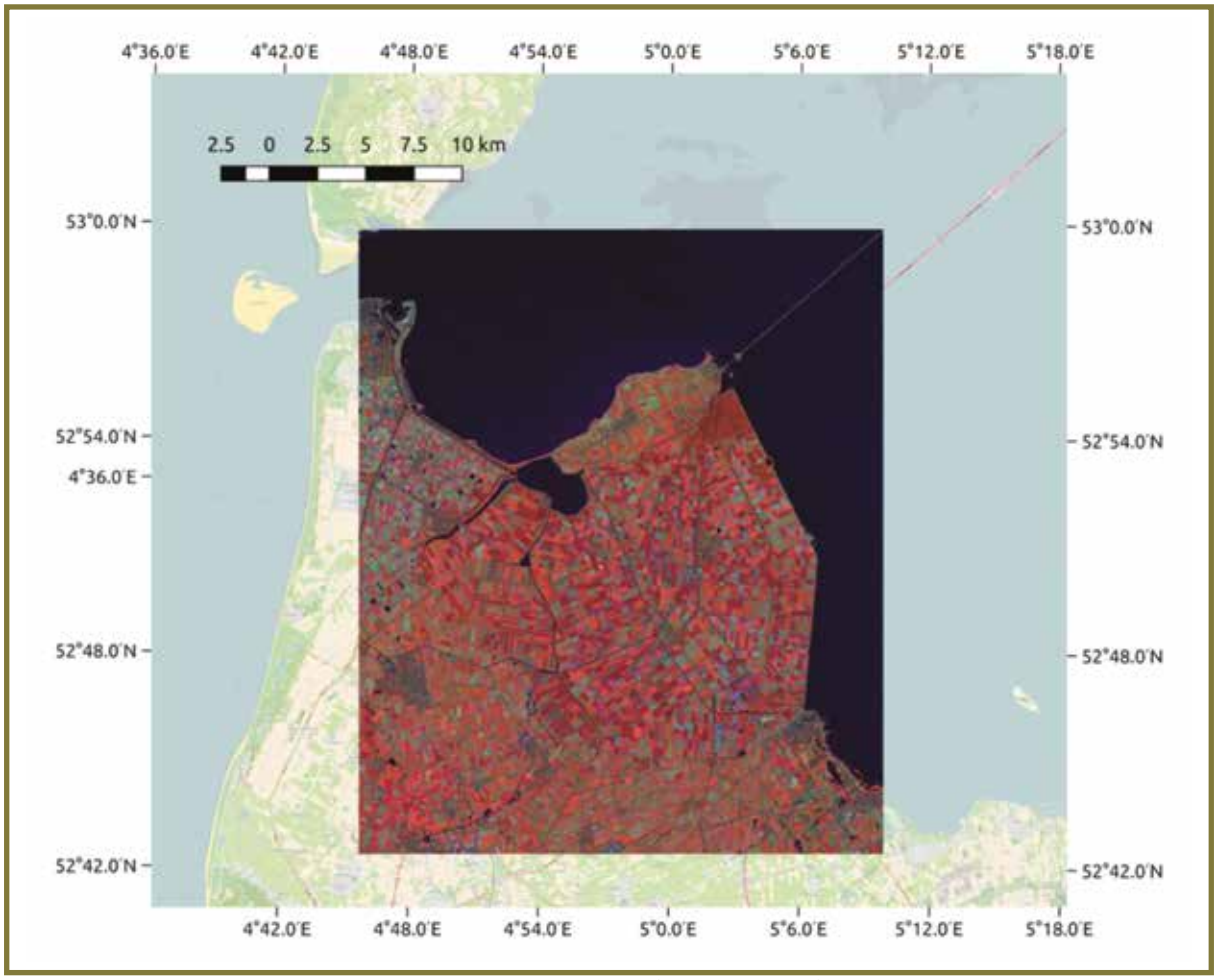

The image is projected in the Dutch national reference coordinate system (RDS, EPSG:28992). Background map data is under the copyright of OpenStreetMap contributors 2017. Sentinel-2 data is under the copyright of the Copernicus programme, 2015.

The example discussed here is of a simple classification using GEE. First, all parcels are selected for 2015 for the municipality of Hollands Kroon, in the North-Holland province of the Netherlands (see figure 3). This municipality includes the Wieringermeer, which is a reclaimed polder, and some surrounding areas. Due to its excellent alluvial soil type, the area is intensively used for arable crop production and horticulture. Of the total municipal area of 37 108 ha, a total of 7 086 parcels covering 27 723 ha are included in the 2015 declarations data. The average size of the declared parcels is 3.91 ha (the range being 0.1 to 47.9 ha).

The relevant parcels are converted to KML format and then uploaded as a Fusion Table to Google Drive, which can be included in the GEE script using the Fusion Table's identification number. The municipality boundaries are included in a similar manner. The municipality boundary is used to select imagery from the GEE catalogues for a given date range and sensor, with the possibility to limit the search against certain criteria. For instance, it is possible to limit the search of optical data with a minimum cloud cover percentage, limit SAR data selection to a particular orbit, etc. For high resolutions, it is possible to choose from Landsat-8, ASTER, Sentinel-1 and Sentinel-2. This example will focus on Sentinel-2, an early commissioning phase acquisition of which is available for 5 July 2015.

Next, a training sample is set up as a selection from the BRP 2015 set. For the purposes of this example, the training parcel size is limited to a minimum of 2 ha, to avoid including mixed pixels across parcel boundaries. In addition, parcels with oblong shape (those in which the long side is four times greater than the short side) are excluded. This is necessary for the Hollands Kroon set, because it includes several parcels of grassland along the inner and outer polder dikes, which are thin but very long strips. The training set selection is further limited to crop types that have at least 50 parcels in the set. This step is intended to avoid including relatively rare crop types. The selection results in a set of 4 473 parcels (covering 24 624 ha).

Finally, 20 percent of the sample (corresponding to 916 parcels) are randomly selected for training and the remaining 80 percent (3 557 parcels) are used to test the classification. All of the parameters used in the selection are variables, which can be easily changed to rerun the classification with other choices and study the influence of different parameter settings.

It is now possible to set up the classifier. To this end, the following bands are selected from the Sentinel-2 image: 2–4 (visible), 5–7 (red edge), 8 and 8A (NIR) and 11 and 12 (SWIR). It should be noted that some bands have a resolution of 10 m (2–4, 8) while others have a resolution of 20 m (5–7, 8A, 11 and 12); however, there is no need to carry out any explicit resampling to prepare the imagery. As the classifier, the random forest classifier is selected, using 10 initial trees per class as the only parameter. The classifier is trained with the selected samples and the training result is then applied to the image bands. For each test parcel, the frequency histogram of the class label that are contained within each parcel boundary is extracted, and the parcel is assigned to the majority class. It is then possible to generate a parcel-based (that is, not pixel-based) confusion matrix, as in figure 4.

FIGURE 4. CONFUSION MATRIX FOR RANDOM FOREST CLASSIFICATION OF SENTINEL-2 IMAGE OF 5 JULY 2015 FOR HOLLANDS KROON, USING BRP 2015 DECLARATION DATA FOR TRAINING AND TESTING.

	ALF	CRT	GRA	HOR	MAI	ONI	POT	SBT	SWH	VEG	WWH	Totals	UA
ALF	**14**	0	1	0	1	0	3	0	0	1	0	20	0.70
CRT	0	**9**	0	0	1	9	0	0	0	2	0	21	0.43
GRA	15	3	**942**	3	8	0	6	1	2	3	0	983	0.96
HOR	8	28	17	**586**	12	31	10	3	1	95	3	794	0.74
MAI	0	3	2	2	**163**	4	5	0	4	5	1	189	0.86
ONI	1	2	0	6	3	**99**	1	4	0	11	0	127	0.78
POT	31	4	5	9	1	0	**571**	3	0	6	0	630	0.91
SBT	1	1	0	12	0	10	2	**232**	0	7	1	266	0.87
SWH	0	0	1	0	2	0	0	0	**50**	0	9	62	0.81
VEG	2	1	0	8	1	0	1	0	0	**12**	0	25	0.48
WWH	0	0	1	0	1	10	0	0	14	0	**403**	429	0.94
Totals	72	51	969	626	193	163	599	243	71	142	417	**3546**	**OA = 0.87**
PA	0.19	0.18	0.97	0.94	0.84	0.61	0.95	0.95	0.70	0.08	0.97		

Crop labels: ALF = alfalfa; CRT = carrots; GRA = grass; HOR = horticulture; MAI = maize; ONI = onions; POT = potato; SBT = sugar beet; SWH = spring wheat; VEG = vegetables; WWH = winter wheat.
Classification labels: PA = producer accuracy; UA = user accuracy; OA = overall accuracy.

It may be noted that relatively good results may be obtained with an overall accuracy of 87 percent for 11 distinct crop types, although only a single Sentinel-2 image is used. Early July is evidently a near-optimal date on which delineate several crop types. At this stage, winter cereals are near harvest, contrasting as senescent canopies with the fully emerged summer crops of sugar beet and potato. Grassland is also well delineated, although considerable variation might be expected in grassland due to varying mowing practices. Horticulture crops are an exception because the majority of this group comprises tulips and other spring flower bulbs, which are typically harvested at the end of June. Confusion is evident for crops such as onions, carrots and other vegetables (that are mixed with horticulture) and spring wheat (that is mixed with winter wheat). Additional optical imagery from before and after July will help to delineate these groups.

While the results prove the potential of Sentinel-2 imagery for crop map generation, the key outcome illustrated by the above example is that it is relatively simple to generate consistent results with GEE. With reference to the example, it is perfectly possible to generate similar results with open-source software alternatives, such as a combination of Python scripts and the open source software modules discussed earlier. The main advantage of using GEE is the ability to change to other image selections, for example Landsat-8 and Sentinel-1 stacks (and hybrid mixes), select other areas and test different parameter settings with minor adaptations to the script. Typically, the use of Sentinel-1 stacks is preferred for classification, because data availability is systematic (there are no cloud cover issues) and overall classification accuracy exceeds 90 percent for arable crop production areas with similar characteristics as Hollands Kroon.

1.7. CONCLUSION

This chapter has sought to explore the availability of imagery for use in crop delineation and characterization processes to support crop area estimation, with an emphasis on free and open-access high-resolution imagery, especially from the new Sentinel-1 and 2-sensors. These sensors, combined with those of other free and open sensors, such as Landsat and ASTER, facilitate new approaches in crop area estimation that combine wide-area coverage at a resolution of 10 m with select VHR imagery from airborne operators and commercial satellite vendors for statistically sound sampling. Generally, software to support analysis of this imagery for the generation of crop classifications and area estimates is now easily available in the open source domain. However, given the large volumes of free and open-access imagery that are now being generated, practical considerations on Big Data processing must be taken into account, depending on the scale of the actual analysis. GEE is an attractive cloud-based platform for rapid data exploration and analysis, because it already hosts free and open-access imagery and provides a rich set of libraries for sophisticated geospatial analysis. Although it is not open-source, it supports a large community of developers and users who share scripted analysis in the same manner as in open-source-software communities. Future developments are expected to further stimulate cloud-based analysis and will probably include fully open-source solutions.

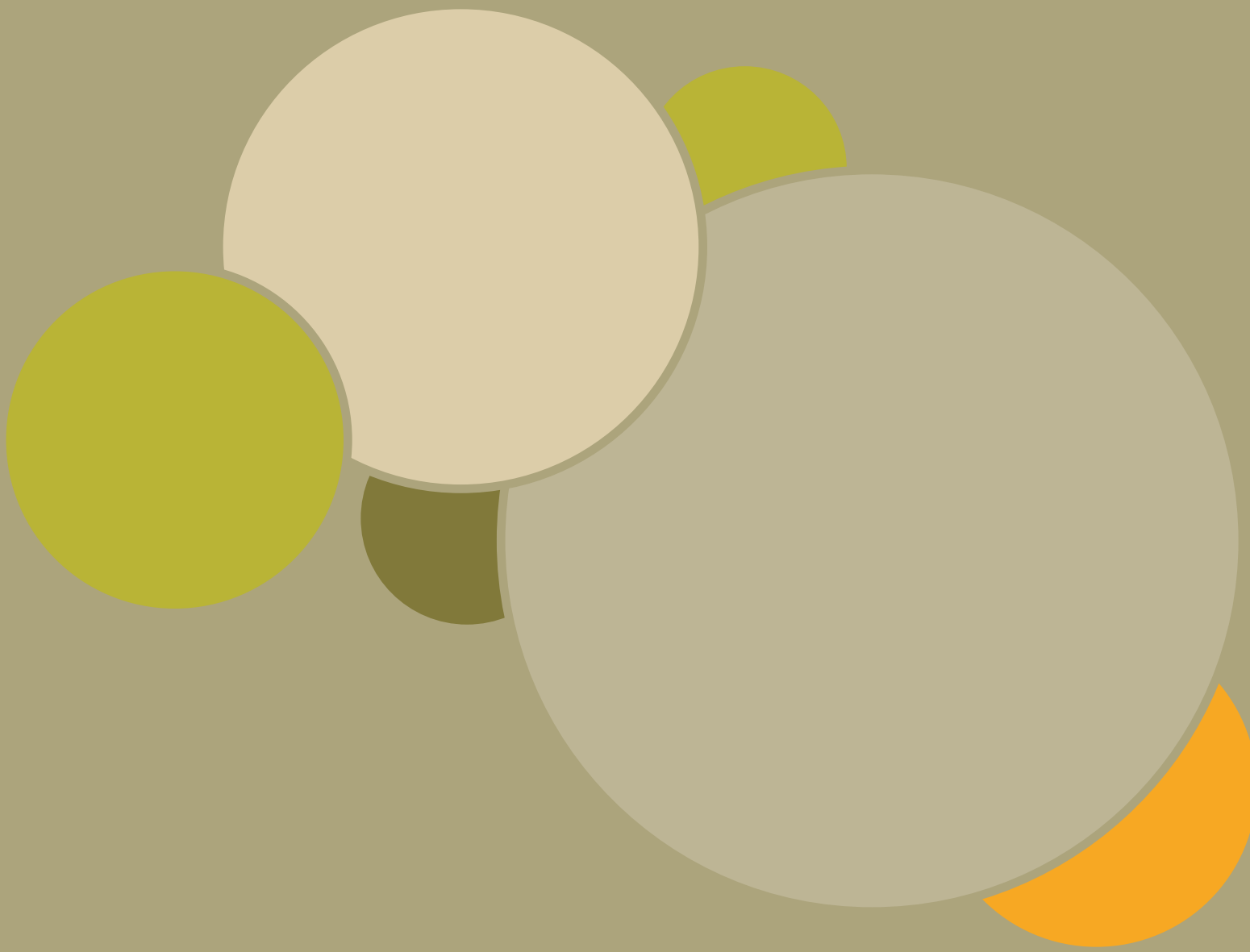

2

Chapter 2

Land cover mapping and monitoring

Pierre Defourny

2.1. INTRODUCTION

Today, there are several ways to describe land surface in light of the unprecedented developments in information technology (IT) and observation capabilities, ranging from the introduction of Unmanned Aerial Vehicles (UAVs) to the creation of in-orbit Earth Observation (EO) platforms. Satellite remote sensing is an undisputed source of land information for a vast range of users at all geographical scales. The gap between remote sensing data producers and map users is increasing, enhanced by the fact that spatial data infrastructures are making a great volume of geographic information widely available; therefore, it is important to understand the various concepts and constraints underlying land cover mapping in the context of agricultural statistics. This is particularly critical in light of the fact that in agricultural surveys, land cover maps are often used to support stratification at the sampling design level. Indeed, simple cropland maps or more specific maps depicting cropping intensity can significantly reduce the sampling variance or the ground sampling effort and associated costs.

Land cover maps can highlight the non-agricultural strata that are not to be sampled or the strata that could be sampled differently. As illustrated by Delincé (2015)[1], if a non-agricultural stratum covers one third of the administrative area of interest, the reallocation of the entire sample to the remaining strata – including cropland areas – will provide a relative stratification efficiency of 1.51 at almost no cost[2]. The efficiency of stratification clearly depends on the relevance of the land cover map selected for the stratification.

This chapter introduces the concept of land cover and reviews some key elements of the land cover mapping process, as organized according to a standard workflow (figure 1). The first steps of this process consist in the selection

1 GSARS. 2015. *Technical Report on Cost-Effectiveness of Remote Sensing for Agricultural Statistics in Developing and Emerging Economies*. GSARS Technical Report: Rome. Available at: http://gsars.org/en/technical-report-on-cost-effectiveness-of-remote-sensing-for-agricultural-statistics-in-developing-and-emerging-economies/. Accessed 9 August 2017.

2 Without stratification, the variance of the mean will be **?**2/(2/3)*n, such that 33 percent of sample size is lost in a region without crops. With stratification, the variance will become **?**2/n, such that the relative efficiency is Er= {**?**2/(2/3)*n}/{**?**2/n} =3/2 =1.5

of the appropriate land cover typology, the collection of the in situ data and the acquisition of the remote sensing imagery. The digital exploitation of these satellite images requires a sequence of standard operations to be completed carefully, and thus derive an accurate land cover map. As land cover maps are readily available for some regions, the relevance of existing maps to agriculture will be discussed systematically on the basis of a set of well-defined criteria. While land cover maps supporting stratification generally refer to previous years, this chapter also reports more recent experiences that enable the production of maps during the current growing season.

FIGURE 1. WORKFLOW FOR LAND COVER MAPPING FROM SATELLITE OBSERVATION TIME SERIES.

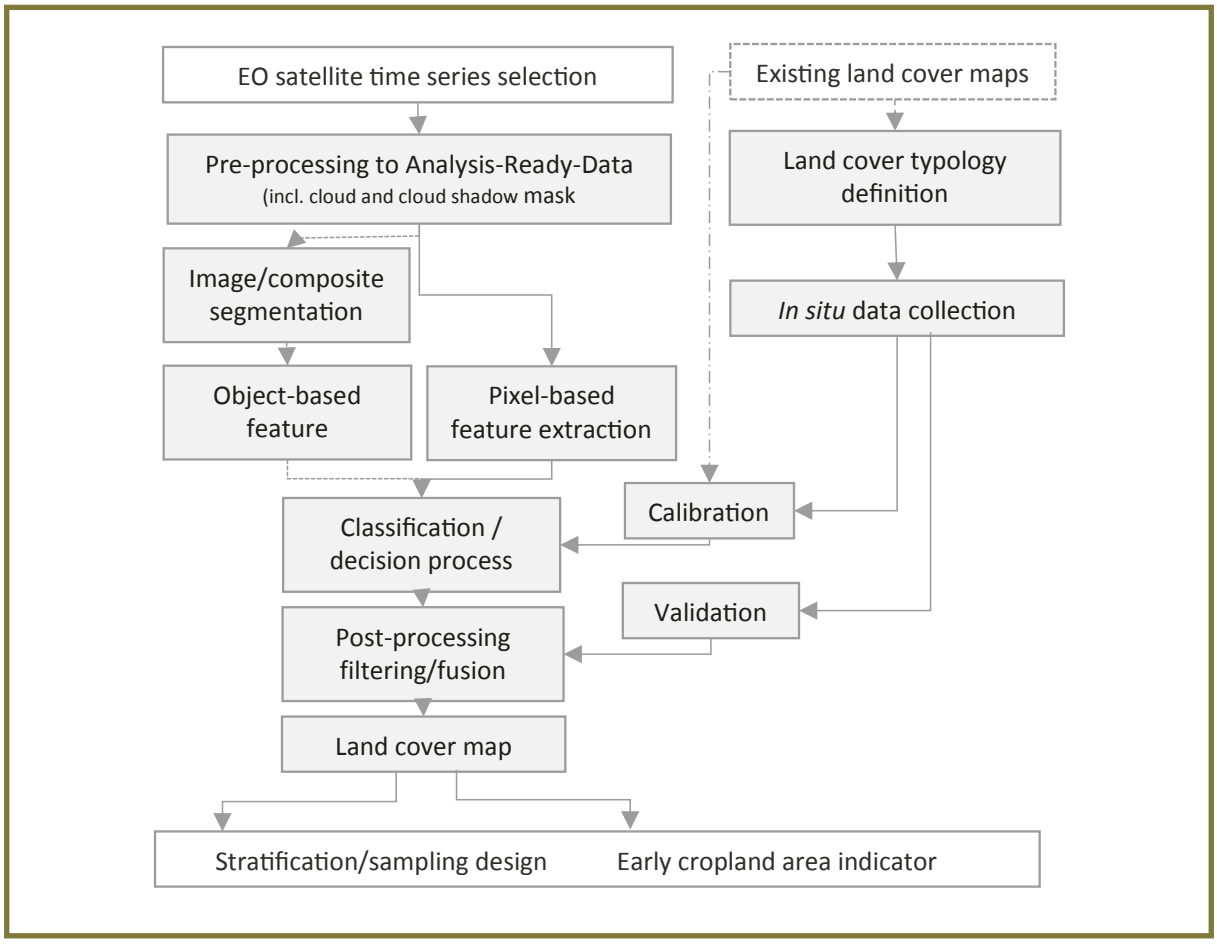

Dashed lines correspond to alternative pathways

2.2. THE CONCEPT OF LAND COVER

Historically, land use is considered more relevant for many applications other than land cover; however, the latter has been elected into a sort of universal panacea for land inventories, due to its reliance upon direct observation and the growing availability of satellite imagery. Land cover is used as a surrogate to describe the structure and character of the landscape by an increasing number of users who may be unaware or ignorant of the origins and semantics of land cover information. Comber *et al*. (2005a) demonstrate that land cover is perceived differently according to the discipline involved. If users do not fully understand the meaning of land cover and the assumptions underpinning it, then they impose their own interpretations of what land cover should encapsulate, relative to their constraints, focus and objectives – an imposition that may affect their assessment of the data and their subsequent analyses.

The real land surface world is infinitely complex, and any interpretation of EO data involves processes such as abstraction, classification, aggregation and simplification. For several decades now, there have been different opinions on what land cover is and how it is distinct from land use. As land observation has no agreed fundamental unit, land cover mapping must be understood as a process of information extraction that is governed by rules grounded in individual or institutional objectives. Most of the major land cover mapping initiatives have created their own classification system, described in great detail. At the very beginning of the satellite observation era, the U.S. Geological Survey (USGS) established a standardized land use and land cover classification system based on 40 years of experience with mapping from aerial photographs (Anderson *et al*., 1976). This is considered to be one of the most influential works in the area of developing national standards to serve various agencies. With the increasing expectations of users, the ever-growing data availability and the large diversity of purposes and contexts, the efforts to document land cover typologies is still very much necessary around the world.

2.2.1. Land Cover Classification Systems (LCCS and LCML)

To ensure full interoperability between typologies and provide common grounds for describing land cover, the Food and Agriculture Organization of the United Nations (FAO) developed the Land Cover Classification System (LCCS) as a conceptual framework for legend definition. Through a dichotomous modular-hierarchical system based on several sets of descriptors, namely the classifiers, the FAO-LCCS tool aims to explicitly clarify each land cover class, and therefore enables translating from one typology to another (Di Gregorio and Jansen, 2000). The system is based on independent and universally valid land cover diagnostic criteria, rather than on a predefined set of land cover classes. Its output is a comprehensive land cover definition, regardless of mapping scale, land cover type, data interpretation method or geographic location (Di Gregorio, 2005).

More recently, the LCCS framework has been modified into the Land Cover Meta-Language (LCML), to improve its flexibility with unbounded classifiers and a richer class description. Since 2012, the LCML framework proposed by FAO has been adopted as an international standard by the Technical Committee of the International Organization for Standardization (ISO)[3]. The LCML is an object-oriented classification system in which each land cover feature is characterized by a series of elements that can be further detailed by a set of attributes. The class meaning is no longer related to a simple class name, but rather to a more exhaustive and modern model populated by the elements and attributes characterizing the features of the land cover. Latham and Rosati (2016) provide further information on the subject[4].

3 The LCML was adopted as ISO standard ISO 19144-2:2012: http://www.din.de/en/getting-involved/standards-committees/nabau/standards/wdc-beuth:din21:155452459/toc-1911111/download.

4 Latham, J. & Rosati, I. 2016. *Land Information in the Context of Agricultural Statistics*. GSARS Technical Report GO-15-2016. Available at: http://gsars.org/wp-content/uploads/2016/08/TR_Information-on-Land-in-the-Context-of-Ag-Statistics-180816.pdf. Last accessed on 10 June 2017.

For the sake of clarity, transparency and intercomparison, it is internationally recommended to use the LCML framework to define any given land cover typology prior to conducting any mapping effort. For instance, the recent land cover Globland30, which was delivered in 2014 thanks to highly intensive and comprehensive efforts, poorly defined the land cover classes related to agriculture; this seriously curtailed its use for many agriculture and livestock applications.

2.2.2. Agriculture in land cover typology

In the context of agricultural statistics, the stratification definition used for the sampling design relies primarily on the land cover classes related to agriculture. It is noteworthy that cultivated land is not, strictly speaking, a land cover class, but rather a land use class[5]. For example, the land cover of a cereal field is more precisely a dense herbaceous vegetation, while only its land use should refer to agriculture or cropping activity. However, all existing land cover typologies integrate agriculture-related classes because of their importance for the landscape structure and for map users.

While agriculture may at first seem to be the easiest 'land cover' class to map for, this is a major source of misunderstanding and discrepancies between existing land cover maps, even when simply considering cropland and no cropland. This situation is exacerbated when considering the vast diversity of agricultural lands throughout the world, from double-cropping rice fields in Asia to the Mesoamerican traditional *milpa* intercropping system, from the European fallow lands to African perennial plantations such as cacao under the forest canopy.

The World Program for the Census of Agriculture 2020 (WCA 2020; Vol. 1, p. 82) proposes the following definitions[6], obtained by aggregating LCML classes:

- **Arable land** is land that is used in most years for growing temporary crops. It includes land used for growing temporary crops during a twelve-month reference period, as well as land that would normally be so used but is lying fallow or has not been sown due to unforeseen circumstances. Arable land does not include land under permanent crops or land that is potentially cultivable but is not normally cultivated. Such land should be classified as "permanent meadows and pastures" if used for grazing or haying, "forest and other wooded land" if overgrown with trees and not used for grazing or haying, or "other area not elsewhere classified" if it becomes wasteland.
- **Cropland** is the total of arable land and land under permanent crops.
- **Agricultural land** is the total of cropland and permanent meadows and pastures.
- **Land used for agriculture** is the total of "agricultural land" and "land under farm buildings and farmyards".

Based on the LCML framework, Di Gregorio (2013) established a precise and comprehensive cropland nomenclature to define cropland. However, in the context of agricultural statistics, the definition may raise additional questions, such as the fact that the cultivated area of interest is neither the sowed surface nor the harvestable one, but rather the area actually harvested. This is not only a semantic discussion for researchers, as the differences can be large in case of drought or floods.

5 See http://faostat.fao.org/beta/en/#data/RL for agriculture land use statistics reported by the countries.
6 WCA 2020, Volume 1, p. 82.

Other than this important discussion, the land cover typology must be workable and compatible with the source of data. For satellite remote sensing, the Joint Experiment for Crop Assessment and Monitoring network (JECAM)[7] endorsed a definition for annual cropland due to the annual nature of the Earth Observation time series:

> "the annual cropland from a remote sensing perspective is a piece of land of minimum 0.25 ha (min. width of 30 m) that is sowed/planted and harvestable at least once within the 12 months after the sowing/planting date. The annual cropland produces an herbaceous cover[8] and is sometimes combined with some tree or woody vegetation[9]."

The focus on annual cropland is more precise from a mapping point of view, and enables dealing with inter-annual changes of land cover, due for example to cropland extension or the abandonment of cultivated lands.

It is important to note that the definition adopted by JECAM also includes the concept of the Minimum Mapping Unit (MMU), which defines the smallest unit to be considered in the mapping process. For example, the mapping process of the EU's CORINE Land Cover Database was initially set at 25 ha, thus considering only landscape features larger than 25 ha. Such a specification may lead to the discarding of small fields scattered in an urban or forest landscape, which may induce a significant bias in the resulting agricultural land map.

2.2.3. Alternative approaches for land characterization

Other initiatives, driven by well-targeted objectives, focus on the delivery of single land cover class products or binary masks. For instance, the global croplands extent was derived from multi-year 250-m MODIS time series using a set of 39 metrics to depict cropland phenology and to derive a global per-pixel cropland probability layer using a global classification decision tree algorithm (Pittman *et al*., 2010). Hansen *et al*. (2013) obtained a bare soil/no bare soil map at global scale by processing the full archive of Landsat data since 2000 for its tree cover product. All of these initiatives offer the advantage of providing a map product that is focused on the land cover class of interest. Conversely, a major drawback is the absence of any concern for complementarities between products, which may lead to significant spatial inconsistencies or semantic incompatibilities.

The European Copernicus programme produced five separate layers (so-called High-Resolution Layers) of information, corresponding, respectively, to forest, grassland, permanent water, impervious surfaces (mainly built-up areas), and wetlands. Such an approach proceeds specifically on a given landscape feature, thus simplifying the data interpretation process. On the other hand, the spatial complementarity between these separately produced layers can only be worked out subsequently as an additional step, and it is not yet possible to obtain a comprehensive land cover map.

Reducing the diversity of land features into a finite number of classes predefined by land cover typology is always a challenge in complex landscapes. As described by Defourny and Bontemps (2013), an alternative strategy was proposed to describe vegetation in terms of continuous fields (Smith *et al*., 1990; DeFries *et al*., 1995). This approach, also known as the continuous fields approach, consists in mapping the respective fraction of the basic components of the land surface, for instance to represent the percentage of bare ground, herbaceous and tree cover

7 www.jecam.org.

8 The herbaceous vegetation expressed as fCover (fraction of soil background covered by the living vegetation) is expected to reach at least 30 percent while the tree or woody (height > 2m) cover should typically not exceed an fCover of 20 percent.

9 There are three known exceptions to this definition. The first concerns sugarcane and cassava, which are included in the cropland class although they have a longer vegetation cycle and are not planted on a yearly basis. Second, taken individually, small plots such as legumes do not meet the minimum size criteria of the cropland definition. However, when considered as a continuous heterogeneous field, they should be included in the cropland. The third case is that of greenhouse crops, which cannot be monitored by remote sensing and are thus excluded from the definition.

for each pixel (Hansen *et al*., 2005). Continuous fields are usually obtained using a regression tree algorithm that matches a continuous and dense training data set covering the whole range of vegetation cover and a large set of multitemporal metrics based on a full time series data set. The properties of continuous fields of vegetation are such as to offer advantages over traditional discrete classifications, because they enable a more precise representation of heterogeneous areas by depicting each pixel as proportions of cover types. In this respect, this approach is appealing and relevant for many natural and semi-natural landscapes. On the other hand, these products were found to be rather difficult to validate, due to the absence of an appropriate reference data set and to the fact that they leave users to define the specific thresholds for converting this continuous products into usable maps.

Similarly, the retrieval of biophysical variables from satellite time series also results in a quantitative description of the land surface thanks to empirical regression or to physically based model inversion. Indeed, remote sensing products corresponding the Leaf Area Index (LAI), the fraction of Absorbed Photosynthetically Active Radiation (fAPAR), albedo, etc. provide direct estimates of undisputable variables that can also be measured on the ground. The seasonal evolution of these biophysical variables can characterize the land surface, and can sometimes be interpreted in agricultural land cover classes of interest or directly used for stratification. However, the capability to identify these biophysical variables from high-resolution, free and open-access satellite imagery, such as that provided by Sentinel-1 and Sentinel-2, has developed only very recently. The time series available for years at coarse spatial resolutions (250 m to 1 km) are only useful for stratification purposes in certain agricultural landscapes, which either have very large field sizes (as typically occurs in Argentina, Ukraine, the United States of America, Russia, etc.), or with uniform and non-fragmented landscapes comprising many small but similar fields cultivated according to a same crop calendar (as for example in the North China plain or in case of irrigated rice plains).

2.3. LAND COVER MAPPING PRODUCTION

Building upon the increasing availability of Earth Observation satellite data, land cover mapping from spectral and temporal signatures has progressively become one of the most popular approaches to describe land surface. Different regions of the world have been mapped and characterized several times, either by national agencies on a routine basis or by international programs (Africover, SERVIR, CORINE Land Cover, etc.), while a number of global land cover maps have been made available with resolutions ranging from 30 m to 500 m.

Chapter 1 of this handbook reviews in detail the various data sources, their evolution and the emergence of new processing environments. The availability of online access to high-speed computing capabilities, along with open-access and free, analysis-ready data time series greatly facilitates the production of land cover map at national scales much more accessible, even compared to only a few years ago. It is, however, important to highlight the conceptual and methodological gaps between the existing classification methods, which are designed to proceed scene by scene or to interactively process a certain number of images over a limited region of interest (local to national), and the automated processing chains that are capable of exploiting all images acquired over a large area of interest (national to regional or continental).

This section systematically reviews the key elements involved in land cover mapping, to help assess the quality of existing land cover maps and support an appropriate design of land cover mapping initiatives at national scale. The intention is to provide an overview of all aspects to consider, rather than to explain specific remote sensing methods. The following chapters of this handbook provide more details on these elements, focusing on particular applications, such as crop type mapping.

2.3.1. Remote sensing data

The selection of the data source strongly constrains the quality and the spatial detail of the mapping output. In addition to data cost and accessibility as reviewed in chapter 1, the optimal trade-off for land cover mapping should be based on four main criteria, seen below and summarized in table 1:

1. The spatial resolution – or more precisely the Ground Sampling Distance (GSD) of the instrument characterized by its point spread function – defines the smallest land feature to be detected and subsequently possibly mapped. It is of paramount importance that the spatial resolution be smaller than the size of most of the agricultural parcels to obtain a sufficient number of pure cropland pixels. However, the most appropriate spatial resolution to use in mapping the cultivated lands also depends on the landscape fragmentation, the diversity of crop types and their spatial distribution; for instance, small but similar adjacent fields of a same crop type can be considered as a very large field if the crop developments are relatively synchronized. While it may be of interest to capture linear landscape features such as hedges, tree alignments or rural roads, this information is not strictly necessary for landscape stratification. It is important to note that higher spatial resolution is not always a better option to when running digital image processing. Improving the spatial resolution exponentially increases the data volume and the relevant computing requirements. For example, an upgrade from a resolution of 30 m to a resolution of 10 m multiplies the data storage by 9. Furthermore, while it is easier to visually interpret an image when its spatial resolution allows capturing landscape elements such as trees or houses, this does not hold true for more automated digital image processing chains. Further investigating this issue, Duveiller and Defourny (2010) propose a conceptual framework to adjust the spatial resolution to a given agricultural landscape field size.

2. The frequency of valid cloud-free observation is the second most important criterion for mapping agricultural landscapes accurately. Indeed, the seasonal dynamics of agricultural lands are only captured with a dense time series of cloud-free observation. A given revisit cycle of an EO system provides very different temporal densities of useable observation depending upon cloud occurrence. Therefore, discriminating between the different types of agricultural land requires consideration of the effective frequency of valid images for the growing season, rather than the revisit capability alone (Whitcraft *et al*., 2015). In heterogeneous landscapes, capturing the entire seasonal profile of the field signature enables distinguishing between the different cultivated lands, such as between permanent meadows, natural grasses and cereals, which may all have very similar appearances for a long period of the growing season. There are constellations of satellites that are equipped with inter-calibrated instruments and can provide competitive options to increase observation frequency using high spatial resolution. In cloudy regions, SAR sensors such as Sentinel-1 or Radarsat-2 may be the best option to ensure a dense time series of observation, as the microwave bands are not affected by most atmospheric perturbations or by clouds.

3. The number of spectral bands and their position along the electromagnetic spectrum is another important criterion, not only for land cover discrimination but also for atmospheric haze correction haze detection and efficient cloud and cloud shadow screening. Today, narrow visible and NIR bands are available for most Earth Observation satellite platforms; ideally, these are complemented with SWIR bands, which are also very useful to discriminate land cover types. Conversely, cloud detection remains a challenging issue. Except for MODIS, Worldview-3 and Sentinel-3OLCI, none of the existing sensors possesses the appropriate spectral bands on the same platform to deal with all aerosols and cloud types, and their confusion with snow and ice. Highly popular satellites, such as Landsat-8 and Sentinel-2, both have a nice set of bands – including an efficient cirrus band – to screen out atmospheric perturbations. However, their operational use continues to face limitations in some regions. Many other sensors are found to be problematic when obtaining consistent time series over large areas, due to atmospheric perturbations of signals that are difficult to detect and to correct. Such corrections are necessary if it is sought to combine in a single image (that is, a composite or a mosaic when only one observation per pixel is available) pixel values captured on different observation dates or different sensors to attain a seamless, cloud-free image. On the other hand, cloud-free observations over large areas that are well distributed over the season may not require atmospheric correction for their classification and could be sufficient for the purposes of land cover mapping.

4. Wide swath sensors cover very large areas in a single overpass (290 km for Sentinel-2, 650 km for DMC satellites, and more than 1 200 km for coarse instruments such as MODIS, Sentinel-3 OLCI and PROBA-V). Therefore, swath width is also a criterion in large-scale application. While smaller images can still be stitched together to form mosaics, they require performing atmospheric correction if they are to be combined in a seamless imagery or in a mapping output consistent over large area. Sensors with a narrow swath (typically approximately 50 km or even below 20 km, for satellites having very high spatial resolution (VHR)) tend to cover large areas by mosaicking small images acquired from different viewing angles. Due to the so-called bidirectional reflectance distribution function, such a viewing angle variability may induce spectral signature differences for a given land surface, which would make the classification process much more challenging.

TABLE 1. CRITERIA SUPPORTING THE SELECTION OF APPROPRIATE REMOTE SENSING DATA SOURCES.

Criteria	Spatial resolution	Valid obs. frequency	Spectral resolution	Swath size
Rationale	Matching the size of the landscape elements	Temporal profile along growing season	Land cover discrimination Cloud screening	Seamless image over large area
Variable according to	Parcel size distribution and fragmentation	Cloud persistence	Land cover diversity Haze and cloud cover frequency	Country size

An additional criterion to select the data source is the level and the quality of data pre-processing. Increasingly, data providers deliver ready-to-use or ready-for-analysis imagery including state-of-the-art radiometric calibration, orthorectification, atmospheric correction and cloud and cloud shadow screening. Otherwise, a pre-processing chain must be implemented to convert the radiance signal recorded at the top-of-atmosphere to bottom-of-atmosphere multispectral reflectance. The only advantage of in-house pre-processing is that some algorithms may be fine-tuned to the area of interest (local availability of better atmospheric information, better DEM, etc.) or that certain more advanced processing steps may be included, such as topographic correction, which is useful wherever significant areas are cultivated in mountainous or hilly regions.

2.3.2. *In situ* data collection

In addition to satellite EO imagery or time series, land cover mapping always relies at least on another source of information to support the classification process (either by training the classification algorithm a priori or to label the output classes a posteriori), and to assess map quality.

The two main purposes of the *in situ* data collection are referred to as algorithm calibration and output validation (figure 1). The calibration data set supports the training of EO data classification algorithms to generate, for instance, a land cover map, a cropland mask or even a crop type map. The requirements for collecting an appropriate calibration data set are examined in detail in section 2.2.3.

Instead of *in situ* data, Matton *et al*. (2015) and Desclée *et al*. (2006) have developed specific methods to use existing obsolete land cover maps as a priori information to train classification algorithms and to produce a cropland mask and a forest mask, respectively. Alternatively, unsupervised classification algorithms do not require a calibration data set; they require a labeling data set, which can consist either of in situ data or of existing obsolete maps, as first implemented in the GlobCover project (Defourny *et al*., 2006).

On the other hand, the validation data set is necessarily a high-quality reference data set, to be used as so-called ground-truth to assess the accuracy of a land cover map. Validation should never be confused with the intercomparison of maps; this process quantifies the discrepancies between the maps, but cannot rigorously attribute errors to one or the other.

Field data collection is a resource-intensive and time-consuming activity, particularly if it is sought to cover large areas. While sampling theory should define the design, logistic and resource constraints impel identification of the optimal trade-off in terms of performance and cost-efficiency. Some basic principles and figures to guide potential map producers and assess map quality are provided further below in this section. In some countries, up-to-date agricultural Land Parcel Information Systems provide a comprehensive ready-to-use set of reference data. In others, field surveys may be impossible for security reasons or due to lack of physical access to the territory.

Training data sets and validation data sets may also be collected by on-screen delineation based on visual and interactive interpretation of multispectral colour composites. Very high spatial resolution images made available on line by Google Earth, Bing, and similar geoportals, are often used for digitizing polygons instead of ground data. The acquisition date of these images displayed on geoportals can be very diverse and does not necessarily correspond to any given year of observation. This is therefore quite efficient for the most stable land cover types but should not be used for crop type for instance as they might change annually. As experimented for GlobCover validation (Defourny *et al*., 2012b), the reliability of the interpretation based only on VHR imagery depends largely on its observation date – a factor that is beyond the control of the interpreter. The interpretation of VHR images is efficiently augmented by the NDVI temporal profiles provided for the corresponding pixel, as proposed by the European Space Agency (ESA) CCI Land Cover interface, which covers the entire world[10]. More recently, several crowdsourcing initiatives have demonstrated that citizen mobilization to collect large amount of data about agriculture or land cover is possible, as seen on programmes such as Google Earth. Geowiki (Fritz *et al*., 2015) and Collect Earth[11] are online applications that guide the visual interpretation of a massive number of non-expert individuals, sometimes through gamification and assuming that the quantity of information somehow also eventually leads to its quality. This is a very active field of research, and a number of worldwide experimental applications have been already proven to be more or less successful.

Calibration

The sampling objective for the calibration data set is to encompass the entire diversity of situations existing in the region of interest (for instance, the national territory) to represent the range of possible spectral and temporal signatures. To produce an agricultural land mask delineating cropland versus non-cropland, all land cover types must be included in the calibration data set. Otherwise, the non-documented land cover types are allocated to the cropland or non-cropland class in an uncontrolled manner.

The samples are targeted to establish the necessary links between a given landscape type (wetlands, urban area, water, etc.) and the existing range of corresponding spectral and temporal signatures. Unlike the case for validation, which should follow a rigorous sampling design, various types of sampling strategies are acceptable for calibration, as long as they are fairly distributed across the territory to capture the full variability of each land cover type.

To cover this diversity and the agroclimatic gradients often observed over large areas (for instance, a national territory), it is recommended to stratify the landscape according to the interactions between agro-ecosystem types, crop type distribution, cropping calendars and overall biophysical contexts (floodplain, mountainous areas, etc.). Such a form of stratification, here called Agro-Ecological Zoning, already exists in many countries. As a rule of thumb, a limited number of zones should be considered, ranging typically from 3 to 12 zones for a country extending

10 http://maps.elie.ucl.ac.be/CCI/viewer/.

11 http://www.mdpi.com/2072-4292/8/10/807/html.

over approximately 500 000 km², to ensure that there are enough training samples for all the classes in each stratum and that the sampling remains manageable.

As described in the JECAM guidelines (2014) for non-agricultural land cover classes, a visual interpretation of existing imagery on geoportals can be very efficient to define at least 15 land cover training samples per class and per stratum, in particular for remote areas and areas with low rates of land cover change. As explained above, the visual interpretation of available up-to-date aerial photographs or VHR imagery is advantageously supplemented by temporal information such as NDVI profiles, to capture the diversity of the non-agricultural land cover types.

As mentioned above, all of the various agricultural classes (that is, different crop types, meadows, pastures, permanent crops, etc.) must be also described in the calibration data set, although they may vary from one year to another. Therefore, a field survey corresponding to the agricultural season of the remote sensing data set to process is the best way to delineate a set of training samples for each stratum, that is for instance approximately 30 samples per crop with an area larger than 5 pixels x 5 pixels9, to capture the signature diversity of a given crop. Classification quality often improves with the quantity of samples. If the objective is to map only the cropland in a single class mask, it may be sufficient to delineate all the different signatures of cropland directly on the color composites, to define different spectral classes, and to regroup them into a single cropland class at a later stage. In countries with strong agricultural seasonality, the selection of an appropriate observation period may dramatically simplify the sampling for agricultural lands: for example, all bare soils at a given specific period of the year could correspond to all annual crop types.

It is worth noting that the comprehensive sampling of crop types often required for land cover mapping may also help in the production of a crop type map. In these cases, it may be more efficient to first produce an agricultural land mask and then classify into crop types only those pixels belonging to the agricultural land mask, rather than classify the entire area again.

A major difference between a cropland mask and a crop type map is the topicality of the map. While the cropland extent varies rather slowly making a given cropland mask probably relevant for several years, the crop type distribution may significantly change every year and is valid only for the year of observation. The same applies for the training data set used for calibration.

BOX 1. MALI. STRATIFICATION AND SAMPLING FOR THE SENTINEL-2 FOR AGRICULTURE, SYSTEM SUPPORTED BY ESA.

Covering over 447 000 km² in Mali, the agro-ecological zoning based on the atlas of the *Projet Inventaire des Ressources Terrestres* (PIRT) delineates five distinct strata, including the cotton belt and the rice production area. For non-cropland, 12 land cover types may be trained separately for the five strata, yielding a total of approximately 1 125 training samples for non-cropland (15 samples x 15 land cover types x 5 strata). The sample distribution within a stratum should cover the expected range along the land cover gradient, and was achieved through Google Earth interpretation of current- or previous-year images, plus corresponding NDVI profile wherever necessary.
To cover crop type diversity as required for crop type mapping, each of the main crop types should be sampled extensively for each stratum. Indeed, the discrimination between similar crop types is expected to require more training data than for contrasted land cover classes. Therefore, a target of 1 800 samples, consisting of 30 samples x 12 crop types x 5 strata is probably a minimum. It should be noted that the 12 main crop types is a simplification of the 40 crop types used by Mali's *Cellule de Planification et Statistiques* (CPS).

It is worth mentioning that for their crop statistics, the 275 CPS officers annually collect 30 000 georeferenced samples, corresponding to cultivated fields distributed throughout the country. Once quality-controlled, this information was found to be valuable as training data for the cropland mapping performed by the Sentinel-2 Agriculture system. For the Southern stratum, the combination of non-cropland samples delineated on Google Earth and the data provided by the CPS allowed for mapping cropland (in white) and non-cropland (in black) at a 10-m resolution, using Sentinel-2 with an overall accuracy of 94 percent. Such a map could definitely optimize the CPS's sampling design for the future.

Validation

The objective of a validation data set is to provide a statistically sound estimate of the accuracy of the output map based on an independent reference information source. The accuracy of a map is assessed by measuring the degree of agreement between the output map and the validation data set.

Several metrics of classification accuracy can be derived from the confusion matrix, which corresponds to a two-dimensional contingency table matching the mapped and observed class for each sample.

The training and validation data set should be completely different and spatially independent. When in situ data are split into two subsets, the first one used for training the algorithm, the second is often expected to assess the quality of the output. In fact, this should not be considered an appropriate validation exercise, as the second set is often spatially correlated to the training one. Such a sampling approach would assess the algorithm calibration performance; however, it would not assess the quality of the entire product. This would be a proper validation data set only if all of the samples were distributed over the entire area of interest and then randomly split into calibration and validation subsets.

The number of observation, the sampling design the response design, and the reliability of the validation data source define the quality of the accuracy estimate. According to sampling theory, random sampling or systematic random sampling are the most suitable to provide independent information and avoid spatial bias resulting from the location of field observations. Similarly, a sampling design based on clusters of samples aligned on a systematic grid with a random start guarantees the selection of a representative and spatially well-distributed data set. These rather theoretical sampling plans are difficult to implement on the ground in operational contexts, because of practical accessibility constraints and limited resources.

A two-stage sampling strategy is often adopted to insure a large distribution of the samples and a random component in the sample selection. First, some Primary Sampling Units (PSUs) delineated by ancillary data (typically, administrative regions) are randomly selected in the different strata according to their cropland area (cropland area-weighted sampling probability). Then, within each PSU, the sampling could proceed as a "windshield survey", identifying Elementary Sampling Units (or ESUs, having minimum dimensions of 3 pixels x 3 pixels) along the roads from a motorized vehicle.

FIGURE 2. SAMPLING BY WINDSHIELD SURVEY

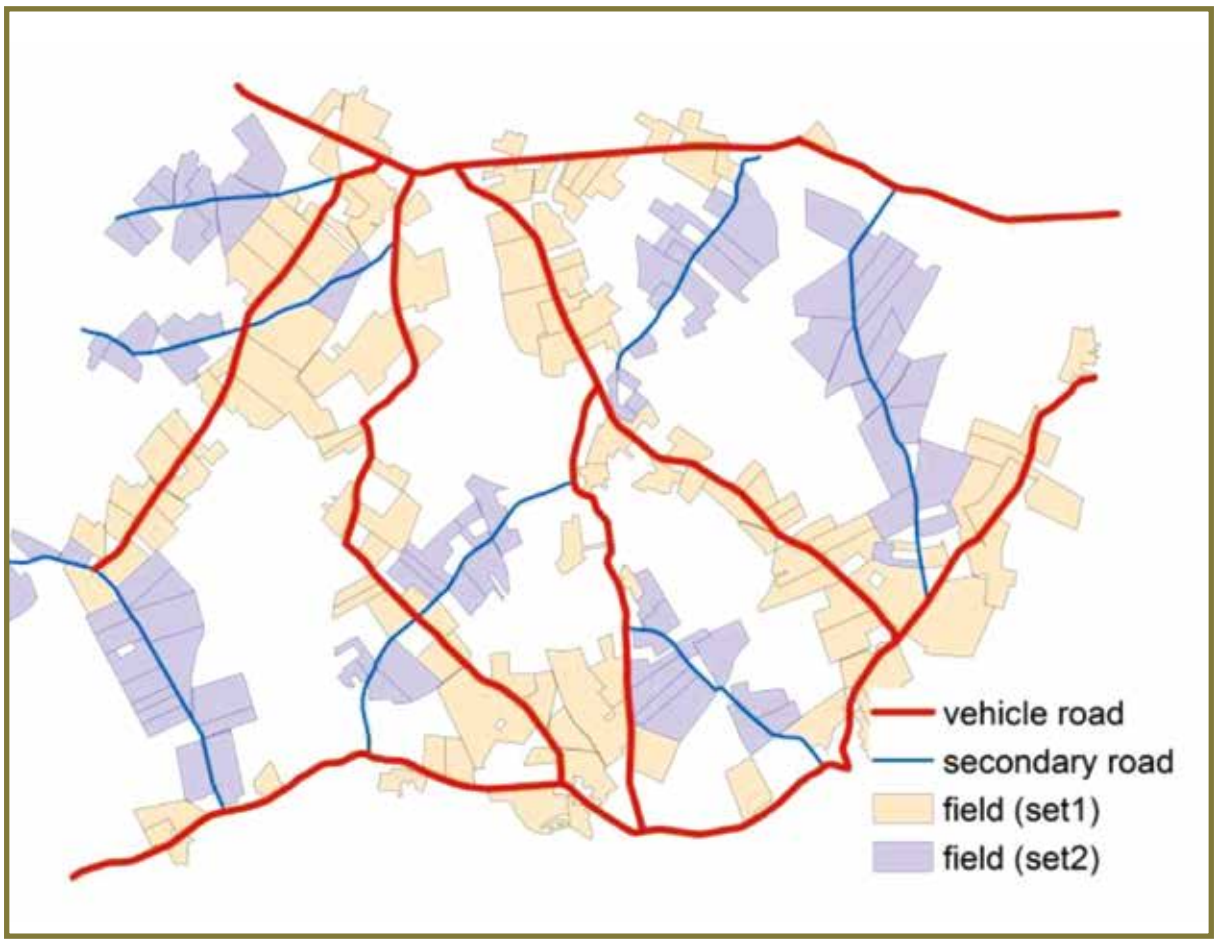

Source: JECAM, 2014.

In terms of response design, this approach allows a data collector to easily and rapidly capture crop diversity from all visible fields (set 1 in figure 4-2). The main objective of this approach is to identify long transects across the PSU by selecting a set of appropriate roads. However, it is recommended that this sampling strategy be complemented by regular additional transects (set 2) using secondary roads and tracks to reduce the spatial bias brought about by roadside sampling. This is crucial when the cropland or crop type distribution varies according to the distance from the main roads. Several transects running in various directions (for example, north-south and east-west) ensure full coverage of the area of interest, while secondary road sampling complements the validation set with less biased data.

As a rule of thumb, the minimum sampling density to validate land cover maps should reach 30 samples for the least represented land cover class, and approximately one observation per 100–150 km2 for large areas. A higher sampling density would improve the quality of the accuracy estimate. As the less frequent or marginal land cover classes are not sufficiently represented with an overall sampling design, a specific sampling strategy is required to target samples for these land cover types while maintaining a random component. When up-to-date VHR imagery is available, a dense systematic random sampling could also allow for collecting, by visual interpretation, a sufficient number of samples over these less-frequent land cover types. Otherwise, a sampling on the ground that is biased towards these classes would be necessary.

In some cases, existing databases may provide appropriate ground-truth for land cover map validation. For instance, the independent LUCAS database of the European Union (EU), designed to derive land statistics, can be used to perform an accuracy assessment of the land cover and cropland mapping for the corresponding year.

The validation data are then used to assess the map accuracy defined by the agreement between the map output and the validation data assumed to be the truth. The most common way to derive the map accuracy is to analyse the confusion matrix, which is a square co-occurrence matrix compiling the number of samples matching a given land cover class with validation information. Diagonal values represent the agreement frequency between the validation data and the map output, while non-diagonal values represent the errors.

TABLE 2. CONFUSION MATRIX WHERE N_{ij} IS THE NUMBER OF VALIDATION SAMPLES CORRESPONDING TO THE LAND COVER MAP CLASS *i* AND VALIDATION INFORMATION *j*.

	Validation data					
Map	**Cropland**	**Forest**	**Grassland**	**Urban**	**Water**	**Total**
Cropland	n_{11}	n_{12}	n_{13}	n_{14}	n_{15}	$n_{1.}$
Forest	n_{21}	n_{22}	n_{23}	n_{24}	n_{25}	$n_{2.}$
Grassland	n_{31}	n_{32}	n_{33}	n_{34}	n_{35}	$n_{3.}$
Urban	n_{41}	n_{42}	n_{43}	n_{44}	n_{45}	$n_{4.}$
Water	n_{51}	n_{52}	n_{53}	n_{54}	n_{55}	$n_{5.}$
Total	$n_{.1}$	$n_{.2}$	$n_{.3}$	$n_{.4}$	$n_{.5}$	$N_{..}$

Among fourteen class-level and twenty map-level accuracy metrics, Liu *et al*. (2007) recommended user accuracy (UA), producer accuracy (PA) and overall accuracy (OA) as primary accuracy measures. For binary maps such as the cropland mask, the OA depends to a large extent on the respective proportion of both classes in the validation data set. In this case, the F-Score, the use of which has been recently adopted, is a more informative accuracy metric.

The OA is computed as the ratio of the number of all correctly classified samples to the total number (N) of all validation samples. A standard target for the overall accuracy of a land cover map is typically 85 percent. In some cases, simple land cover maps that include very few classes can reach 90 percent.

$$OA\ (\%) = (100 \times \sum_{k=1}^{q} n_{kk}) / N \qquad \text{(equation 1)}$$

The UA for a given land cover class *i* is the ratio between the number of correctly classified samples as belonging to this class and all samples classified in this class.

$$UA_i\ (\%) = 100 \times \frac{n_{ii}}{n_{i+}} \qquad \text{(equation 2)}$$

The PA for a given class *i* is the ratio between the number of correctly classified samples and all sampl belonging to this class, according to the validation data.

$$PA_i\ (\%) = 100 \times \frac{n_{ii}}{n_{+i}} \qquad \text{(equation 3)}$$

The F-score is calculated as a combination of PA and UA for a given land cover class *i*:

2.3.3 Image processing and map production

The extraction of land surface information from remotely sensed data relies on a series of complex processes, because the radiance measured by the sensors in watt/m².str does not allow for direct inference of the land cover. In the past, several operational mapping systems were based on on-screen interactive visual interpretation of one or two images acquired at specific periods of the year, and mainly relied on expert interpretation. This approach has been progressively supported by image processing tools, which are either interactively run or applied once for all. Moving from best-image or pair-of-images selection to full-time series processing, digital processing tends to reduce labour-intensive data handling to focus interactive human intervention on the most critical steps.

Any land cover map production consists of a sequence of main processing steps. For each of these steps, several conceptual and algorithmic choices are possible. Waldner *et al*. (2016) have shown that crop mask accuracy varies more from one agricultural region to another rather than from one state-of-the-art method to another. Clearly, certain methodological choices may be more appropriate than others; however, ultimately, the quality and quantity of the remote sensing input and of the calibration data set play an even more important role, in most cases. The key to success is probably the adequacy of the methodological choices adopted for a given quantity and quality of input Earth Observation and in situ calibration data, and with regard to the landscape characteristics to be mapped.

As introduced in figure 1, four main steps in the land cover production chain may be clearly identified: (1) image segmentation; (2) feature extraction; (3) classification; and (4) postprocessing, including filtering and/or fusion.

Image segmentation

The land is discretized into pixels by satellite imagery, while on-screen visual interpretation delineates homogeneous patterns. An image raster made of pixels and a vector made of objects are the two main conceptual models designed to describe the spatial dimension of the world. When the spatial resolution is close or larger than the size of the land cover elements to be mapped, land cover information is generally extracted at the pixel level and the segmentation step is not necessary. For VHR or high-spatial-resolution imagery providing pixels much smaller than the land cover elements, the vector model is usually preferred and the image should be segmented into objects by means of image segmentation algorithms.

Image segmentation groups adjacent pixels into spatially continuous objects according to their spectral characteristics and their spatial context, aiming to capture meaningful spatially discrete land objects. The object-based approach is well adapted to image texture extraction, has intrinsic contextual information avoiding a salt-and-pepper effect in the classification output, and supports multiscale interpretation thanks to hierarchical or multilevel segmentation (Radoux and Defourny, 2008). On the other hand, this step is also an additional source of error compared to the pixel-based approach. As explained above, it is mostly recommended to proceed with object-based classification when the pixel size is much smaller than the landscape elements. Typically, metric and decametric images are often segmented into objects, while hectometric-resolution images are not. In exceptional cases, pixel- and object-based production chains have been designed; consider the interactive production of the GlobeLand30 land cover map (Jun Chen *et al*. 2015).

Image segmentation can be performed on the basis of two distinct approaches: the gradient-based methods, which rely on a local detection of edges (such as watershed delineation from the intensity gradient), and the region-growing methods, which identify spatial clusters of coherent pixels. One of the most popular region-growing algorithms in remote sensing consists in grouping objects together as long as the normalized variance of the pixel values within the merged object remains below a given threshold (Baatz and Schäape, 2000). In addition to spectral homogeneity, the merging of objects can also be constrained by the object shape, to improve the matching with spatial land cover objects. This algorithm has been implemented in the commercial software eCognition, while the watershed delineation and mean-shift algorithms are implemented in the open source ORFEO toolbox (https://www.orfeo-toolbox.org/) and available in the open-source Quantum GIS (QGIS) through the SEXTANTE plugin.

Feature extraction

The feature extraction step consists in computing, from the remote sensing images or time series, the most discriminant variables to be used as input for the classification algorithm. These features may be of various natures: (1) spectral, as the multispectral reflectance or the derived indices, such as the NDVI or any other vegetation, chlorophyll or soil index; (2) temporal, as the minimum, maximum or amplitude of a variable over a given time period; (3) textural, as the local contrast, entropy or any other variable derived from the co-occurrence matrix; and (4) a spatial or contextual variable that is particularly suited to the object-based approach.

Currently, three main strategies may be observed in the field of land cover mapping. First, classical strategies rely mainly on spectral features and, possibly, some simple temporal features based on NDVI time series, considering that these are the sources of all other features in any case. In light of increasingly powerful computing performances and the dissemination of machine-learning algorithms, many remote sensing specialists now consider that "more is better" (in terms of features) and rely on classification algorithms to select the most discriminant ones. Third, knowledge-based strategies aim to integrate external expert knowledge by designing ad hoc features according to the classification target and by retaining only those features deemed meaningful according to experts' rationale (Lambert *et al*., 2016).

Classification

The classification step consists in one or many numerical processes to finally allocate every pixel or object to one of the classes of the land cover typology. The vast diversity of classification algorithms can be split into two main types: the supervised type, which uses a training data set to calibrate the algorithm a priori; and the unsupervised type, which produces clusters of pixels to be labelled a posteriori as land cover class in light of in situ or ancillary information. More recently, forerunning steps of supervised classification are very useful and consist in automatic cleaning of *in situ* training data sets or active learning to build a more efficient training data set, by iteratively improving the performance of the classifier model.

The set of methods used to classify images in land cover classes is constantly expanding and is summarized in table 3 in terms of strengths and disadvantages. A review of these methods was recently completed by Davidson (2016) and is included below.

TABLE 3. STRENGTHS AND WEAKNESSES OF ALGORITHMS USED FOR LARGE-AREA CLASSIFICATION OF SATELLITE IMAGE DATA (BASED ON GÓMEZ *et al.*, 2016).

Algorithm	Strengths/characteristics	Weaknesses
Maximum Likelihood (Parametric)	• Simple application • Easy to understand and interpret • Predicts class membership probability	• Parametric • Assumes normal distribution of data • Large training sample necessary
Artificial Neural Networks (Non-parametric)	• Manages large feature space well • Indicates strength of class membership • Generally high classification accuracy • Resistant to training data deficiencies – requires less training data than Decision Trees (DTs)	• Needs parameters for network design • Tends to overfit data • Black box (rules are unknown) • Computationally intense • Slow training
Support Vector Machines (Non-parametric)	• Manages large feature space well • Insensitive to Hughes effect • Works well with small training data set • Does not overfit	• Needs parameters: regularization and kernel • Poor performance with small feature space • Computationally intense • Designed as binary, although variations exist
Decision Trees (Non-parametric)	• No need for any kind of parameter • Easy to apply and interpret • Handles missing data • Handles data of different types (e.g. continuous, categorical) and scales • Handles non-linear relationships • Insensitive to noise	• Sensitive to noise • Tends to overfit • Does not perform as well as others in large feature spaces • Large training sample required
Random Forests (Non-parametric)	• Capacity to determine variable importance • Robust to data reduction • Does not overfit • Produces unbiased accuracy estimate • Higher accuracy than DTs	• Decision rules unknown (black box) • Computationally intense • Requires input parameters (#trees and #variables per node)

Classification based on Maximum Likelihood

Until recently, the Maximum Likelihood (ML) classification method was the most widely used method for the supervised classification of remote sensor data (Lu and Weng, 2007; Bhatta, 2008; Kumar *et al.*, 2016). The ML decision rule is based on probability. In this approach, training data are used to describe target classes statistically by their multivariate probability density functions. Each density function represents the probability that the spectral pattern of a class falls within a given region in multidimensional spectral space. The spectral signature of each pixel is then assigned to the class of which it has the highest likelihood of being a member (Jensen, 1986).

While the primary advantage of the ML approach is the full control that an analyst has over the land cover classes to be used in the final classification, its application is limited by its reliance on the Gaussian distribution of input data, an assumption that is often violated when using multitemporal data of many spectral features and multimodal distributions (Gislason *et al.*, 2006; Glanz *et al.*, 2014). In addition, classification through ML uses the same set of features for all classes and requires a large number of computations to completely classify image data. This is particularly true when a large number of features are used as input to the classification process, or where a large number of spectral classes must be differentiated. In such cases, the implementation of the ML classifier can be significantly slower than other supervised classification techniques. The various limitations associated with ML classification translate into the active development of novel classification algorithms for the field of remote sensing. Of these new methods, artificial neural networks (ANNs: Rumelhart *et al.*, 1986;

Rigol-Sanchez *et al*., 2003), support vector machines (SVMs, Abedi *et al*., 2013; Al-Anazi and Gates, 2010; Cortes and Vapnik, 1995; Ghimire *et al*., 2012; Zuo and Carranza, 2011), Decision Trees (DTs) (Breiman, 1984) and ensembles of classification trees such as Random Forest (RF, Breiman, 2001; Vincenzi *et al*., 2011; Waske and Braun, 2009; Ghimire *et al*., 2012; Rodriguez-Galiano and Chica-Olmo, 2012) have shown great promise.

Artificial Neural Networks

The use of ANNs for remote sensing classification is motivated by the realization that the human brain is efficient at processing vast quantities of data from a variety of different sources, and that mathematical renderings of this approach may be useful for processing and interpreting image data. When applied to image classification, an ANN is a massively parallel distributed processor made up of simple processing units that acquires knowledge from its environment through a self-learning process, to adaptively construct linkages between the input data, such as satellite imagery features, and the output data, such as target cover classes (Rumelhart *et al*., 1986; Rigol-Sanchez *et al*., 2003). Notable ANNs are the Back-Propagating Multi-Layer Perceptron (MLP) (Wilkinson, 1997), Kohonen's Self-Organizing Feature Map (KSOFM) (Ji, 2000; Pal *et al*., 2005) and Fuzzy ARTMAP (Carpenter *et al*., 1992; Mannan *et al*., 1998). While these approaches vary in terms of their exact implementation, they all require training and classification to extract useful information from remotely sensed image data (Jensen, 2016). In the training stage, image data from locations whose attributes (classes) are known are passed as input to the network. The network uses this information in an iterative procedure that defines the rules that produce the best classification results. These rules are then used in the classification stage to assign features data to the training class of which it has the highest probability (fuzzy membership grade) of being a member.

The advantages to ANNs include their ability to: (1) perform more accurately when input data comprise many large data sets that are measured at different scales and the frequency distributions of which are non-normal; (2) learn and continuously update complex patterns, such as non-linear relationships between input data and output classes, as more data are provided in a changing environment; (3) provide, through generalization, robust solutions in the presence of incomplete or imprecise data; and (4) incorporate a priori knowledge and realistic physical constraints into the analysis (Atkinson and Tatnall, 1997; Pal and Mather, 2003; Rogan *et al*., 2008; Hansen, 2012; Jensen, 2016). However, the disadvantages to ANNs have limited their adoption to critical real world applications (Pal and Mather, 2003; Qiu and Jensen, 2004; Jensen, 2016). Arguably, the biggest drawback of ANNs is that they are a "black box" for interpretation (Rodriguez-Galiano *et al*., 2012; Gómez *et al*., 2016). Indeed, it has traditionally been difficult to explain in a meaningful way the process through which the output has been obtained, because the rules for image classification and interpretation learned by the network are not easily accessible or describable (Qiu and Jensen, 2004; Jensen, 2016). As a result, other classification methods with more readily understandable explanation capabilities tend to be used instead.

Support Vector Machines

Support Vector Machines (SVMs), a supervised non-parametric statistical learning technique for solving classification problems (Smola and Schoelkopf, 1998; Vapnik, 2000), show great potential for the classification of remotely sensed image data (Melgani and Bruzzone, 2004; Pal and Mather, 2005). SVMs solve a quadratic optimization problem to determine the optimal separating boundaries (hyperplanes) between two classes in multidimensional feature space (Foody and Mathur, 2004). SVMs do this by focusing only on the training data that lie at the edge of the class distributions (that is, the support vectors). When classes cannot be separated, the training data are projected into a higher-dimensional space using kernel techniques, where the new data distribution enables the better fitting of a linear hyperplane (Van der Linden *et al*., 2009). This procedure is repeated for each pair of classes to divide the data into the predefined number of classes. The rules for optimal class separation are then used to assign all image data into the predefined target classes. The basis of the SVM approach to classification is, therefore, the notion that only the training samples that lie on the class boundaries are necessary for discrimination (Foody and Mathur, 2004).

The advantage to using SVMs is their ability to outperform traditional classification methods when only small training data sets are available (Foody and Mathur, 2004; Waske and Benediktsson, 2007). The underlying principle that benefits SVMs is that the learning process is based on structural risk minimization (Van der Linden *et al*., 2009). Under this scheme, SVMs minimize classification error on unseen data without making any a priori assumptions on the statistical distribution of the data (Mountrakis *et al*., 2011). The major disadvantage to using SVMs concerns the selection of the most appropriate kernel function type and its associated parameters. Although many options exist, some kernel functions are unable to provide optimal SVM configuration for remote sensing applications (Mountrakis *et al*., 2011). This is important because inappropriate choices may lead to overfitting or oversmoothing, which may bear a significant negative influence on SVM performance and classification accuracy (Ustuner, 2015; Martins *et al*., 2016). In addition, SVMs are not optimized to deal with noisy data, such as the outlier effects frequently encountered in remote sensing data, the inclusion of which can dramatically reduce classifier performance (Mountrakis *et al*., 2011). Despite these issues, SVMs remain a popular option for land cover classification.

Classification based on Decision Trees

Decision Trees (DTs), supervised classification methods based on recursive binary partitions complying with a set of optimized rules, have become an attractive option for extracting discrete class information for land cover classification (Huang and Jensen, 1997 Friedl *et al*., 2002). A DT takes a set of features as input, and returns an output (that is, a decision) through a sequence of tests. Trees build the rule by recursive binary partitioning regions (nodes) that are increasingly homogeneous with respect to their class variable (Breiman, 1984). DT classifiers create multivariate models based on a set of decision rules defined by combinations of features and a set of linear discriminant functions that are applied at each test node (Champagne *et al*., 2014). Typically, after a sufficient number of training samples have been collected (Lu and Weng, 2007), a DT learning algorithm uses the training data to generate DTs that are then transformed into another representation of knowledge representation, called production rules. Because production rules are easy to understand, they can be examined by human experts and, with caution, can be edited directly (Jensen, 1986).

The use of DTs for image classification has various advantages, such as the ability to handle data at different measurement scales (Brown de Colstoun *et al*., 2003), non-normal (non-parametric) input data frequency distributions (Friedl and Brodley, 1997; Hansen *et al*., 1996), and non-linear relationships between input data and classes (Friedl *et al*., 2002). These are similar to those described for ANNs. However, in addition, DTs are easy to apply because fewer numbers of parameters need to be estimated (Friedl *et al*., 2010; Gómez *et al*., 2016); they provide a hierarchical structure that is transparent and easy to interpret (Hansen *et al*., 1996; Rodriguez-Galiano and Chica-Olmo, 2012); and they can be trained by creating rules and conditions directly from training data with little human interaction (Huang and Jensen, 1997). One of the most important features of DTs is that they can adapt when new learning data are provided and, because the output of the system itself, can be evaluated to examine how a conclusion was reached (Jensen, 2016). The disadvantage to using DTs include the sensitivity of DTs to feature spaces with high dimensionality (Pal and Mather, 2003), noisy data (Ghimire *et al*., 2012) and overfitting (Breiman, 1984). A better understanding of the influences on DT classification performance is an area of remote sensing that is currently undergoing further research (Hansen, 2012), and has led to the development of ensemble DT-based methods – such as the Random Forest (RF) method – that improve classification performance through the combination of many individual DTs.

Classification based on Random Forests

Random Forest (RF), an improved implementation of DT, is an ensemble-learning algorithm that combines multiple classifications of the same data to produce higher classification accuracies than other forms of DT (Cutler *et al*., 2007; Ghimire *et al*., 2012). RF works by fitting many DT-based classifications to a data set, and then uses a rule-based approach to combine the predictions from all the trees. During this process, individual trees are grown from differing subsets of training data using a process called "bagging". Bagging involves the

random subsampling (with replacement) of the original data for growing each tree. Generally, for each tree grown, two thirds of the training data are used to grow the tree, while the remaining one third are left unused (out-of-bag, or OOB) for later error assessment (Breiman, 2001). A classification is then fit to each bootstrap sample; however, at each node (split), only a small number of randomly selected predictor variables are used in the binary partitioning (Rodriguez-Galiano and Chica-Olmo, 2012). The splitting process continues until further subdivision no longer reduces the Gini index (Cutler *et al*., 2007). Each tree contributes to the assignment of the most frequent class to the input data with a single vote (Breiman, 1984; Rodriguez-Galiano and Chica-Olmo, 2012). The predicted class of an observation is calculated by the majority vote for that observation, with ties split randomly (Cutler *et al*., 2007).

The biggest advantage of RF is that it is potentially more accurate and robust than conventional parametric or DT machine-learning methods (Rodriguez-Galiano and Chica-Olmo, 2012). This is because the group of classifiers performs more accurately than any individual classifier, while circumventing classifier weaknesses (Breiman, 1984; Ghimire *et al*., 2010; Kotsiantis and Pintelas, 2004). In addition, RF requires the definition of only two parameters to generate the prediction model (that is, the number of classification trees desired and the number of prediction variables used in each node to grow the tree), and is therefore considered fairly straightforward to parameterize (Rodriguez-Galiano and Chica-Olmo, 2012). Further advantages result from the RF's use of bagging to make individual trees grow from training data subsets. Fully grown trees are used to compute accuracies and error rates for each observation using the OOB predictions, which are then averaged over all observations. Because the OOB observations are not used to fit the trees, the OOB estimates are essentially cross-validated accuracy estimates (Rodriguez-Galiano and Chica-Olmo, 2012). RF is also able to assess the importance of a single variable. For this purpose, RF switches one of the input variables, maintaining the rest constant, and measures the decrease in accuracy that has taken place by means of the OOB error (Breiman, 1984; Rodriguez-Galiano and Chica-Olmo, 2012). This is useful when it is important to know how each predictive variable influences the classification model (Ghimire *et al*., 2010; Gislason *et al*., 2006; Pal and Mather, 2005). The disadvantage to using RF is that with a large number of trees, it becomes less feasible to examine individual trees and understand their structure (Deschamps *et al*., 2012), thus leading to a black box nature that obfuscates decision rules (Gómez *et al*., 2016)

To conclude, a comprehensive synthesis of this body of work was recently completed by Khatami *et al*. (2016) thanks to a statistical meta-analysis of research on supervised pixel-based land cover image classification. Based on research published from 1998 to 2012 in five high-impact remote sensing journals, this study aimed to provide coherent guidance on the relative performances of different classification processes for generating land cover products. Unfortunately, it is not possible to identify a single best solution for all possible situations; however, various versions of RF or SVM tend to be preferred as single classifier, because of the maturity of these machine-learning classifiers and their suitability to handle very large features dimensions. Alternatively, more sophisticated processing strategies may also be designed on an ad hoc basis to combine different classifiers for different classification outputs, for instance, to proceed in a hierarchical way (in other words, operating a first discrimination between water, bare soil, urban, forest, cropland and others, and then a second classification to separate the various agricultural classes).

Postprocessing

Postprocessing operations can improve the classification output thanks to the possibility to apply various filtering techniques or to fuse various classification outputs. First, macroscopic errors can be corrected interactively, as they are clearly identified by systematic visual inspection. Basic filtering operators over sliding window of 3 pixels x 3 pixels or 5 pixels x 5 pixels, such as a majority filter removes the salt-and-pepper effect induced by pixel-based classification. More interestingly, such a majority filter could also be applied to pixel-based classification output using objects obtained by multispectral reflectance image segmentation, thus providing a much smoother land cover map.

Fusion techniques are required to merge outputs from the ensemble classifier. A single output map can be obtained by majority voting either where the ensemble chooses the class on which all classifiers agree (unanimous voting); at least one more than half of the classifiers agree (simple majority); or several classifiers agree (plurality voting). Weighted majority voting can be used when some classifiers are expected to perform better than others, or are weighted by the associated probability or membership of the classification output.

It is important to note that the various steps described above are largely interrelated, and each decision must consider the entire land cover mapping production chain to ensure that an appropriate solution is achieved.

2.4. CURRENT PRACTICES AND EXISTING LAND COVER DATA SETS

As an alternative to producing a new land cover map, the fusion of several existing land cover products may sometimes yield a better map – with reduced uncertainties and the desired classification legend – for specific applications (Jung *et al*., 2006). Compiling all available information on a single land cover or land use class from multiple sources, a global cropland map was derived (Thenkabail *et al*., 2009). Two other global maps were similarly derived to map cropland with an emphasis on water management: the Global Map of Rain-fed Cropland Areas (GMRCA) and the Global Irrigated Area Map (GIAM). However, the coarse spatial resolution (10 km) of these products does not meet the needs of operational applications and entail large uncertainties, especially with regard to complex farming systems such as those prevailing in Africa.

For their land cover information, national or regional programs often use imagery at resolutions ranging from 5 m to 30 m, or rely upon the integration of multisensor images. Most of these national land use land cover programs are listed in the appendix to this chapter, in particular when the output map was available. Some countries have established dedicated annual national crop type mapping based on satellite remote sensing, such as the 30-m Cropland Data Layer (CDL) of the United States of America, or Canada's 30-m Annual Crop Inventory. On the other hand, to manage the distribution of subsidies from the EU Common Agricultural Policy, most EU countries maintain a Land Parcel Identification System (LPIS) for farmer's declarations. Such annual information over most of the agriculture area proved highly efficient in supporting national land cover and cropland mapping, for example using the Sentinel-2 Agriculture system (see section 2.4.2 below).

Other efforts, such as Africover and the Global Land Cover Network (GLCN) program, have completed detailed land cover maps at the country level on the basis of visual interpretation of 30-m spatial resolution images rather than automatic classification. Therefore, they are updated less frequently. In addition, various global land mapping initiatives have recently delivered global land cover products, such as the GlobeLand30[12], the Globcover 2005 & 2009[13], the MODIS land cover[14] and, most recently, the ESA CCI Land Cover database[15].

Despite the availability of multiple land cover maps for a given country, it is not readily apparent which of these is the most useful for specific applications, nor how to combine them to provide an improved data set. The standards in terms of land cover map documentation, and then a systematic review of all currently available data sets, are given below.

12 http://glc30.tianditu.com/.
13 http://due.esrin.esa.int/page_globcover.php.
14 http://modis-land.gsfc.nasa.gov/landcover.html.
15 http://maps.elie.ucl.ac.be/CCI/viewer/.

2.4.1 Metadata, data policy and crowdsourcing

Metadata are data that provide information on other data. In the geospatial domain, these metadata are essential to make appropriate use of any raster or vector layer. ISO standard 19115-1:2014 defines the schema required for describing geographic information and services by means of metadata. Metadata should provide information on the identification, extent, quality, spatial and temporal aspects, content, spatial cartographic reference, portrayal, availability and distribution policy, as well as other properties of digital geographic data and services. When metadata records are formatted to a common standard, it facilitates the location and readability of the metadata by both humans and machines, enabling it to be automatically used for software data catalogues. More specifically for purposes of land cover information, ISO standard 19144-2:2012 introduced in section 2.1.1 above defines the LCML framework to fully document the land cover typology.

Open-source data policies are increasingly frequently applied to government data, thus allowing wider use of the available information and possibly collaborative efforts to keep them updated. While the open policies adopted in the United States of America with regard to GIS and EO paved the way, the EU INSPIRE Directive[16] now recommends that all EU Member States document, with precise metadata, all of the geospatial information produced by administration and governmental agencies and to make these data publicly available. Furthermore, creative commons licenses[17] are a very good solution for sharing geospatial data while assuring that the credit remains with the authors and, possibly, setting restrictions on the commercial use of the data in question.

More recently, collaborative initiatives for land cover data collection have also been rapidly developing. The Geo-Wiki platform[18] has proposed various crowdsourcing applications to compare global land cover maps or to collect reference data. An impressive amount of in situ data or photointerpreted samples can be quickly collected when such a platform is well designed and promoted. However, the scientific exploitation of crowdsourcing data still requires methodological development. A good example of open-source geospatial collaborative data collection is the Open Street Map initiative[19], which provides an open global baseline map that can inspire advanced land cover mapping initiatives, for example for designing in situ data collection.

2.4.2 Comprehensive review of existing land cover and cropland data sets

To assess the fitness of existing land cover maps to cropland mapping, Waldner *et al*. (2015) propose an analytical framework to assess the effectively available land cover data set for each country. This framework uses four criteria to quantitatively evaluate land cover maps with regard to cropland information: (1) thematic information relevant to cropland definition; (2) timeliness; (3) spatial resolution; and (4) confidence level. Based on this initial analysis, it has been possible to identify the priority areas for cropland mapping efforts at the global scale.

The identification and collection of national, regional and global land cover maps is a long-term enterprise, because of the variety of sources and producers involved and the many different data distribution policies. The elaboration of an exhaustive inventory and spatial database is a continuous effort, in light of the constant product releases, updates and changes made to policies on data access. Global, regional and national data sets were identified by means of systematic review during working sessions with key individual experts, literature reviews and web-based searches. While collecting these data sets, it was necessary to distinguish existing data sets from free-of-charge, publicly available data (see appendix); with regard to the former, a distribution policy is generally in place that prevents

16 Directive 2007/2/EC of the European Parliament and of the Council of 14 March 2007 establishing an Infrastructure for Spatial Information in the European Community (INSPIRE), available at http://eur-lex.europa.eu/legal-content/EN/ALL/?uri=CELEX:32007L0002 (last accessed 10 June 2017).

17 https://creativecommons.org/share-your-work/.

18 http://www.geo-wiki.org/.

19 https://www.openstreetmap.org/#map=5/51.500/-0.100.

their use, or it may be difficult to access the actual georeferenced data set (and not merely an image of the maps embedded in a website). Therefore, the general rule is that a data set that is not available is considered non-existent and is not considered in the review.

Global land cover products such as GLC2000, GlobCover 2005/2009, MODIS Land Cover, GlobeLand30, and ESA Climate Change Initiative (CCI) Land Cover products do not specifically target the agriculture component of the landscape. Poor semantic definition of the classes may prevent their use for agricultural applications; however, several other reasons exist to explain the poor accuracy of the cropland class in most of these products: (1) the heterogeneous and dynamic intrinsic nature of the world's agrosystems; (2) the spatial structure of the landscape (parcel size) and its crop diversity; (3) differences in crop cycles; (4) differences in cropping practices and calendars within the same class; (5) spectral similarity with other land cover classes; and (6) for optical-derived maps, persistent cloud coverage.

After the land cover maps have been comprehensively identified and collected, each criterion was quantified for each map and the multicriteria analysis was applied at the country level to identify the priority areas for cropland mapping. Three critical priority areas were identified: African countries (mainly in West Africa), Southeast Asia (especially Indonesia) and South America (Brazil). Other countries, such as Ethiopia, Madagascar, Mozambique and Pakistan, should also be strongly considered.

FIGURE 3. (A) PRIORITY INDICATOR MAP AND (B) ITS UPDATE TYPOLOGY.

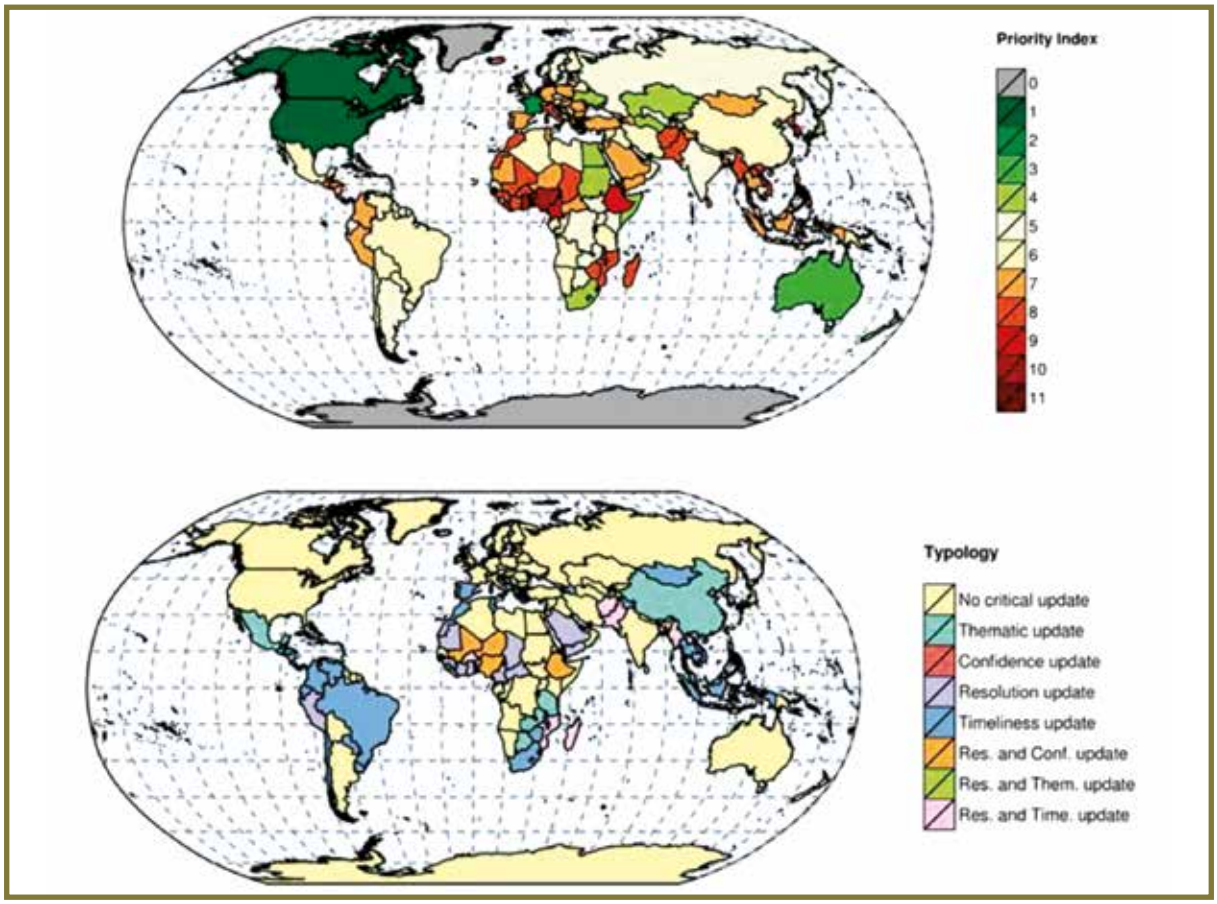

Areas with a high priority index (reddish shades) characterize priority areas for cropland mapping, whereas areas with low scores correspond to accurate and precise current maps (greenish shades). West Africa, Ethiopia and Southeast Asia (Indonesia) clearly appear as priority areas for cropland mapping (Waldner *et al.*, 2015).

Realizing the richness and the range of the quality of existing land cover maps, the study capitalized on previous works to harmonize them. Building on the priority analysis, a Unified Cropland Layer[20] is created by combining the fittest products. The Layer was assessed against available global validation data sets and yields an overall accuracy ranging from 84 to 95 percent, thus outperforming most global land cover maps.

2.4.3 Land cover change detection

In the literature (see for example Jung *et al*., 2006; McCallum *et al*., 2006), the discrepancy between several and/or successive land cover products is often explained by the incompatibility between land cover typologies and by current map accuracies, which are ranging from 70 percent to 85 percent for global land cover products. These overall accuracies make it impossible to derive any land cover change information from direct comparison of such products as the annual land cover change rate is significantly lower than the error rate in the land cover maps.

At coarse resolutions, significant year-to-year variations in land cover labels that are not associated with land cover change may be observed. This problem appears to be partly explained by the fact that several landscapes include mixtures of classes at a spatial resolution between 300 m and 500 m. Furthermore, year-to-year variability in vegetation phenology, and disturbances such as fire, drought, and insect infestation, make it rather difficult to attain a consistent annual characterization.

For these reasons, the Land Cover component of the ESA Climate Change Initiative has developed a strategy to decouple land cover mapping from land cover change detection. This allows delivering a unique and consistent time series of 24 annual global land cover maps from 1992 to 2015 at a resolution of 300 m, highlighting the changes occurring from one year to another and from one land cover to another (figure 3). This long set of maps was only possible with 1-km^2 observation from AVHRR, SPOT-Vegetation, and PROBA-V. At such a resolution, only major land cover changes are expected to be detected at an annual interval; however, the daily observation capabilities of these instruments allow for dealing with the interannual variability of the seasonality observed in different biomes. Once the land cover change is detected, imagery at a resolution of 300 m is used to delineate the change precisely.

20 http://maps.elie.ucl.ac.be/geoportail/.

FIGURE 4.

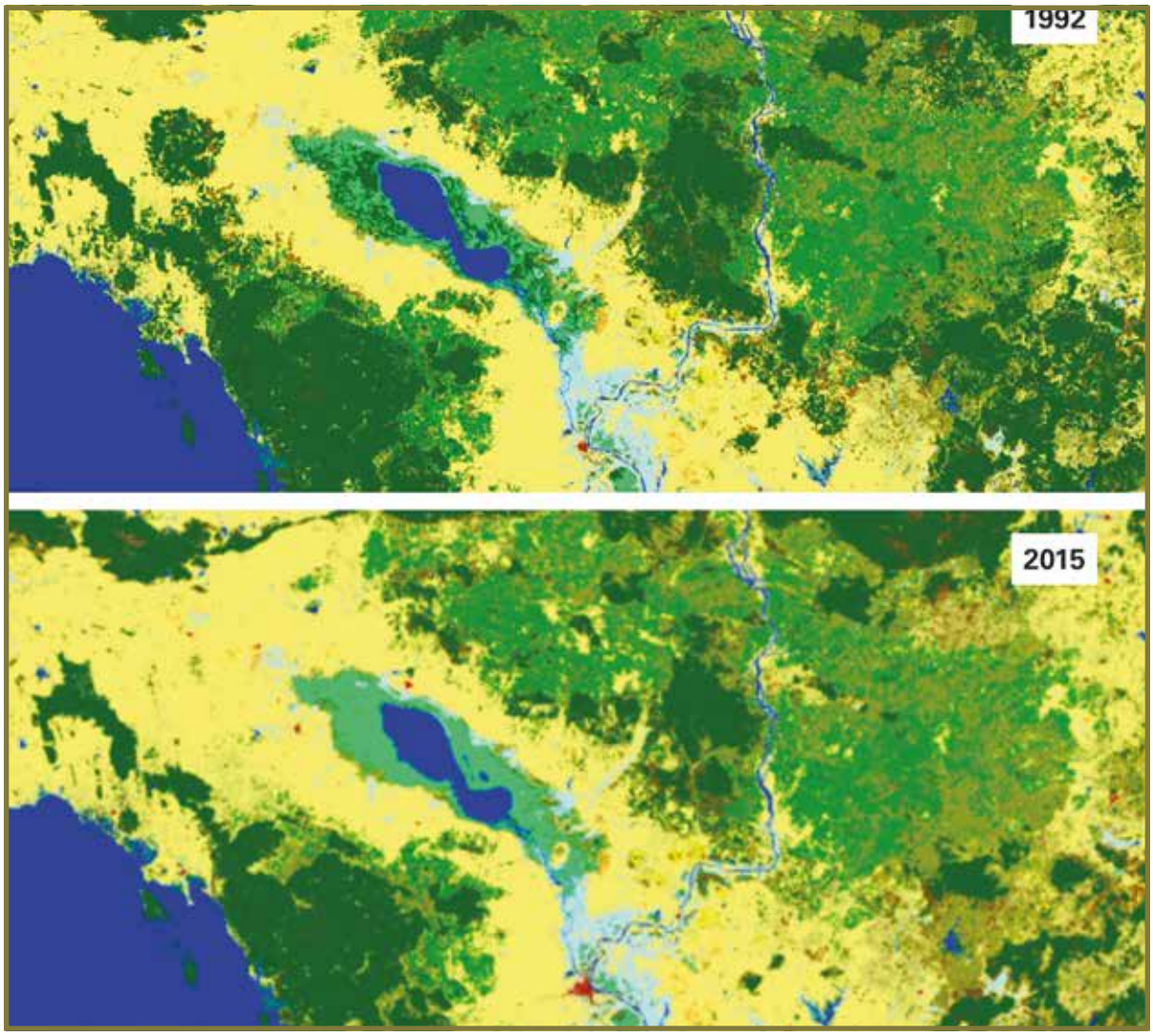

Land cover changes occurring from 1992 to 2015 in Cambodia as detected at 1 km and mapped at a resolution of 300 m, showing, among other phenomena, urban expansion (red) and large cropland (yellow) encroachments into the different forest types (shades of green). These maps, drawn from the CCI Land Cover project, and their full legends, are available at http://maps.elie.ucl.ac.be/CCI/viewer/.

Even using high-resolution land cover mapping outputs such as the CORINE Land Cover program, it is challenging to attain the expected product stability over time, and a specific procedure for change detection is required. Such instability across products clearly calls for the adoption of alternative approaches or alternative concepts.

Two main challenges must be addressed if land cover change detection is to be reliable. First, specific change detection methods must be developed and extensively tested to capture the very low percentage of annual land cover change (the fastest cropland extension ever observed in Brazil and Argentina was below 4 percent per year and in Africa, it remains mostly below 1 percent). To date, a method validated for various agro-ecosystems is not currently available for annual cropland change detection. However, several change detection methods – either object-based (for instance, Desclée *et al.*, 2006; Ernst *et al.*, 2013) or pixel-based (for instance, Hansen *et al.*, 2013) – have reached a good stage of maturity and are able to deliver accurate information on forest change, mainly but not exclusively relating to agricultural clearings. Most of these methods directly compare reflectance values or sets of vegetation index values to identify the land surface change, rather than classifying the land cover. In addition, precise change detection for agricultural lands was hampered by the lack of dense time series of high-resolution

data. The recent availability of Sentinel-1, Sentinel-2 and Landsat-8 time series and their long-term continuity call for new developments of annual cropland change detection methods.

2.5. ONGOING MAPPING INITIATIVES AT MULTINATIONAL OR GLOBAL SCALE

Several international initiatives are currently seeking to attain breakthroughs in the field of land cover mapping. This section introduces three of these initiatives, focusing specifically on agricultural lands.

2.5.1. Global Cropland

The possibility provided by Google Engine to access high-power computing facilities and the entire Landsat archive online paves the way for major initiatives to be launched, such as the Global Food Security Analysis-Support Data at 30 meters (GFSAD30) project, led by USGS (Thenkabail *et al*., 2012). From Landsat and MODIS archives, classification methods based on temporal analysis of the signal aim to complete a 30-m global cropland map from a multi-source data set (figure 4). A mobile application and access to their ready-to-use data set opens the way to collaborative efforts.

FIGURE 5.

Current (March 2017) achievement of the USGS GFSAD30 project to deliver croplands at a resolution of 30 m (https://croplands.org/).

2.5.2 The Sentinel-2 for Agriculture system

Driven by the information needs defined by major international stakeholders and supported by ESA, the ESA Sentinel-2 for Agriculture (Sen2-Agri) project, led by the *Université catholique de Louvain* (Bontemps *et al*., 2016) has developed and released an open-source processing system to automatically download all Sentinel-2 and Landsat-8 images captured during the growing season to deliver in near real-time a suite of four different nationwide products at a resolution of 10 m: (i) monthly cloud-free temporal syntheses of surface reflectance values in the ten Sentinel-2 bands, at resolutions of either 10 or 20 m according to the band; (ii) monthly cropland masks at a resolution of 10 m delivered during the agricultural season(s) to map the annual cropland; (iii) crop type maps and early area indicators for five main crop types, delivered at mid- and end-season; (iv) vegetation status describing crop development on a seven-day basis whenever cloud-free observation is available –. The latter consists of a set of maps of indicators including the NDVI, the Leaf Area Index (LAI) and phenology metrics derived from the NDVI time profiles.

This Sen2-Agri system has been successfully demonstrated at national scale in Ukraine, Mali (see text box above) and South Africa, and over nine additional sites around the world. Its nominal operation requires both Sentinel-2 A and B satellites in orbit in addition to the Landsat-8, to enhance the observation frequency. While the cropland mask can be produced without *in situ* data, the capacity to collect quality-controlled *in situ* data in a timely manner was found to be critical to the production of crop-type maps in the course of the growing season. Released in June 2017 to the public as an operational production system, the Sen2-Agri system is expected to serve as a key source of remote sensing products for various applications in agriculture monitoring, for precise stratification of the sampling design and the compilation of early crop statistics (Defourny *et al*., 2016). The specificity of this production system lies in its near real-time and automated capabilities for the scalable processing of image time series that are remotely sensed throughout the season at a resolution of 10 m for entire national territories.

FIGURE 6.

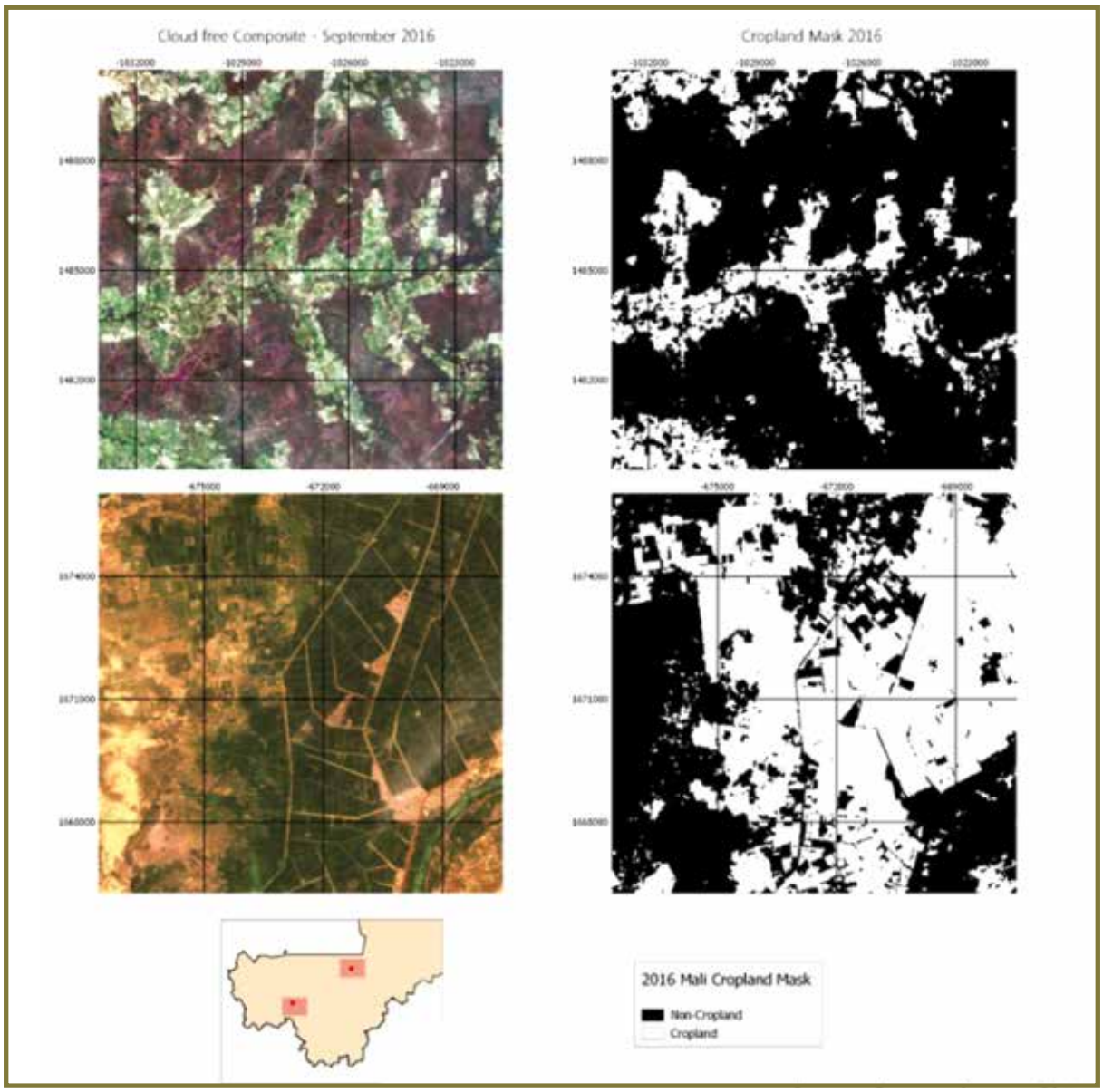

Sen2Agri 10-m natural colour composites (left) and corresponding cropland maps (right) for the 2016 growing season in Mali, as automatically derived in September from Sentinel-2A time series: upper zoom in the region of Kita, and lower zoom in the rice production area of the Office du Niger.

2.5.3 Irrigated rice mapping

The mapping of irrigated rice systems has been an active research field, in particular using Synthetic Aperture Radar (SAR) observations. Rice has a highly specific spectrotemporal signature, such that it is usually not addressed in a land cover mapping perspective but rather in a context of rice monitoring. With the advent of several operational SAR systems in orbit that are capable of providing dense and consistent time series, such as those from PALSAR, Radarsat-2 or Sentinel-1a and Sentinel-1b, the mapping of irrigated land is now mature. For example, the International Rice Research Institute (IRRI) has been working very actively to detect the planting dates and the planted area for the entire Philippines (PRISM project), while Asia-Rice, supported by JAXA, and GEO-Rice, supported by ESA, are other two ambitious activities currently taking place in the context of the GEOGLAM.

PERSPECTIVES

With the advent of the fleet of Sentinel satellites (Sentinel-1a and Sentinel-1b, Sentinel-2a and Sentinel-2b) providing (often) free global-level Earth Observation at resolutions ranging from 10 to 20 m for the entire world on a regular basis (five days revisit time for Sentinel-2 and 12 days for Sentinel-1), EO is entering a new era of fully operational applications that are also sustainable in the long term. This is particularly useful for regular nationwide land cover mapping initiatives for the purposes of agricultural landscape stratification. It can be predicted that other disciplines, such as statistics and agro-economics, will soon clearly identify the benefits of this evolution and make appropriate adjustments in terms of information flows.

This seamless revolution concerns not only the availability of space technology and related data policies, but also the cloud computing infrastructure and the methodological progress linked to machine learning and artificial intelligence algorithms. Even field data collection strategies take advantage of IT evolutions such as crowdsourcing initiatives, mobile applications and the growth in the use of UAVs.

Moving away from the static perspective of a map, time series of annual maps allow for the yearly consolidation of their quality and enhancement of their capacity for change detection. The map will increasingly become a georeferenced land cover land use database, continuously updated with the flow of incoming satellite observation. In the context of agricultural statistics, both the increasing computing capacities and the enhanced data flows directly from the field make a strong contribution to the timeliness and cost-effectiveness of land cover and cropland map production.

This evolution is also considered in the context of policy-making. Land cover is deemed a key source of information, to be used by countries for reporting on the Sustainable Development Goal (SDG) indicators. Similarly, it is worth mentioning that land cover and land use classifications are crucial components of the international Central Framework of System of Environmental and Economic Accounting (SEEA) standard, and even more so of its satellite accounting system for Agriculture, Forestry and Fisheries (SEEA AFF), jointly developed by FAO and the UN Statistics Division (UNSD). SEEA AFF provides a statistical framework to report on agricultural statistics and develop related agri-environmental indicators, and the SEEA land cover classification itself is based on the Land Cover Meta Language (LCML) classifiers.

Beyond the land cover use for sampling stratification, the development of SEEA-compliant land cover products at a national scale should ensure a reporting of agri-environmental statistics that is inherently coherent with the System of National Accounting, and the development of agricultural policies that better capture the environmental aspects of agricultural activities. The necessary close links between policy-making processes, agricultural statistics, indicators and land cover information are key arguments in enhancing the national capacity for operational and efficient land mapping on the basis of remote sensing data.

2.6. REFERENCES

Abdulaziz, A.M., Hurtado, J.M. & Al- Douri, R. 2009. Application of Multitemporal Landsat Data to Monitor Land Cover Changes in the Eastern Nile Delta Region, Egypt. *International Journal of Remote Sensing*, 30(11): 2977–96.

Abedi, M., Gholam-Hossain, N. & Fathianpour, N. 2013. Fuzzy Outranking Approach: A Knowledge-Driven Method for Mineral Prospectivity Mapping. *International Journal of Applied Earth Observation and Geoinformation*, 21: 556–67.

Al-Anazi, A.F. & Gates, I.D. 2010. Support Vector Regression for Porosity Prediction in a Heterogeneous Reservoir: A Comparative Study. *Computers & Geosciences*, 36(12): 1494–1503.

Atkinson, P.M. & Tatnall, A.R.L. 1997. Introduction Neural Networks in Remote Sensing. *International Journal of Remote Sensing*, 18(4): 699–709.

Baatz, M. & Schäpe, A. 2000. Multiresolution segmentation - an optimization approach for high quality multi-scale image segmentation. In: Strobl, J., Blaschke, T. and Griesebner, G. (eds), *Angewandte Geographische Informationsverarbeitung XII* (pp. 12–23), Wichmann-Verlag: Heidelberg.

Bagan, H., Kinoshita, T. & Yamagata, Y. 2012. Combination of AVNIR-2, PALSAR, and Polarimetric Parameters for Land Cover Classification. *IEEE Transactions on Geoscience and Remote Sensing*, 50(4): 1318–28.

Bagan, H. & Yamagata, Y. 2010. Improved Subspace Classification Method for Multispectral Remote Sensing Image Classification. *Photogrammetric Engineering and Remote Sensing*, 76(11): 1239–51.

Beltran, C.M. & Calera Belmonte, A. 2001. Irrigated Crop Area Estimation Using Landsat TM Imagery in La Mancha, Spain. *Photogrammetric Engineering and Remote Sensing*, 67(10): 1177–1184.

Bhatta, B. 2008. *Remote Sensing and GIS*. Oxford University Press: Oxford, UK.

Bontemps, S., Arias, M. *et al.* 2015. Building a Data Set over 12 Globally Distributed Sites to Support the Development of Agriculture Monitoring Applications with Sentinel-2. *Remote Sensing*, 7(9): 16062–16090.

Bontemps, S., Herold, M., Kooistra, L., van Groenestijn, A., Hartley, A., Arino, O., Moreau, I. & Defourny, P. 2012. Revisiting land cover observation to address the needs of the climate modeling community. *Biogeosciences*, 9(6): 2145–2157.

Breiman, L. 1984. *Classification and Regression Trees*. CRC Press: Boca Raton, FL, USA.

Breiman, L. 2001. "Random Forests." *Machine Learning*, 45(1): 5–32.

Brown de Colstoun, E.C., Story, M.H., Thompson, C., Commisso, K., Smith, T.G. & Irons, J.R. 2003. National Park Vegetation Mapping Using Multitemporal Landsat 7 Data and a Decision Tree Classifier. *Remote Sensing of Environment*, 85(3): 316–27.

Carpenter, G.A., Grossberg, S., Markuzon, N., Reynolds, J.H. & Rosen, D.B. 1992. Fuzzy ARTMAP: A Neural Network Architecture for Incremental Supervised Learning of Analog Multidimensional Maps. *IEEE Transactions on Neural Networks*, (35): 698–713. doi

Carreiras, J.M.B., Pereira, J.M.C., Campagnolo, M.L. & Shimabukuro, Y.E. 2006. Assessing the Extent of Agriculture/Pasture and Secondary Succession Forest in the Brazilian Legal Amazon Using SPOT VEGETATION Data. *Remote Sensing of Environment*, 101(3 2006): 283–98.

Champagne, C., McNairn, H., Daneshfar, B. & Shang, J.L. 2014. A Bootstrap Method for Assessing Classification Accuracy and Confidence for Agricultural Land Use Mapping in Canada. *International Journal of Applied Earth Observation and Geoinformation*, 29: 44–52.

Chen, J., Chen, J., Liao, A., Cao, X., Chen, L., Chen, X., He, C., Han, G., Peng, S., Lu, M. *et al.* 2015. Global land cover mapping at 30m resolution: A POK-based operational approach. *ISPRS Journal of Photogrammetry and Remote Sensing*, 103:7–27.

Chen, C. & Mcnairn, H. 2006. A Neural Network Integrated Approach for Rice Crop Monitoring. *International Journal of Remote Sensing*, 27(72006): 1367–93.

Congalton, R.G., Balogh, M., Bell, C., Green, K., Milliken, J.A. & Ottman, R. 1998. Mapping and Monitoring Agricultural Crops and Other Land Cover in the Lower Colorado River Basin. *Photogrammetric Engineering and Remote Sensing*, 64(11): 1107–1114.

Cortes, C. & Vapnik, V. 1995. Support-Vector Networks. *Machine Learning*, 20(3): 273–297.

Cutler, D.R., Edwards, T.C., Beard, K.B., Cutler, A., Hess, K.T., Gibson, J. & Lawler, J.J. 2007. Random Forests for Classification in Ecology. *Ecology*, 88(11 2007): 2783–92.

Davidson, A.M. 2016. *Review of satellite image classification methods*. Internal document. Agriculture and Agri-Food Canada: Ottawa.

DeFries, R.S., Hansen, M.C. & Townshend, J.R.G. 2000. Global Continuous Fields of Vegetation Characteristics: A Linear Mixture Model Applied to Multi-Year 8 Km AVHRR Data. *International Journal of Remote Sensing*, 21(6–7 January 1, 2000): 1389–1414.

DeFries, R.S. & Chan, J.C.W. 2000. Multiple Criteria for Evaluating Machine Learning Algorithms for Land Cover Classification from Satellite Data. *Remote Sensing of Environment*, 74(3 2000): 503–15.

Defourny, P. & and Bontemps S. 2012a. Revisiting Land-Cover Mapping Concepts. In Giri, C. (ed.), *Remote Sensing of Land Use and Land Cover* (pp. 45–64), CRC Press: Boca Raton, FL, USA.

Defourny, P., Bontemps, S., Mayaux, P., Herold, M. & Bontemps, S. 2012b. Global Land-Cover Map Validation Experiences: Toward the Characterization of Uncertainty. In Giri, C. (ed.), *Remote Sensing of Land Use and Land Cover* (pp. 207-224), CRC Press: Boca Raton, FL, USA.

Defourny, P., Vancutsem, C., Bicheron, P., Brockmann, C., Nino, F., Schouten, L., Leroy, M., *et al.* 2006. GLOBCOVER: a 300 m global land cover product for 2005 using Envisat MERIS time series. In Kerle, N. & Skidmore, A., *Proceedings of the ISPRS Commission VII mid-term symposium, Remote sensing: from pixels to processes* (pp. 8–11).

Defourny, P., Bontemps, S., Bellemans, N., Cara, C. *et al.* 2016. Nationwide demonstration cases of Sentinel-2 satellite exploitation towards early crop area indicator. Paper prepared for the Seventh International Conference on Agriculture Statistics (ICAS VII), 26–28 October 2016. Rome.

Denègre, J. 2013. *Thematic Mapping From Satellite Imagery: A Guidebook*. Elsevier.

Deschamps, B., McNairn, H., Shang, J. & Jiao, X. 2012. Towards Operational Radar-Only Crop Type Classification: Comparison of a Traditional Decision Tree with a Random Forest Classifier. *Canadian Journal of Remote Sensing*, 38(1): 60–68.

Desclée, B., Bogaert, P. & Defourny, P. 2006. Forest change detection by statistical object-based method. *Remote Sensing of Environment*, 102: 1–11.

DiGregorio, A. 2013. *A cropland nomenclature conform to the FAO Land Cover Meta-Language*. SIGMA Technical Report.

Di Gregorio, A. & Leonardi, U. 2016. *Land Cover Classification System: User manual. Software version 3*. Available at: http://www.fao.org/3/ai5428e.pdf. Last accessed on 10 June 2017.

Duveiller G., Defourny P., Desclée B. & Mayaux P. 2008. Deforestation in Central Africa: estimates at regional, national and landscape levels by advanced processing of systematically-distributed Landsat extracts. *Remote Sensing of Environment*, 112: 1969–1981.

Duveiller, G. & Defourny, P. 2010. A conceptual framework to define the spatial resolution requirements for agricultural monitoring using remote sensing. *Remote Sensing of Environment*, 114: 2637–2650.

Duro, D.C., Franklin, S.E. & Dubé, M.G. 2012. A Comparison of Pixel-Based and Object-Based Image Analysis with Selected Machine Learning Algorithms for the Classification of Agricultural Landscapes Using SPOT-5 HRG Imagery. *Remote Sensing of Environment* 118: 259–72.

Enderle, W. & Weih, J.C. 2005. Integrating Supervised and Unsupervised Classification Methods to Develop a More Accurate Land Cover Classification. *Journal of the Arkansas Academy of Science*, 59: 65–73.

Ernst, C., Mayaux, P., Verhegghen, A., Bodart, C., Musampa, C. & Defourny, P. 2013. National forest cover change in Congo Basin : deforestation, reforestation, degradation and regeneration for the years 1990, 2000 and 2005. *Global Change Biology*, (194): 1173-1187.

Foody, G.M. 2008. RVM- based Multi- class Classification of Remotely Sensed Data. *International Journal of Remote Sensing*, 29(6): 1817–23.

———. Supervised Image Classification by MLP and RBF Neural Networks with and without an Exhaustively Defined Set of Classes. 2004. *International Journal of Remote Sensing*, 25(15): 3091–3104.

Foody, G.M., Boyd D.S. & Sanchez- Hernandez, C. 2007. Mapping a Specific Class with an Ensemble of Classifiers. *International Journal of Remote Sensing*, 28(8): 1733–46.

Foody, G.M. & Mathur, A. 2004. A Relative Evaluation of Multiclass Image Classification by Support Vector Machines. *IEEE Transactions on Geoscience and Remote Sensing*, 42(6): 1335–43.

Friedl, M.A., McIver, D.K., Hodges, J.C.F., Zhang, X.Y., Muchoney, D., Strahler, A.H., Woodcock, C.E. *et al*. Global Land Cover Mapping from MODIS: Algorithms and Early Results. *Remote Sensing of Environment*, 83(1–2): 287–302.

Friedl, M.A. & Brodley, C.E. 1997. Decision Tree Classification of Land Cover from Remotely Sensed Data. *Remote Sensing of Environment*, 61(): 399–409.

Friedl, M.A., Sulla-Menashe, D., Tan, B., Schneider, A., Ramankutty, N., Sibley, A. & Huang, X. 2010. MODIS Collection 5 Global Land Cover: Algorithm Refinements and Characterization of New Datasets. *Remote Sensing of Environment*, 114(1): 168–82.

Fritz, F., Se, L. & Mc Callum, I. 2015. Mapping global cropland and field size. *Global Change Biology*, 21: 1980–1992.

Frizzelle, B.G. & Moody, A. 2001. Mapping Continuous Distributions of Land Cover. *Photogrammetric Engineering and Remote Sensing*, 67(6): 693–705.

Ghimire, B., Rogan, J. & Miller, J. 2010. Contextual Land-Cover Classification: Incorporating Spatial Dependence in Land-Cover Classification Models Using Random Forests and the Getis Statistic. *Remote Sensing Letters* 1(1): 45–54.

Ghimire, B., Rogan, J., Rodríguez Galiano, V., Panday, P. & Neeti, N. An Evaluation of Bagging, Boosting, and Random Forests for Land-Cover Classification in Cape Cod, Massachusetts, USA. *GIScience & Remote Sensing*, 49(5): 623–643.

Giri, C.P. 2012. *Remote Sensing of Land Use and Land Cover: Principles and Applications*. CRC Press: Boca Raton, FL, USA.

Gislason, P.O., Benediktsson, J.A. & Sveinsson, J.R. 2006. Random Forests for Land Cover Classification. *Pattern Recognition in Remote Sensing (PRRS 2004)* 27(4): 294–300.

Glanz, H., Carvalho, L., Sulla-Menashe, D. & Friedl, M.A. 2014. A Parametric Model for Classifying Land Cover and Evaluating Training Data Based on Multi-Temporal Remote Sensing Data. *ISPRS Journal of Photogrammetry and Remote Sensing*, 97: 219–28.

Gómez, C., White, J.C. & Wulder, M.A. 2016. Optical Remotely Sensed Time Series Data for Land Cover Classification: A Review. *ISPRS Journal of Photogrammetry and Remote Sensing*, 116: 55–72.

Hansen, M., Dubayah, R. & Defries, R. 1996. Classification Trees: An Alternative to Traditional Land Cover Classifiers. *International Journal of Remote Sensing*, 17(5): 1075–81.

Hansen, M. 2012. "Classification Trees and Mixed Pixel Training Data." In Giri, C. (ed.), *Remote Sensing of Land Use and Land Cover* (pp. 127–36), CRC Press: Boca Raton, FL, USA.

Huang, C., Davis, L.S. & Townshend, J.R.G. 2002. An Assessment of Support Vector Machines for Land Cover Classification. *International Journal of Remote Sensing* 23(4): 725–49.

Huang, X. & Jensen, J.R. 1997. A Machine-Learning Approach to Automated Knowledge-Base Building for Remote Sensing Image Analysis with GIS Data. *Photogrammetric Engineering and Remote Sensing*, 63(10): 1185–94.

Inglada, J., Arias, M., Tardy, B., Hagolle, O., Valero, S., Morin, D., Dedieu, G., Sepulcre Canto, G., Bontemps, S., Defourny, P. & Koetz, B. 2015. Assessment of an Operational System for Crop Type Map Production Using High Temporal and Spatial Resolution Satellite Optical Imagery. *Remote Sensing*, 7(9): 12356–12379.

Joint Experiment of Crop Assessment and Monitoring (JECAM). 2014. JECAM Guidelines: Definition of the Minimum Earth Observation Dataset Requirements. JECAM Standards documents. Available at http://www.jecam.org/JECAM_EO_Guidelines_v1_0.pdf. Accessed on 10 June 2017.Jensen, J.R. 1986. "Introductory Digital Image Processing: A Remote Sensing Perspective". SciTech Connect, University of South Carolina, Columbus, USA. 1 January 1986. Available at: http://www.osti.gov/scitech/biblio/5166368. Last accessed on 10 June 2017.

Jensen, J.R. 2016. *Introductory Digital Image Processing: A Remote Sensing Perspective*, 4th ed. Pearson: Glenview, IL, USA.

Ji, C.Y. 2000. Land-Use Classification of Remotely Sensed Data Using Kohonen Self-Organizing Feature Map Neural Networks. *Photogrammetric Engineering and Remote Sensing*, 66(12): 1451–60.

Jones, H.G. & Vaughan, R.A. 2010. *Remote Sensing of Vegetation: Principles, Techniques, and Applications*. Oxford University Press: Oxford, UK – New York, USA.

Kamusoko, C. & Aniya, M. 2009. Hybrid Classification of Landsat Data and GIS for Land Use/Cover Change Analysis of the Bindura District, Zimbabwe. *International Journal of Remote Sensing*, 30(1 2009): 97–115.

Khatami, R., Mountrakis, G. & Stehman, S.V. 2016. A Meta-Analysis of Remote Sensing Research on Supervised Pixel-Based Land-Cover Image Classification Processes: General Guidelines for Practitioners and Future Research. *Remote Sensing of Environment*, 177: 89–100.

Kotsiantis, S.B. & Pintelas, P.E. 2004. Combining Bagging and Boosting. *International Journal of Computational Intelligence*, 1(4): 324–333.

Kumar, L., Priyakant, S., Brown, J.F., Ramsey, R.D., Rigge, M., Stam, C.A., Hernandez, A.J., Hunt Jr., E.R. & Reeves, M.C. 2016. Characterization, Mapping and Monitoring of Rangelands: Methods and Approaches. In Thenkabail, P.S. (ed.), *Land Resources Monitoring, Modeling, and Mapping with Remote Sensing,* vol. 2 (pp. 309–350). Remote Sensing Handbook series. CRC Press: Boca Raton, FL, USA.

Laba, M., Smith, S.D. & Degloria, S.D. 1997. Landsat-Based Land Cover Mapping in the Lower Yuna River Watershed in the Dominican Republic. *International Journal of Remote Sensing*, 18(14): 3011–25.

Lambert, M.-J., Waldner, F. & Defourny, P. 2016. Cropland Mapping over Sahelian and Sudanian Agrosystems: A Knowledge-Based Approach Using PROBA-V Time Series at 100-m. *Remote Sensing*, 8(3): 1–23.

Latham, J. & Rosati, I. 2016. *Land Information in the Context of Agricultural Statistics*. GSARS Technical Report GO-15-2016. Available at: http://gsars.org/wp-content/uploads/2016/08/TR_Information-on-Land-in-the-Context-of-Ag-Statistics-180816.pdf. Last accessed on 10 June 2017.

Liu, C., Frazier, P. & Kumar, L. 2007. Comparative assessment of the measures of thematic classification accuracy. *Remote Sensing of Environment*, 107(4): 606–616.

Lu, D. & Weng, Q. 2007. A Survey of Image Classification Methods and Techniques for Improving Classification Performance. *International Journal of Remote Sensing*, 28(5): 823–70.

Mannan, B., Roy, J. & Ray, A.K. 1998. Fuzzy ARTMAP Supervised Classification of Multi-Spectral Remotely-Sensed Images. *International Journal of Remote Sensing*, 19(4): 767–74.

Matton, N., Sepulcre Canto, G., Waldner, F., Valero, S., Morin, D., Inglada, J., Arias, M., Bontemps, S., Koetz, B. & Defourny, P. 2015. An Automated Method for Annual Cropland Mapping along the Season for Various Globally-Distributed Agrosystems Using High Spatial and Temporal Resolution Time Series. *Remote Sensing*, 7(10): 13208–13232.

Martins, S., Bernardo, N., Ogashawara, I. & Alcantara, E. 2016. Support Vector Machine Algorithm Optimal Parameterization for Change Detection Mapping in Funil Hydroelectric Reservoir (Rio de Janeiro State, Brazil). *Modeling Earth Systems and Environment*, 2(3 2016).

Melgani, F. & Bruzzone, L. 2004. Classification of Hyperspectral Remote Sensing Images with Support Vector Machines. *IEEE Transactions on Geoscience and Remote Sensing*, 42(8): 1778–90.

Mountrakis, G., Watts, R., Luo, L. & Wang, J. 2009. Developing Collaborative Classifiers Using an Expert-Based Model. *Photogrammetric Engineering and Remote Sensing*, 75(7): 831–43.

Mountrakis, G., Im, J. & Ogole, C. Support Vector Machines in Remote Sensing: A Review. *ISPRS Journal of Photogrammetry and Remote Sensing*, 66(3): 247–59.

Pal, M. & Mather, P.M. 2005. Support Vector Machines for Classification in Remote Sensing. *International Journal of Remote Sensing*, 26(5): 1007–1011.

Pal, M. & Mather, P.M. 2006. Some Issues in the Classification of DAIS Hyperspectral Data. *International Journal of Remote Sensing*, 27(14): 2895–2916.

Pal, M. & Mather, P.M. 2003. An Assessment of the Effectiveness of Decision Tree Methods for Land Cover Classification. *Remote Sensing of Environment*, 86(4 August 30, 2003): 554–65.

Pal, N.R., Laha, A. & Das, J. 2005. Designing Fuzzy Rule Based Classifier Using Self□organizing Feature Map for Analysis of Multispectral Satellite Images. *International Journal of Remote Sensing*, 26(10): 2219–40.

Qiu, F. & Jensen, J.R. 2004. Opening the Black Box of Neural Networks for Remote Sensing Image Classification. *International Journal of Remote Sensing*, 25(9): 1749–68.

Radoux, J. & Defourny, P. 2008. Quality assessment of segmentation results devoted to object-based classification. In Blaschke, T., Lang, S. & Hay, G.J. (eds), *Object-Based Image Analysis : Spatial concepts for knowledge driven remote sensing applications* (pp. 257–271), Springer-Verlag: Berlin – Heidelberg.

Rigol-Sanchez, J.P., Chica-Olmo, M. & Abarca-Hernandez, F. 2003. Artificial Neural Networks as a Tool for Mineral Potential Mapping with GIS. *International Journal of Remote Sensing*, 24(5): 1151–56.

Rodriguez-Galiano, V. & Chica-Olmo, M. 2012. Land Cover Change Analysis of a Mediterranean Area in Spain Using Different Sources of Data: Multi-Seasonal Landsat Images, Land Surface Temperature, Digital Terrain Models and Texture. *Applied Geography*, 35(1–2): 208–18.

Rogan, J., Franklin, J., Stow, D., Miller, J., Woodcock, C. & Roberts, D. 2008. Mapping Land-Cover Modifications over Large Areas: A Comparison of Machine Learning Algorithms. *Earth Observations for Terrestrial Biodiversity and Ecosystems Special Issue*, 112(5): 2272–83.

Rumelhart, D.E., Hinton, G.E. & Williams, R.J. 1986. Learning Representations by Back-Propagating Errors. *Nature*, 323(6088): 533–36.

Sluiter, R. & Pebesma, E.J. 2010. Comparing Techniques for Vegetation Classification Using Multi- and Hyperspectral Images and Ancillary Environmental Data. *International Journal of Remote Sensing*, 31(23): 6143–61.

Smola, A. & Schoelkopf, B. 1998. A Tutorial on Support Vector Regression. NeuroCOLT2 Technical Report Series, NC2-TR-1998-030. Available at: http://citeseer. ist. psu. edu/smola98tutorial. html. Last accessed on 10 June 2017.

Thenkabail, P.S., Knox, J.W., Ozdogan, M., Gumma, M.K., Congalton, R.G., Wu, Z., Milesi, C., Finkral, A., Marshall, M., Mariotto, I., You, S. Giri, C. & Nagler, P. 2012. Assessing future risks to agricultural productivity, water resources and food security: how can remote sensing help?. *Photogrammetric Engineering and Remote Sensing*, *August 2012 Special Issue on Global Croplands: Highlight Article*, 78(8): 773–782.

Ustuner, M. 2015. Application of Support Vector Machines for Landuse Classification Using High-Resolution RapidEye Images: A Sensitivity Analysis. *European Journal of Remote Sensing*:403.

Valero, S., Morin, D., Inglada, J., Sepulcre Canto, G., Arias, M., Hagolle, O., Dedieu, G., Bontemps, S., Defourny, P. & Koetz, B. Production of a Dynamic Cropland Mask by Processing Remote Sensing Image Series at High Temporal and Spatial Resolutions. *Remote Sensing*, 8(55): 1–21.

Van der Linden, S., Rabe, A., Okujeni, A. & Hostert, P. 2009. *Image SVM Classification, Manual for Application: Image SVM Version 2*. Available at: http://dev.geo.hu-berlin.de/trac/enmap-box/export/8/enmap-box/tags/Save20150115/SourceCode/applications/imageSVM/_help/svc_manual.pdf. Last accessed on 10 June 2017. Publication of the Humboldt-Universität zu Berlin, Germany.

Vapnik, V.N. 2000. *The Nature of Statistical Learning Theory*. 2nd edition. Statistics for Engineering and Information Science. Springer: New York, USA.

Vincenzi, S., Zucchetta, M., Franzoi, P., Pellizzato, M. Pranovi, F., De Leo, G.A. & Torricelli, P. 2011. Application of a Random Forest Algorithm to Predict Spatial Distribution of the Potential Yield of Ruditapes Philippinarum in the Venice Lagoon, Italy. *Ecological Modelling*, 222(8): 1471–1478.

Waldner, F., Fritz, S., Lamarche, C., Bontemps, S. & Defourny, P. 2016. A Unified Cropland Layer at 250 m for Global Agriculture Monitoring. *Data*, 1(1), no. 3: 1–13.

Waldner, F., De Abelleyra, D., Veron, S.R., Zhang, M., Wu, B., Plotnikov, D., Bartalev, S., Lavreniuk, M., Skakun, S., Kussul, N., Le Maire, G., Dupuy, S., Jarvis, I, & Defourny, P. 2016. Towards a set of agrosystem-specific cropland mapping methods to address the global cropland diversity. *International Journal of Remote Sensing*, 37(14): 3196–3231.

Waldner, F., Fritz, S., Di Gregorio, A. & Defourny, P. 2015. Mapping Priorities to Focus Cropland Mapping Activities: Fitness Assessment of Existing Global, Regional and National Cropland Maps. *Remote Sensing*, 7(6): 7959–7986.

Waske, B. & Benediktsson, J.A. Fusion of Support Vector Machines for Classification of Multisensor Data. *IEEE Transactions on Geoscience and Remote Sensing*, 45(12): 3858–3866.

Waske, B. & Braun, M. 2009. Classifier Ensembles for Land Cover Mapping Using Multitemporal SAR Imagery. *ISPRS Journal of Photogrammetry and Remote Sensing, Theme Issue: Mapping with SAR: Techniques and Applications*, 64(5): 450–457.

Wilkinson, G.G. 1997. Open Questions in Neurocomputing for Earth Observation. In Kanellopoulos, I., Wilkinson, G.G., Roli, F. & Austin, J. (eds), *Neurocomputation in Remote Sensing Data Analysis* (pp. 3–13). Springer: Berlin–Heidelberg.

Xiuwan, C. Using Remote Sensing and GIS to Analyse Land Cover Change and Its Impacts on Regional Sustainable Development. *International Journal of Remote Sensing*, 23(1): 107–124.

Zhong, Y., Zhang, L., Gong, J. & Li, P. 2007. A Supervised Artificial Immune Classifier for Remote-Sensing Imagery. *IEEE Transactions on Geoscience and Remote Sensing*, 45(12): 3957–3966.

Zuo, R. & Carranza, E.J.M. 2011. Support Vector Machine: A Tool for Mapping Mineral Prospectivity. *Computers & Geosciences*, 37(12): 1967–1975.

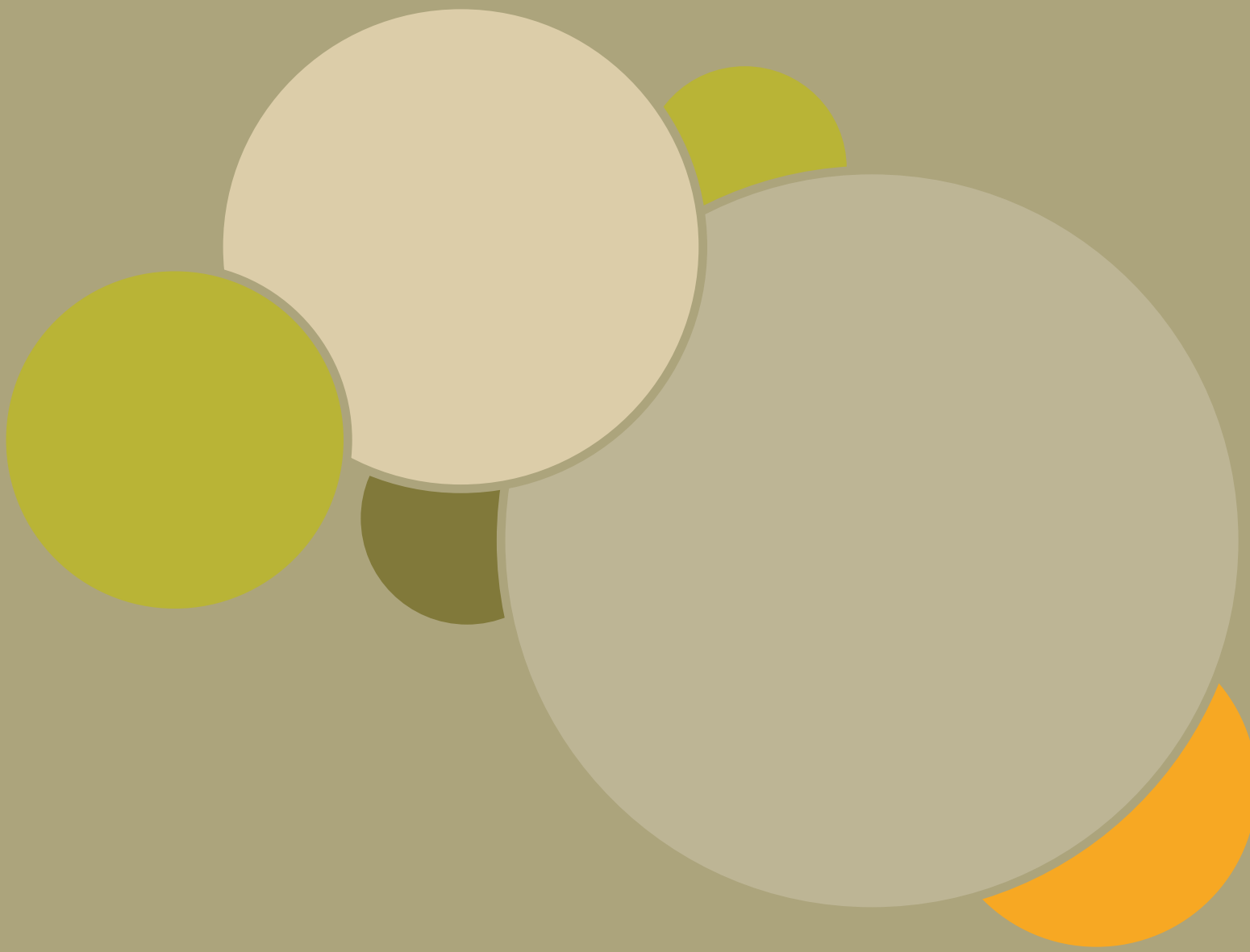

3

Chapter 3

Use of remote sensing for the design of sampling frames

Javier Gallego

The topic of this chapter overlaps to a great extent with that covered in chapters 4 and 6 of the recent GSARS handbook on Master Sampling Frames for Agricultural Statistics (GSARS, 2015). Chapter 4 of that handbook provides guidelines on the use of Geographic Information Systems (GIS), Global Navigation Satellite Systems (GNSS, better known as GPS) and remote sensing, while chapter 6 focuses on Area Sampling frames (ASFs). Readers are invited to consult the aforementioned handbook for additional details; however, the present chapter is intended to be self-explanatory.

Most applications of remote sensing to agricultural statistics correspond to optical sensors, which are generally classified on the basis of their spatial resolution. This is closely linked with the repetitiveness of image acquisition: VHR satellite images, with a pixel size between approximately 0.5 m and 2.5 m, are usually too expensive for exhaustive coverage unless publicly accessible layers such as Google Earth or Bing are considered. The acquisition year of these images is often highly heterogeneous, thus making them of limited use for crop area estimation in a specific year or season. However, they can be very useful in building a sampling frame unless the agricultural landscape in question is subject to rapid change.

Several images with a resolution between 10 and 30 m are now available free of charge, and full coverages are feasible. However, they can be used to build a sampling frame only if the dominant plot size is not excessively small and the parcel structure in the landscape can be distinguished.

Other types of images, in particular radar images, appear to be promising and in continuous improvement; however, to date, their only major validated application to agriculture is in monitoring paddy rice.

3.1. LIST FRAMES AND AREA FRAMES

Sampling frames for agricultural statistics are often classified into two main categories: list sampling frames (LSF) and ASFs. An LSF may be an agricultural census or a list of farms, holdings or households obtained from administrative registers. In an ASF, the sampling units are elements of geographic space: points, lines (transects) or polygons (segments).

The difference between LSFs and ASFs is far from clear:

- List frames often use Enumeration Areas (EAs) as Primary Sampling Units (PSUs). If the boundaries of EAs are available (hopefully as a GIS layer), the first stage of the LSF can be treated as an ASF;
- The first time a survey is run on an ASF, a list of farms is associated to the sampled points or segments. Although identifying the farms associated to points or segments may be difficult in the first year, the list thus built can be treated as a list sample with probability proportional to size (PPS) and is easier to update in consecutive years than the full list of farms in the EA.

Remote sensing plays a major role with regard to ASFs, while for the more traditional LSFs, its role is more modest. However, the usability of remote sensing for LSFs is not negligible, in particular when a GIS layer of EA boundaries is available and a stratification can integrate the land cover information derived from remote sensing.

3.1.1. Stratification

Defining a stratification is probably the most common application of remote sensing to agricultural sampling frames. Remote-sensing-based stratifications may be conceived in various ways for ASFs. For LSFs, the applicability is more limited, generally to their "area frame" aspect. In particular, images can be used to stratify EAs when they are used as PSUs and a GIS layer of EAs is available.

Classified images or land cover maps elaborated from images can be used to define strata according to criteria that can be linked to the overall percentage of cropland or to the dominance of specific crops. For example, strata can be defined as the sets of units having over 60 percent of cropland, 30 to 60 percent of cropland, 10 to 30 percent of cropland or less than 10 percent of cropland. Certain strata may also be associated to specific crops, such as the set of units in which olive trees occupy more than 50 percent, or in which there is a strong presence of irrigated land. If classified images or land cover maps are strongly biased, this will reduce the efficiency of stratification in terms of variance; however, it will not introduce bias on the estimators generated on the basis of a survey using such a stratification. Bias in the area estimators may derive from the presence of systematic mistakes in the observations made by surveyors, but not from inaccurate stratification.

3.1.2. Inaccuracies in stratification

Often, the survey observation of a sample unit is not consistent with the definition of the stratum to which it belongs. For example, in the Sétif example (section 2.3 below), a segment i was sampled in stratum 3, defined as having between 40 and 70 percent of cropland. Suppose that the field observation reveals that the total crop area in the segment is actually 25 percent. The survey manager may believe that this segment was wrongly allocated in the stratification and that the stratification will be improved if this segment is reallocated to stratum 2. This would be wrong and may introduce a significant bias in the estimators because the rule cannot be applied to similar segments that are not in the sample (and thus upon which no information available). It is important to respect the principle that the stratification takes place prior to sampling and that the quality of stratification is the same within and outside the selected sample. Identifying frequent misclassifications in the sample may raise concerns as to whether the

stratification should be reviewed; in this case, it should be reviewed for future surveys with a homogeneous rule and level of information on the territory. The stratification cannot be reviewed on the basis of information collected on the sample alone.

3.2. AREA SAMPLING FRAMES

3.2.1. Frames of segments with physical boundaries

The segments of an area frame can be delimited by physical boundaries, such as rivers or roads. This was the choice made by the U.S. Department of Agriculture (USDA) in the 1930s, and remains operational to this day (Davies, 2009). The delineation of sampling units is based to a large extent on photointerpretation. The availability of crop classification layers[1] has introduced a new tool for stratification (Boryan and Yang, 2012); however, this does not eliminate the time- and resource-intensive visual task of identifying boundaries. The amount of photointerpretation can be reduced by introducing an intermediate step in which PSUs are delineated and sampled. The PSUs selected are subdivided into segments, and one of them is selected in the second step (figure 1). Readers should note that this scheme is not a proper two-stage sampling system because only one segment per PSU is selected in the second step.

In defining sampling units, photointerpretation is essential for area frames of segments having physical boundaries. At the same time, it is capable of providing excellent information for stratification. However, this type of area frame is seldom a good solution in developing countries with small agricultural plots.

FIGURE 1. A PSU HAVING PHYSICAL BOUNDARIES AND WITHIN WHICH A SEGMENT IS SELECTED.

1 https://www.nass.usda.gov/Research_and_Science/Cropland/Release/index.php.

3.2.2. Frames on regular grids

One alternative is to define segments by applying a geometric grid on a given cartographic projection, usually square segments. When defining the frame, square segments usually provide similar accuracy levels as segments with physical boundaries, with lower costs. A first definition of such an area frame can be a simple overlay of a square grid onto the administrative boundaries. On the borders, small polygons arise that can be eliminated if their area is less than half the area of a full grid cell. The generated undercover can be approximately compensated for by attributing the weight of a full cell to the incomplete boundary cells retained. In the example of figure 2, this introduces a very low bias of only 0.05 percent in the overall area. For these operations, no use of remote sensing has been made, but rather only of basic GIS operations.

FIGURE 2. A SQUARE GRID ON AN ADMINISTRATIVE REGION. RIGHT: SQUARE GRID AFTER ELIMINATING SMALL GRID CELL PIECES.

In the example above, a homogeneous grid size was used. A first level of refinement may consist in adapting the grid size to the plot size. Several approaches can be used for this purpose, such as using a remote-sensing-derived map of dominant field size. Figure 3 represents a global field size map that can be used (Fritz *et al*., 2015), although some users may prefer to use their own local knowledge to refine or improve the field size mapping.

FIGURE 3. GLOBAL MAP OF DOMINANT FIELD SIZE.

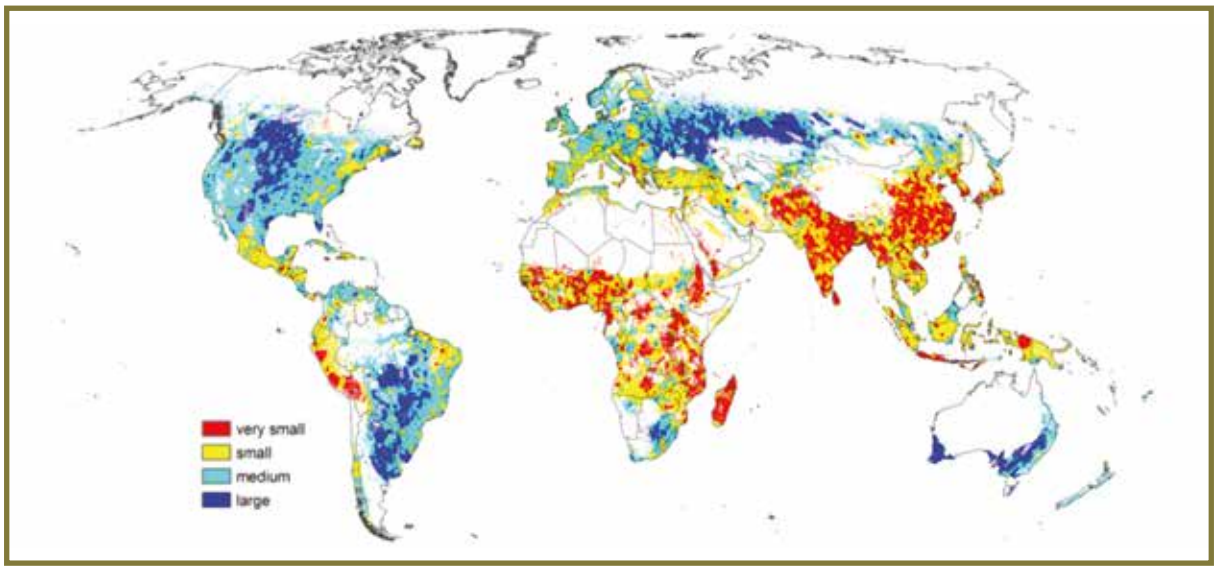

Another option is starting with a large grid size and viewing the sampled cells on a very-high-resolution (VHR) image. A rule can be defined to reduce the area to be observed if the number of fields is larger than a given threshold (figure 4). This partial observation does not introduce any bias in area estimation as long as the rule is fixed (for example, by retaining only the central part of the large segment) and applied independently of the land cover observed. However, it does introduce complications in the computation of variances of the estimators.

A frequent rule of thumb on the suitable size of segments is that the average number of fields or land cover patches per segment should be between 10 and 20, so that the working time required for the field visit is less than half a day (Taylor *et al*., 1997).

FIGURE 4. REDUCED SEGMENT DUE TO AN EXCESSIVE NUMBER OF FIELDS.

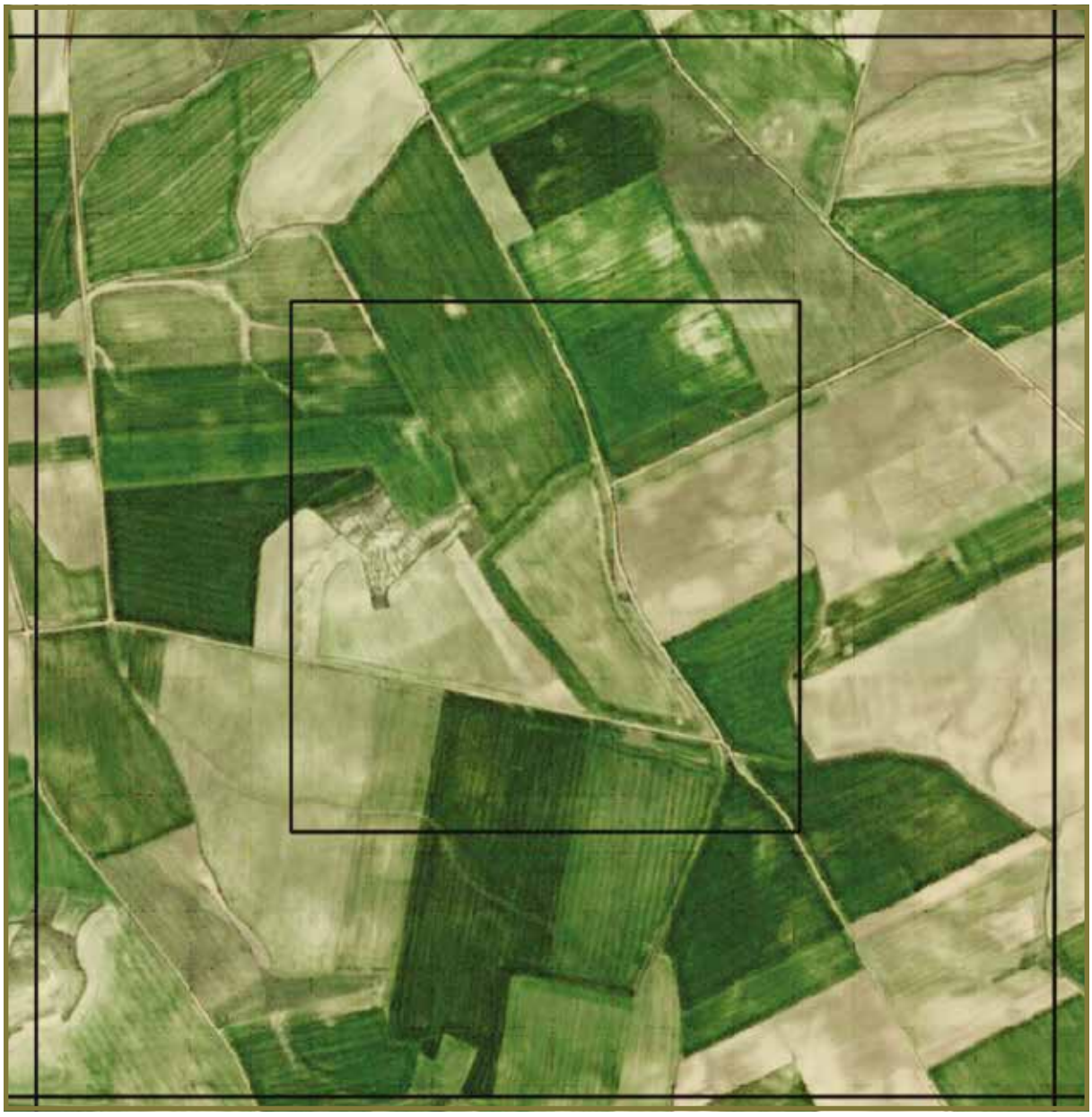

3.2.2.1. Stratification with existing national or regional land cover maps

If land cover maps or classified satellite images are available, it is possible to compute a cropland area indicator for each cell of the grid on the basis of the available information. The result of this computation is usually of insufficient quality to be termed "statistics"; however, it is very useful to stratify the territory. This type of stratification is particularly useful for the cheap sampling frames based on regular grids. For area frames based on segments with physical boundaries, this type of stratification is generally unnecessary, because the proportion of cropland or of specific crop types within each PSU may be visually assessed when their perimeters are delineated.

FIGURE 5. OVERLAY OF A LAND COVER MAP ONTO A SAMPLING GRID.

Figure 5 illustrates the overlay of an available land cover map onto an image. In this example, the map is the CORINE Land Cover (CLC) map. As may be seen, the map is not perfect and contains classes with a vague label, such as "complex land cover". In any case, this type of map can be used to attribute a cropland index to each unit of the sampling grid (in this case, squares). The index may be, for example:

*Arable land index=arable+0.4*complex+0.2*perm.crops+0.2*grassland*

FIGURE 6. A SAMPLING GRID OVERLAID ONTO A HIGH-RESOLUTION LAND COVER MAP (LEFT) AND A DERIVED STRATIFICATION (RIGHT).

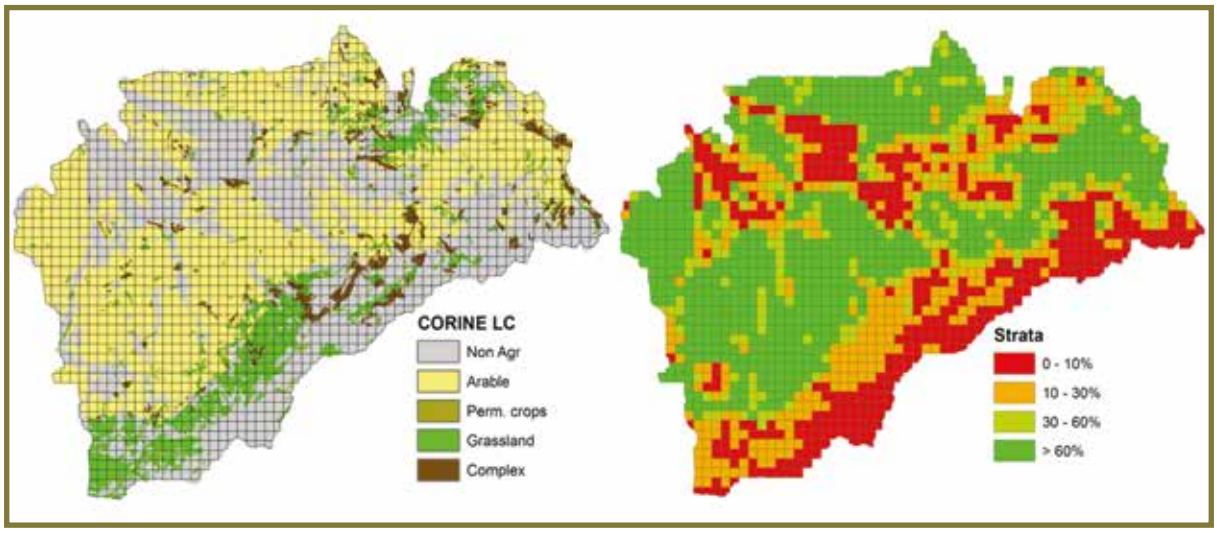

Figure 6 illustrates the definition of this type of stratification for the area frame of figure 2. In this example, the area of permanent crops is used to compute the index because it has been observed that the polygons labelled as permanent crops in the CLC actually contain a certain amount of arable land. The index can be further refined by introducing the knowledge that the user may have of the land cover map and the thresholds to define the strata. Despite the imperfections of the CLC and of the index, this method of stratification has proven to yield a relative efficiency of approximately 2, for major crops in Spain (Gallego et al., 1999)

Similar land cover maps are available in many parts of the world. For example, the Africover project has produced a large number of maps for African countries (Latham, 2009). Many Africover land cover maps should be updated, but even outdated maps may provide a good basis for stratification[2]. The main risk of using outdated maps is that the sampling plan usually excludes the stratum labelled as "non-cropland", while a significant change from non-cropland to cropland may have occurred. This factor will generate an important bias in the estimations if it is ignored by the statistician. A possible way to address this issue in the absence of resources for a full update of the map is to use a two-phase sampling for the non-cropland stratum.

3.2.3. Stratification based on global cropland maps

Figure 7 provides an example of stratification defined in Sétif (Algeria) with the help of a cropland probability map that was obtained comparing different existing land cover maps (Fritz and See, 2008). In this example, the sampling cells were rectangles of 1 500 m x 600 m. In each of the sampled cells, two rows of six points were to be visited (incomplete observation of segments in a two-stage sampling scheme). For the stratification, each 1 500 m x 600 m cell was given a "crop probability index", which was computed from the map by weighted average. The meaning of this crop probability index was not entirely clear and did not correspond to an expected proportion of cropland; nonetheless, it still led to a reasonable stratification defined by the intervals 0–10 percent, 10–40 percent, 40–70 percent and greater than 70 percent.

2 http://www.fao.org/geonetwork/srv/en/main.search?title=africover%20landcover.

FIGURE 7. STRATIFICATION WITH A CROP PROBABILITY MAP AND A SAMPLING GRID OF RECTANGLES IN SÉTIF (ALGERIA).

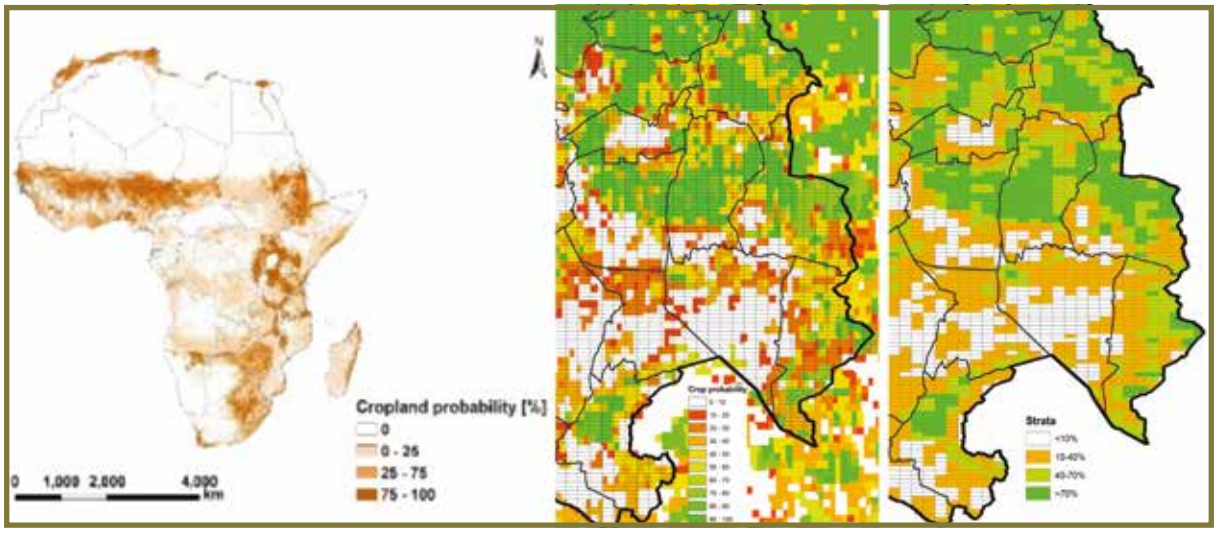

A similar global product is the FAO Global Land Cover-SHARE[3]. This database may be considered more complete, in the sense that it estimates the proportion of 11 major land cover types in each pixel.

3.2.4. Stratification on more detailed data relating to a previous year

In some countries, more detailed GIS layers are available, if not necessarily up-to-date. The USDA has developed a stratification method based on the cropland data layer (Boryan and Yang, 2012), consisting in a large mosaic of classified images. In some cases, detailed mappings at the parcel level may have been produced some years earlier. This type of layer has been used, for example, for stratification in a test pilot conducted in the Siliana Governorate in Tunisia (Sghaier, 2016). The procedure is the same as that illustrated above for coarser-resolution products: for each element of the sampling frame (usually a grid cell), an indicator of arable land or cropland proportion is estimated by weighted average of the available map proportions; the stratification is then defined by intervals of the indicator or on the basis of alternative indicators linked to specific crops. Figure 8 shows an example of a classified image on a grid of square segments that can be used for stratification.

3 http://www.glcn.org/databases/lc_glcshare_en.jsp.

FIGURE 8. A GRID OF SQUARE SEGMENTS OVERLAID ONTO A CLASSIFIED IMAGE.

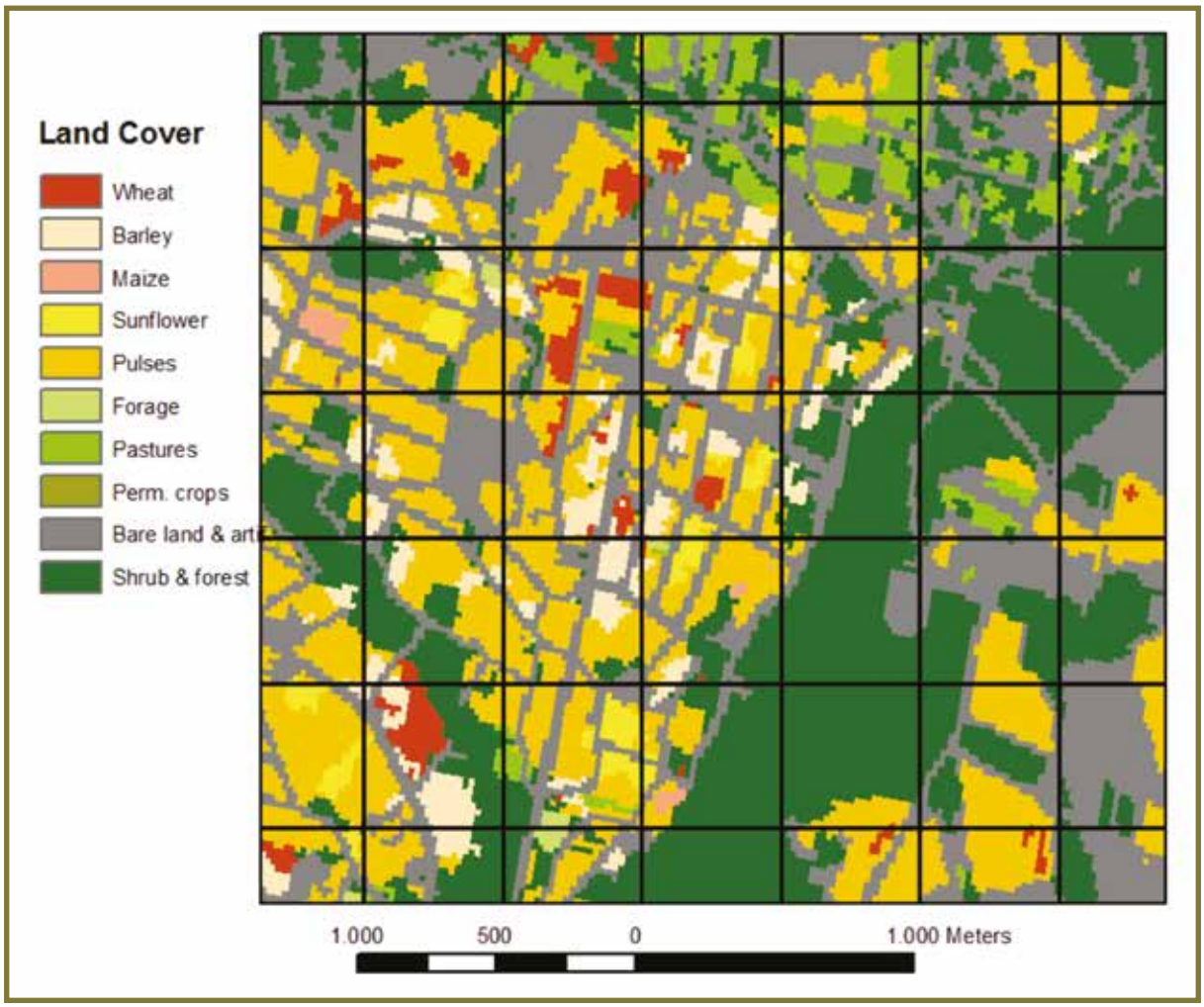

3.2.5. Photointerpretation of public domain images and crowdsourcing

The availability of free VHR images in tools such as Google Earth or Bing suggests the opportunity of their use for collecting agricultural information. However, the production of a land cover map from these with standard methods and a relatively fine spatial resolution requires a great deal of work by skilled photointerpreters and therefore a considerable budget.

Crowdsourcing can provide a cheap alternative and is worth exploring, without underestimating its limitations but rather identifying ways to limit their impact. The Geo-wiki network is making interesting progress on tools to exploit volunteer photointerpreters[4] in this regard:

- Volunteers may be not able to edit a polygon layer. On the other hand, allowing a large number of people to modify the polygon geometry can be risky. Instead of asking photointerpreters to delineate polygons, they can be asked to assess predefined polygons (grid cells or polygons that have been determined with a pattern recognition software). The question put to volunteers may be very simple; with regard to figure 9, it could be, for example, "Do you see any cropland inside the rectangle?" However, a slightly more precise question will be more useful for the purposes of stratification, such as "Is the percentage of cropland you see in the rectangle very high, high, medium, low, or zero?" A self-assessment of confidence may also be informative: "Is your level of confidence

4 http://www.laco-wiki.net/, http://www.geo-wiki.org/.

high, reasonable, or are you not sure at all?" With this type of questions, the photointerpretation time per cell ranges between 30 seconds and one minute, if good Internet access is available (and this is a critical limiting factor), such that a volunteer working three hours per day can assess between 150 and 300 cells during that time.

- A more elaborated system is illustrated in figure 10. The landscape had been previously divided into polygons with an automatic segmentation software. Each intersection of these polygons with the current grid cell is labelled by the photointerpreter as cropland or non-cropland. A general opinion of the reliability level is also provided. The photointerpretation tool will compute an index of likely cropland proportions that are useful for stratification.
- Assessing the reliability of each volunteer is essential. The Geo-wiki network examines the photointerpretation provided by different volunteers or by volunteers and experts to attribute reliability scores. When volunteers have a consistently high score, they receive a higher weight in attributing a score to other volunteers.
- Motivating volunteers is also important. Rewards such as smartphones to the top photointerpreter of the month are being tested, with promising results.

It may not be feasible to perform a full stratification with the high-score volunteers available. Suppose, for example, that the dominant field size is between 0.5 ha and 1 ha. A suitable segment size may be 300 m x 300 m. If the agricultural strata of the country occupy 300 000 km2, more than 3 million cells would have to be photointerpreted to conduct a full stratification. In this case, a two-phase sampling scheme similar to the method used in the EU LUCAS survey may be a reasonable solution. For example, a systematic first-phase sample of one cell out of a 5 x 5 grid would provide a more reasonable sample size of approximately 130 000 cells to be photointerpreted.

FIGURE 9. A SIMPLE SCREEN DESIGN FOR CROWD PHOTOINTERPRETATION.

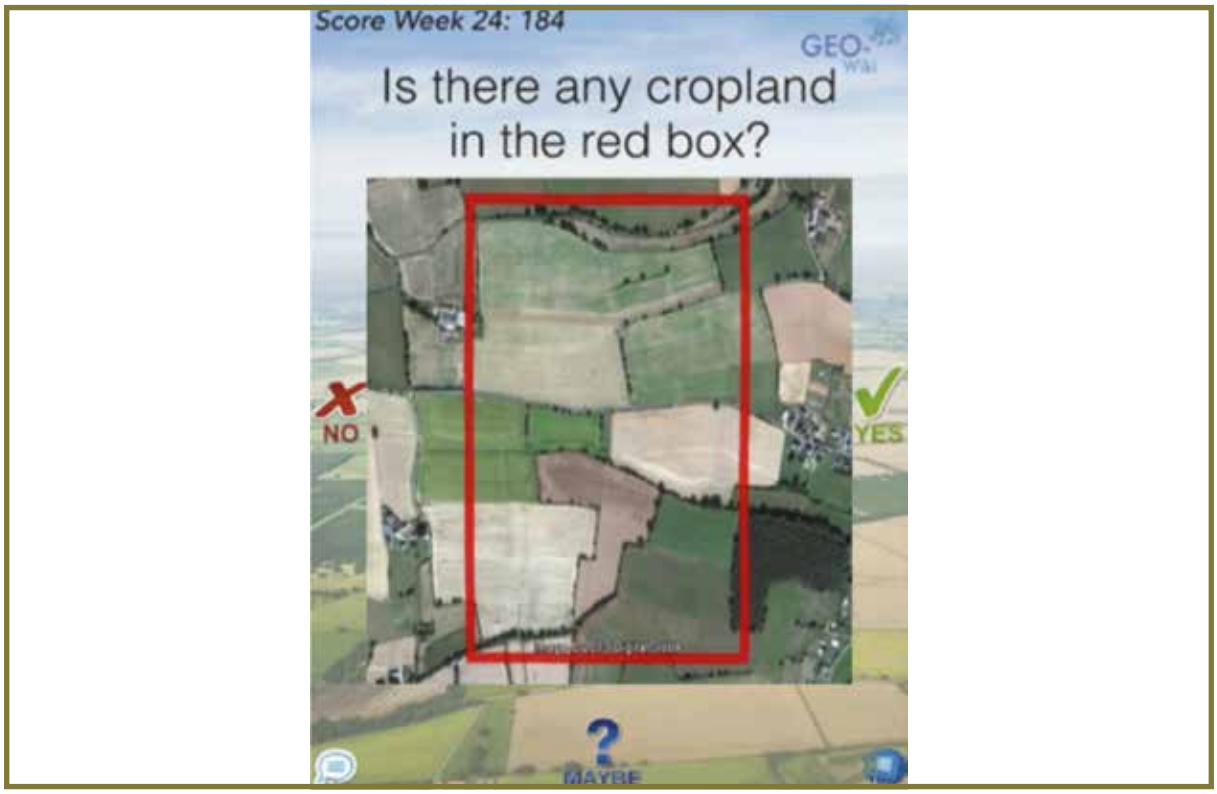

FIGURE 10. A MORE ELABORATE PHOTOINTERPRETATION BASIS, WITH POLYGONS PREVIOUSLY DELINEATED BY AN AUTOMATIC SEGMENTATION SOFTWARE.

3.2.6. Area frames of clustered points

For area frames of (clustered or unclustered) points or segments with geometric shapes, images are not necessary to define the sampling units, but may be essential for:

- Stratification, in particular when using a two-phase sampling for points with stratification based on photointerpretation of the first-phase sample; and
- Field survey documents: when the location of a point on the image fails to correspond to the location provided by GPS, it is preferable to give precedence to the image, which is more stable and traceable, especially if land cover change is an important target.

The two main types of area sampling frames of points are clustered and unclustered points. Frames of clustered points correspond to a traditional two-stage sampling scheme. If preferred, these may also be seen as frames of segments with an incomplete observation of the segment: instead of delineating all the fields and patches in the segment, only the land cover types (crop or other land cover classes) corresponding to a sample of points are recorded. The sample of points within regular segments is usually a regular grid (figure 11). This solution significantly reduces the workload while entailing only a small degradation of accuracy. An example of this approach is the French TER-UTI survey (FAO, 1998), which has been operational since the 1960s. TER-UTI uses a 6 x 6 points cluster with a distance between points of 300 m; however, when the dominant field size is smaller, a distance of 100 m may be more cost-efficient.

FIGURE 11. A REGULAR GRID OF POINTS ON A SQUARE SEGMENT FOR A TWO-STAGE SAMPLING SCHEME.

The stratification of such a sampling frame can be performed with the same procedures illustrated above for area frames of segments on a regular grid: the full square or rectangle is allocated to a stratum on the basis of the information available, even if only a grid of points inside it is surveyed.

3.2.7. Area frames of unclustered points

Unclustered points are generally used with a two-phase sampling technique (which is not to be confused with two-stage sampling): a large first-phase sample is selected to build an incomplete stratification, which is then used to select the final sample. Examples of this approach are the Italian Agrit survey after the modification introduced in 2002 (Martino, 2003) and the Eurostat LUCAS survey (Gallego and Delincé, 2010).

The comparison of results and costs relating to the old and the new versions of Agrit (Martino, 2003; Gallego and Delincé, 2010) indicates that unclustered points are capable of providing better cost-efficiency for area frame surveys in the European context (in light of the landscape and road networks prevailing therein); however, the results of the comparison are likely to be very different in developing countries, due to the greater impact of travelling expenses.

FIGURE 12. STRATIFIED FIRST-PHASE SAMPLE IN CENTRAL EUROPE.

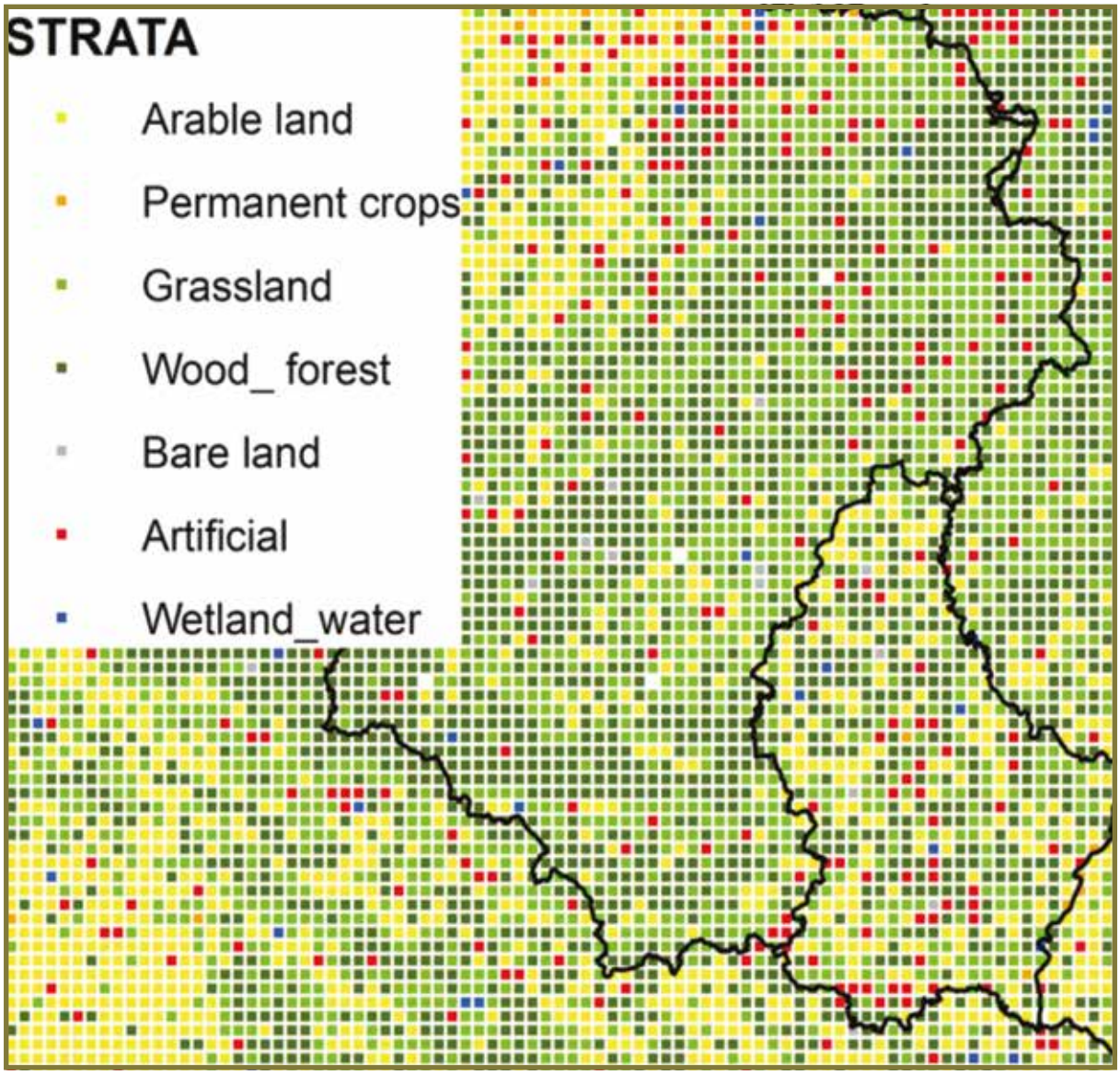

The main steps are the following:

- Select a large sample of points (first-phase sample). In Agrit and LUCAS, regular grids with more than 1 000 000 points each were selected.
- The first-phase sample was stratified by means of photointerpretation with a simple nomenclature (figure 12).
- A subsample is selected with a sampling rate that depends on the survey's priorities.

3.2.8. Comparing frames of segments with frames of points

Data collection and processing is easier for points than for area segments. Groundwork with segments requires a delineation of fields within the segment and digitizing them before area estimates are computed. This requires a certain amount of time (which may range from a few weeks to several months) for large samples and, consequently, delays for the production of estimates. The improvement of low-cost navigation devices, including smartphones, has had a greater impact on improving the cost-efficiency of point surveys rather than for segments.

Area segments provide better information for geometric co-registration, to overlay the ground information on satellite images; they are also capable of giving better information on plot structure and size. This may be useful for agri-environmental indicators, such as landscape indexes. Segments may also be better adapted for combination with satellite images with a regression estimator (Carfagna, 2007).

Comparisons between segments with physical boundaries and square segments have shown that the two approaches yield a very similar level of accuracy. Square segments would be preferable, since building the relative sampling frame is much cheaper (González et al., 1991).

3.2.9. Area frames of transects

A transect is a piece of a straight line of a certain length. It corresponds to the meaning of the word "segment" in basic geometry, and is used in area frame sampling because the term "segment" is given a different meaning in this context.

Transects can be combined with point sampling. This option may be suitable for landscapes containing mostly thin cultivation stripes to overcome the difficulty of locating a point in such landscapes; it has been tested in a pilot project in China (Kerdiles et al., 2013). A point is located within an image and determines the selection of a block of stripes. The point is given the proportion of each crop along a transect perpendicular to the stripes estimated in practice by step-counting on the border of the large plot (figure 13). This approach has drawbacks that are yet to be assessed, but may provide a practical solution for this difficult type of landscape.

FIGURE 13. A TRANSECT GENERATED BY A SAMPLED POINT TO SURVEY PARCELS WITH THIN CROP STRIPES.

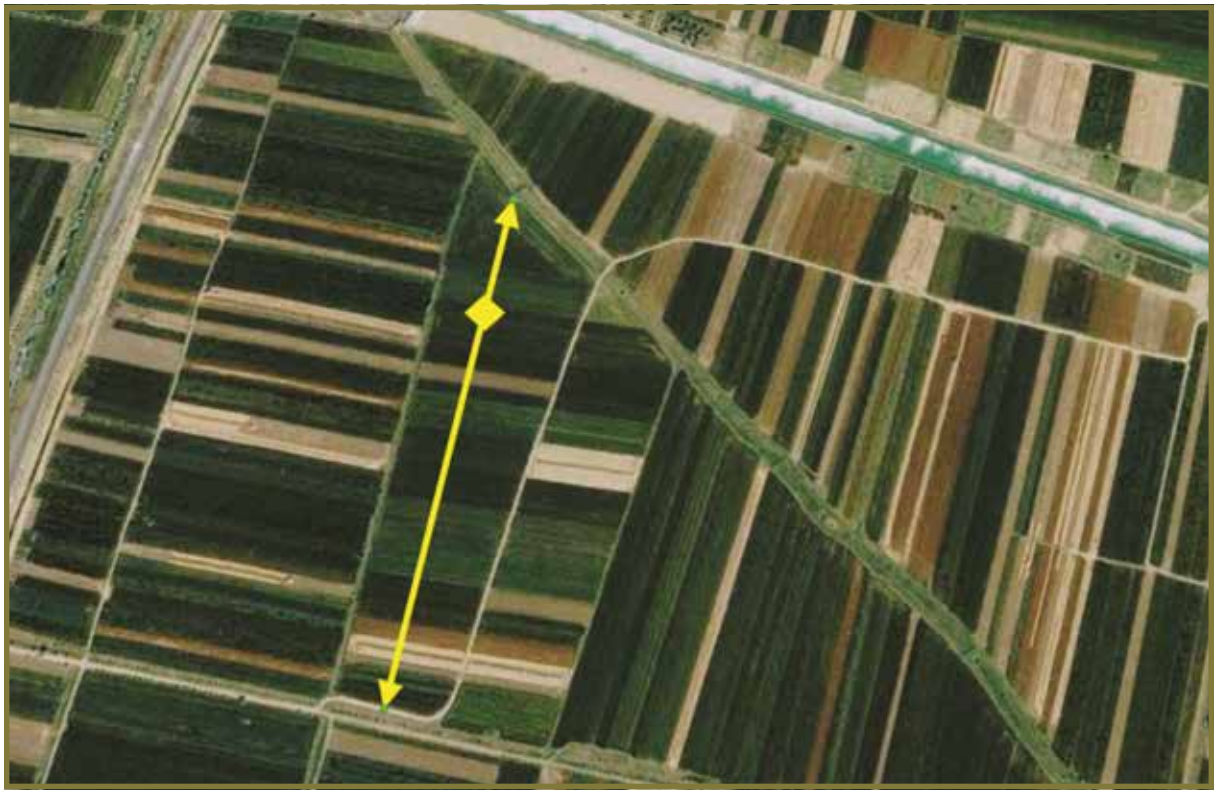

Transects are often used in environmental surveys to estimate the length of linear elements (de Vries, 1986; Gallego and Delincé, 2010), but are seldom employed in the context of agricultural statistics.

In principle, a transect has only one dimension (its width is 0); however, the term is also used to indicate long and thin polygons, for example measuring 100 m x 50 km. This type of sampling units are well-adapted to low-altitude flights (Jolly and Watson, 1979). They have been used for nomadic livestock estimation and may be applied more frequently if regulations allow relatively long Unmanned Aerial Vehicle (UAV) (also known as drone) flights. Otherwise, small piloted aircraft should be reassessed, taking into account the improvements made to cameras (3–5 cm resolution) and to the orthorectification of images (Gallego et al., 2016). Simulations made with data from the Netherlands show that thin and long stripes, which are better adapted to low-altitude flights, are much more efficient than square segments (figure 14).

FIGURE 14. SAMPLING SCHEME OF STRIPES FOR A SIMULATION STUDY WITH DATA FROM THE NETHERLANDS.

3.3. REMOTE SENSING FOR LSFS

3.3.1. The location of a farm: a difficult problem

The information provided by images from satellites or airplanes is closely linked to the precise location of a pixel. For this reason, the potential use of remote sensing for LSFs depends to a great extent on the location information of the elements of an LSF. The basic units of an LSF are farms or households. Although the following sections refer to farms, the reasoning explained can be applied to households too, to a large extent. Farms are often linked to an EA or other type of small administrative unit; this is often the only location information available for a farm. The explicit GIS representation of EAs determines the potential use of remote sensing.

3.3.2. Administrative registers

In some countries, the administrative information systems allow for a good georeferenced description of each farm (headquarters or managed fields). The term "registers" is used to denote such detailed GIS-based information systems. Registers report agricultural fields or plots with the support of orthophotographic documents or satellite images. However, they are suitable for use in the direct production of unbiased and timely statistics only under specific conditions of timeliness, accuracy and completeness that are difficult to reach in practice. On the other hand, the parcels delineated in a register are not necessarily conceived to match plots having a single crop. However, even outdated or incomplete registers may provide an excellent data source to build an efficient sampling frame. This is more clearly applicable in ASFs rather than to LSFs.

If a register is available, a satisfactory solution may be provided to the problem of GIS representation of a farm. A simpler solution is attributing to a farm the coordinates of its headquarters. However, defining the term "headquarters" is complicated and may have to adapt to the specific agricultural reality of each geographical area.

3.3.3. Using EAs as first-stage sampling units

GIS-based layers of small administrative areas, such as Enumeration Areas (EA) used for a census, communes, villages, etc. have a variety of uses that go far beyond defining a sampling frame for agricultural statistics. Compared to GIS administrative registers of farms, the cost of building a layer of small administrative units is much lower, even though it is not low in absolute terms. Building such a layer in the context of a strong agricultural statistical programme may be affordable, and at the same time prove useful for other territorial management tasks. For the purpose of agricultural statistics, such a layer of EA boundaries is useful for both list frames and area frames.

In this chapter, the term "EA" is used in a generic way. It may correspond to EAs as used in a population or agricultural census, or to administrative units, such as communes or villages. Producing, updating and improving the GIS layers of EAs may be an important step in an agricultural survey. Several situations are possible, depending on the legal or operational definition of the EA:

- The EA are defined on paper topographic maps. In this case, the topographic maps are first scanned to produce a raster image. Then, polygon boundaries are digitized with the scanned maps as a background. Each EA will be defined by a polygon layer (usually a single polygon). All EA layers should be georeferenced and merged in a single layer. The last step is correcting overlaps and missing splinters, to obtain a seamless layer. For this step, it is useful to have an image of the finest possible spatial resolution in the background, because EA boundaries often correspond to roads, rivers or other visible landscape features.
- A variant of the situation above occurs when a polygon GIS layer of boundaries exists, but must be refined, updated or corrected. In this case, only the last steps described above apply. If the boundaries of EAs are refined on the basis of satellite images, it is important to ascertain first that the geometry of the images is of adequate

quality in terms of spatial resolution and orthorectification. In particular, at the time of writing, the quality of the orthorectification of the image layers available in Google Earth may be insufficient. Figure 15 illustrates an example of an EA where the boundaries appear to have followed physical features and may require editing. Checks against additional documents (cadastral maps, for example) is necessary to ensure that appropriate corrections are made.

FIGURE 15. EXAMPLE OF AN EA WITH REGARD TO WHICH DOUBTS ARISE AS TO GEOMETRIC ACCURACY.

- EAs are legally defined by the text description of their boundaries. At best, the formal or legal definition of an EA refers to the visible landscape features. In these cases, imagery is essential to convert textual descriptions into georeferenced boundaries. To this, office-based work and fieldwork with local experts are essential.
- In some cases, the legal definition is more vague and may refer to households instead of to the territory. For example, the specification may be provided by the mention of a small population nucleus and a generic reference to neghbouring households. Local administrators or extension workers are generally able to determine the EA to which a given household belongs, but its precise geographic delimitation may be problematic. In this case, high-resolution imagery is very useful as a working tool; however, the core of the task remains the interaction between the different levels of local and national administrators. Building a GIS layer of EAs is a major task for the good administration of the territory; the layer can be used for a vast range of purposes beyond agricultural surveys alone.

The imagery basis upon which to build, improve or update a GIS layer of EA boundaries should enable a clear recognition of those landscape features that define EA boundaries. Possible choices are:

- Orthophotographic airborne coverage;
- Publicly available layers such as Google Earth or Bing – These solutions are attractive because they are accessible and free, although caution is required to ensure that the geometric accuracy is sufficiently homogeneous and the dates of the imagery are known (although the date of the images is less important than its spatial resolution, which should be as fine as possible); and
- Archives of private companies that may be accessed with a moderately priced subscription, such as Digital Globe.

3.3.4. Sampling EAs with probability proportional to the area

It is assumed here EAs are to be sampled in a country or a region for which a GIS layer of EA boundaries is available. It may be sought to sample EAs with a probability proportional to the geographical area Di of each EA. The standard approach is to apply a random PPS sampling, as illustrated in figure 17(a). A simple geographical method is to sample points with uniform probability and then selecting the EAs on which those points fall. However, the spatial layout of the sample is irregular, as often occurs in random sampling: several groups of contiguous communes are selected, while relatively wide areas remain empty. This drawback of random sampling is well known and is most easily overcome with systematic sampling. Some area frame surveys have used one-dimensional systematic sampling of EAs or PSUs by ordering the population with a rule linked to their location. A zig-zag ordering is often used for this ranking, as in the case of the USDA's AFS (Cotter and Tomczac, 1994). Figure 16 illustrates a zig-zag ordering of small administrative units that have been ordered by west–east bands. In this way, the two-dimensional layout is converted into a one-dimensional array in which a traditional PPS systematic sampling may be applied. It may be seen that the irregularity of the spatial layout remains.

FIGURE 16. ORDERING COMMUNES ACCORDING TO A ZIG-ZAG PATTERN PRIOR TO CONDUCTING A SYSTEMATIC SAMPLING.

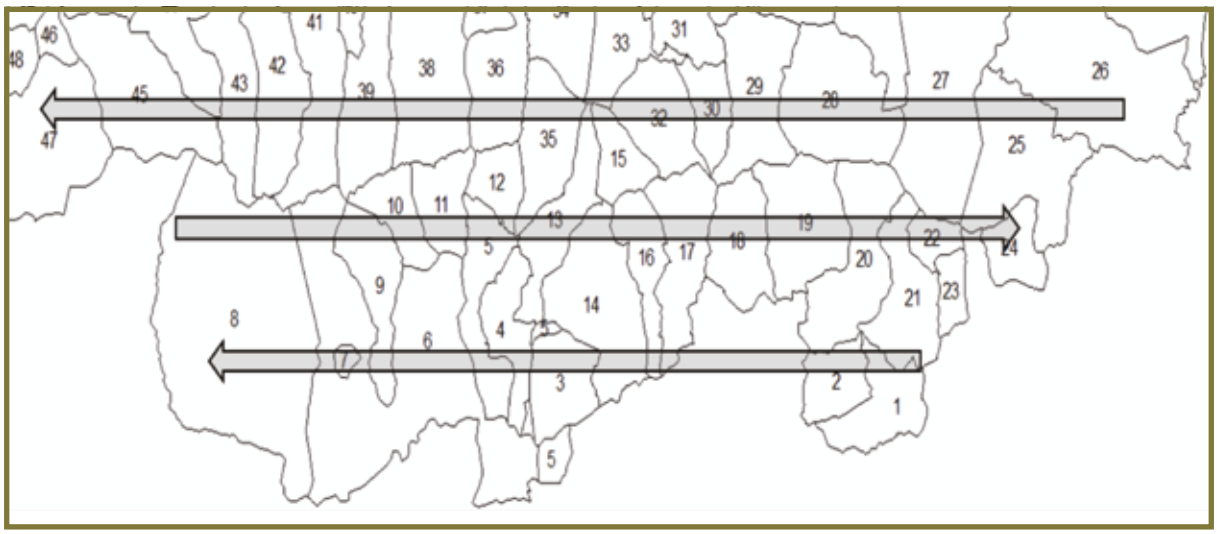

FIGURE 17. DIFFERENT PPS SAMPLES OF COMMUNES IN CASTILLA Y LEÓN (SPAIN) WITH THEIR GEOGRAPHIC AREA AS SIZE MEASURE.

(a) Random

(b) One-dimensional systematic with zig-zag array.

(c) Bidimensional systematic

Two-dimensional PPS sampling can be applied with a systematic grid of points (figure 17(c)) that provides a more regular distribution. Such a regular geographic layout improves the efficiency (Dunn and Harrison, 1993) if the spatial correlation decreases with the distance. The most important drawback is that there is no unbiased estimate of the variance. The standard variance formulas will generally yield an overestimation, so that the improvement can be hidden by the variance estimation bias. The traceability of the sampling process is probably the main gain in systematic sampling. Figure 17(c) shows an example from Castilla y León (Spain), where a regular grid of 30-km steps is used to select a sample of communes.

Sampling with a probability proportional to the geographical area is not the best option for agricultural statistics. A more reasonable solution is sampling with probability proportional to the cropland area in each EA. Other criteria may be based on the utilized agricultural area, current annual crops or other categories. This can be achieved by photointerpreting a sample of points, if cropland can be identified on the images. It may provide an alternative if no recent data are available for the total cropland per EA that can be used for PPS sampling. Photointerpreting a sample of points and selecting the EA if the point falls on cropland (figure 18) automatically produces a PPS EA sampling, even if the cropland area in each EA and in the whole region are unknown. The problem with this approach is that the computation of estimators for the total of any additive variable Z requires knowledge of the cropland in each EA and in the region:

$$\hat{Z} = \sum_i z_i \frac{A}{n\, a_i}$$

where A and a_i refer to the cropland area in the region and in the i^{th} EA respectively. To cope with this problem, one option is photointerpreting a larger sample that will be considered as a first-phase sample, or using a proxy, such as classified images or land cover maps. If a suitable land cover map or classified image is available, the parameter driving the PPS sampling may be the cropland area (or a similar concept) according to the map.

FIGURE 18. A POINT THAT IS PHOTOINTERPRETED AS CROPLAND (LEFT) AND A POINT THAT IS PHOTOINTERPRETED AS NON-CROPLAND (RIGHT).

Figure 19 maps the arable land area according to the CLC (EEA, 2007), and is available for the EU and some neighbouring countries. In Castilla y León, arable land is concentrated in the central zones, and therefore the sample of EAs with a probability proportional to arable land is mainly located in the centre of the region (figure 19). In this case, there are two sampling steps: first, defining a systematic grid; and second, selecting the EAs corresponding to the points of the grid that fall on arable land according to the CLC.

FIGURE 19. ARABLE LAND DISTRIBUTION AND A SYSTEMATIC SAMPLE OF COMMUNES WITH A PROBABILITY PROPORTIONAL TO THE AREA OF ARABLE LAND.

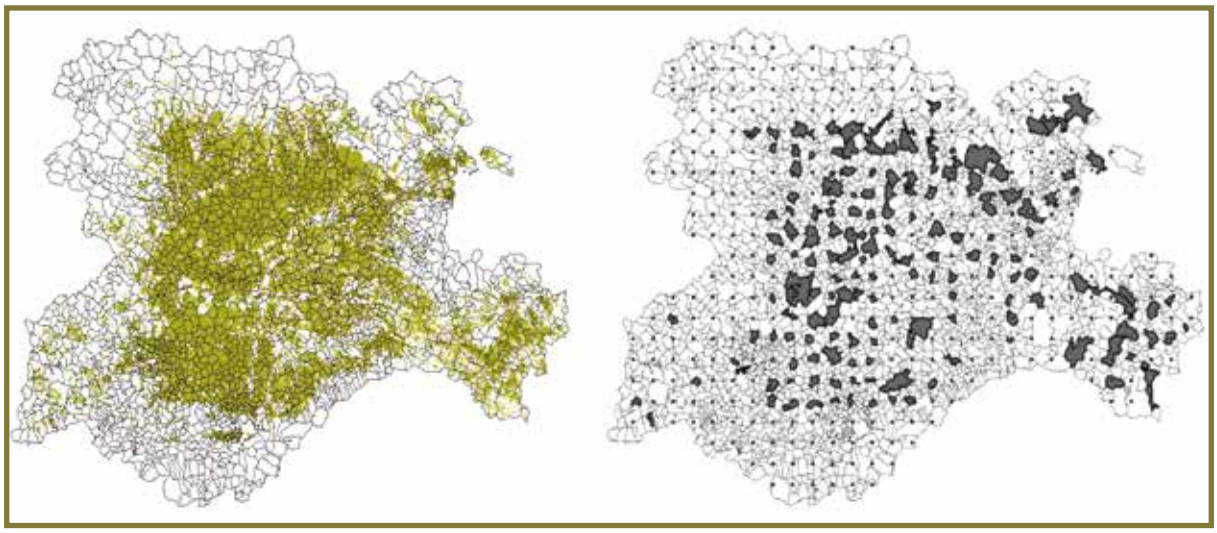

3.3.5. EA stratification

Traditionally, EAs are stratified on the basis of data from a census or other information sources, such as total cropland or number of cattle units from administrative reports provided by local extension workers. If such information is unavailable, too old or considered unreliable, remote sensing can provide an alternative. The approaches mentioned in section 2 above may be applied to stratify EAs if a GIS layer of their boundaries is available. In this case, it is possible to stratify by direct photointerpretation or by computation of indicators from available GIS layers: land cover maps detailed image classifications or farm registers.

A two-stage sampling scheme can be also considered, with EAs as PSUs and points as SSUs. In the second stage, we can use a two-phase sampling scheme with a regular grid of points in the first phase (figure 20). These points would be photointerpreted as cropland, non-cropland or doubt, for a simple stratification that would lead to the final sample of points. The identification of farms or holdings operating the plots that correspond to the selected field would produce a sample with a probability proportional to the cropland area (Gallego et al., 1994). This scheme illustrates how fuzzy the discrimination between list frames and area frames can be: the starting point are EAs, a typical element of list frames; then, a sample of points is introduced, a typical element of area frames; last, from the points, a sample of holdings is obtained, the basic unit of list frames. Figure 20 illustrates a strongly unbalanced grid (the long distance being in a west–east direction and the short distance in a north–south direction) to emphasize that grids need not necessarily be square and that this may have the advantage of reducing the walking distance between points in the field survey.

FIGURE 20. A GRID OF POINTS IN AN EA, WHICH CAN BE USED AS THE FIRST-PHASE SAMPLE IN A SECOND SAMPLING STAGE.

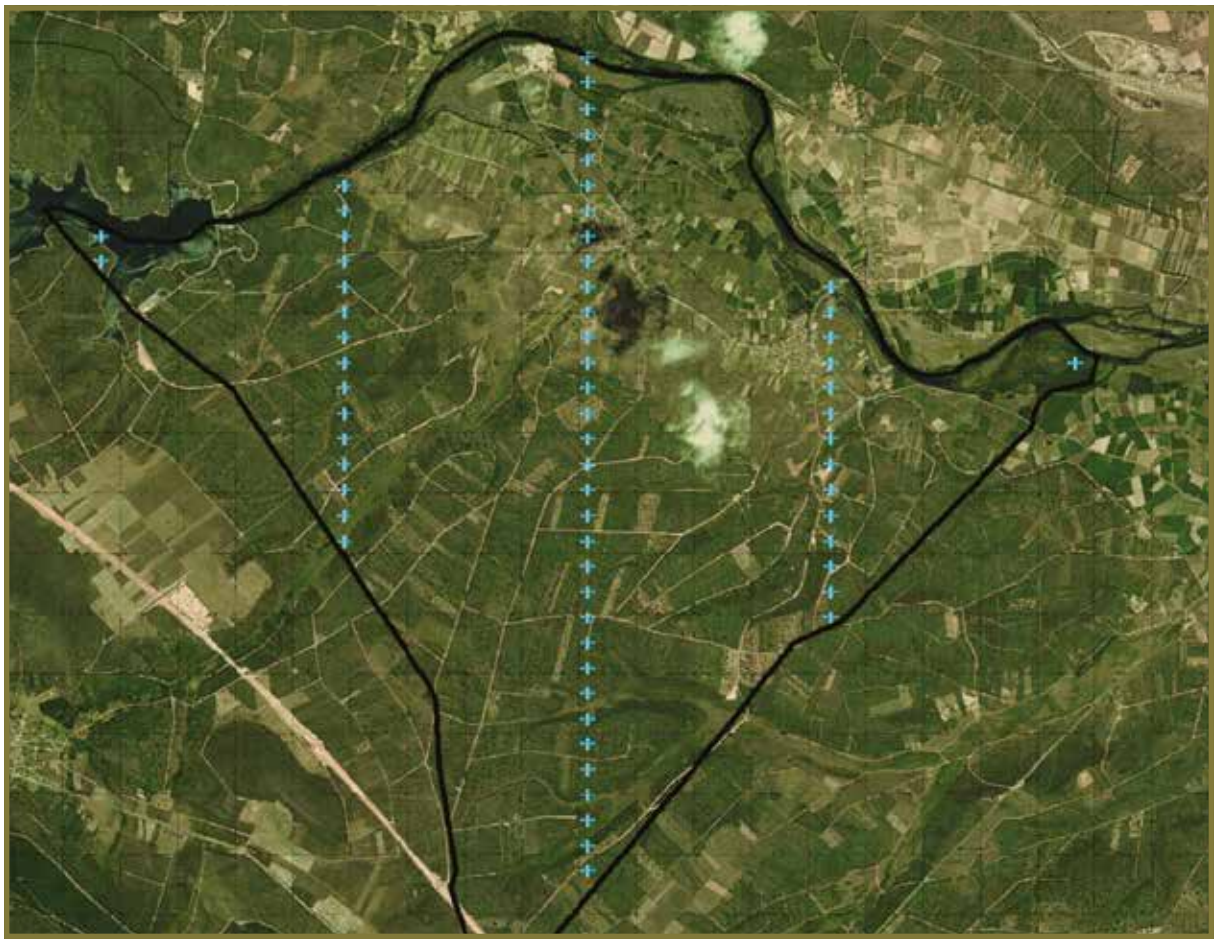

3.4. MEASURING PLOTS

Measuring agricultural plots is usually a necessary task in agricultural surveys, both in list frames and in area frames. Indeed, in most developing countries the information provided by farmers on the area of a specific plot tends to be unreliable, often due to lack of knowledge. Photointerpretation may be a valid alternative to the traditional measuring-tape-and-compass method. Depending on the characteristics of the images or plot boundaries, it can be more or less precise than GPS-based measurement. In principle, when photointerpreting, the delineation accuracy is approximately of the same order of magnitude of the resolution of the image, if the contrast between objects is sufficient. Thus, measuring plots on images with a resolution lower than 3–4 m should be preferable to measuring with a basic GPS device having a location accuracy of approximately 5 m. However, the issue is much more complex.

Figure 20 represents an example of an area dominated by agricultural plots smaller than 1 ha. The image on the left is an aerial orthophotograph (having a resolution of 0.5 m) dated 2007, while that on the right is a SPOT satellite image (with a 2.5 m resolution) dated 2012. The plot marked as "1" can be approximately delineated on both images, because the contrast with neighbouring plots is good. However, the difference in the shapes identified is rather significant, only partly because of the different dates. Plot 2 is easy to delineate in the orthophotograph, but is virtually impossible to identify on the image on the right. Photointerpretation should be performed on the field with a portable device, to identify possible changes intervening between the date when the image was captured and the date of the survey. When selecting the harware, care should be taken to ensure that the screen enables a good visibility.

FIGURE 21. PHOTOINTERPRETING PLOTS WITH AN AERIAL ORTHOPHOTOGRAPH (0.5 M RESOLUTION) AND A SATELLITE IMAGE (2.5 M RESOLUTION).

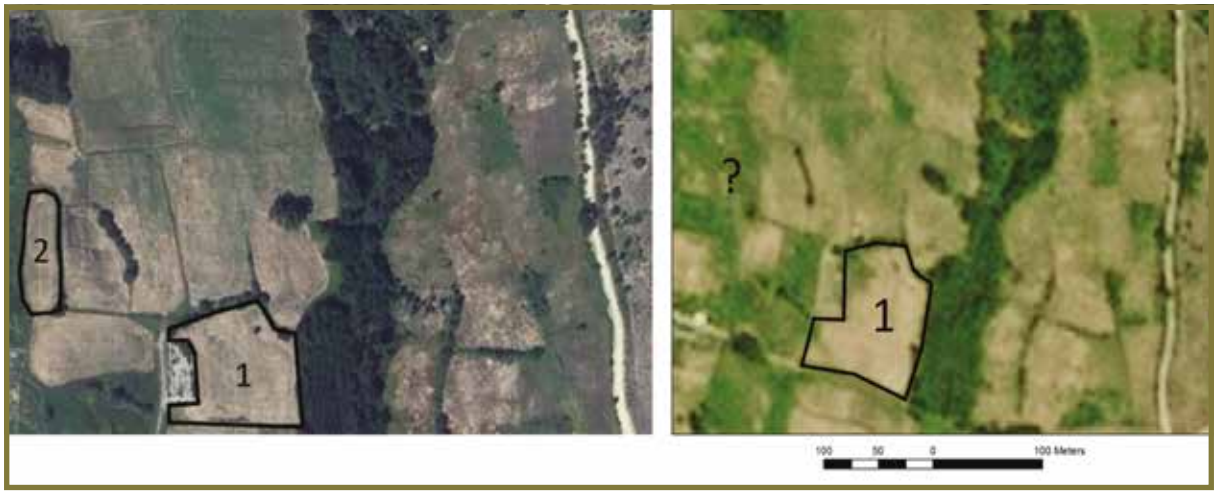

3.5. SAMPLING SATELLITE IMAGES

3.5.1. The experiences of the 1970s

In the LACIE project, the first to explore the application of remote sensing to agricultural statistics, Landsat-MSS images were cut into tiles of 5 x 6 nautical miles (Mc Donald and Hall, 1980), and a sample of these was classified. The reason for this selection was not clearly given in the publications explaining the project, although it seems that the classification of a full Landsat-MSS scene required computing facilities that the USDA/NASS did not have in-house (Hanuschak, personal communication, 2001). Although NASA had the capacity to classify a full MSS image, it was decided to design a method that the NASS could use without external support. Sampling errors were computed; however, the impact of estimating by pixels counting the crop areas in each tile was disregarded. This was corrected in the late 1970s, when the USDA gained the capability to classify full images and started to use regression estimators combining field data of the June Enumerative Survey (approximately 16 000 segments with physical boundaries) with classified images as auxiliary data (Hanuschak et al., 1979; Chhikara et al., 1986; Allen, 1990).

3.5.2. Sampling medium-resolution images

In the 1980s, cutting an image into tiles and sampling them for automatic classification became meaningless; however, sampling satellite images continued to be justified in certain cases. Such images have a spatial resolution between 20 m and 60 m, and were called "high-resolution images" at the time. Sampling satellite images was reasonable when the region of interest was large and a full coverage of images was not affordable for a specific project (the free-distribution policy was not applied to this type of images). For example, the "Rapid crop area change estimates" of the EU MARS Project used a sample of 60 sites, of 40 x 40 km each. The target was to cover each site with four SPOT-XS images throughout the crop growth season, although the maximum number of images was not always reached. For several years, the project gave estimates that matched other available sources of information; however, further analysis concluded that the use of pixel counting as a basis for the estimates gave image analysts a subjectivity margin of approximately 20–30 percent, so that the estimates could be adjusted to match external sources (Gallego, 2006).

Satellite images have often been sampled for forest resource assessment at global scale or for very large areas, such as the tropical belt (figure 21). For forest applications, it may happen that an image is subdivided into tiles and only one of these, or a sample thereof, is analysed when images are visually photointerpreted. In this case, the cost of each sample unit is proportional to its size; this justifies the choice of smaller units (Achard et al., 2002).

FIGURE 22. STRATIFIED SAMPLE OF LANDSAT SCENES AND QUARTERS OF SCENE USED TO ESTIMATE CHANGES IN TROPICAL FOREST.

3.5.3. Sampling VHR images

VHR images (currently, having a pixel size between 0.3 m and 3m) have become increasingly frequent and the question of their usability for area estimation has arisen. Full coverage is extremely expensive and complicated to manage. Therefore, a sample of units with a suitable size to be covered by VHR images may be created. The size covered by a VHR image varies from one satellite to another. Squares of 10 x 10 km or 15 x 15 km may be considered suitable for coverage by a VHR image (figure 22). The EU's Geoland2 project has explored the use of such samples to estimate land cover change (Aleksandrowicz et al., 2014).

The sampling efficiency of 10 x 10 km units has been explored under the optimistic assumption that single crops can be accurately identified (Gallego and Stibig, 2013). The conclusion was that VHR crop identification with this type of samples can be cost-efficient compared with EU-LUCAS ground-based point surveys if the cost per 10 x 10 km unit, including image purchase and processing, is less than approximately US$500. The cost threshold depends on the spatial correlation structure and therefore varies from one crop to another in each landscape. Currently, this cost is not achievable. However, the system may become interesting in the future, for crops that can be reliably identified on images, if the cost of image purchasing and processing is substantially reduced.

FIGURE 23. A SAMPLE OF SITES OF 10 X 10 KM TO BE ANALYSED WITH VHR IMAGES IN THE GEOLAND 2 PROJECT.

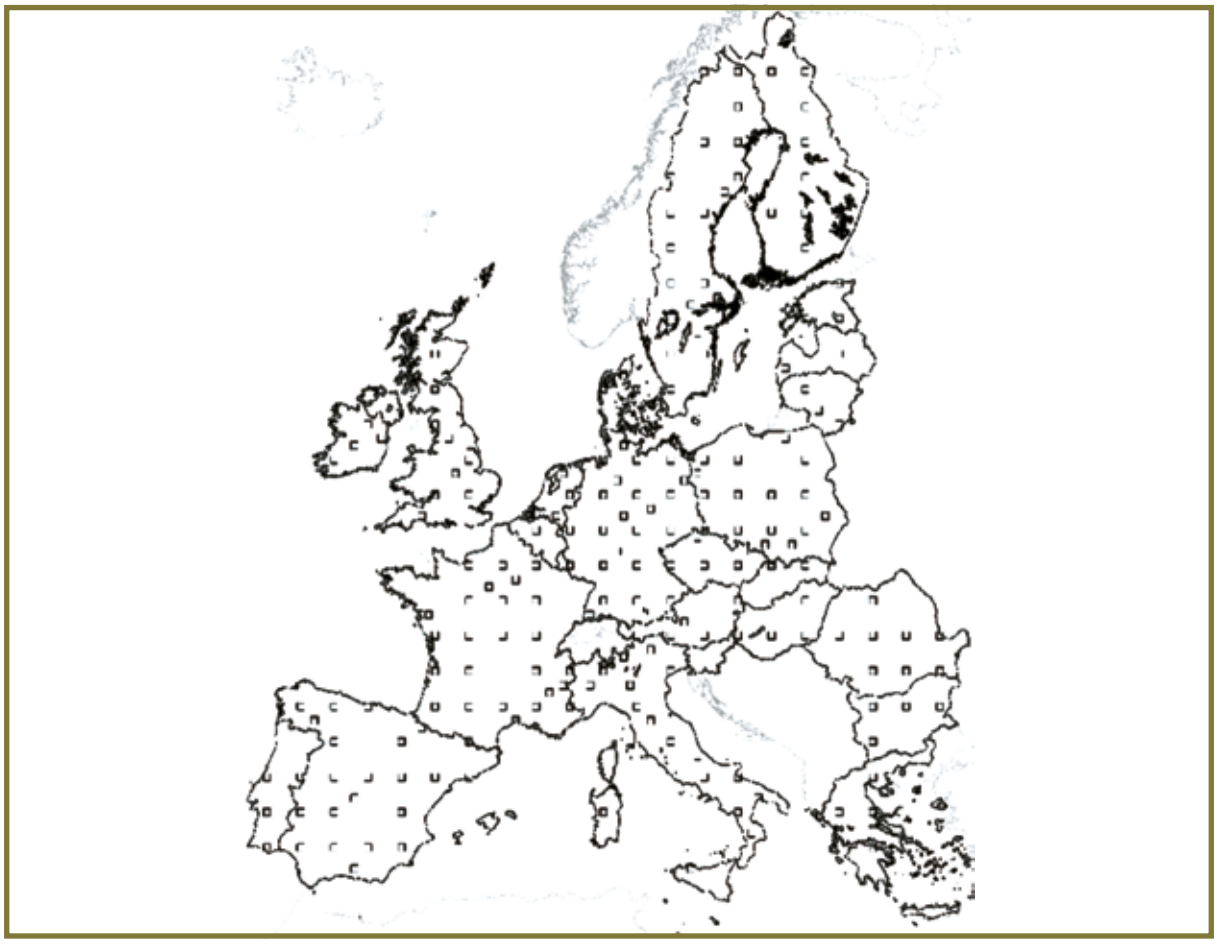

3.6. SURVEYS ALONG ROADS

Many area frame surveys have faced difficulties with sample units that are far from roads and require a long walking time to be reached. This is particularly serious in countries in which the road network is not dense or when time constraints are particularly strict. Surveys along roads are used by several international agencies in assessing the agricultural situation in third countries. However, in most cases, there does not appear to be any methodological note describing how to sample the routes along which the observations are made.

Concentrating observations along roads appears to be a practical solution, and several options can be considered: Moisen (1996) proposes a stratification based on buffers around roads. This seems to be practical for his model-based approach to the monitoring of vegetation; however, it is likely to be inefficient for crop area estimates, because most of the variance would derive from the areas far from the roads, with a lower sampling rate.

The CropWatch system uses a system that assumes the availability of reliable figures for the total area of a more general class, such as arable land or overall cropland (Wu and Li, 2012). The more general figure can be obtained, for example, with a small regression model extrapolating FAOSTAT figures, or through remote sensing, such as by photointerpreting a large sample of points into cropland and non-cropland. The survey along the road is used to estimate the proportion of each single crop compared to the overall cropland. The underlying assumption is that the ratio between the areas of different crops is similar close to the roads and far from the roads. This assumption has

been tested in the EU with the help of a GIS road network and the LUCAS 2009 field survey. Sampling pieces of road with a probability proportional to their length and sampling points in a 100-m buffer leads to a positive bias for wheat (+ 2.5 percent) and a negative bias for barley (-4.3 percent). The bias is reduced by half with a modified sampling scheme: large square segments of 3 x 3 km are sampled, a regular grid is selected therein, and only the points within a 100-m buffer from any road in the square segment are visited (figure 23). With this sampling scheme, the bias is reduced to +1.4 percent for wheat and to -2.4 percent for barley. The reason is that part of the bias comes from the fact that barley is more often cultivated in areas with less fertile land, and these areas also have a less dense road network; this receives a higher weight when sampling segments rather than sampling road arcs.

FIGURE 24. SAMPLE OF POINTS FOR A SURVEY ALONG THE ROAD BY SAMPLING LARGE SQUARE SEGMENTS.

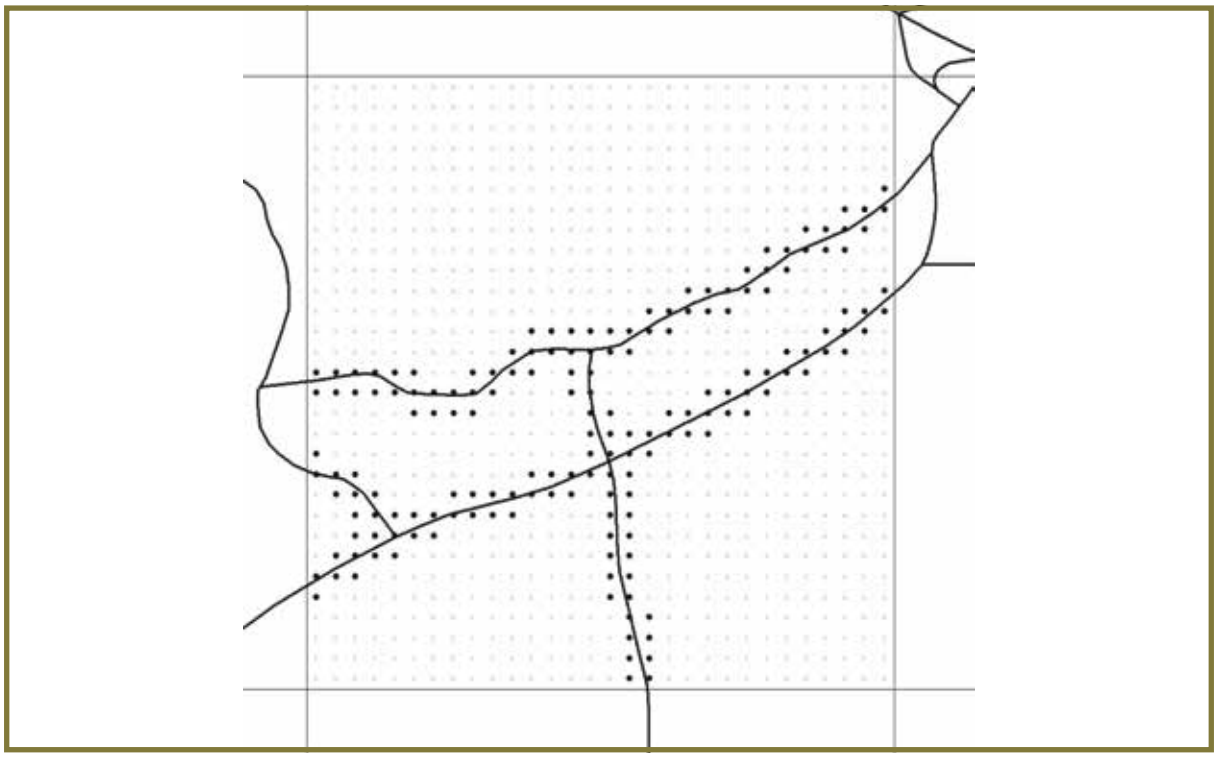

3.7. REFERENCES

Achard, F., Eva, H.D., Stibig, H.J., Mayaux, Ph., Gallego, J., Richards, T. & Malingreau, J.P. 2002, Determination of deforestation rates of the world's humid tropical forests, *Science*, 297(5583): 999–1002.

Aleksandrowicz, S., Turlej, K., Lewiński, S. & Bochenek, Z. Change detection algorithm for the production of land cover change maps over the European Union countries. *Remote Sensing*, 6: 5976–5994.

Allen, J.D. 1990. A Look at the Remote Sensing Applications Program of the National Agricultural Statistics Service. *Journal of Official Statistics*, 6(4): 393–409.

Boryan, C.G. & Yang, Z. 2012. *A new land cover classification based stratification method for area sampling frame construction*. In *Proceedings of 2012 First International Conference on Agro-Geoinformatics,* 2–4 August 2012. Shanghai, China. Available at http://ieeexplore.ieee.org/xpl/articleDetails.jsp?tp=&arnumber=6311727&queryText%3DBoryan. Accessed on 5 May 2017.

Boryan, C.G. & Yang, Z. 2012. *A new land cover classification based stratification method for area sampling frame construction*. In *Proceedings of the First International Conference on Agro-Geoinformatics*, 2–4 August 2012. Shanghai, China. Available at http://ieeexplore.ieee.org/xpl/articleDetails.jsp?tp=&arnumber=6311727&queryText%3DBoryan. Accessed on 5 May 2017.

Carfagna E. 2007. A comparison of area frame sample designs for agricultural statistics. *Bulletin of the International Statistical Institute, 56th Session. Proceedings of the Meeting STCPM11 on Agricultural and Rural Statistics*, 22–29 August 2007. Lisbon.

Carfagna, E. & Gallego, F.J. 2005. The use of remote sensing in agricultural statistics. *International Statistical Review* 73(3): 389–404.

Chhikara, R.S., Houston, A.G. & Lundgren, J.C. 1986. Crop acreage estimation using a LANDSAT-based estimator as an auxiliary variable. *IEEE Transactions on Geoscience and Remote Sensing*, vol. GE-24 1: 157–168.

Cotter, J. & Tomczac, C. 1994. An Image Analysis System to Develop Area Sampling Frames for Agricultural Surveys. *Photogrammetric Engineering and Remote Sensing*, 60(3): 299–306.

Davies, C. 2009. *Area frame design for agricultural surveys*. RDD Research Report N. RDD-09-xx. USDA-NASS Publication: Washington, DC. Available at: http://www.nass.usda.gov/Publications/Methodology_and_Data_Quality/Advanced_Topics/AREA%20FRAME%20DESIGN.pdf. Accessed on 5 May 2017.

De Vries, P.G. 1986. *Sampling Theory for Forest Inventory. A Teach-yourself Course*. Springer-Verlag: Berlin – Heidelberg (Germany) – Wageningen (The Netherlands).

Dunn, R. & Harrison, A.R. 1993, Two-dimensional systematic sampling of land use. *Journal of the Royal Statistical Society series: Applied Statistics*, 42(4): 585–601.

European Environment Agency (EEA). 2007. *CLC2006 technical guidelines*. Technical report no. 17/2007. EEA Publication: Copenhagen. Available at http://www.eea.europa.eu/publications/technical_report_2007_17. Accessed on 5 May 2017.

Food and Agriculture Organization of the United Nations (FAO). 1996. *Multiple frame agricultural surveys, Volume 1: Current surveys based on area and list sampling methods*. FAO Statistical Development Series, n.7. Available at http://www.fao.org/fileadmin/templates/ess/documents/meetings_and_workshops/regional_workshop_sampling_2010/FSDS_7_Multiple_frame_AS_Volume_1.pdf. Accessed on 5 May 2017.

FAO. 1998. *Multiple frame agricultural surveys, Volume 2: Agricultural survey programmes based on area frame or dual frame sample designs*. FAO Statistical Development Series, n. 10. Available at http://www.fao.org/fileadmin/templates/ess/ess_test_folder/Publications/SDS/10_multiple_frame_agricultural_surveys.pdf. Accessed on 5 May 2017.

Fritz, S. & See, L. 2008. Identifying and quantifying uncertainty and spatial disagreement in the comparison of global land cover for different applications. *Global Change Biology*: 14, 1057–1075.

Fritz, S., See, L., Mccallum, I., You, L., Bun, A., Moltchanova, E. & Obersteiner, M. 2015. Mapping global cropland and field size. *Global Change Biology*, 21(5): 1980–1992.

Gallego, F.J. & Stibig, H.J. 2013. Area estimation from a sample of satellite images: the impact of stratification on the clustering efficiency. *Journal of Applied Earth Observation and Geoinformation,* 22: 139–146.

Gallego, F.J. 2006. *Review of the Main Remote Sensing Methods for Crop Area Estimates*. In *Workshop proceedings: Remote sensing support to crop yield forecast and area estimates*. ISPRS archives, XXXVI, 8/W48, 65–70. Available at http://www.isprs.org/publications/PDF/ISPRS_Archives_WorkshopStresa2006.pdf. Accessed on 5 May 2017.

Gallego, F.J., Carfagna, E. & Peedell, S. 1999. The use of CORINE Land Cover to improve area frame survey estimates. *Research in Official Statistics*. 2(2): 99–122.

Gallego, F.J., Delincé, J. & Carfagna, E. 1994. Two-Stage Area Frame Sampling on Square Segments for Farm Surveys. *Survey Methodology*, 20(2): 107–115.

Gallego, J., Giovacchini, A. & Downie, M. 2016. Sampling stripes (transects) for crop area estimation with drones. Presentation prepared for the Seventh International Conference on Agricultural Statistics (ICAS VII), 26–28 October 2016. Rome.

Gallego, F.J., Carfagna, E. & Baruth, B. 2010. Accuracy, Objectivity and Efficiency of Remote Sensing for Agricultural Statistics. In Benedetti, R., Bee, M., Espa, G. & Piersimoni, F. (eds), (pp. 193–211). John Wiley & Sons: Chichester, UK.

Gallego, F.J. & Delincé, J. 2010, The European Land Use and Cover Area-frame statistical Survey (LUCAS). In Benedetti, R., Bee, M., Espa, G. & Piersimoni, F. (eds), *Agricultural Survey Methods* (pp. 151–168). John Wiley & Sons: Chichester, UK.

Global Strategy to improve Agricultural and Rural Statistics (GSARS) 2015. *Handbook on Master Sampling Frames for Agricultural Statistics: Frame Development, Sample Design and Estimation*. GSARS Handbook: Rome. Available at http://gsars.org/wp-content/uploads/2016/02/MSF-010216-web.pdf. Accessed 5 May 2017.

González F., López, S. & Cuevas, J.M. 1991. Comparing Two Methodologies for Crop Area Estimation in Spain Using Landsat TM Images and Ground Gathered Data. *Remote sensing of the environment*, 35: 29–36.

Hanuschak, G., Sigman, R., Craig, M., Ozga, M., Luebbe, R., Cook, P., Kleweno, D. & Miller, Ch. 1979. Obtaining timely crop area estimates using ground gathered and Landsat data. USDA Technical Bulletin 1609. Available at https://play.google.com/store/books/details?id=wYwoAAAAYAAJ&rdid=book-wYwoAAAAYAAJ&rdot=1. Accessed on 5 May 2017.

Hendricks, W.A., Searls, D.T. & Horvitz, D.G. 1965. A comparison of three rules for associating farms and farmland with sample area segments in agricultural surveys. In S.S. Zarkovich (ed.), *Estimation of areas in Agricultural Statistic*s, (pp. 191–198). FAO Publication: Rome.

Jolly, G.M. & Watson, R.M. 1979. Aerial sample survey methods in the quantitative assessment of ecological resources. In Cormack, R.M., Patil, G.P. & Robson, D.S. (eds), *Sampling Biological Populations* (pp. 203–216). International Co-Operative Publishing House: Fairland, US.

Kerdiles, H., Spyratos, S., Gallego, J., & Dong, Q. 2013. Assessing the crop acreage in Mengcheng county on the North China plain using adapted regression estimator method. In *2nd International Conference on Agro-Geoinformatics: Information for Sustainable Agriculture, Agro-Geoinformatics 2013,* 577–582 http://iopscience.iop.org/1755-1315/17/1/012057.

Latham, J. 2009. FAO land cover mapping initiatives. In Campbell, J.C. *et al*. (eds), *North America Land Cover Summit* (pp. 75–95). Association of American Geographers Publication: Washington, D.C. Available at http://www.aag.org/galleries/nalcs/CH6.pdf. Accessed on 5 May 2017.

Mac Donald, R.B. & Hall, F.G. 1980. Global crop forecasting. *Science*, 208: 670–679.

Martino, L. 2003. The Agrit system for short-term estimates in agriculture. Paper presented at the DRAGON Seminar, 9–11 July 2003. Krakow/Balice, Poland.

Moisen, G.G. 1996, Generalized linear mixed models for analyzing error in a satellite-based vegetation map of Utah. In Mowrer, H.T., Czaplewski, R.L. & Hamre, R.H. (eds), *Spatial accuracy assessment in natural resources and environmental sciences* (pp. 459–466). USDA Forest Service General Technical Report RM-GTR-277.

Taylor, J., Sannier, C., Delincé, J. & Gallego, F.J. 1997. *Regional Crop Inventories in Europe Assisted by Remote Sensing: 1988-1993*. Synthesis Report, EUR 17319 EN. European Commission Publication: Luxembourg. Available at : http://mars.jrc.ec.europa.eu/mars/Bulletins-Publications/Regional-Crop-Inventories-in-Europe-Assisted-by-Remote-Sensing-1988-1993.

Wu, B. & Li, Q. 2012. Crop planting and type proportion method for crop acreage estimation of complex agricultural landscapes. *International Journal of Applied Earth Observation*, 16: 101–112.

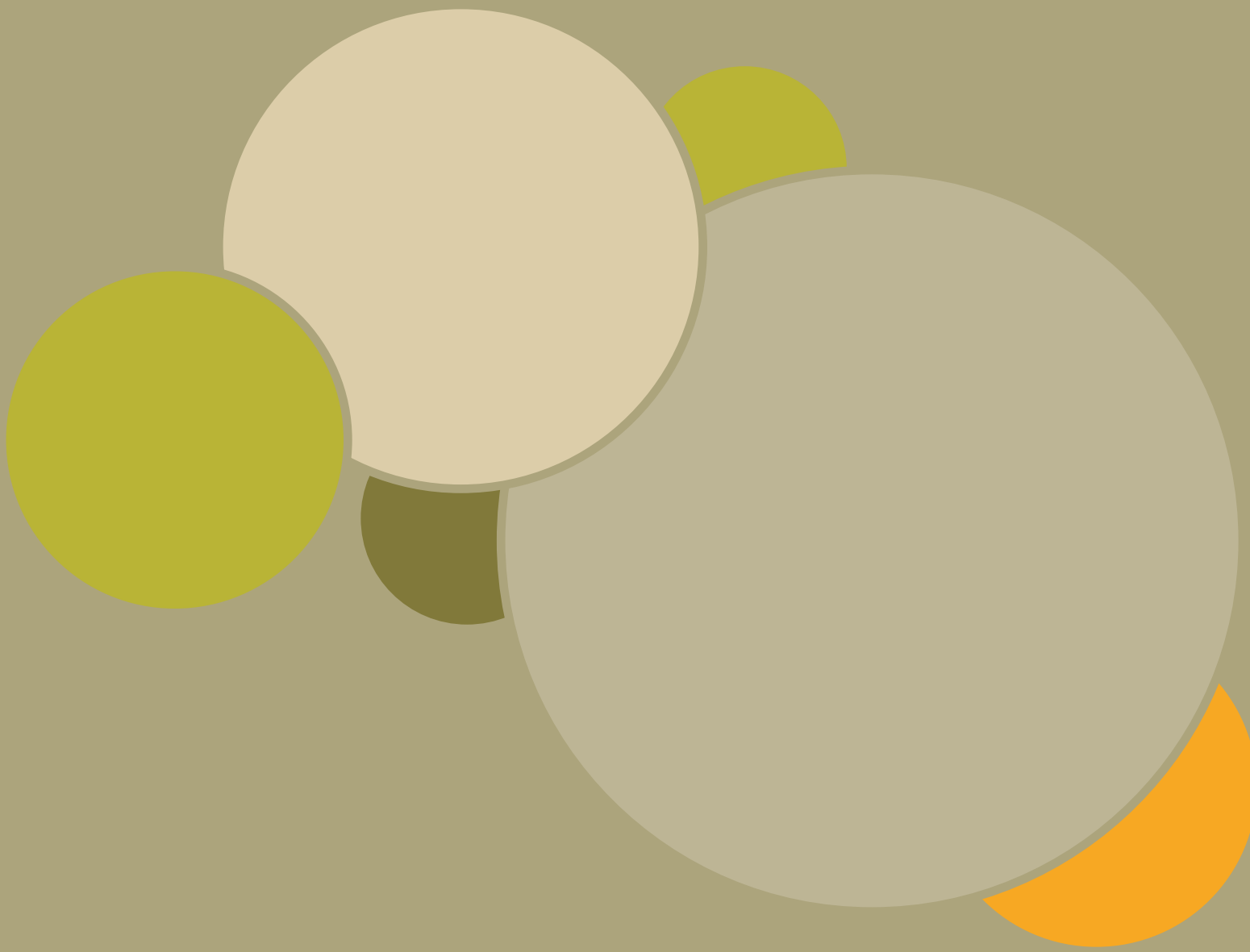

4

Chapter 4

Detailed crop mapping using remote sensing data (Crop Data Layers)

Andrew M. Davidson, Thierry Fisette, Heather McNairn and Bahram Daneshfar

4.1. INTRODUCTION

Understanding the state and trends in agricultural production at a national scale is essential to combat short- and long-term threats to the stable and reliable access to food for all. However, quantifying food supply can be difficult because national, regional and global crop production fluctuates due to local land management decisions and ever-changing meteorological conditions (Fischer *et al.*, 2005). Forecasting food supply (production) necessitates ongoing and frequent updates on the crop acres seeded and their yields (Lobell and Field, 2007; World Bank, UN & FAO, 2010; Waldner *et al.*, 2015). Obtaining this information requires detailed, routine and rapid mapping of croplands with sufficiently high accuracy (Gallego *et al.*, 2008).

Remotely sensed data from Earth Observation (EO) satellites are the most cost-effective means for gathering spatially explicit, timely, detailed and reliable information over large land areas with high revisit frequency (Atzberger *et al.*, 2016). Such information, integrated with national statistics, in situ (ground) observations and secondary (ancillary) data and information, show potential for mapping crop acreages (Gallego, 2004; Kussul *et al.*, 2016). However, delivering an accurate inventory of crops requires the selection of appropriate satellite data, the collection of quality ground information, the application of suitable pre- and post-processing methods and the implementation of robust methodologies. This is a challenge because cropping systems are often diverse and complex, and the types of crops grown and the timing of their growth vary from region to region, as do the management practices implemented. Consequently, the success of remote sensing approaches requires their adaptation to local cropping systems and environmental conditions.

The last decade has seen many attempts to articulate the spatially explicit remote sensing data requirements to map cropping systems, and particularly, where (Fritz *et al.*, 2015), when (Whitcraft *et al.*, 2015a), how frequently

(Whitcraft *et al*., 2015b), over which spectral range, and at what spatial resolution data are needed (Whitcraft *et al*., 2015c). Elucidating the best data and methodologies for crop mapping remains a high priority commitment on the international research agenda. Indeed, various international efforts have been established to reach a convergence of approaches and develop monitoring and reporting protocols and best practices for a variety of global agricultural systems (such as the Group on Earth Observations Global Agricultural Monitoring (GEOGLAM) initiative, which includes the Joint Experiment of Crop Assessment and Monitoring (JECAM), the Asian Rice Crop Estimation and Monitoring initiative (Asia-RiCE), the Stimulating Innovation for Global Monitoring of Agriculture activity (SIGMA), and contributions from the Sentinel-2 for Agriculture system (Sen2-Agri)).

The overarching goal of this chapter is to provide an overview of remote-sensing-based approaches for detailed (field-level) annual crop mapping at a national scale. First, an overview of existing remote-sensing-based approaches used for cropland mapping is presented. This includes a brief overview of supervised image classification and pixel-based versus object-based classification. Second, the various types of satellite data, ground data and secondary data used for detailed crop mapping are discussed. Third, the operational implementation of a national crop mapping program is demonstrated with specific reference to the Annual Crop Inventory for Canada. Finally, the main future challenges and opportunities for crop type mapping at national scales are outlined.

4.2. SATELLITE IMAGE CLASSIFICATION FOR DETAILED CROP MAPPING

4.2.1. The supervised classification of satellite imagery

Satellite image classification is a fundamental tool for many remote sensing applications. In the broadest sense, it involves the implementation of automated techniques that can identify different surface types in one or more spectral bands to produce a thematic map with little or no user interaction (Jones and Vaughan, 2010). During this process, image data (pixels or objects, see section 2.2) are sorted automatically into one of a finite number of target classes on the basis of their spectral characteristics.

In most cases, crop maps are generated using supervised classification (Beltran and Belmonte, 2001; Congalton *et al*., 1998). The supervised classification approach requires significant a priori human intervention, and is generally implemented in four main steps: (i) an image analyst uses in situ (ground) observations to identify locations in the image data that correspond to each of the surface types (target classes) to be mapped (this reference data set is often referred to as a training sample, because it is used in subsequent steps to "train" the computer to recognize spectrally similar areas for each class); (ii) the classification algorithm matches these reference locations to the image data (and secondary data, if available) to statistically define the spectral (and non-spectral, if secondary data are available) characteristics of each target class; (iii) the algorithm then compares each pixel in the image to these signatures and assigns it to the target class which it most closely resembles; and (iv) the accuracy of the final classification is evaluated (validated) using a selection of ground reference points not used to train the classification (that is, the validation sample). The entire supervised classification process for detailed crop mapping is summarized in detail in figure 1.

Until recently, the Maximum Likelihood (ML) classification method was the most widely used method for the supervised classification of remote sensor data (Lu and Weng, 2007; Bhatta, 2008; Kumar *et al*., 2016). In this approach, training data are used to describe target classes statistically by their multivariate probability density functions. Each density function represents the probability that the spectral pattern of a class falls within a given region in multidimensional spectral space (Denègre, 2013). Image data are then assigned to the training class of which it has the highest likelihood of being a member (Jensen, 1986). The ML approach has been widely applied in different studies for the satellite image classification of agricultural regions (Laba *et al*., 1997; Xiuwan, 2002; Abdulaziz *et al*., 2009; Kamusoko and Aniya, 2009; Rogan *et al*., 2008). However, limitations associated with this

approach – particularly, its reliance on the Gaussian distribution of input data, an assumption that is often violated when using multi-temporal image data (Gislason *et al*., 2006; Glanz *et al*., 2014) – mean that the development of alternative classification techniques continues to be an active area of research in agricultural remote sensing. Of these new methods, artificial neural networks (ANNs – see Rumelhart *et al*., 1986; Rigol-Sanchez *et al*., 2003), support vector machines (SVMs – see Abedi *et al*., 2013; Al-Anazi and Gates, 2010; Cortes and Vapnik, 1995; Ghimire *et al*., 2012; Zuo and Carranza, 2011), Decision Trees (DTs – see Breiman, 1984) and ensembles of classification trees such as Random Forest (RF – see Breiman, 2001; Vincenzi *et al*., 2011; Waske and Braun, 2009; Ghimire *et al*., 2012; Rodriguez-Galiano and Chica-Olmo, 2012) have all shown great promise.

FIGURE 1. THE STEPS IN A SUPERVISED CLASSIFICATION. THE AGRICULTURE AND AGRI-FOOD CANADA (AAFC) APPROACH TO CROP MAPPING AT THE FIELD (PARCEL) LEVEL FOLLOWS THE RED ARROWS.

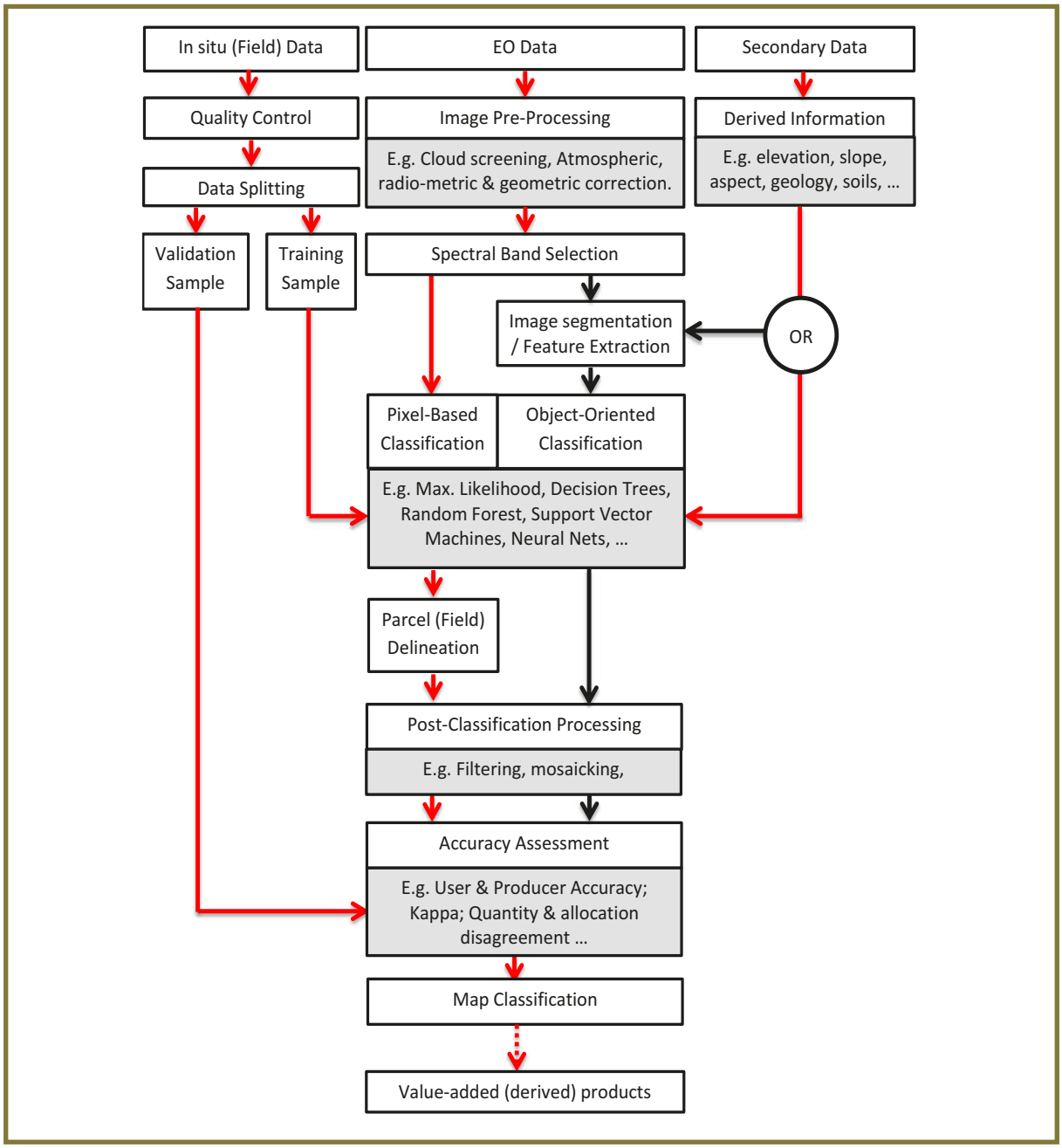

4.2.2. Pixel-based versus object-based classification

The supervised classification of satellite imagery has traditionally been implemented on a pixel-by-pixel basis. However, the spatial variability of each input layer or band is much less within the field of a single crop than between fields of different crops. As a result, more recent attempts to improve pixel-based crop mapping accuracies have focused on the development of methods that focus on the classification of homogeneous aggregations of pixels, known as objects. The most common approach used to generate image objects is image segmentation (Benz *et al*., 2004). Image segmentation involves the decomposition of an image into homogeneous non-overlapping regions through the grouping of pixels in accordance with determined criteria of homogeneity and heterogeneity to produce objects that are spatially and spectrally heterogeneous (Haralick and Shapiro, 1985; Comaniciu and Meer, 2002; Benz *et al*., 2004). Feature extraction involves the subsequent extraction of the various spectral, textual, morphic and contextual attributes associated with each of the objects created in the segmentation process (Blaschke, 2010). Classifications can then be performed on image objects, using the object-specific feature information as an additional input to the classifier. This is referred to as object-oriented classification (Jensen, 1986). Successful applications of this approach for crop identification and mapping have been demonstrated by Evans *et al*. (2002), Brown de Coulston *et al*. (2003), Castillejo-González *et al*. (2009), McNairn *et al*. (2009), Peña-Barragán *et al*. (2011) and Vieira *et al*. (2012).

4.3. INPUT DATA LAYERS REQUIRED FOR CROP CLASSIFICATION

Irrespective of the exact method(s) used, the supervised classification of crop types involves the use of multiple types of data during the classification process. These are: (i) in situ (ground) data; (ii) satellite data; and (iii) ancillary (secondary) data and information (Teleguntla *et al*., 2016). When these data are of high quality and are used in an integrated fashion, the output mapping produces the highest possible accuracies (Thenkabail *et al*., 2009a and 2009b). In this section, we outline the main considerations when collecting high quality in situ, satellite and ancillary data for agricultural classification.

4.3.1. Ground (*in situ*) data

The quality of in situ (ground) observations is of great importance to cropland mapping because these data are used not only to train the supervised image classifications from which crop maps are derived, but also because they are used as independent reference data to validate these maps. The quality of ground data has a significant impact on the delivery of an accurate classification; therefore, practitioners must pay careful attention to how these data are collected. Traditionally, ground data used in crop classification have been collected via crop field surveys. In this approach, users visit fields and record information about the crop grown – such as crop type, cultivar, growth stage, etc. – along with the geographic location of the observation with a Global Positioning System (GPS). The objective of surveying is to sample the diversity of crop types within the region of interest as representatively as possible. Doing so requires that a sufficient number of samples be collected for each target class.

The temporal and spatial characteristics of the sampling designs used to collect in situ observations influence the quality of satellite-derived crop maps. The timing of field surveys is usually determined by the local crop calendar. Crop calendars describe when the major growing phases of particular crops occur each year (see figure 2). For best results, site visits should coincide with the period in crop growth during which the crop type can most easily be identified. Typically, this will occur during the periods of flowering, fruit development and reproduction. For regions with a simple single cropping season, one observation per field per season is usually adequate. If multiple crops are

grown on the same field over the course of a year (at the same time or separately), one visit to the site per crop cycle is required. While the most appropriate ways to locate representative, non-biased and spatially independent field samples are well documented, these approaches can rarely be implemented operationally. Instead, sampling is often provided by "windshield surveys", in which data are collected along road networks from motorized vehicles. While this approach allows a data collector to easily and rapidly capture the entire crop diversity from all visible fields, the spatial non-randomness of collected data can introduce statistical bias that must be evaluated carefully before use.

FIGURE 2. CROP CALENDARS FOR (A) WHEAT AND (B) RICE.

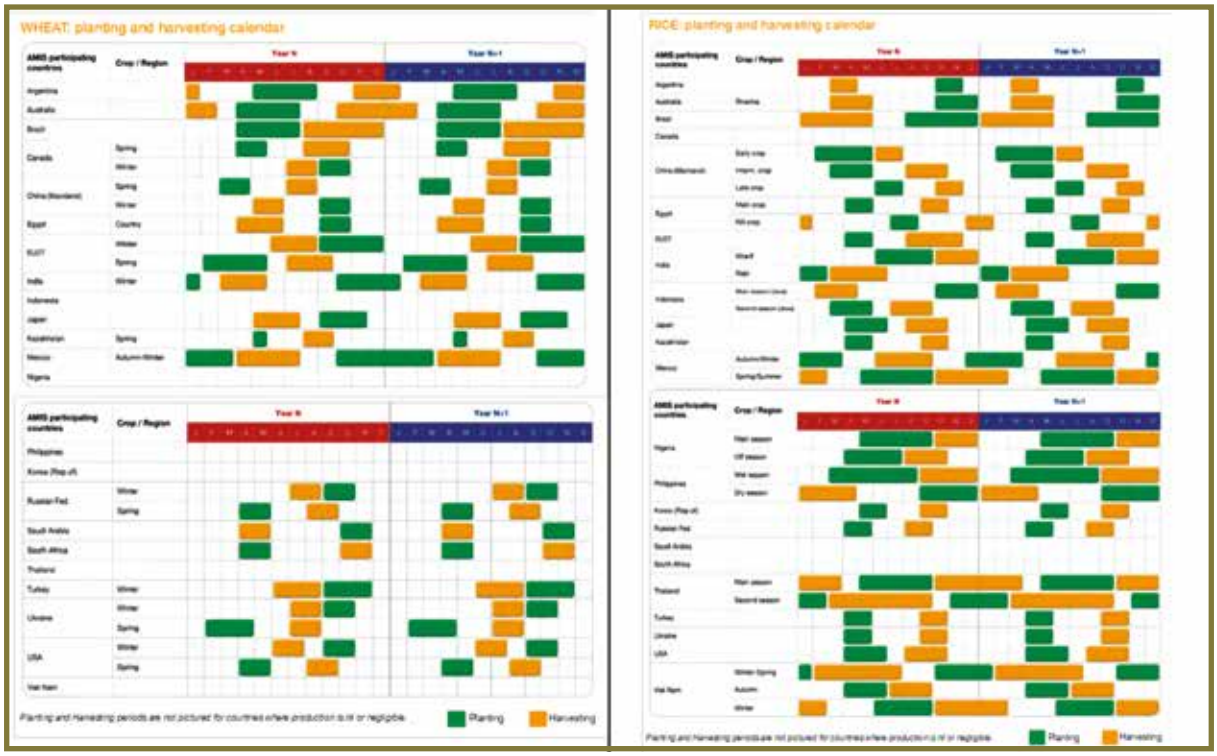

The dates of planting and harvesting determine the sampling period over which remote sensing and ground observations must be acquired for space-based crop mapping (AMIS, 2012).

It is often difficult to determine a priori the sample size necessary to train the image classifier. Although overall classification accuracies generally increase with the number of fields used in the training process, the exact nature of this relationship is complex and differs among crop classes. The number and quality of the images acquired as input to the classification also influence the number of fields to be sampled. For example, larger sample sizes are required if the variability in spectral response within each crop class is not sufficiently characterized to permit crop discrimination. However, because such factors cannot generally be predicted a priori, ground sampling often results in undersampling for some crop types and oversampling for others.

The biggest disadvantage of field surveys is that they are labour-intensive, time-consuming and challenging when the goal is to acquire representative data at national and regional scales. Consequently, other reliable sources of data must usually be considered to supplement ground surveys (or replace them entirely). These sources include data collected by local, regional or national government agencies or, more informally, through crowdsourcing. Ground data provided by government agencies are usually the most accurate, detailed and complete sources of information available for crop type mapping, although they still require considerable evaluation to ensure their readiness for use in classification. Although future potential exists, crowdsourcing – the process of obtaining information by enlisting

the services of a large number of people, either paid or unpaid, via the Internet – has not yet become a widely used method for collecting ground data for crop classification purposes.

4.3.2. Earth Observation (EO) Data

4.3.2.1. EO data sources for successful crop classification

The coordination of Earth Observation (EO) data for agricultural monitoring necessitates the articulation of spatially explicit EO data requirements, including on where (Fritz *et al*., 2015), when (Whitcraft *et al*., 2015a), how frequently (Whitcraft *et al*., 2015b), over which spectral range, and at what spatial resolution these data are needed (Whitcraft *et al*., 2015c). Because cropping systems are often diverse and complex, and the types of crops grown and the timing of their growth vary from region to region, the best choice of sensors to be used, the optimal number of images required, and the timing of image acquisitions are usually geographically specific.

The decision to use optical or synthetic aperture radar (SAR) is usually determined by the trade-off among a number of factors, including: (a) the heterogeneous and dynamic intrinsic nature of the agro-ecosystem being studied; (b) the geographical extent to be mapped; (c) the Minimum Mapping Unit (MMU) required to resolve individual fields and other meaningful ecological units (wetlands, woodlots, etc.); (d) differences in crop cycles; (e) differences in cropping practices and calendars within the same class; (f) the spectral similarity with other land cover classes; and (g) the engineering constraints of the remote sensing systems (swath size; spatial, temporal, spectral and radiometric resolutions; and cloud coverage for optical systems); and (g) data availability (whether open or fee-based; Waldner *et al*., 2015). These sensor-focused considerations are summarized in table 1, which briefly illustrates the sensor characteristics required to create various crop-related map information products for the Group on Earth Observation's (GEO) Global Agricultural Monitoring (GLAM) initiative (also known as GEOGLAM).

TABLE 1. THE TABLE OF REQUIREMENTS FOR SATELLITE-BASED EARTH OBSERVATIONS DATA, DEVELOPED BY THE CEOS AD HOC TEAM FOR GEOGLAM (CEOS, 2014; GEOGLAM, 2014).

Spatial Resolution	Spectral Range	Effective observ. frequency (cloud free)	Field Size	Target Information Products and Applications						
				Crop Mask	Crop Type Area and Growing Calendar	Crop Condition	Crop Yield	Crop Biophysical Variables	Environ. Variables	Ag Practices / Cropping Systems
Coarse Resolution Sampling (>100m)										
>500-2000 m	optical	Daily	All			X		L		
100-500 m	optical	2 to 5 per week	All	X	X	X	L	L	X	L
5-50 km	microwave	Daily	All			X	X	X	X	
Moderate Resolution Sampling (10 to 100m)										
10-70m	optical	Monthly (min 2 out of season + 3 in season). Required every 1-3 years.	All	X	L/M					X
10-70m	optical	~Weekly (8 days; min. 1 per 16 days)	All	X	X	X	X	X	X	X
10-100m	SAR Dual Polarization	~Weekly (8 days; min. 1 per 16 days)	All	X	X	X	X	X	X	X
Fine Resolution Sampling (5 to 10m)										
5-10 m	VIS, NIR, SWIR	Monthly (min. 3 in season)	M/S	M/S	M/S					
5-10 m	VIS, NIR, SWIR	~Weekly (8 days; min. 1 per 16 days)	All		M/S	X		X	X	X
5-10 m	SAR Dual Polarization	Monthly	M/S	M/S	M/S					M/S
Very Fine Resolution Sampling (<5m)										
< 5 m	VIS, NIR	3 per year (2 in season + 1 out of season); Required every 3 years	S	S	S					
< 5 m	VIS, NIR	1 to 2 per month	All		X		X			X

Requirements are broken down by spatial & spectral range, frequency with which reasonably cloud-free data are required, geographic extent, as well as the application or target product for which the data would be used. Requirements are refined based on field size over which acquisitions are required, or the field sizes for which a certain data type would be useful. "L" refers to "Large fields" (>15 ha), "M" refers to "Medium fields" (1.5–15 ha), and "S" refers to "small fields" (<1.5 ha). The symbol "x" or the word "All" indicates that these data are useful for that product's generation for all field sizes (Whitcraft *et al.*, 2015c).

4.3.2.2. Optical satellite data

Optical remote sensors collect spectral observations in the visible, near-infrared (NIR) and short-wave infrared (SWIR) wavelengths to form images of the Earth's surface by detecting the solar radiation reflected from targets on the ground. These sensors are well-suited for mapping vegetation because observations from their primary imaging bands (usually, blue, green, red, NIR and SWIR) can be used to readily distinguish the unique spectral signatures of vegetation from other surface covers. In the visible, NIR and SWIR regions of the electromagnetic spectrum, the amount of ambient solar energy absorbed, reflected and transmitted by vegetation is mainly determined by plant pigmentation, internal leaf structure and moisture content, respectively (Jensen, 1986). These physical and chemical responses (at the atom level) are crop-specific and indicative of the growth stage and condition of the plant. As a result, the shape and magnitude of reflectance spectra spanning these wavelengths is often used to differentiate among different vegetation types. However, using optical sensors for crop monitoring is not without challenge. Because these sensors are passive and depend on the Sun as the sole source of illumination, their images can only be collected during the daytime and under clear skies. In addition, factors other than the presence and amount of green vegetation (senescent vegetation, woody biomass, soil and shadow) often combine to form composite spectra, and this often makes the discrimination of green vegetation difficult (Colwell, 1974). This has prompted the development and application of spectral vegetation indices (VIs), which combine two or more spectral bands to enhance the vegetative signal, while minimizing background effects.

At national to global scales, agricultural mapping has mostly been undertaken using cloud-free coarse resolution (greater than 100 m) observations from sensors such as SPOT-VGT (Bartholomé and Belward, 2005 – Global Land Cover 2000), NOAA-AVHRR (Loveland *et al*., 2000 – IGBP DISCover; Hansen *et al*., 2000 – UMD Global Land Cover; Defries *et al*., 2003 – Global AVHRR Land Cover; Defries and Townshend, 2003 – Global AVHRR NDVI Land Cover), NASA-MODIS (Friedl *et al*., 2002 - MODIS Global Land Cover; Tateishi *et al*., 2011 – Global Land Cover by National Mapping Organizations) and ENVISAT-MERIS (Arino *et al*., 2008 – GlobCover). While the large swath width of these systems provide the large synoptic views and daily revisit frequencies required for the phenology-based classification of vegetation, their use in detailed crop classification of smallholder agriculture is limited by their coarse resolution pixels, which are often unable to resolve individual fields (Wardlow *et al*., 2007; Wardlow and Egbert, 2008; Ozdogan, 2010). As a result, these efforts have tended to map agriculture using one or two very broad classes that are insufficient for detailed crop area estimation, or provide additional phenologically related information to supplement studies using finer-resolution observations. Nonetheless, exceptions occur in agricultural regions with large fields, or where techniques for unmixing the contributing surface components of mixed pixel spectra can be implemented (Jakubauskas *et al*., 2002; Lunetta *et al*., 2006; Chang *et al*., 2007; Fritz *et al*., 2008; Galford *et al*., 2008; Lunetta *et al*., 2010; Sakamoto *et al*., 2010; Pan *et al*., 2012; Brown *et al*., 2013; Waldner *et al*., 2016).

At regional to national scales, agricultural mapping has mostly been undertaken using multispectral observations from moderate-resolution (10 m to 100 m) sensors, particularly Landsat, whose data are available free of charge (Badhwar, 1984; Reese *et al*., 2002; Guerschman *et al*., 2003; Turker and Arikan, 2005; McNairn *et al*., 2009; Fisette *et al*., 2013; Johnson, 2013; Fisette *et al*., 2014; Yan and Roy, 2014; Fisette *et al*., 2015). However, while the spatial resolution of these sensors is sufficient to resolve individual fields, their temporal revisit times are much less frequent than the daily overpasses of the NOAA-AVHRR, SPOT-VGT and NASA-MODIS orbiters (Landsat-7 and Landsat-8 missions offer an eight-day revisit time, with each individual satellite revisiting every 16 days). Such large gaps between revisit times are problematic in regions with persistent cloud cover, where the number of cloud-free images necessary for detailed crop mapping is rarely obtained (Jewell, 1989; McNairn *et al*., 2002; Blaes *et al*., 2005; McNairn *et al*., 2009). In such cases, data from other moderate-resolution multispectral sensors are available to fill the data gaps, though these may be fee-based (such as SPOT, AWIFS and DMC), operate at coarser spatial resolutions (such as AWIFS, the resolution of which is 56 m), contain fewer spectral imaging bands (SPOT, DMC), or be subject to other technical or access constraints. In the future, synergies between operational programs such as Landsat and Sentinel-2 (Wulder *et al*., 2015) will contribute greatly to filling these data gaps by raising

the frequency of geometrically and radiometrically compatible acquisitions (Gómez *et al*., 2016), and providing global observations with a two- to five-day frequency (Drusch *et al*., 2012; Irons *et al*., 2012; Wulder *et al*., 2015).

At local scales, agricultural mapping has mostly been undertaken using observations from fine-resolution (lesser than 10 m) sensors, such as RapidEye (Tapsall *et al*., 2010; Conrad *et al*., 2011; Kim and Yeom, 2014; Ustuner *et al*., 2014; Beyer *et al*., 2015; Schuster *et al*., 2015; Lussem *et al*., 2016; Xu *et al*., 2016), and to a lesser degree, IKONOS (Xie *et al*., 2007; Turker and Ozdarici, 2011), Quickbird (Yang *et al*., 2007) and WorldView (Alabi *et al*., 2016). While fine-resolution remote sensing has been shown to increase field-level crop mapping accuracies in regions with small field sizes (Salehi *et al*., 2013), they have generally not been used operationally for comprehensive wall-to-wall national-scale agricultural mapping over large regions or countries (mostly due to their cost and the computational overhead of processing such large data volumes). Instead, their suitability for characterizing subfield variability in growth conditions has seen these data targeted towards precision agriculture, and the management of farm inputs such as fertilizers, herbicides, seed and fuel (used during tillage, planting, spraying, etc.).

4.3.2.3. SAR Data

SAR remote sensors propagate energy at microwave frequencies and measure the intensity and phase of energy scattered following interaction with a target. These sensors provide their own source of energy and are thus able to operate both day and night. The lower-frequency microwaves used by SARs are unaffected by atmospheric conditions, meaning that data collection is successful even in the presence of cloud cover. Sensing in the microwave portion of the electromagnetic spectrum makes SARs well-suited for discriminating among vegetation types because the scattering at these longer wavelength is driven by crop-specific larger-scale structures (size, shape and orientation of leaves, stems and fruit) as well as by the volume of water in the vegetation canopy (at the molecule level). However, as in the case of optical data, using data from SARs for crop monitoring is not without challenge. This is primarily due to the confounding contributions of soil properties (moisture and roughness) to the radar signal. The significance of the effects of these soil conditions depends upon the crop type and growth stage, and the configuration of the microwave sensor. Nevertheless, results from research (Blaes *et al*., 2005; McNairn *et al*., 2009; Larrañaga *et al*., 2011) and operations (Fisette *et al*., 2015) have shown that the integration of SARs can increase accuracies over the use of optical data alone.

SAR sensors are defined by their operating frequency, incident angle and polarization. Frequency (GHz or wavelength (in cm)) determines the penetration depth of the microwave into the crop canopy, and which crop canopy components (leaves, fruit, stalks) interact with the signal, and how. No single frequency is best for separating all crops, because penetration into the canopy must be deep enough to allow the microwaves to interact with the dominant plant structure, but not so deep that soil properties affect the SAR response. This optimal depth of penetration, and matching of the wavelength to the size of crop structures, varies from crop to crop and throughout each crop's development. As such, most researchers advocate the use of multiple frequencies for crop classification (Skriver *et al*., 1999; Hill *et al*., 2005; Baghdadi *et al*., 2009; McNairn *et al*., 2009; Shang *et al*., 2009; Hoekman *et al*., 2011; Haldar *et al*., 2012; Jia *et al*., 2012; Skriver, 2012). Currently, implementing a multi-frequency approach is challenging due to limitations in the availability, in operational terms, of data from sensors at different frequencies. Thus, approaches to date have generally been to integrate single-frequency SAR with optical data (see for example McNairn *et al*., 2009; Hütt *et al*., 2016).

The optimal SAR polarizations for crop classification are easily defined. The linear cross-polarization (either horizontal-vertical – HV – or vertical-horizontal – VH) provides the best separation of crops (McNairn *et al*., 2009; Koppe *et al*., 2013; Sonobe *et al*., 2014). The repolarization which must occur to produce a significant HV or VH response happens when the signal undergoes multiple scattering within the canopy. The vertical-vertical (VV) polarization is also useful in identifying crops as the vertical transmit waves are attenuated or scattered by the

vertical structure of many crops. Horizontal-horizontal (HH) is the least informative polarization. The incident angle also has an impact on penetration into the crop canopy; however, the selection of this angle is the least important consideration.

As with optical sensors, the selection of the SAR swath and resolution depends upon the region in question on the trade-off between the field size and the area to be mapped. The selection of the SAR orbit (ascending or descending) must also be considered. In temperate regions, humidity coupled with low overnight temperatures can cause dew to form on canopies. This early morning dew affects the backscatter (Gillespie *et al*., 1990). Some research has suggested that although backscatter increases in the presence of dew, the effect is observed across crop types and may have minimal effect on crop separability (Wood *et al*., 2002). Nevertheless, research on dew effects is limited; therefore, early-morning acquisitions should be avoided where possible.

4.3.2.4. Optical and SAR data pre-processing

Optical and SAR data must usually be subject to various pre-processing routines before they can be used as input to classification algorithms for mapping agricultural landscapes. The exact natures of these routines – which are used to correct for radiometric and geometric distortions of data – depend on the specific sensors and platforms used to acquire the data, the atmospheric conditions during data acquisition and the methods used in the classification process. Radiometric distortions can result from variations in scene illumination and viewing geometry, atmospheric conditions, and sensor noise and response. Geometric distortions may result from the motion of the platform, the motion of scanning systems, variations in platform altitude, attitude and velocity, terrain relief and the Earth's curvature and rotation. Corrections are intended to compensate for these distortions so that the geometric and radiometric representations of the imagery will be as close as possible to the real world. However, in reality, the actual amount of image preprocessing required from users will depend on the processing level of data acquired. Higher-level data products – often made available by space agencies as analysis-ready data suitable for direct use in scientific publications – have more pre-processing done at source compared to lower-level products, which require more preprocessing to be completed by the end user.

4.3.3. Ancillary (secondary) data and information

Ancillary (secondary) data and information come from sources other than remote sensing, and can be used to improve classification accuracy. Ancillary data refers to additional context variables that can be integrated with remote sensing data at various stages during the image classification process. These variables may include, but are not limited to, elevation, slope, aspect, hydrology, geology, soils, transportation networks, political boundaries and vegetation maps (Jensen, 2016). Ancillary data can be incorporated before the image classification process (such as for a priori image stratification; see Jensen, 2016), during the image classification process (for example, as input into classification: Maselli *et al*., 1995; Huang and Jensen, 1997; Stow *et al*., 2003; Qiu and Jensen, 2004) or after the image classification process (for example, for post-classification sorting: see Rocha and Queluz, 2002). Ancillary information refers to additional expert knowledge that can be incorporated into the classification process. This may include evidence regarding the most plausible landscape configurations resulting from the classification process. For example, ancillary information, implemented through Bayesian networks (Jensen and Nielsen, 2007), has been shown to allow for the incorporation of expert knowledge into complex classification tasks and the characterization of phenomena through plausible reasoning inferences based on evidence (Atzberger *et al*., 2016). However, while useful, great care must be taken to minimize the introduction of new errors while incorporating ancillary data and information into a classification system.

4.4 OPERATIONAL CROP MAPPING AT THE NATIONAL SCALE

4.4.1. Moving from the research to the operations domain

National operational agricultural monitoring systems should provide timely, standardized and interchangeable crop-related information with statistically valid precision and accuracy (Atzberger *et al*., 2016) and be based on robust, consistent and repeatable data and methodologies (Franklin and Wulder, 2002). The implementation of such systems, built on a foundation of research and development, requires confidence that the methods developed (and data used) at regional scales are robust enough to be geographically portable over much larger areas where access to data (EO or in situ) may not be as easy (Bontemps *et al*., 2012; Gong *et al*., 2013). However, the actual transition from the research domain to the operations domain is usually non-trivial. This is because the transition pathways from research to operations and applications are characterized by a variety of challenges and potential barriers. These include, but are not limited to: (a) the lack of scientific understanding; (b) difficulties associated with extending scientific understanding or technological capability to operational utility; and (c) limitations to observing technologies, to the understanding of how to use the observations effectively or to the computational power required to use the observations in operational models (National Research Council of the National Academies, 2003). It is also important to note that the research-operations relationship is not unidirectional. Operational systems must be dynamic, and require ongoing improvements based on changing needs, emerging research and ever-improving and changing satellite data streams and in situ data networks. Consequently, research must remain at the core of the operational system throughout and beyond implementation (GEOGLAM, 2015).

4.4.2. Agricultural monitoring systems

In the past 40 years, numerous initiatives have focused on the derivation of cropland from satellite imagery. These initiatives have been carried out using a vast diversity of mapping strategies at global, subcontinental and national scales (table 2; Waldner *et al*., 2015). While most of these initiatives lasted only a short period of time, some continue today in an operational context.

The primary global monitoring systems include: (a) the USAID Famine Early Warning System (FEWS-NET); (b) the Food and Agriculture Organization of the United Nations (FAO) Global Information and Early Warning System (GIEWS); (c) the Monitoring Agriculture by Remote Sensing (MARS) Project of the European Commission, at the Joint Research Center (JRC); (d) the Crop Watch Program at the Institute of Remote Sensing Applications (IRSA) of the Chinese Academy of Sciences; and € the USDA Foreign Agricultural Service (FAS) Global Agriculture Monitoring (GLAM) System (Becker-Reshef *et al*., 2010). Despite the utility of these initiatives for global agricultural monitoring, they are generally limited by their relatively coarse sampling resolutions (often greater than 10km), lack of detail within crop classes, lack of validation and large uncertainties (Vancutsem *et al*., 2012; Waldner *et al*., 2015) that make them unsuitable for detailed national crop mapping at the parcel level.

At the subcontinental or national scale, the use of much finer-resolution imagery (that is, 30 m or finer) has allowed for more detailed and more accurate crop mapping to be implemented at the parcel (field) level. Examples of such activities include:

a. the United States Cropland Data Layer (CDL), generated annually by the United States Department of Agriculture (USDA) National Agricultural Statistics Service (NASS) (using UK-DMC 2 and Landsat-8 optical imagery);
b. the United Kingdom Land Cover Plus: Crops (LC+ Crops) data set, generated annually by the United Kingdom's Centre for Ecology & Hydrology (CEH) in collaboration with Remote Sensing Applications Consultants Ltd (RSAC) (using Sentinel-2 optical imagery and Sentinel-1 C-band SAR);
c. the Chinese Agriculture Remote Sensing Monitoring System (CHARMS) and the China Crop Watch System (CCWS), with products generated submonthly by the Ministry of Agriculture (MOA) and the Chinese Academy of Sciences (CAS) (using medium- (lesser than 30 m; for example, HJ-1 CCD, GF-1, Landsat-5,-7 and -8, SPOT, IRS, Envisat) and low-resolution imagery (from 250 m to 1000 m; such as MODIS, AVHRR));
d. the Pakistan Agricultural information System (AIS), with products generated seasonally by the Pakistan National Space Agency (SUPARCO) and the Ministry of Food and Agriculture (MINFA), in collaboration with FAO (using SPOT-5 optical imagery);
e. the Indian Crop Acreage and Production Estimation (CAPE) program, with land use mapped annually by the Indian Ministry of Agriculture (using RESOURCESAT-1 and -2 optical imagery and RISAT-1 and -2 SAR data);
f. the Russian VEGA-PRO satellite-based service for vegetation monitoring, generated sub-annually by the Russian Academy of Sciences, with support from the Skolkovo Foundation;
g. the Sentinel-2 for Agriculture system (Sen2-Agri), with products generated frequently during the growing season by the European Space Agency (ESA) (using Sentinel-2 optical imagery).

TABLE 2. A SURVEY OF NATIONAL, REGIONAL AND GLOBAL LAND COVER MAPS (BASED ON WALDNER *et al.*, 2015). THE TABLE ONLY CONTAINS PUBLICLY-AVAILABLE DATA. DATA SETS HAVING A DISTRIBUTION POLICY THAT PREVENTS THEIR USE OR ACCESS ARE NOT CONSIDERED.

Extent	Product Name and Reference	Time Period
Global		
	FROM-GLC (Gong *et al.*, 2013)	2013
	Global Cropland Extent (Pittman *et al.*, 2010)	2000–2008
	GlobCover 2009 (Arino *et al.*, 2008)	2009
	Climate Change Initiative Land Cover (CCI) (Defourny *et al.*, 201X)	2000, 2005, 2010
	MODIS Land Cover Type MOD12Q1, 2005 (NASA)	2005
	GLC-Share, Food and Agriculture Organization (Latham *et al.*)	1990–2014
	IIASA-IFPRI Cropland (Fritz *et al.*, 2015)	1990–2012
	GLC2000 (Bartholomé and Belward, 2005)	1999–2000
	International Geosphere-Biosphere Programme (IGBP) (Eidenshink and Faundeen, 1994)	1992–1993
	Global Map-Global Land Cover (GLCNMO) (Tateishi *et al.*, 2011)	2007–2009
Regional		
	Corine Land Cover, European Environment Agency (EEA)	2006
	Southern African Development Community Land Cover database, Council for Scientific and Industrial Research (CSIR)	2002
	Cropland Mask of Africa, Joint Research Centre (JRC) (Vancutsem *et al.*, 2012)	2012
	North American Environmental Atlas, Commission for Environmental Cooperation (CEC)	2005
	Land Cover Map of Latin America and the Caribbean (Blanco *et al.*, 2013)	2008
	Congo Basin Map (Verhegghen *et al.*, 2012)	2000–2007
Congo, Burundi, Egypt, Eritrea, Kenya, Rwanda, Somalia, Sudan, United Republic of Tanzania, Uganda	Africover, Food and Agriculture Organization (FAO)	1999–2001
Senegal, Bhutan, Nepal	Global Land Cover Network (GLCN)	2005–2007
France, Belgium, the Netherlands	Land Parcel Identification System	2012–2014
Barbados, Rep. Dominicana, Dominica, Grenada, Puerto Rico, Saint Kit and Nevis, Virgin Islands	United States Geological Survey (USGS)	2000–2001
Fiji, Solomon Islands, Timor Leste, Niue, Naurau, Palau, Tonga, Tuvalu, Vanuatu, Kiribati, Marshall Islands, Micronesia, Cook Islands	Applied Geoscience and Technology Division (SOPAC)	1999–2010
Botswana, Namibia, Rwanda, Zambia, United Republic of Tanzania, Malawi	Land Cover Scheme II, the Regional Visualization and Monitoring System (ICIMOD-SERVIR)	2010

Extent	Product Name and Reference	Time Period
National		
China	GlobeLand30 (Chen *et al.*, 2015)	2009–2010
Japan	High Resolution Land Use-Land Cover Map, Japan Aerospace Exploration Agency (JAXA) (Takahashi *et al.*, 2013)	2006–2011
Tajikistan	(Thenkabail and Wu, 2012)	2010
Burkina Faso	Corine Database of Burkina Faso	2000
Canada	Annual Crop Inventory, Agri-Food Canada (AAFC) (Fisette *et al.*, 2013, 2014, 2015)	2011-present
Canada	National Resources of Canada (Latifovic *et al.*, 2004)	2005
USA	Cropland Data Layer, US Department of Agriculture (USDA) (USDA National Agricultural Statistics Service Cropland Data Layer. 2015).	2008-present
China	National Land Cover Map of China (Liu *et al.*, 2005)	1995–1996
Australia	Digital Land Cover Database (Lymburner *et al.*, 2011)	2011
Cambodia	Land Cover of Cambodia, Japan International Cooperation Agency (JICA)	2002
New Zealand	Land Cover DataBase v4 Ministry for the Environment	2004
South Africa	National Land Cover, CSIR	2000–2001
South Africa	National Land Cover, South African National Biodiversity Institute (SANBI)	2009
Uruguay	Land Cover of Uruguay, FAO	2010
Mexico	Land Cover of Mexico,Comisión Nacional para el Conocimiento y Uso de la Biodiversidad (CONABIO)	1999
Argentina	Cobertura y uso del suelo, Instituto Nacional de Tecnología Agropecuaria (INTA)	2006
Ecuador	Uso del Suelo departamento de Informacíon Ambiental	2001
Thailand	Royal Forest Department of Thailand	2000
Chile	Chile Corporacion Nacional Forestal	1999
India	Land Use Land Cover of India, National Remote Sensing Centre (NRSC) (Sreenivas *et al.*, 2015)	2012
Gambia	(Holecz *et al.*, 2013)	2013
United Kingdom	United Kingdom Land Cover Plus Crop Dataset (Natural Environment Research Council, 2015)	2015-present
Ukraine	Land Cover Ukraine (Lavreniuk *et al.*, 2015)	2010
Russia	TerraNorte Arable Lands of Russia (Bartalev *et al.*, 2011)	2014

4.4.3. Case Study: Canada's operational space-based Annual Crop Inventory

4.4.3.1. Adoption of EO by the Government of Canada

Agriculture and Agri-Food Canada (AAFC) – the government department responsible for Canada's agriculture and agrifood sector – has taken advantage of recent advances in satellite and sensor engineering and the proliferation of space-based EO missions to map and monitor agricultural land use and its change. This includes image data acquired by a multitude of satellites/sensors (such as Landsat-5, -7 and -8, RADARSAT-2, SPOT, DMC, RapidEye and Resourcesat-1) that span the optical and microwave regions of the electromagnetic spectrum and a range of spatial (pixel) resolutions (from 5 m to 56 m). There is already a significant body of published work by AAFC scientists that demonstrate the value of EO to provide useful national-extent, cost-effective, timely, accurate and scalable information on land use (McNairn *et al*., 2009; Shang *et al*., 2009; Deschamps *et al*., 2012; Fisette *et al*., 2013 and 2014; Champagne *et al*., 2014; Jiao *et al*., 2014; Liu *et al*., 2016) and its changes in time (Pei *et al*., 2011; Li *et al*., 2013; El-Khoury *et al*., 2014, 2015; Huffman *et al*., 2015). In the future, the AAFC's ability to meet the sector's informational needs is expected to improve as new satellite sensor technologies are launched, brought online and made available (such as Sentinel-1, -2 and -3; RADARSAT-Constellation). In this respect, the EO approach will be critical to the development of the AAFC's next generation of useful and authoritative informational products.

4.4.3.2. The space-based Annual Crop Inventory for Canada

One of the most valuable EO-based information products produced operationally by AAFC is the Annual Crop Inventory for Canada (or ACI; see figure 3). This information product – which is updated annually and available free of charge to the public via the Government of Canada's Open Data Portal – comprises a gridded (raster) map of the agricultural land use and non-agricultural land cover found within Canada's agricultural extent (Fisette *et al*., 2013 and 2014). While the earliest versions of the ACI (2009 and 2010) focused on the mapping of Canada's Prairie Provinces (Alberta, Saskatchewan and Manitoba), subsequent versions (2012 – present) have included the whole country. By providing highly accurate field-level information on detailed crop types, pasture and grassland, the ACI is an important foundational data set for supporting the development of programs and policy at the AAFC. Beyond the AAFC, the ACI provides important land use information for other departments of the Government of Canada, various provincial governments, producers, non-governmental organizations, universities and colleges, the private sector and the public.

FIGURE 3. MAP OF THE 2016 ANNUAL CROP INVENTORY FOR CANADA.

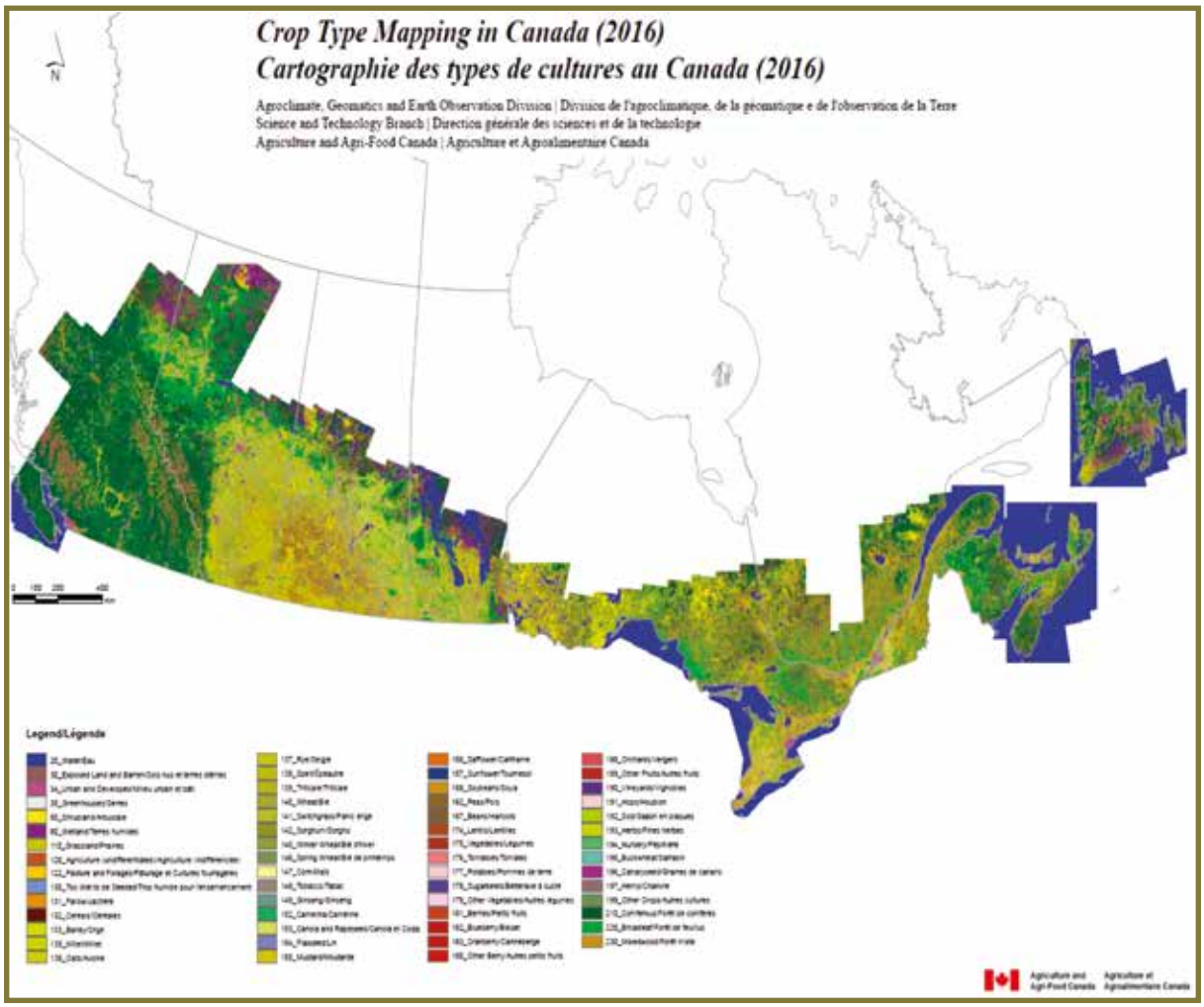

4.4.3.3. A Random Forest classification approach to land use and land cover mapping

The ACI is created by the application of classification methodologies that were developed and customized in-house at the AAFC (McNairn *et al*., 2009; Shang *et al*., 2009; Deschamps *et al*., 2012; Fisette *et al*., 2013, 2014; Champagne *et al*., 2014; Jiao *et al*., 2014; Liu *et al*., 2016). Original versions of the ACI used a classification methodology based on the application of DTs. This was primarily due to its successful implementation in various land use classifications compared to other supervised classification approaches (see, for example, Friedl and Brodley, 1997; Brown de Colstoun *et al*., 2003; Pal and Mather, 2003; Xu *et al*., 2005; Peña-Barragán *et al*., 2011; Deschamps *et al*., 2012; Vieira *et al*., 2012; Liu *et al*., 2016), and especially, its operational application to the annual CDL of the United States of America (Boryan *et al*., 2011). More recently, the AAFC switched its focus to use Random Forest (RF) classification approaches. RF has performed particularly well in agricultural monitoring, and high classification accuracies have been obtained for cropland sites not only in Canada (McNairn *et al*., 2009; Deschamps *et al*., 2012; Fisette *et al*., 2013, 2014 and 2015) but also elsewhere in the world (such as in the United States of America (Xie *et al*., 2007; Watts *et al*., 2009; Zhong *et al*., 2014), Argentina (Valero *et al*., 2016; Waldner *et al*., 2016), Brazil (Müller *et al*., 2015; Waldner *et al*., 2016), Peru (Tatsumi *et al*., 2015), China (Valero *et al*., 2016; Waldner *et al*., 2016; Hütt *et al*., 2016), the Russian Federation (Valero *et al*., 2016; Waldner *et al*., 2016) and the Ukraine (Valero *et al*., 2016; Waldner *et al*., 2016), Japan (Sonobe *et al*., 2014), Iran (Eisavi *et al*., 2015), Australia (Pringle *et al*., 2012), France (Valero *et al*., 2016), Burkina Faso (Valero *et al*., 2016) and South Africa (Valero *et al*., 2016)).

Since 2009, the AAFC has created its ACI by applying RF to various combinations of optical (Landsat-5, -7 and -8; Resourcesat-1; DMC; SPOT) and SAR (RADARSAT-2) imagery using discriminate functions estimated empirically from hundreds of thousands of ground-based (in situ) training data samples. The RF method is preferred because of its advantages over other methods and, with particular reference to AAFC operations, its demonstrated ability to handle discrete data, its processing speed (18 times faster than DT, according to Deschamps *et al*., 2012), its independence of the distribution of class signatures, its interpretable classification rules, its cost-effectiveness and demonstrated higher accuracies (Friedl and Brodley, 1997; Pal and Mather, 2003). The AAFC has also incorporated advanced options, such as pruning and boosting, into the DT classification process to improve the accuracy of the algorithm.

The AAFC performs its annual RF classifications on a region-by-region basis. This is because the dynamic nature of crop rotations, crop growth and harvest patterns create significant reflectance differences between adjacent satellite scenes within the temporal period encompassed by scene availability. While each classification region combines several dates of optical and SAR imagery, the actual combination of imagery per region can vary based on data availability. Region-by-region classification should be a consideration of any agency attempting to perform large-scale national mapping.

4.4.3.4. Ground (*in situ*) data

In situ (ground) truth information used in model training and validation is critical to successful crop classification. Currently, annual crop insurance data provided by four Canadian Provinces (Alberta, Saskatchewan, Manitoba and Québec, which together represent 87 percent of the total agricultural extent) are the most accurate, detailed and complete sources of information for geospatial crop type information in Canada. For provinces where insurance data cannot be accessed, ground-truth information is provided by in situ observations from AAFC staff. In situ data are screened and evaluated for bias by the AAFC before they are input into the RF classifications. In situ observations present two major sources of bias. In crop insurance data, bias can occur because some crops are less likely to be insured than others. When this occurs, uninsured crops are not represented in crop insurance databases, and underrepresented in the training data input to the RF classifications. In the AAFC's field surveys, bias can occur when the timing of field surveys does not coincide with the stages of crop growth that are most useful for accurately identifying crop types. When this happens, crop misidentification is more common, and systematic errors occur in the training data input to the RF classifications. Both cases of bias can result in land use maps containing lower classification accuracies.

4.4.3.5. Optical and SAR satellite data requirements and their pre-processing

Research suggests that optical and SAR satellite data are both required to adequately characterize the key crop-growing (phenological) stages required for high-accuracy crop mapping at a national scale across Canada (McNairn *et al*., 2009; Shang *et al*., 2009; Deschamps *et al*., 2012; Fisette *et al*., 2013, 2014; Champagne *et al*., 2014; Jiao *et al*., 2014; Liu *et al*., 2016). This is because both optical and SAR data streams provide unique and valuable information relating to plant growth and type. Optical imagery is important because observations acquired in the NIR and SWIR regions of the electromagnetic spectrum have been shown to be extremely useful for differentiating among crop types (Clark *et al*., 1995). Dual-polarization SAR data is much more sensitive to plant structure than optical data and is also able to fill gaps in the optical image record brought about by non-ideal weather conditions during key growth stages. Results from research (McNairn *et al*., 2009) and operations (Fisette *et al*., 2015) have shown that the integration of SAR can increase accuracies over the use of optical data alone. For example, the addition of the dual-polarization RADARSAT-2 data to optical imagery has increased overall accuracies by up to 16 percent (Fisette *et al*., 2015).

Before using optical and SAR data as input to the RF classification used to generate the ACI, some pre-processing of these data must be carried out. If not already geometrically corrected, images are orthorectified using a 3-D multisensor physical model (Toutin, 2005). Because the AAFC performs its RF classifications on a region-by-region basis, the mosaicking and atmospheric correction of multidate optical data is unnecessary. However, because clouds may still be present in these data, an automated cloud and shadow masking technique (Zhu and Woodcock, 2012) is applied to every optical image to remove poor-quality retrievals. A gamma maximum-a-posteriori filter is applied to radar data to remove noise (speckle) and the data are resampled to a 16-bit size to reduce processing time. Along-track images of the same date are mosaicked together. This process enables the creation of large classification regions with more training sites.

4.4.3.6. Evolution of optical and SAR imagery input

The ACI has evolved since its first release in 2009 in terms of the satellite data used as input to the classification process (figure 4). While the ACI has always incorporated SAR data from RADARSAT-2, the satellites and sensors used to provide optical data have changed throughout the years. These changes have been driven by a combination of push-and-pull factors. Push factors refer to the undesirable characteristics of a data stream that make its use so limiting that other sources must be sought. Conversely, pull factors refer to the desirable qualities of a new (or newly available) data stream that make its use preferable to existing streams. Push-and-pull factors usually include issues relating to data availability, data cost, spatial resolution, spectral resolution and temporal revisit frequency.

In 2009 and 2010, the ACI was geographically restricted to the Canadian Prairie Provinces (Alberta, Saskatchewan and Manitoba) and based on the integration of multidate optical and SAR data from Resourcesat-1 and RADARSAT-2. The resulting crop maps, which were gridded to the 56-m spatial resolution of Resourcesat-1, provided acceptable mapping accuracies (greater than 75 percent) for the relatively large fields in western Canada. However, testing showed that the extrapolation of this approach to eastern Canada – where fields tend to be much smaller, longer and/or narrower – resulted in lower mapping accuracies in these regions. As a result, the Resourcesat-1 data stream was considered unsuitable for national-scale crop mapping in Canada.

FIGURE 4. DATA SOURCES AND VOLUMES FOR AAFC ANNUAL CROP INVENTORY, 2011–2015.

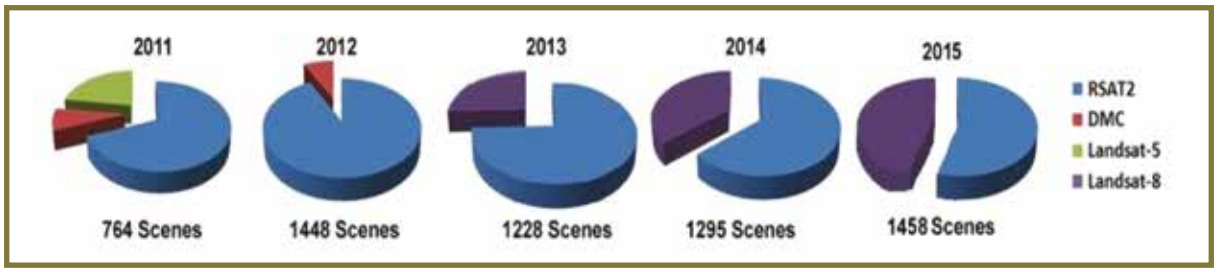

In 2011 and 2012, the geographical scope of the ACI was extended to encompass all but two Canadian Provinces (British Columbia, and Newfoundland and Labrador). Limitations brought about by the coarse spatial resolution of Resourcesat-1 data were directly addressed by using finer-resolution data from other optical satellite sensors. In 2011, these streams comprised multidate observations from Landsat-5 and single-date observations from the Disaster Monitoring Constellation (DMC), which were then integrated with RADARSAT-2 imagery. The resulting crop maps, which were gridded to a 30-m spatial resolution, provided high mapping accuracies not only for western Canada but also for the majority of the eastern part of the country (with the exceptions of the Provinces of Prince Edward Island (PEI) and Nova Scotia (NS), whose mapping accuracies fell below 70 percent). In 2012, after the mid-year failure of the Landsat-5 satellite, the EO input to the ACI was limited to multidate RADARSAT-2 imagery

and single-date observations from DMC. The significant reduction in optical data availability was partially offset by the doubling of RADARSAT-2 acquisitions over those of the previous year. The resulting crop maps, gridded to the same 30-m spatial resolution as in 2011, provided high mapping accuracies (over 75 percent) for all Provinces mapped, including those that were poorly mapped in 2011. The higher classification accuracies for PEI and NS in 2012 were explained by the ability of SAR data to make up for missing optical data, and the use of a higher-quality in situ training data set in 2012.

In 2013, the geographic scope of the ACI was extended even further, to include all Canadian agricultural Provinces. At the same time, data from the newly operational Landsat-8 became the sole optical data stream to provide input to the ACI. These data, integrated with SAR data from RADARSAT-2, were able to provide high mapping accuracies (over 75 percent) for all Provinces mapped. At the time of writing (2016), the Landsat-8/RADARSAT-2 imagery combination continues to provide a reliable and high-quality data source for the ACI, with mapping accuracies for 2016 expected to exceed 85 percent for all Provinces. The now stable source of EO information means that improvements seen in the ACI mapping accuracies since 2013 are largely due to non-imagery reasons, such as better and more reliable ground sampling, and tweaks to the RF classification methodologies that result in higher classification performance.

4.4.3.7. Classification postprocessing

The random forest classification used by the AAFC does not produce a land cover/use map that is immediately appropriate for universal distribution. Instead, three postprocessing steps – filtering, mosaicking and permanent class addition – must be undertaken before final product validation and accuracy assessment are conducted, and the data are made available (figure 1). First, post-classification filtering must be applied to the outputs generated by the random forest classification. This is because pixel-based classification approaches tend to render classified maps containing isolated and erroneously classified pixels. Misclassified pixels are often due to variations in crop growth within a single field and, left alone, will give the (usually wrong) impression that a farmer has planted multiple crops within a field. The application of post-classification filtering directly addresses this problem by assigning the majority class value within each field to each pixel in the field. This process has been shown to increase the classification accuracies of certain crop classes in the ACI by as much as 5 to 10 percent (McNairn *et al*., 2009; Fisette *et al*., 2014 and 2015). Second, the mosaicking of individual classification regions is undertaken to produce individual crop maps for each of the Canadian Provinces that contains agriculture. This is done using an automated process that prioritizes (chooses) zones with higher accuracies where there is overlap between classification regions. The third and final step in map preparation is the addition of permanent classes to the ACI. Every year, the AAFC updates a database containing "permanent" features – such as golf courses, sports fields, ski hills and airports – that generally remain unchanged from one year to another. The identification of these classes is important because they may otherwise be confused with spectrally-similar agricultural classes. Permanent features are added a posteriori to the filtered and mosaicked land use/cover classifications.

4.4.3.8. Product validation and accuracy

Once the ACI has been created, its accuracy is evaluated. To do this, the AAFC uses the confusion (error) matrix approach that has been adopted by the remote sensing community as the standard reporting convention of map accuracy (Congalton, 1991). Confusion matrices not only provide the overall accuracy of a classification technique, but also the errors of exclusion (omission errors), errors of inclusion (commission errors) and F-scores associated with each class in a classification. The overall accuracy of the ACI is calculated by dividing the total number of correctly classified fields in the error matrix by the total number of fields in the matrix. Omission error (producer accuracy) refers to the probability that a reference field of crop class X is correctly classified as class X. Commission

error (user accuracy) refers to the probability that a field classified as class X is in reality class X. Where no fields are classified as one of the predefined reference classes, user accuracy is undefined. Finally, the F-score for each class, a class-specific indicator that is not affected by the information from other classes, is calculated as the harmonic mean of user accuracy and producer accuracy (Waldner *et al*., 2015).

As part of the imagery classification process, the overall crop accuracy of the ACI is validated for each unique image-date combination. When mapped, these data provide detailed insight into the spatial variations in crop accuracy across Canada's entire agricultural extent (figure 5). Although the ACI consistently achieves an overall target accuracy of 85 percent at the national scale, map accuracy varies from crop to crop, region to region, and year to year, depending on satellite data availability and the geographic representativeness of in situ training data (table 3). In general, the highest mapping accuracies (greater than 90 percent) are found where crops display significantly different spectral characteristics at the time of the EO data acquisition, such as in the Canadian Prairie Provinces of Saskatchewan and Alberta. Elsewhere, however, accuracies are lower, and may vary from approximately 70 to 80 percent. This variability is explained by two main factors that relate to limitations associated with the in situ and satellite data used in the classification process.

FIGURE 5. GEOGRAPHIC COVERAGE AND OVERALL MAPPING ACCURACIES FOR AAFC ANNUAL CROP INVENTORY, 2016.

TABLE 3.

Province	2009	2010	2011	2012	2013	2014	2015
NFL	--	--	--	--	--	--	--
PE	--	--	67.5	78.7	87.9	81.0	83.7
NB	--	--	88.1	88.0	87.3	89.1	86.1
NS	--	--	64.2	89.9	74.2	64.4	85.2
QC	--	--	81.4	81.8	87.5	83.9	87.1
ON	--	--	80.8	76.2	88.2	87.9	89.6
MB	80.0	85.1	79.0	85.9	85.4	90.3	90.0
SK			87.1	82.4	86.5	85.9	89.7
AB			87.7	88.4	89.9	89.4	88.9
BC	--	--	--	--	79.2	88.4	--
CANADA	**80.0**	**85.1**	**85.3**	**83.9**	**86.0**	**87.4**	**85.0**

Provincial variability in classification accuracy for the AAFC Annual Crop Inventory, 2015. (NFL = Newfoundland and Labrador, PE = Prince Edward Island, NB = New Brunswick, NS = Nova Scotia, QC = Québec, ON = Ontario, MB = Manitoba, SK = Saskatchewan, AB = Alberta, BC = British Columbia). Accuracies are not calculated for Provinces and years where insufficient ground validation data exists (or, not required to assure a high quality product, as in the case of NFL that is known to be 95% pasture).

First, there can be significant Province-to-Province variability in the number, density and quality (detail and accuracy) of in situ data used for training the RF classification and its validation. This variability is directly related to the different sources of the data. The highest-quality data tend to be those that: (a) are the most spatially representative of the agricultural landscape; (b) are of the highest accuracy through both space and time; (c) use the most detailed crop (thematic) classes; and (d) contain the large sample sizes required for training and validating the RF classifications. Data provided by the Provincial Governments of Alberta, Saskatchewan, Manitoba and Québec generally meet these all of these requirements (Note: while detailed data is provided by the Provincial Government of British Columbia, it focuses only on specific classes, and is thus not spatially comprehensive). In comparison, data for the remaining Provinces (Ontario, New Brunswick, NS, PEI and Newfoundland) are collected by AAFC staff using windshield surveys that paint a less spatially representative picture of the agricultural landscape as a whole. While crop maps generated from these data generally meet the AAFC's target mapping accuracies, they can only do so at the cost of generalization, such that detailed classes (for example, wheat, barley and oats) are aggregated to a single broader class (such as cereals). Wider access to Provincially-collected ground data for all Provinces would eliminate discontinuities in class detail across the country.

Second, there is often significant regional variability in cloud cover, which can limit the amount of optical satellite data (currently Landsat-8) available for input to the RF classification. For example, while as many as three or four clear-sky Landsat-8 images can be acquired over the Canadian Prairie Provinces each growing season, this availability can be reduced to a single image (or, in the worst cases, no images) in Canada's coastal regions (mainly the agricultural regions in the eastern Maritime Provinces of Newfoundland and Labrador, New Brunswick, NS and PEI). While the AAFC places a heavier reliance on the monthly acquisition of microwave (RADARSAT-2) imagery for input to the RF classification process in these regions, the lack or absence of optical imagery still results in a 10 to 15 percent drop in map accuracy compared to other regions where optical data is more available. This issue should become less problematic in the future as access to new streams of optical (such as Sentinel-2) and microwave imagery (such as Sentinel-1; RADARSAT Constellation Mission, 2018) increases.

It should finally be noted here that confusion matrices, despite their common use, are limited in their inability to provide more detail on the source of error that can be linked to the performance of the classification algorithm or to the spatial resolution of the remote sensing data (Boschetti *et al*., 2004). For this reason, the AAFC is currently evaluating the use of another method – the De Finetti Entropy Triangle (ET) (Valverde-Albacete and Peláez-Moreno, 2010) – for their classification error assessment. This approach, with a solid information-theoretical basis, has not yet found common use in remote sensing classification studies, but may provide a more faithful indication of classifier performance than the accuracies derived from confusion matrices (Valverde-Albacete and Peláez-Moreno, 2014).

4.4.3.9. Comparisons with crop area estimates from statistical surveys (Census of Agriculture)

An additional validation of the AAFC ACI is undertaken every five years using statistical information obtained during the national Census of Agriculture by Statistics Canada. Statistics Canada is the agency responsible for collecting, compiling, analysing, reporting and publishing information relating to the commercial, industrial, financial, social, economic and general activities and condition of the people of Canada (Government of Canada, 2008). A comparison of the ACI and the Census of Agriculture (figure 6) for the most recent census year of 2011 by Fisette *et al*. (2014) revealed that: (a) at the national scale, the ACI overestimates the agricultural area of Canada by 15 percent compared to the 2011 Census of Agriculture; and (b) at more regional scales, the ACI tends to overestimate the cultivated areas of major crops (for example, forage, cereals, oilseeds) and, with the exception of corn and fruits, underestimate acreages of minor crops, sometimes drastically (such as fallow, pulses). The differences between the estimates provided by these two different sources of information must be reconciled.

The disagreements between the 2011 ACI and the Census of Agriculture are explained by inconsistencies in the sample size and spatial distribution of in situ data used to train the RF classification. The accuracy of mapped crop classes depends greatly on the adequacy of the training data to represent each class (Pal and Mather, 2003). Of particular importance is whether a mapped class is under- or overrepresented in the sample data. Classes in the ACI that are overrepresented in training data are typically overrepresented in the output map at the expense of marginal (minor) crops, the acreages of which are underrepresented. These biases generally support the observation that remotely sensed crop area estimation through simple pixel counting is insufficient to provide unbiased estimates of seeded area (Gallego, 2004 and 2006).

FIGURE 6. COMPARISON OF CROP AREA ESTIMATES DERIVED FROM AAFC ANNUAL CROP INVENTORY (2011) WITH THE CANADIAN CENSUS OF AGRICULTURE (2011).

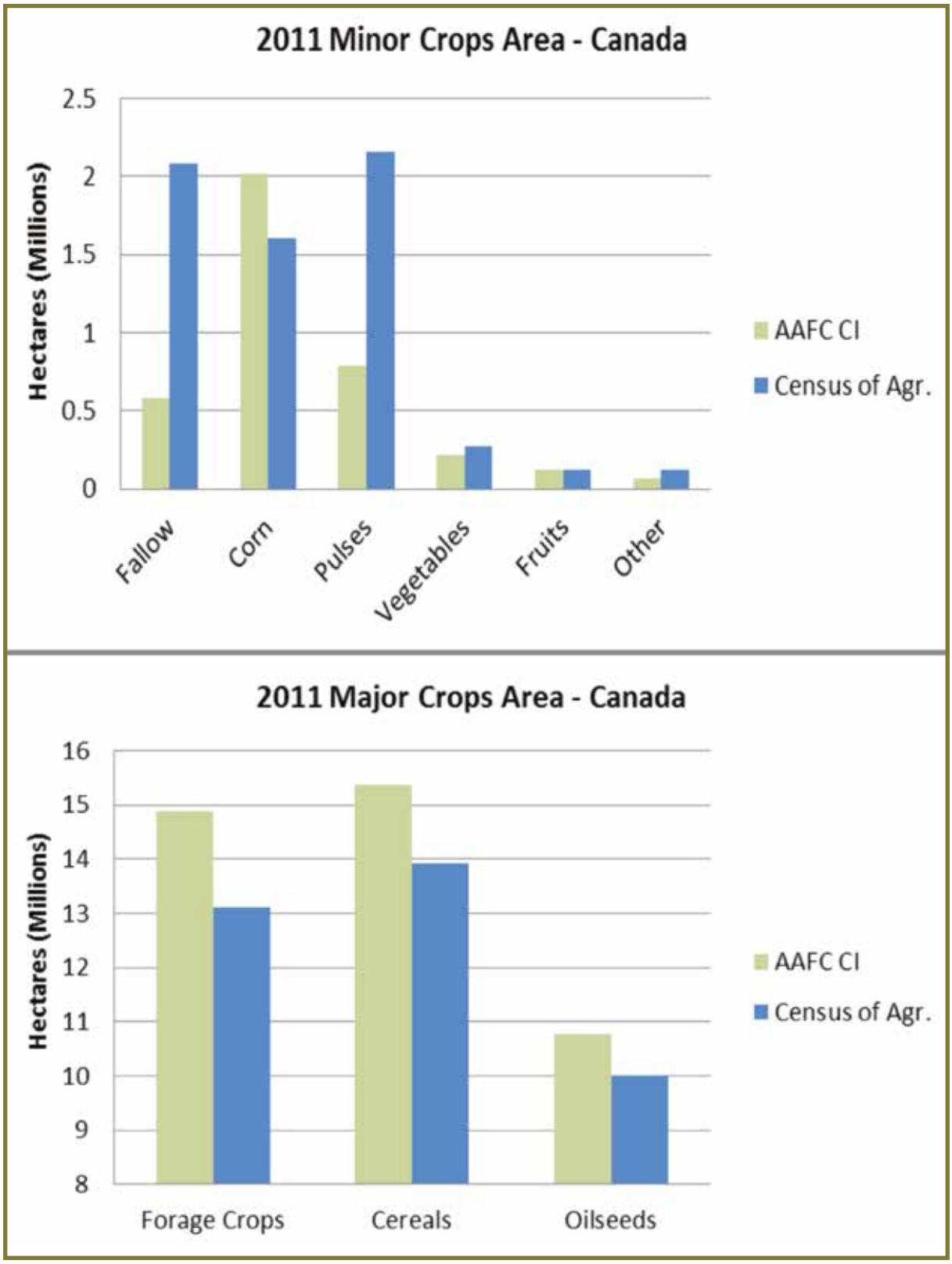

Various statistical techniques have been proposed (and applied) to reduce the bias of simple pixel counting for crop area estimation. One such approach is the regression estimator, a method that combines unbiased information measured on a sample (that is, by means of ground surveys) with exhaustive but inaccurate and biased information (that is, classified satellite images) (Gallego, 2004 and 2006; Gallego *et al*., 2010 and 2014). The regression estimator uses a classified satellite image as an auxiliary variable to reduce the bias of estimates derived from ground surveys. While this approach has been widely applied in large operational projects for crop area estimation with remote sensing (see for example Wall *et al*., 1984; Chhikara *et al*., 1986; González-Alonso and Cuevas, 1993), the value added by the remote sensing strongly depends on the accuracy of the classification and is directly proportional to the effort made in the ground survey (Gallego *et al*., 2010).

The AAFC has developed a modified version of the regression estimator to directly address bias in its ACI-derived estimates of crop area. This approach, not yet operational, supplements existing ground survey information with very-high-accuracy local (24 km x 24 km) crop maps that are derived from fine-resolution remote sensing observations and high-quality ground survey points. The high quality of these maps means that they can be used to compensate statistically for the sparse and inconsistent coverage of ground survey points in these regions and, in effect, can be treated as the equivalent of unbiased ground surveys. Matching area estimates from these high-accuracy local maps with those derived from corresponding locations in the ACI enables crop-specific mathematical relationships to be derived for area estimates based on sampling (area estimates from the high-quality remote sensing maps) and pixel counting (area estimates from the ACI). These relationships are then used to adjust the ACI-based area estimates so that the accuracies of individual crop area estimates, as well as total cropped area, are increased.

4.4.3.10. Map legend standardization

The thematic classes used during the crop classification process can vary from application to application and from country to country. This is problematic because these incompatibilities hamper the aggregation toward broader regional and global data sets (Giri, 2012). As a result, the classes used for crop identification and mapping are usually based on national or international classification schemes that provide the best semantic interoperability with other land cover classifications, and facilitate direct classification-to-classification comparisons (Jensen, 1986; Teleguntla *et al*., 2016). To this end, the AAFC ACI uses a harmonized legend based on the Canadian Forest Service (CFS) Earth Observation for Sustainable Development (EOSD) Land Cover Classification (Wulder and Nelson, 2001). This legend is compatible with a number of internationally recognized legends, including FAO's Land Cover Classification System (LCCS) (Di Gregorio and Jansen, 2000).

4.4.3.11. Data publication and use

As part of the Canadian Government's commitment to open science, the ACI data are made available at no cost to the public. ACI data are distributed in raster format (GeoTIFF) in the Albers Equal Area (AEA) projection. The AAFC metadata – information that accompanies and describes the data set – are based on ISO 19131 standards and made available in Canada's two official languages (English and French). To date, annual crop maps are typically made available approximately eight months after the end of growing season (that is, the March following the end of the growing season mapped). Downloads of the ACI have increased annually since 2009, making it one of the Government of Canada's most downloaded geospatial data sets.

The downstream uses of the ACI are varied. The ACI has been extensively used by the Canadian public sector at various levels. At the federal government level, the ACI has been used to support applications and assessments relating to a diverse range of issues, including: (a) crop area estimation; (b) regional-scale yield modeling; (c) climate-related production risk; (d) soil erosion modelling; (e) agriculture-related greenhouse gas emissions and

removals; (f) bird population changes; (g) environmental sustainability indicator reporting; (h) urban changes in Canadian metropolitan areas; and (i) air quality assessment. At the provincial government level, uses of the ACI include: (a) assessing general agricultural trends; (b) wetland biodiversity assessment; (c) agriculture-related stewardship program design; (d) mapping riparian land use; (e) modelling nutrient transport through watersheds; and (f) urban expansion and land use planning. However, this data set has also found wide use in other sectors of the economy. For example, commodity groups have used the ACI to not only target and implement strategies to meet regionally specific needs of growers, but also as a screening function to demonstrate compliance with international sustainability certification criteria (for example, the European Union's Renewable Energy Directive (EU-RED) relating to land use conversion). Universities and colleges have used the ACI to support research activities relating to pest occurrence and management, trends in crop rotation, and pollinator distribution and conservation. Agribusinesses have used the ACI to independently validate agricultural land use for aggregating carbon offset credits in the agricultural sector, map flooded areas by crop type for insurance claim verification, calibrate models for estimating seeded areas immediately after harvest, and analyse draw areas for grain elevators.

4.4.3.12. Applicability of ACI methodologies to other countries

The methodologies used to generate the ACI are already being used to guide international standards for data products and reporting, and will help support the development of a global system of systems for agricultural crop assessment and monitoring under the GEOGLAM Joint Experiment for Crop Assessment and Monitoring (JECAM) initiative. To this end, and to facilitate the transfer of methodologies to other nations with similar cropping systems, the AAFC is in the process of documenting its processing methodologies in detail for future open distribution. While the data processing chain implemented at the AAFC relies mostly on proprietary image processing and Geographical Information System (GIS) software packages and modules, it could also be implemented using other software systems, including open-source software. Open-source software – computer software the source code of which is made available with a license that allows the copyright holder to study, change and distribute the software to anyone and for any purpose – is particularly attractive because it is usually available at no cost. The attractiveness of the Canadian approach to crop mapping lies in its relatively modest requirements in terms of human resources (five full-time staff) and cost (Can$150 000 annually) compared to other large nations (such as the United States of America or China).

4.4.3.13. Future development and implementations

Despite the demonstrated success of the ACI, certain areas of development yet remain to be addressed if it to be capable of meeting the future needs of the AAFC and its clients in a cost-effective and computationally efficient manner. Of particular interest is the production of within-season crop acreage estimates that would be released as precursors to the final ACI product release. Achieving this objective will require: (a) negotiations for earlier access to the ground observations provided by provincial agencies that are used to train and validate the ACI; (b) further optimization of classification routines – such as a switch from pixel-based to object-based mapping – to reduce the computational overhead that makes within season-estimates impossible; and (c) incorporation of new and future data streams (such as Sentinel-1, Sentinel-2 and Sentinel-3; and the RADARSAT Constellation Mission – RCM – that is scheduled for launch in 2018). In addition, the extrapolation of the ACI methodologies to more complex cropping systems – such as multiple cropping systems (agriculture that involves planting more than one crop on the same land in one year) and mixed cropping systems (agriculture that involves planting two or more types of plants simultaneously in the same field) – requires further development and testing.

4.5. CONCLUSION

This chapter has summarized recent progress made to advance applications of remote sensing technologies for the creation of national-scale detailed crop maps (CDLs) at the field (parcel) level.

The creation of accurate and detailed crop maps requires high-quality ground and high quality multitemporal satellite data. High-quality ground data are for training and validating the supervised classification approach used to classify satellite imagery. While ground data provided by local, regional and national government agencies are usually the most accurate, detailed and complete, other sources of data are required in their absence. This leads to additional challenges for crop mapping in parts of the world where authoritative spatially explicit field-level information is unavailable (in other words, where the data are not collected or are not made available for use), and particularly, where ground data collection through alternative methods is difficult or impossible (for example due to limited resources (money, time, people); limited accessibility (poor road infrastructures and remote agricultural regions); or armed conflict)). Nonetheless, no matter the source, acquired ground data require considerable evaluation ensure that the data is ready for use in classification. High-quality satellite observations can be obtained from various optical or SAR sensors; however, they must be collected at a spatial resolution that allows individual fields to be resolved, and at times, during the growing season, that coincides with the key growth stages of crops being assessed. The most accurate detailed national crop mapping generally occurs when moderate-resolution spectrally rich time series are acquired that contain no gaps.

An extensive review of the published literature suggests that while there is no single best image classification method for detailed crop mapping, methodologies based on machine learning generally outperform others. Of these methods, Random Forest has already been incorporated operationally into national mapping strategies using optical data (United States) and optical and SAR data (Canada) and SAR data (United Kingdom). Other approaches – such as artificial neural networks and support vector machines – have also shown great potential. However, until now, such methods have mainly been limited to applications in the research (non-operational) domain.

Crop area estimation based on satellite-derived crop maps must be carried out with caution and incorporate methods for assessing and correcting bias. Bias occurs because pixel counting frequently underestimates the seeded area of minor crops and overestimates the seeded area of major crops. These disparities caused by inconsistencies in the sample size and spatial distribution of in situ data used to train classifications, and generally support the observation that current remotely sensed crop area estimation is insufficient to provide unbiased estimates of seeded area. Bias can be reduced through the use of statistical tools, such as the regression estimator, a method that combines unbiased information measured on a sample (ground surveys) with exhaustive but inaccurate and biased information (classified satellite images).

Future opportunities for detailed crop mapping will be great and come from the adoption of new and improved optical and SAR data satellite streams that, in combination or isolation, will allow a better characterization of crop-specific growth cycles at the field level. However, this will not be without challenge. The ability of national mapping agencies to incorporate this information in a timely and efficient manner will require significant investment in information technology infrastructure to facilitate the processing of significantly greater volumes of data.

4.6. REFERENCES

Abdulaziz, A.M., Hurtado, J.J.M. & Al- Douri, R. 2009. Application of multitemporal Landsat data to monitor land cover changes in the Eastern Nile Delta region, Egypt. Int*ernational Journal of Remote Sensing*, 30: 2977–2996.

Abedi, M., Norouzi, G.-H. & Fathianpour, N. 2013. Fuzzy outranking approach: A knowledge-driven method for mineral prospectivity mapping. In*ternational Journal of Applied Earth Observation and Geoinformation*, 21: 556–567.

Alabi, T., Haertel, M. & Chiejile, S. 2016. Investigating the Use of High Resolution Multi-spectral Satellite Imagery for Crop Mapping in Nigeria - Crop and Landuse Classification using WorldView-3 High Resolution Multispectral Imagery and LANDSAT8 Data. Proceedings of the 2nd International Conference on Geographical Information Systems Theory, Applications and Management (GISTAM 2016), pp. 109–120), SCITEPRESS - Science and Technology Publications.

Al-Anazi, A.F. & Gates, I.D. 2010. Support vector regression for porosity prediction in a heterogeneous reservoir: A comparative study. *Computers & Geoscience*, 36: 1494–1503.

Arino, O., Bicheron, P., Achard, F., Latham, J., Witt, R. & Weber, J.-L. 2008. GlobCover: The most detailed portrait of Earth. *European Space Agency Bulletin*, 136: 24–31.

Atzberger, C., Vuolo, F., Klisch, A., Rembold, F., Meroni, M., Mello, M.P. & Formaggio, A.R. 2016. *Agriculture*. In Thenkabail, P.S. (ed.), Land Resources Monitoring, Modeling and Mapping with Remote Sensing, (pp. 71–112). CRC Press Inc.: Boca Raton, FL, USA,.

Badhwar, G.D. 1984. Automatic corn-soybean classification using landsat MSS data. I. Near-harvest crop proportion estimation. *Remote Sensing of Environment*, 14: 15–29.

Baghdadi, N., Boyer, N., Todoroff, P., El Hajj, M. & Bégué, A. 2009. Potential of SAR sensors TerraSAR-X, ASAR/ENVISAT and PALSAR/ALOS for monitoring sugarcane crops on Reunion Island. *Remote Sensing of Environment*, 113: 1724–1738.

Bartalev, S., Egorov, C., Loupian, E., Plotnikov, D. & Uvarov, I. 2011. Recognition of arable lands using multi-annual satellite data from spectroradiometer MODIS and locally adaptive supervised classification. *Computer Optics*, 35: 103–116.

Bartholomé, E. & Belward, A.S. 2005. GLC2000: a new approach to global land cover mapping from Earth observation data. *International Journal of Remote Sensing*, 26: 1959–1977.

Becker-Reshef, I., Justice, C., Sullivan, M., Vermote, E., Tucker, C., Anyamba, A., Small, J., Pak, E., Masuoka, E., Schmaltz, J. *et al.* 2010. Monitoring Global Croplands with Coarse Resolution Earth Observations: The Global Agriculture Monitoring (GLAM) Project. *Remote Sensing*, 2: 1589–1609.

Beltran, C.M. & Belmonte, A.C. 2001. Irrigated crop area estimation using Landsat TM imagery in La Mancha, Spain. *Photogrammetric Engineering & Remote Sensing*, 67: 1177–1184.

Benz, U.C., Hofmann, P., Willhauck, G., Lingenfelder, I. & Heynen, M. 2004. Multi-resolution, object-oriented fuzzy analysis of remote sensing data for GIS-ready information. *ISPRS Journal of Photogrammetry and Remote Sensing*, 58: 239–258.

Beyer, F., Jarmer, T., Siegmann, B. & Fischer, P. 2015. Improved crop classification using multitemporal RapidEye data. Paper presented at the 8th International Workshop on the Analysis of Multitemporal Remote Sensing Images (Multi-Temp), 22–24 July 2015. Annecy, France, IEEE.

Bhatta, B. 2008. *Remote Sensing and GIS*. Oxford University Press: Oxford, UK.

Blaes, X., Vanhalle, L. & Defourny, P. 2005. Efficiency of crop identification based on optical and SAR image time series. *Remote Sensing of Environment*, 96: 352–365.

Blanco, P.D., Colditz, R.R., Saldaña, G.L., Hardtke, L.A., Llamas, R.M., Mari, N.A., Fischer, A., Caride, C., Aceñolaza, P.G. & del Valle, H.F. 2013. A land cover map of Latin America and the Caribbean in the framework of the SERENA project. *Remote Sensing of Environment*, 132: 13–31.

Blaschke, T. 2010. Object based image analysis for remote sensing. *ISPRS Journal of Photogrammetry and Remote Sensing*, 65: 2–16.

Bontemps, S., Arino, O., Bicheron, P., Brockman, C.C., Leroy, M., Vancutsem, C. & Defourny, P. 2012. Operational Service Demonstration for Global Land-Cover Mapping: The GlobCover and GlobCorine Experiences for 2005 and 2009. In Giri, C.P. (ed.), *Remote Sensing of Land Use and Land Cover: Principles and Applications* (pp. 243–265) CRC Press: Boca Raton, FL, USA.

Boryan, C., Yang, Z., Mueller, R. & Craig, M. 2011. Monitoring US agriculture: the US Department of Agriculture, National Agricultural Statistics Service, Cropland Data Layer Program. Geocarto International: 26, 341–358.

Boschetti, L., Flasse, S.P. & Brivio, P.A. 2004. Analysis of the Conflict between Omission and Commission in Low Spatial Resolution Dichotomic Thematic Products: The Pareto Boundary. *Remote Sensing of Environment* 91(3–4): 280–92.

Breiman, L. 1984. *Classification and regression trees*. CRC Press: Boca Raton, FL, USA.

Breiman, L. 2001. *Random Forests*. Machine Learning, 45: 5–32.

Brown, J.C., Kastens, J.H., Coutinho, A.C., Victoria, D. de C. & Bishop, C.R. 2013. Classifying multiyear agricultural land use data from Mato Grosso using time-series MODIS vegetation index data. *Remote Sensing of Environment*, 130: 39–50.

Brown de Colstoun, E.C., Story, M.H., Thompson, C., Commisso, K., Smith, T.G. & Irons, J.R. 2003. National Park vegetation mapping using multitemporal Landsat 7 data and a decision tree classifier. *Remote Sensing of Environment*, 85: 316–327.

Castillejo-González, I.L., López-Granados, F., García-Ferrer, A., Peña-Barragán, J.M., Jurado-Expósito, M., de la Orden, M.S. & González-Audicana, M. 2009. Object- and pixel-based analysis for mapping crops and their agro-environmental associated measures using QuickBird imagery. *Computers and Electronics in Agriculture*, 68: 207–215.

Chang, J., Hansen, M.C., Pittman, K., Carroll, M. & DiMiceli, C. 2007. Corn and Soybean Mapping in the United States Using MODIS Time-Series Data Sets. *Agronomy Journal*, 99: 1654.

Chen, J., Chen, J., Liao, A., Cao, X., Chen, L., Chen, X., He, C., Han, G., Peng, S. & Lu, M. 2015. Global land cover mapping at 30m resolution: A POK-based operational approach. *ISPRS Journal of Photogrammetry and Remote Sensing*, 103: 7–27.

Chhikara, R., Lundgren, J. & Houston, A. 1986. Crop Acreage Estimation Using a Landsat-Based Estimator as an Auxiliary Variable. *IEEE Transactions on Geoscience and Remote Sensing*, *GE-24*: 157–168.

Clark, R.N., King, T.V., Ager, C. & Swayze, G.A. 1995. Initial vegetation species and senescence/stress indicator mapping in the San Luis Valley, Colorado using imaging spectrometer data. USGS Publication: Denver, CO, USA.

Colwell, J.E. 1974. Vegetation canopy reflectance. *Remote Sensing of Environment*, 3: 175–183.

Comaniciu, D. & Meer, P. 2002. Mean shift: a robust approach toward feature space analysis. *IEEE Transactions on Pattern Analysis and Machine Intelligence*, 24: 603–619.

Congalton, R.G. 1991. A review of assessing the accuracy of classifications of remotely sensed data. Remote Sensing of Environment, *37*: 35–46.

Congalton, R.G., Balogh, M., Bell, C., Green, K., Milliken, J.A. & Ottman, R. 1998. Mapping and monitoring agricultural crops and other land cover in the Lower Colorado River Basin. *Photogrammetric Engineering & Remote Sensing*, 64: 1107–1114.

Conrad, C., Machwitz, M., Schorcht, G., Löw, F., Fritsch, S. & Dech, S. 2011. Potentials of RapidEye time series for improved classification of crop rotations in heterogeneous agricultural landscapes: experiences from irrigation systems in Central Asia. In Neale, C.M.U. & Maltese, A. (eds), *Remote Sensing for Agriculture, Ecosystems, and Hydrology XIII* (p. 817412), SPIE Proceedings Vol. 8174, Publication of the Society of Photo-Optical Instrumentation Engineers: Washington, D.C.

Cortes, C. & Vapnik, V. 1995. Support-vector networks. *Machine Learning*, 20: 273–297.

Defries, R.S.&d Townshend, J.R.G. 2003. LBA Regional Land Cover from AVHRR, 1-Degree, 1987 (Defries and Townshend). ORNL DAAC, Oak Ridge, TN, USA.

Defries, R.S., Hansen, M., Sohlberg, R. & Townshend, J.R.G. 2003. LBA Regional Land Cover from AVHRR, 8-km, 1984 (Defries et al.). ORNL DAAC, Oak Ridge, TN, USA.

Denègre, J. 2013. Thematic Mapping From Satellite Imagery: A Guidebook. Elsevier: Kidlington, Oxford, U.K.

Deschamps, B., McNairn, H., Shang, J. & Jiao, X. 2012. Towards operational radar-only crop type classification: comparison of a traditional decision tree with a random forest classifier. *Canadian Journal of Remote Sensing*, 38: 60–68.

Di Gregorio, A. & Jansen, L.J.M. 2000. *Land cover classification system: Classification concepts and user manual*. FAO Publication: Rome.

Drusch, M., Del Bello, U., Carlier, S., Colin, O., Fernandez, V., Gascon, F., Hoersch, B., Isola, C., Laberinti, P., Martimort, P. *et al.* 2012. Sentinel-2: ESA's Optical High-Resolution Mission for GMES Operational Services. *The Sentinel Missions - New Opportunities for Science*, 120: 25–36.

Eidenshink, J.C. & Faundeen, J.L. 1994. The 1 km AVHRR global land data set: first stages in implementation. *International Journal of Remote Sensing*, 15: 3443–3462.

Eisavi, V., Homayouni, S., Yazdi, A.M. & Alimohammadi, A. 2015. Land cover mapping based on random forest classification of multitemporal spectral and thermal images. *Environmental Monitoring and Assessment*, 187(5): 291 ff.

El-Khoury, A., Seidou, O., Lapen, D.R., Sunohara, M., Zhenyang, Q., Mohammadian, M. & Daneshfar, B. 2014. Prediction of land-use conversions for use in watershed-scale hydrological modeling: a Canadian case study. *The Canadian Geographer/Le Géographe Canadien*, 58: 499–516.

El-Khoury, A., Seidou, O., Lapen, D.R., Que, Z., Mohammadian, M., Sunohara, M. & Bahram, D. 2015. Combined impacts of future climate and land use changes on discharge, nitrogen and phosphorus loads for a Canadian river basin. *Journal of Environmental Management*, 151: 76–86.

Evans, C., Jones, R., Svalbe, I. & Berman, M. 2002. Segmenting multispectral Landsat TM images into field units. *IEEE Transactions on Geoscience and Remote Sensing*, 40: 1054–1064.

Fischer, G., Shah, M., N. Tubiello, F. & van Velhuizen, H. 2005. Socio-economic and climate change impacts on agriculture: an integrated assessment, 1990-2080. *Philosophical Transactions of the Royal Society B: Biological Sciences*, 360: 2067–2083.

Fisette, T., Rollin, P., Aly, Z., Campbell, L., Daneshfar, B., Filyer, P., Smith, A., Davidson, A., Shang, J. & Jarvis, I. 2013. *AAFC annual crop inventory*. In IEEE, *2013 Second International Conference on Agro-Geoinformatics (Agro-Geoinformatics)* (pp. 270–274), IEEE Publication.

Fisette, T., Davidson, A., Daneshfar, B., Rollin, P., Aly, Z. & Campbell, L. 2014. Annual space-based crop inventory for Canada: 2009–2014. In IEEE, *2014 IEEE International Geoscience and Remote Sensing Symposium* (pp. 5095–5098), IEEE Publication.

Fisette, T., McNairn, H. & Davidson, A. 2015. An Operational Annual Space-Based Crop Inventory Based on the Integration of Optical and Microwave Remote Sensing Data: Protocol Document. Agriculture and Agri-Food Canada Publication: Ottawa.

Franklin, S.E. & Wulder, M.A. 2002. Remote sensing methods in medium spatial resolution satellite data land cover classification of large areas. *Progress in Physical Geography*, 26: 173–205.

Friedl, M.A. & Brodley, C.E. 1997. Decision tree classification of land cover from remotely sensed data. *Remote Sensing of Environment*, 61: 399–409.

Friedl, M.A., McIver, D.K., Hodges, J.C.F., Zhang, X.Y., Muchoney, D., Strahler, A.H., Woodcock, C.E., Gopal, S., Schneider, A., Cooper, A. *et al.* 2002. Global land cover mapping from MODIS: algorithms and early results. Remote Sensing of Environment, 83: 287–302.

Fritz, S., Massart, M., Savin, I., Gallego, J. & Rembold, F. 2008. The use of MODIS data to derive acreage estimations for larger fields: A case study in the south-western Rostov region of Russia. *International Journal of Applied Earth Observation and Geoinformation*, 10: 453–466.

Fritz, S., See, L., McCallum, I., You, L., Bun, A., Moltchanova, E., Duerauer, M., Albrecht, F., Schill, C. & Perger, C. 2015. Mapping global cropland and field size. Global Change Biology, 21: 1980–1992.

Galford, G.L., Mustard, J.F., Melillo, J., Gendrin, A., Cerri, C.C. & Cerri, C.E.P. 2008. Wavelet analysis of MODIS time series to detect expansion and intensification of row-crop agriculture in Brazil. *Remote Sensing of Environment Special Issue*, 112: 576–587.

Gallego, F.J. 2004. Remote sensing and land cover area estimation. International Journal of Remote Sensing, 25: 3019–3047.

Gallego, F.J. 2006. *Review of the Main Remote Sensing Methods for Crop Area Estimates*. In *Workshop proceedings: Remote sensing support to crop yield forecast and area estimates*. ISPRS archives, XXXVI, 8/W48, 65–70. Available at http://www.isprs.org/publications/PDF/ISPRS_Archives_WorkshopStresa2006.pdf. Accessed on 5 May 2017.

Gallego, F.J., Craig, M., Michaelsen, J. Bossyns, B. & Fritz S. (eds). 2008. *Best practices for crop area estimation with Remote Sensing*. GEOSS Community of Practice Ag 0703a. European Communities Publication: Luxembourg.

Gallego, F.J., Kussul, N., Skakun, S., Kravchenko, O., Shelestov, A. & Kussul, O. 2014. Efficiency assessment of using satellite data for crop area estimation in Ukraine. *International Journal of Applied Earth Observation and Geoinformation*, 29: 22–30.

Ghimire, B., Rogan, J., Galiano, V.R., Panday, P. & Neeti, N. 2012. An evaluation of bagging, boosting, and random forests for land-cover classification in Cape Cod, Massachusetts, USA. *GIScience & Remote Sensing*, 49: 623–643.

Gillespie, T.J. 1990. Radar detection of a dew event in wheat. *Remote Sensing of Environment*, 33(3): 151–156.

Giri, C.P. 2012. *Remote sensing of land use and land cover: principles and applications*. CRC Press: Boca Raton, FL, USA.

Gislason, P.O., Benediktsson, J.A. & Sveinsson, J.R. 2006. Random Forests for land cover classification. *Pattern Recognition Letters*, 27(4): 294–300.

Glanz, H., Carvalho, L., Sulla-Menashe, D. & Friedl, M.A. 2014. A parametric model for classifying land cover and evaluating training data based on multi-temporal remote sensing data. *ISPRS Journal of Photogrammetry and Remote Sensing*, 97: 219–228.

Gómez, C., White, J.C. & Wulder, M.A. 2016. Optical remotely sensed time series data for land cover classification: A review. *ISPRS Journal of Photogrammetry and Remote Sensing*, 116: 55–72.

Gong, P., Wang, J., Yu, L., Zhao, Y., Zhao, Y., Liang, L., Niu, Z., Huang, X., Fu, H., Liu, S. *et al*. 2013a. Finer resolution observation and monitoring of global land cover: first mapping results with Landsat TM and ETM+ data. *International Journal of Remote Sensing*, 34: 2607–2654.

Gong, P., Wang, J., Yu, L., Zhao, Y., Zhao, Y., Liang, L., Niu, Z., Huang, X., Fu, H., Liu, S. *et al.* 2013b. Finer resolution observation and monitoring of global land cover: first mapping results with Landsat TM and ETM+ data. *International Journal of Remote Sensing*, 34: 2607–2654.

González-Alonso, F. & Cuevas, J.M. 1993. Remote sensing and agricultural statistics: crop area estimation through regression estimators and confusion matrices. *International Journal of Remote Sensing*, 14: 1215–1219.

Government of Canada. Statistics Canada. 2008. *Mandate and objectives*. Available at: http://www.statcan.gc.ca/eng/about/mandate. Accessed on 10 June 2017.

Guerschman, J.P., Paruelo, J.M., Bella, C.D., Giallorenzi, M.C. & Pacin, F. 2003. Land cover classification in the Argentine Pampas using multi-temporal Landsat TM data. International Journal of Remote Sensing, 24: 3381–3402.

Haldar, D., Das, A., Mohan, S., Pal, O., Hooda, R.S. & Chakraborty, M. 2012. Assessment of L-Band SAR Data at Different Polarization Combinations for Crop and Other Landuse Classification, *Progress in Electromagnetics Research B*, 36: 303–321.

Hansen, M.C., DeFries, R.S., Townshend, J.R. & Sohlberg, R. 2000. Global land cover classification at 1 km spatial resolution using a classification tree approach. *International Journal of Remote Sensing*, 21: 1331–1364.

Haralick, R.M. & Shapiro, L.G. 1985. Image Segmentation Techniques. In Gilmore, J.F. (ed.), *SPIE Proceedings Vol. 0548: Applications of Artificial Intelligence II* (pp. 2–9). SPIE Publication: Bellingham, WA, USA.

Hill, M.J., Ticehurst, C.J., Lee, J.-S., Grunes, M.R., Donald, G.E. & Henry, D. 2005. Integration of optical and radar classifications for mapping pasture type in Western Australia. *IEEE Transactions on Geoscience and Remote Sensing*, 43: 1665–1681.

Hoekman, D.H., Vissers, M.A.M. & Tran, T.N. 2011. Unsupervised Full-Polarimetric SAR Data Segmentation as a Tool for Classification of Agricultural Areas. *IEEE Journal of Selected Topics in Applied Earth Observations and Remote Sensing*, 4: 402–411.

Holecz, F., Collivignarelli, F., Barbieri, M., Gatti, L., Boschetti, M., Manfron, G., Brivio, P.A., Abukari, M. & Bondo, T. 2013. *Establishing National Baseline Land Cover Map Including Annual and Seasonal Variations for the Understanding of Current Agricultural Practices in the Gambia*. IFAD document. Unpublished. Available at: https://operations.ifad.org/documents/654016/fd0979c5-e1f2-483c-8247-922d4ac27c2d. Last accessed 3 July 2017.

Hütt, C., Koppe, W., Miao, Y. & Bareth, G. 2016. Best Accuracy Land Use/Land Cover (LULC) Classification to Derive Crop Types Using Multitemporal, Multisensor, and Multi-Polarization SAR Satellite Images. *Remote Sensing*, 8: 684.

Irons, J.R., Dwyer, J.L. & Barsi, J.A. 2012. The next Landsat satellite: The Landsat Data Continuity Mission. *Remote Sensing of Environment*, 122: 11–21.

Jakubauskas, M.E., Legates, D.R. & Kastens, J.H. 2002. Crop identification using harmonic analysis of time-series AVHRR NDVI data. *Computers and Electronics in Agriculture*, 37: 127–139.

Jensen, J.R. 1986. *Introductory digital image processing: A remote sensing perspective*.Pearson Education, Inc.: Glenview, IL, USA.

Jensen, F.V. & Nielsen, T.D. 2007. *Bayesian Networks and Decision Graphs*. Springer: New York, NY, USA.

Jewell, N. 1989. An evaluation of multi-date SPOT data for agriculture and land use mapping in the United Kingdom. *International Journal of Remote Sensing*, 10: 939–951.

Jia, K., Li, Q., Tian, Y., Wu, B., Zhang, F. & Meng, J. 2012. Crop classification using multi-configuration SAR data in the North China Plain. International Journal of Remote Sensing, 33. 170–183.

Jiao, X., Kovacs, J.M., Shang, J., McNairn, H., Walters, D., Ma, B. & Geng, X. 2014. Object-oriented crop mapping and monitoring using multi-temporal polarimetric RADARSAT-2 data. ISPRS Journal of Photogrammetry and Remote Sensing, 96: 38–46.

Johnson, D.M. 2013. A 2010 map estimate of annually tilled cropland within the coterminous United States. Agricultural Systems, 114: 95–105.

Jones, H.G. & Vaughan, R.A. 2010. *Remote Sensing of Vegetation: Principles, Techniques, and Applications*. Oxford University Press: Oxford, UK – New York, USA.

Kamusoko, C. & Aniya, M. 2009. Hybrid classification of Landsat data and GIS for land use/cover change analysis of the Bindura district, Zimbabwe. *International Journal of Remote Sensing,* 30: 97–115.

Kim, H.-O. & Yeom, J.-M. 2014. Effect of red-edge and texture features for object-based paddy rice crop classification using RapidEye multi-spectral satellite image data. *International Journal of Remote Sensing*: 1–23.

Kumar, L., Priyakant, S., Brown, J.F., Ramsey, R.D., Rigge, M., Stam, C.A., Hernandez, A.J., Hunt Jr., E.R. & Reeves, M. 2016. Characterization, mapping and monitoring of rangelands: Methods and approaches. In Thenkabail, P.S. (ed.), *Land Resources Monitoring, Modeling and Mapping with Remote Sensing* (pp. 309–350), CRC Press Inc.: Boca Raton, FL, USA.

Kussul, N., Lemoine, G., Gallego, F.J., Skakun, S.V., Lavreniuk, M. & Shelestov, A.Y. 2016. Parcel-Based Crop Classification in Ukraine Using Landsat-8 Data and Sentinel-1A Data. *IEEE Journal of Selected Topics in Applied Earth Observations and Remote Sensing*, 9: 2500–2508.

Laba, M., Smith, S.D. & Degloria, S.D. 1997. Landsat-based land cover mapping in the lower Yuna River watershed in the Dominican Republic. *International Journal of Remote Sensing*, 18: 3011–3025.

Larrañaga, A., Álvarez-Mozos, J. & Albizua, L. 2011. Crop classification in rain-fed and irrigated agricultural areas using Landsat TM and ALOS/PALSAR data. *Canadian Journal of Remote Sensing*, 37: 157–170.

Latham, J., Cumani, R., Rosati, I. & Bloise, M. 2014. *Global Land Cover SHARE (GLC-SHARE) Database Beta-Release Version 1.0-2-14*. Available at: http://www.fao.org/uploads/media/glc-share-doc.pdf. Last accessed 3 July 2017.

Latifovic, R., Zhu, Z.-L., Cihlar, J. & Olthof, I. 2004. Land cover mapping of North America - Global Land Cover 2000. *Remote Sensing of Environment*, 89: 116–127.

Lavreniuk, M., Kussul, N., Skakun, S., Shelestov, A. & Yailymov, B. 2015. Regional retrospective high resolution land cover for Ukraine: Methodology and results. In *2015 IEEE International Geoscience and Remote Sensing Symposium (IGARSS)* (pp. 3965–3968. IEEE Publication.

Li, Z., Huffman, T., McConkey, B. & Townley-Smith, L. 2013. Monitoring and modeling spatial and temporal patterns of grassland dynamics using time-series MODIS NDVI with climate and stocking data. *Remote Sensing of Environment*, 138: 232–244.

Liu, J., Liu, M., Tian, H., Zhuang, D., Zhang, Z., Zhang, W., Tang, X. & Deng, X. 2005. Spatial and temporal patterns of China's cropland during 1990–2000: an analysis based on Landsat TM data. *Remote Sensing of Environment*, 98: 442–456.

Loveland, T.R., Reed, B.C., Brown, J.F., Ohlen, D.O., Zhu, Z., Yang, L. & Merchant, J.W. 2000. Development of a global land cover characteristics database and IGBP DISCover from 1 km AVHRR data. International *Journal of Remote Sensing*, 21: 1303–1330.

Lu, D. & Weng, Q. 2007. A survey of image classification methods and techniques for improving classification performance. *International Journal of Remote Sensing*, 28: 823–870.

Lunetta, R.S., Knight, J.F., Ediriwickrema, J., Lyon, J.G. & Worthy, L.D. 2006. Land-cover change detection using multi-temporal MODIS NDVI data. *Remote Sensing of Environment*, 105: 142–154.

Lunetta, R.S., Shao, Y., Ediriwickrema, J. & Lyon, J.G. 2010. Monitoring agricultural cropping patterns across the Laurentian Great Lakes Basin using MODIS-NDVI data. *International Journal of Applied Earth Observation and Geoinformation*, 12: 81–88.

Lussem, U., Hütt, C. & Waldhoff, G. 2016. Combined Analysis of Sentinel-1 and Rapideye Data for Improved Crop Type Classification: An Early Season Approach for Rapeseed and Cereals. In: *ISPRS - International Archives of the Photogrammetry, Remote Sensing and Spatial Information Sciences*, Vol. XLI-B8 (pp. 959–963). ISPRS Publication.

Lymburner, L., Geoscience Australia, and Australian Bureau of Agricultural and Resource Economics. (2011). *The National Dynamic Land Cover Dataset*. Geoscience Australia Publication: (Canberra:.

Maselli, F., Conese, C., De Filippis, T. & Romani, M. 1995. Integration of ancillary data into a maximum-likelihood classifier with nonparametric priors. *ISPRS Journal of Photogrammetry and Remote Sensing*, 50: 2–11.

McNairn, H., Ellis, J., Van Der Sanden, J.J., Hirose, T. & Brown, R.J. 2002. Providing crop information using RADARSAT-1 and satellite optical imagery. *International Journal of Remote Sensing*, 23: 851–870.

McNairn, H., Champagne, C., Shang, J., Holmstrom, D. & Reichert, G. 2009. Integration of optical and Synthetic Aperture Radar (SAR) imagery for delivering operational annual crop inventories. *ISPRS Journal of Photogrammetry and Remote Sensing*, 64: 434–449.

National Research Council of the National Academies. 2003. *Satellite Observations of the Earth's Environment: Accelerating the Transition of Research to Operations*. National Academies Press: Washington, D.C.

Pal, M. & Mather, P.M. 2003. An assessment of the effectiveness of decision tree methods for land cover classification. *Remote Sensing of Environment*, 86: 554–565.

Pan, Y., Li, L., Zhang, J., Liang, S., Zhu, X. & Sulla-Menashe, D. 2012. Winter wheat area estimation from MODIS-EVI time series data using the Crop Proportion Phenology Index. *Remote Sensing of Environment*, 119: 232–242.

Pei, Z., Zhang, S., Guo, L., McNairn, H., Shang, J. & Jiao, X. 2011. Rice identification and change detection using TerraSAR-X data. *Canadian Journal of Remote Sensing*, 37: 151–156.

Peña-Barragán, J.M., Ngugi, M.K., Plant, R.E. & Six, J. 2011. Object-based crop identification using multiple vegetation indices, textural features and crop phenology. *Remote Sensing of Environment*, 115: 1301–1316.

Pittman, K., Hansen, M.C., Becker-Reshef, I., Potapov, P.V. & Justice, C.O. 2010. Estimating Global Cropland Extent with Multi-year MODIS Data. *Remote Sensing*, 2: 1844–1863.

Pringle, M.J., Denham, R.J. & Devadas, R. 2012. Identification of cropping activity in central and southern Queensland, Australia, with the aid of MODIS MOD13Q1 imagery. *International Journal of Applied Earth Observations and Geoinformation*, 19: 276–285.

Reese, H.M., Lillesand, T.M., Nagel, D.E., Stewart, J.S., Goldmann, R.A., Simmons, T.E., Chipman, J.W. & Tessar, P.A. 2002. Statewide land cover derived from multiseasonal Landsat TM data. *Remote Sensing of Environment*, 82: 224–237.

Rigol-Sanchez, J.P., Chica-Olmo, M. & Abarca-Hernandez, F. 2003. Artificial neural networks as a tool for mineral potential mapping with GIS. *International Journal of Remote Sensing*, 24: 1151–1156.

Rocha, J. & Queluz, M.P. 2002. Integration of census data, remote sensing, and GIS techniques for land-use and cover classification. In Ehlers, M. (ed.), *SPIE Proceedings: Remote Sensing for Environmental Monitoring, GIS Applications, and Geology* (pp. 73–83), Conference Volume 4545. SPIE Publication.

Rodriguez-Galiano, V. & Chica-Olmo, M. 2012. Land cover change analysis of a Mediterranean area in Spain using different sources of data: Multi-seasonal Landsat images, land surface temperature, digital terrain models and texture. *Applied Geography*, 35: 208–218.

Rogan, J., Franklin, J., Stow, D., Miller, J., Woodcock, C. & Roberts, D. 2008. Mapping land-cover modifications over large areas: A comparison of machine learning algorithms. *Remote Sensing of Environment*, 112: 2272–2283.

Rumelhart, D.E., Hinton, G.E. & Williams, R.J. 1986. Learning representations by back-propagating errors. *Nature*, 323: 533–536.

Sakamoto, T., Wardlow, B.D., Gitelson, A.A., Verma, S.B., Suyker, A.E. & Arkebauer, T.J. 2010. A Two-Step Filtering approach for detecting maize and soybean phenology with time-series MODIS data. *Remote Sensing of Environment*, 114: 2146–2159.

Schuster, C., Schmidt, T., Conrad, C., Kleinschmit, B. & Förster, M. 2015. Grassland habitat mapping by intra-annual time series analysis – Comparison of RapidEye and TerraSAR-X satellite data. *International Journal of Applied Earth Observations and Geoinformation*, 34: 25–34.

Shang, J., McNairn, H., Champagne, C. & Jiao, X. 2009. Application of Multi-Frequency Synthetic Aperture Radar (SAR) in Crop Classification. In Jedlovec, G. (ed.), *Advances in Geoscience and Remote Sensing* (pp. 557–568), InTech: Rijeka, Croatia.

Skriver, H. 2012. Crop Classification by Multitemporal C- and L-Band Single- and Dual-Polarization and Fully Polarimetric SAR. *IEEE Transactions on Geoscience and Remote Sensing*, 50: 2138–2149.

Skriver, H., Svendsen, M.T. & Thomsen, A.G. 1999. Multitemporal C-and L-band polarimetric signatures of crops. *IEEE Transactions on Geoscience and Remote Sensing*, 37: 2413–2429.

Sonobe, R., Tani, H., Wang, X., Kobayashi, N. & Shimamura, H. 2014. Random forest classification of crop type using multi-temporal TerraSAR-X dual-polarimetric data. *Remote Sensing Letters*, 5: 157–164.

Sreenivas, K., Sekhar, N.S., Saxena, M., Paliwal, R., Pathak, S., Porwal, M.C., Fyzee, M.A., Rao, S.K., Wadodkar, M. & Anasuya, T. 2015. Estimating inter-annual diversity of seasonal agricultural area using multi-temporal resourcesat data. *Journal of Environmental Management*, 161: 433–442.

Takahashi, M., Nasahara, K.N., Tadono, T., Watanabe, T., Dotsu, M., Sugimura, T. & Tomiyama, N. 2013. *High-Resolution Land Use and Land Cover Map of Japan*. Japan Aerospace Exploration Agency, pp. 2384–2387.

Tapsall, B., Milenov, P. & Tasdemir, K. 2010. Analysis of RapidEye imagery for annual landcover mapping as an aid to European Union (EU) common agricultural policy. In: Wagner, W. & Székely, B. (eds), Proceedings of the ISPRS TC VII Symposium – 100 Years ISPRS, (pp. 568–573), ISPRS Publication.

Tateishi, R., Uriyangqai, B., Al-Bilbisi, H., Ghar, M.A., Tsend-Ayush, J., Kobayashi, T., Kasimu, A., Hoan, N.T., Shalaby, A., Alsaaideh, B. *et al.* 2011a. Production of global land cover data – GLCNMO. *International Journal of Digital Earth*, 4. 22–49.

Tateishi, R., Uriyangqai, B., Al-Bilbisi, H., Ghar, M.A., Tsend-Ayush, J., Kobayashi, T., Kasimu, A., Hoan, N.T., Shalaby, A., Alsaaideh, B. *et al.* 2011b. Production of global land cover data – GLCNMO. *International Journal of Digital Earth* 4: 22–49.

Tatsumi, K., Yamashiki, Y., Canales Torres, M.A. & Taipe, C.L.R. 2015. Crop classification of upland fields using Random forest of time-series Landsat 7 ETM+ data. *Computers and Electronics in Agriculture*, 115: 171–179.

Teleguntla, P., Thenkabail, P.S., Xiong, J., Gumma, M.K., Giri, C., Milesi, C., Ozdogan, M., Congalton, R.G. & Tilton, J. 2016. Global food security support analysis data at nominal 1km (GFSAD1km) derived from remote sensing in support of food security in the twenty-first century: current achievements and future possibilities. In Thenkabail, P.S. (ed.), *Land Resources Monitoring, Modeling and Mapping with Remote Sensing*, (pp. 131–159), CRC Press: Boca Raton, FL, USA.

Thenkabail, P.S. and Wu, Z. 2012. An automated cropland classification algorithm (ACCA) for Tajikistan by combining Landsat, MODIS, and secondary data. *Remote Sensing*, 4: 2890–2918.

Thenkabail, P.S., Biradar, C.M., Noojipady, P., Dheeravath, V., Li, Y., Velpuri, M., Gumma, M., Gangalakunta, O.R.P., Turral, H., Cai, X. *et al.* 2009. Global irrigated area map (GIAM), derived from remote sensing, for the end of the last millennium. *International Journal of Remote Sensing*, 30: 3679–3733.

Toutin, T. 2005. Multisource Data Fusion with an Integrated and Unified Geometric Modelling. EARSeL *Advanced Remote Sensing*, : 118–129.

Turker, M. & Arikan, M. 2005. Sequential masking classification of multi-temporal Landsat7 ETM+ images for field-based crop mapping in Karacabey, Turkey. *International Journal of Remote Sensing*, 26: 3813–3830.

Turker, M. & Ozdarici, A. 2011. Field-based crop classification using SPOT4, SPOT5, IKONOS and QuickBird imagery for agricultural areas: a comparison study. *International Journal of Remote Sensing*, 32: 9735–9768.

Ustuner, M., Sanli, F.B., Abdikan, S., Esetlili, M.T. & Kurucu, Y. 2014. Crop Type Classification Using Vegetation Indices of RapidEye Imagery. In: *ISPRS - International Archives of the Photogrammetry, Remote Sensing and Spatial Information Sciences*, Vol. XL-7 (pp. 195–198). ISPRS Publication.

Valero, S., Morin, D., Inglada, J., Sepulcre, G., Arias, M., Hagolle, O., Dedieu, G., Bontemps, S., Defourny, P. & Koetz, B. 2016. Production of a Dynamic Cropland Mask by Processing Remote Sensing Image Series at High Temporal and Spatial Resolutions. *Remote Sensing*, 8: 55.

Valverde-Albacete, F.J. & Peláez-Moreno, C. 2010. Two Information-Theoretic Tools to Assess the Performance of Multi-Class Classifiers. *Pattern Recognition Letters*, 31(12): 1665–1671.

Valverde-Albacete, F.J. & Peláez-Moreno, C. 2014. 100% Classification Accuracy Considered Harmful: The Normalized Information Transfer Factor Explains the Accuracy Paradox. *PLoS ONE*, 9(1): e84217. Available at: doi:10.1371/journal.pone.0084217. Accessed on 10 June 2017.

Vancutsem, C., Marinho, E., Kayitakire, F., See, L. & Fritz, S. 2012. Harmonizing and Combining Existing Land Cover/Land Use Datasets for Cropland Area Monitoring at the African Continental Scale. *Remote Sensing*, 5: 19–41.

Verhegghen, A., Mayaux, P., de Wasseige, C. & Defourny, P. 2012. Mapping Congo Basin vegetation types from 300 m and 1 km multi-sensor time series for carbon stocks and forest areas estimation. *Biogeosciences*, 9: 5061–5079.

Vieira, M.A., Formaggio, A.R., Rennó, C.D., Atzberger, C., Aguiar, D.A. & Mello, M.P. 2012. Object Based Image Analysis and Data Mining applied to a remotely sensed Landsat time-series to map sugarcane over large areas. *Remote Sensing of Environment*, 123: 553–562.

Vincenzi, S., Zucchetta, M., Franzoi, P., Pellizzato, M., Pranovi, F., De Leo, G.A. & Torricelli, P. 2011. Application of a Random Forest algorithm to predict spatial distribution of the potential yield of Ruditapes philippinarum in the Venice lagoon, Italy. *Ecological Modelling,* 222: 1471–1478.

Waldner, F., Fritz, S., Di Gregorio, A. & Defourny, P. 2015. Mapping Priorities to Focus Cropland Mapping Activities: Fitness Assessment of Existing Global, Regional and National Cropland Maps. *Remote Sensing*, 7: 7959–7986.

Waldner, F., De Abelleyra, D., Verón, S.R., Zhang, M., Wu, B., Plotnikov, D., Bartalev, S., Lavreniuk, M., Skakun, S., Kussul, N. *et al.* 2016. Towards a set of agrosystem-specific cropland mapping methods to address the global cropland diversity. *International Journal of Remote Sensing*, 37: 3196–3231.

Wall, S.L., Thomas, R.W., Brown, C.E. & Bauer, E.H. 1984. Landsat-based inventory system for agriculture in California. *Remote Sensing of Environment*, 14: 267–278.

Wardlow, B.D. & Egbert, S.L. 2008. Large-area crop mapping using time-series MODIS 250 m NDVI data: An assessment for the U.S. Central Great Plains. *Remote Sensing of Environment*, 112: 1096–1116.

Wardlow, B., Egbert, S. & Kastens, J. 2007. Analysis of time-series MODIS 250 m vegetation index data for crop classification in the U.S. Central Great Plains. *Remote Sensing of Environment*, 108: 290–310.

Waske, B. & Braun, M. 2009. Classifier ensembles for land cover mapping using multitemporal SAR imagery. *ISPRS Journal of Photogrammetry and Remote Sensing*, 64: 450–457.

Watts, J.D., Lawrence, R.L., Miller, P.R. & Montagne, C. 2009. Monitoring of cropland practices for carbon sequestration purposes in north central Montana by Landsat remote sensing. *Remote Sensing of Environment*, 113: 1843–1852.

Whitcraft, A.K., Becker-Reshef, I. & Justice, C.O. 2015a. Agricultural growing season calendars derived from MODIS surface reflectance. *International Journal of Digital Earth*, 8: 173–197.

Whitcraft, A.K., Vermote, E.F., Becker-Reshef, I. & Justice, C.O. 2015b. Cloud cover throughout the agricultural growing season: Impacts on passive optical earth observations. *Remote Sensing of Environment*, 156: 438–447.

Whitcraft, A.K., Becker-Reshef, I. & Justice, C. 2015c. A Framework for Defining Spatially Explicit Earth Observation Requirements for a Global Agricultural Monitoring Initiative (GEOGLAM). *Remote Sensing*, 7: 1461–1481.

Wood, D., McNairn, H., Brown, R. & Dixon, R. 2002. The effect of dew on the use of RADARSAT-1 for crop monitoring. *Remote Sensing of Environment*, 80: 241–247.

World Bank, United Nations (UN) & Food and Agriculture Organization of the United Nations (FAO). 2010. Global strategy to improve agricultural and rural statistics. Report No. 56719-GLB. World Bank Publication: Washington, D.C. Available at: http://www.fao.org/docrep/015/am082e/am082e00.pdf. Last accessed 3 July 2017.

Wulder, M.A. & Nelson, T. 2001. *EOSD Land Cover Classification Legend Report*. Canadian Forest Service Publication: Victoria, BC, Canada.

Wulder, M.A., Hilker, T., White, J.C., Coops, N.C., Masek, J.G., Pflugmacher, D. & Crevier, Y. 2015. Virtual constellations for global terrestrial monitoring. *Remote Sensing of Environment*, 170: 62–76.

Xiuwan, C. 2002. Using remote sensing and GIS to analyse land cover change and its impacts on regional sustainable development. *International Journal of Remote Sensing*, 23: 107–124.

Xu, X., Doktor, D. & Conrad, C. 2016. Phenological Metrics Extraction for Agricultural Land-use Types Using RapidEye and MODIS. *Geophysical Research Abstracts*, 18: 10375.

Yan, L. & Roy, D.P. 2014. Automated crop field extraction from multi-temporal Web Enabled Landsat Data. *Remote Sensing of Environment*, 144: 42–64.

Yang, C., Everitt, J.H., Fletcher, R.S. & Murden, D. 2007. Using high resolution QuickBird imagery for crop identification and area estimation. *Geocarto International*, 22: 219–233.

Zhu, Z. & Woodcock, C.E. 2012. Object-based cloud and cloud shadow detection in Landsat imagery. *Remote Sensing of Environment*, 118: 83–94.

Zuo, R. & Carranza, E.J.M. 2011. Support vector machine: A tool for mapping mineral prospectivity. *Computers & Geosciences*, 37: 1967–1975.

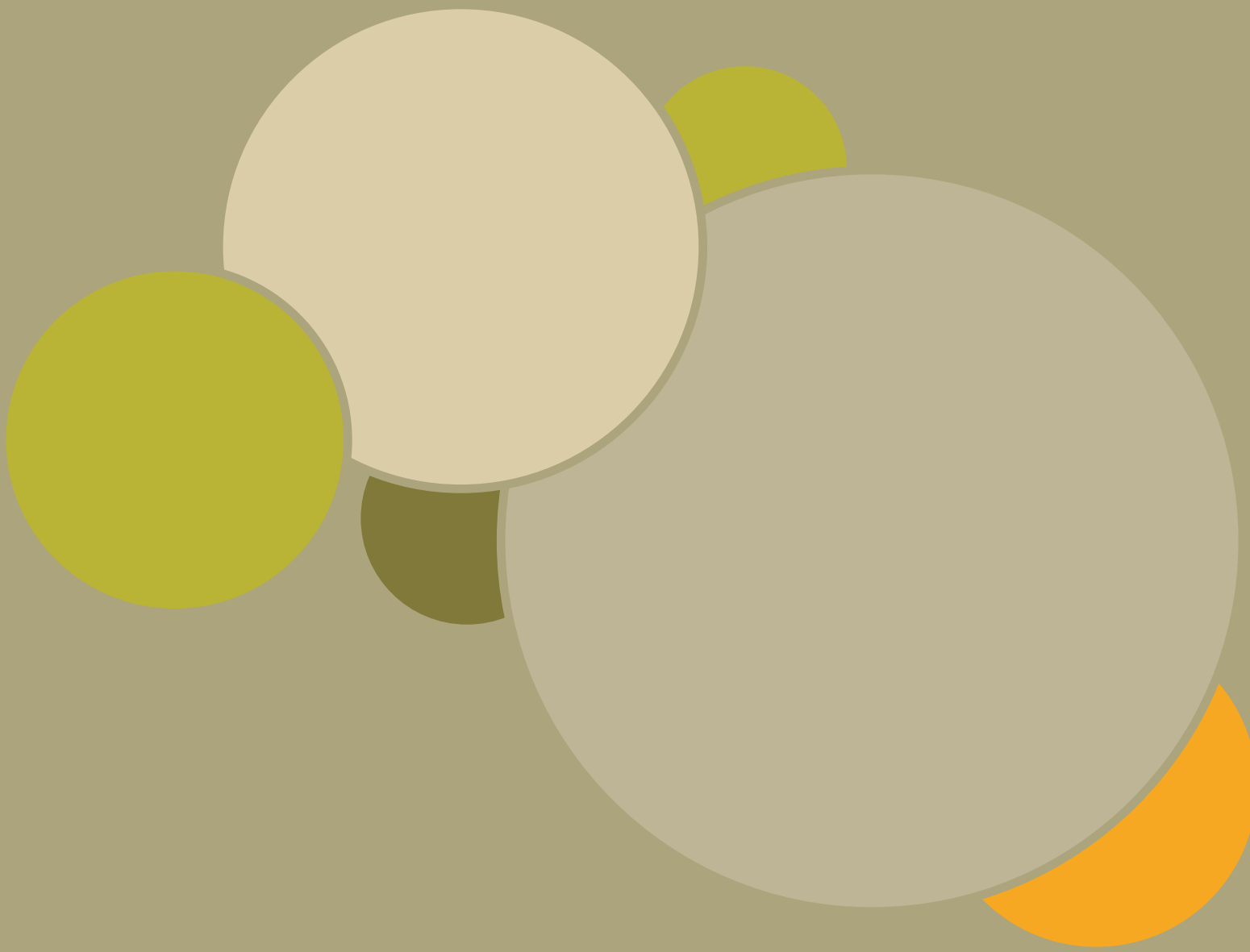

5

Chapter 5

Crop area estimation with remote sensing

Shibendu S. Ray & Neetu

5.1. CROP AREA ESTIMATION: INTRODUCTION

Crop production information, which is essential for various economic planning and agricultural market management (Gallego *et al*., 2014), has two components: crop area and crop yield. Among these two, it is always assumed that estimation of the area is comparatively simpler and more straightforward than estimation of the crop yield. However, crop area estimation presents several challenges and complexities, which may not be readily apparent (Craig and Atkinson, 2013).

Factors which determine the complexity of crop area estimation include, but are not limited to, the following: small field size, scattered and diversified cropping patterns, mixed cropping system with phenological differences, extended sowing process (for example, in India, the planting of rice progresses from June to September), changes in cropping pattern, short-duration crops, cropping in homesteads, complex physiography (such as crops grown on hillsides through terrace or contour farming), complex seasonality (sugarcane having a main crop and a ratoon crop; or crops growing in multiple seasons depending upon climate diversity). In addition, there may be changes in the crop sown area due to damage, which may be caused by both biotic (weather) and abiotic (pest and disease) factors. Furthermore, the crop area estimation must take place at multiple stages: before sowing (specifically, the date of intended sowing, which depends upon the profits obtained in the previous year from the crop and weather forecasts); during early sowing; at mid-season and before harvest (Vogel and Bange, 1999).

Craig and Atkinson (2013) have provided a review of the methods used for crop area estimation. Conventionally, crop area is estimated either by complete enumeration of all farms or by samples. The sampling may be Area Frame Sampling (AFS), farm list sampling or a combination of both; the latter case is called multiple frame sampling. In some cases, it also involves the expert opinion of voluntary crop reporters. Other sources of crop area may be

administrative surveys, crop processing units (for example, cotton or jute mills) and markets. The final estimate is generated either by direct reference to the survey data or by a panel of experts, which reviews data from different sources and finalizes the estimates.

However, the conventional method of crop area estimation is time-consuming, costly, tedious and subject to human bias. It is also extremely difficult in several land types, such as hilly terrains. To overcome these problems, satellite remote sensing has been used for crop area estimation, either directly or to support the area sampling schemes. Satellite remote sensing provides temporal, synoptic, multispectral and multiresolution images of land use and land cover and offers the ability to classify different crops.

Use of satellite-based remote sensing data for crop area estimation dates back to the early 1970s, when the Corn Blight Watch Experiment was jointly carried out in 1971 by the U.S. Department of Agriculture (USDA), the National Aeronautics and Space Administration (NASA) and a number of universities (Sharples, 1973). In 1972, the ERTS-A was successfully launched and NASA conducted joint experiments with the USDA to establish the feasibility of surveying major crop types from space with multispectral remote sensing technology (Bryan, 1974). Experiments such as the Crop Identification Technology Assessment for Remote Sensing (CITARS) experiment and the Large Area Crop Inventory Experiment (LACIE) were conducted to demonstrate the capabilities of remote sensing in the context of crop inventory (MacDonald, 1984). The CITARS experiment evaluated classification procedures and alternative analysis techniques for corn and soybean crops.

LACIE was the first program sponsored by the Government of the United States of America aimed at examining the feasibility of using remotely sensed satellite data – specifically, Landsat data – to estimate wheat production over large geographic areas (Nellis *et al*., 2009). The LACIE programme was first operated in 1974 in the Great Plains of the United States of America, and was extended to include Canada and the former Soviet Union (MacDonald, 1984). The successes of LACIE led to a follow-on project in 1980 called Agriculture and Resources Inventory Surveys Through Aerospace Remote Sensing (AgRISTARS). The goal of this new program was to expand upon LACIE and include monitoring of other crops such as barley, corn, cotton, rice, soybeans and wheat (Holmes *et al*., 1979). The AgRISTARS program was successful in demonstrating the value of timely data and limited ground reference information for identifying crops and predicting yield.

5.1.1. LACIE

The LACIE experiment proved to be a potential model for other programmes designed to globally measure other terrestrial plant communities by remote sensing from satellites (Erickson, 1984; MacDonald and Hall, 1980). The LACIE experiment was a joint programme of NASA, the National Oceanic and Atmospheric Administration (NOAA) and the USDA, and was the first operational agricultural assessment programme to demonstrate the potential uses of Landsat data. LACIE envisaged three phases: Phase I (conducted between 1974 and 1975) developed a methodology in the Great Plains (area estimation was performed in a quasi-operational mode, while yield and production estimation were performed in a feasibility test mode); Phase II (1975-1976) evaluated the methodology in the Great Plains, Canada, and in "indicator regions" in the former USSR (the quasi-operational wheat area estimation was extended to yield and production); Phase III (1976-1977), in which a second-generation technology, developed in Phases I and II, was used to forecast the 1977 Soviet wheat crop at country level. The project also conducted exploratory studies in India, China, Australia, Argentina, and Brazil (MacDonald and Hall, 1980). The area was estimated from selected sample segments using Landsat data, while yield was estimated using weather-based models with data from the World Meteorological Organization (WMO).

LACIE used a performance envelope of 90/90, which means that in 90 percent of the cases, the error was within a 10 percent range. The results from LACIE were more reliable for the former USSR, and also met the 90/90 accuracy

criterion for the Great Plains. Although the results for Canada, India, China, Australia, Brazil and Argentina were encouraging, they did not meet the 90/90 accuracy goal (MacDonald and Hall, 1980).

Hanuschak *et al*. (1982) have described how Landsat was successfully used from 1972 to 1982 for the USDA's Statistical Reporting Service (SRS), towards improving (i) the area sampling frame (ASF) and (ii) the regression estimation of crop area.

Subsequently, many methodology development and demonstration programmes were carried out in various countries to explore the use of satellite-based remote sensing data in crop area estimation (Dadhwal *et al*., 2002).

Currently, many countries use remotely sensed satellite data for different aspects of crop area estimations. Table 1 presents a summary of satellite data utilization in various operational national crop area estimation programmes. Countries use different types of satellite data and various approaches, which are described in the subsequent sections. In section 3, two national programmes (USDA/NASS's Cropland Data Layer (CDL) programme and India's Forecasting Agricultural Output using Space, Agrometeorology and Land-based observations (FASAL programme), one regional programme (the European Union's Joint Research Centre's Monitoring Agriculture with Remote Sensing (EU JRC/MARS) Area Estimate) and two global programmes (the USDA's Foreign Agriculture Service (FAS) and China's CropWatch) are discussed in detail to understand various aspects of satellite data use.

5.2. APPROACHES TO CROP AREA ESTIMATION USING REMOTE SENSING

The basic principle guiding the use of remote sensing in the context of crop identification and classification is founded on the fact that crops look different (have different spectral signatures) in multispectral data due to their different structure, physiology, cultural practice and phenology. With the support of selected ground information, called ground truth, crops may be identified. This concept is used in four broad approaches for crop area estimation using remote sensing data: (i) ASF design; (ii) direct estimation or pixel counting; (iii) regression estimator; and (iv) calibration estimator.

5.2.1. ASF design

Chapter 3 of this handbook addressed the use of remote sensing for sampling frame design. For this purpose, satellite imagery is of the utmost value, as it provides a table of reference when elaborating the population frame; in particular, it may be used to subdivide areas of interest into enumeration areas (EAs) in which list frames of holdings are defined, and it helps with the definition of area frames composed of primary and secondary sampling units (PSUs and SSUs respectively), which are readily identifiable in the digital imagery (Delincé, 2015). The crop proportion derived from remote sensing data, either through visual interpretation or digital classification, is used to characterize spatial variability and, in turn, a parameter of stratification for area frame sample design. There are two types of area frame: (i) an area frame with physical or natural boundaries; and (ii) an area frame having a regular shape (grid sampling).

In figure 1, an example of a regularly shaped (5 x 5 km grid) area frame is shown for India's Bihar State, as assessed under India's FASAL project. The classified crop map (figure 1a) is used to stratify the 5 x 5 km segments into four strata (A type: over 50 percent constituted by crop area; B type: between 30 and 50 percent, C type: between

15 and 30 percent, D type: between 5 and 15 percent). A unique identification number is provided for each 5 x 5 km segment. After stratification, approximately 15 percent of the sample segments (table 2) are selected from each type for final analysis. Approximately 50 percent of these sample segments are visited in the field for ground truth data collection.

FIGURE 1. AFS DESIGN FOR BIHAR STATE, INDIA, UNDER THE FASAL PROGRAMME.

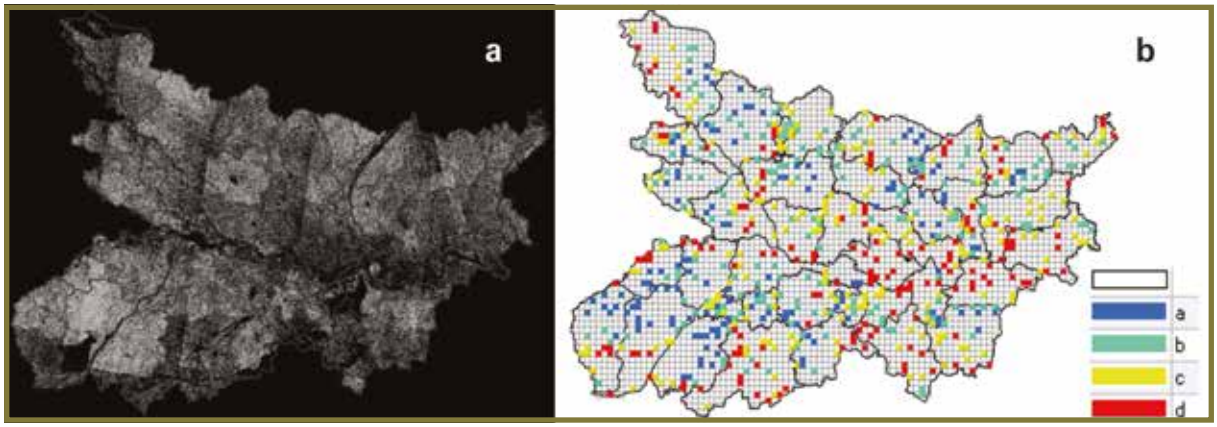

1a) Classified crop map of Bihar State. 1b) 5 x 5 km grids overlaid onto the classified image, with each grid stratified into four classes (A, B, C and D) based on crop proportion. The figure shows selected sample segments (approximately 15 percent) from each type.

Square segments are not the only possible approach for constructing area frames. In FAO's study on rice area estimation in Afghanistan (FAO, 2017), irregular segments, with limits constituted by physical boundaries, were used. Due to a complex local landscape, the ASF was designed at multiple levels: there were PSUs (of 500 to 700 ha), SSUs (from 200 to 300 ha) and Terminal Sampling Units (between 25 and 35 ha). The stratification was based on crop intensity (greater than 75 percent, between 50 and 75 percent, between 25 and 50 percent, and lower than 25 percent). Frame design definition and survey optimization were based on imagery from Pleiades to MODIS.

ASF design using remote sensing data provides a high stratification efficiency. Carfagna (2013) noted that in the pilot areas of the MARS Project, in most cases, efficiency ranged from 1.1 to 1.6 percent. Gallego *et al*. (1999) found the efficiency to lie between 1.7 and 2.2 percent for main crops in Spain. In India, for rice crop estimation using microwave data (Special Aperture Radar, or SAR), the efficiency of stratification ranged from 1.0 to 2.68 percent (table 2).

The Coefficient of Variation (CV) is another parameter that characterizes the usefulness of stratification. In India, for rice areas between 1 million and 3 million ha (at state level), the CVs ranged between 1.15 to 3 percent for sample sizes of 1229 and 450 ha respectively. For rice crops, a significant negative correlation was found between the CV and the crop area at a fixed sampling rate (approximately 15 percent). From the study of ASF design in various countries, Delincé (2015) also found that the CVs increased as crop area decreased.

TABLE 1. USE OF REMOTE SENSING FOR CROP AREA ESTIMATION IN DIFFERENT COUNTRIES

Country	Organization	Name of The Programme	Satellite Data	Scale	Crops	Approach	Ref.
Afghanistan	FAO		ProbaV, Aqua/Terra, Landsat 8, Sentinel 1, Sentinel 2, SPOT 5, 6 &7 and Pleiades 1A & 1B	District, Province	Rice	AFS design, image classification and regression estimator	FAO, 2017
Argentina	*Secretaría de Agricultura, Ganadería, Pesca y Alimentos de la Nación Argentina (SAGPyA)*		Landsat		Wheat, corn, soybean	ASF and classification	Justice and Becker-Reshef, 2007
Asia (6 countries)	International Rice Research Institute (IRRI)	Remote Sensing based Information and Insurance for crops in Emerging economies (RIICE)	X-band SAR from COSMO-SkyMed; TerraSAR-X	Selected sites	Rice	Image classification	Nelson *et al.*, 2014
Australia	University of Queensland		MODIS EVI		Wheat, barley, chickpea	Harmonic analysis, Principal component analysis	Potgieter *et al.*, 2007
Brazil	*Companhia Nacional de Abastecimento* (CONAB)	GeoSafras	Landsat & MODIS		Corn, soybean & wheat	Regression analysis	Fontana *et al.*, 2006
Canada	Statistics Canada	Still at research level	Landsat 8			Classification	Brisbane and Mohl, 2014
China	National Bureau of Statistics (NBS), Ministry of Agriculture	Crop Acreage Estimation by using Remote Sensing and Sample Survey (CAERSS) China Agricultural Remote Sensing Monitoring System (CHARMS)	Province	Corn, rice and soybean	AFS system and regression/ calibration		Pan *et al.*, 2012
Ethiopia	University of California	Research study	Ikonos, Landsat	District	Cropped area	AFS and classification	Husak *et al.*, 2008
European Union (28 countries)	JRC	MARS	Landsat TM & SPOT XS	EU, Member State	Wheat, barley, maize, rice, pulses; rape, sunflower, sugar beet	Stratification and regression estimator	Gallego, 2000 and 2006

Country	Organization	Name of The Programme	Satellite Data	Scale	Crops	Approach	Ref.
Hungary	FÖMI Remote Sensing Centre	Crop Monitoring and Production Forecast Program (CROPMON)	Landsat and IRS-1C/1D	County	Wheat, maize	Image classification	Csornai et al, 2006
India	Mahalanobis National Crop Forecast Centre (MNCFC), (Department of Agricultural Cooperation & Farmers Welfare, or DAC&FW)	FASAL	Resourcesat 2: AWiFS& LISS III; Landsat & Sentinel 2; RISAT-1 SAR	District, State, National	Rice, wheat, cotton, sugarcane, sorghum, jute, rapeseed and mustard, potato	ASF design and Image classification	Ray *et al.*, 2015
Pakistan	Space and Upper Atmosphere Research Commission (SUPARCO)		SPOT 5	Province	Wheat, rice, cotton, sugarcane, maize, potato	Image classification and AFS system	Ahmad *et al.*, 2015
Russian Federation	Ministry of Agriculture	Agrocosmos	MODIS 16 Day NDVI Product	Oblast/ District	To support agricultural censuses		Temnikov and Sergey, 2007
Spain	Regional Ministry of Agriculture	Castile and León crops and natural land map	Deimos 1 & Landsat 8		CDL	Classification using a machine learning algorithm	Medina and Garcia, 2015
South Africa	National Crop Statistics Consortium	Producer Independent Crop Estimate System (PICES)	Landsat	Province	Sunflower, maize	Image classification	Ferreira *et al.*, 2006
USA	USDA/NASS	CDL	Resourcesat AWiFS, Landsat ETM+	State	Cotton, wheat, sorghum, rice, soybean, etc.	Regression estimator	Bailey and Boryan, 2010

TABLE 2. RICE SAMPLING PLAN, CVS AND STRATIFICATION EFFICIENCY FOR VARIOUS STATES OF INDIA AS USED UNDER THE FASAL PROJECT.

State	Population of 5 x 5 km grids				Samples of 5 x 5 km grids				Population total	Sample total	Sampling fraction	CV (%)	Stratification efficiency
	A	B	C	D	a	b	c	d	N	n	%		
Andhra Pradesh	316	581	736	1201	49	91	111	174	2 834	425	15	2.37	2.68
Assam	524	840	937	681	96	120	125	84	3 000	425	14	1.77	1.46
Bihar	646	989	1091	784	109	145	166	109	3 510	529	15	1.60	1.230
Chhattisgarh	711	979	1042	1 347	111	154	159	203	4 079	642	15	1.31	1.56
Haryana	273	265	339	499	46	53	61	93	1 376	253	18.4	2.28	2.66
Jharkhand	233	552	747	872	47	89	127	141	2 404	404	16.8	1.81	1.234
Karnataka	195	521	741	1 350	41	91	123	203	2 807	458	16.3	3.09	1.22
Madhya Pradesh	273	460	826	848	59	79	130	128	2 407	396	16.4	2.95	1.00
Punjab	462	554	503	387	72	105	93	78	1 906	348	18.2	1.52	1.53
Uttar Pradesh	1 332	2 218	2 154	1 826	227	364	367	318	7 530	1 276	16.9	1.15	1.40

A type: > 50% crop area; B type: 30–50%, C type: 15–30%, D type: 5–15%
Stratification efficiency is the ratio between the variances of Simple Random Sampling (SRS) and stratified sampling.

FIGURE 2. CVS OF ESTIMATES AS A FUNCTION OF RICE CROP AREA IN DIFFERENT STATES OF INDIA.

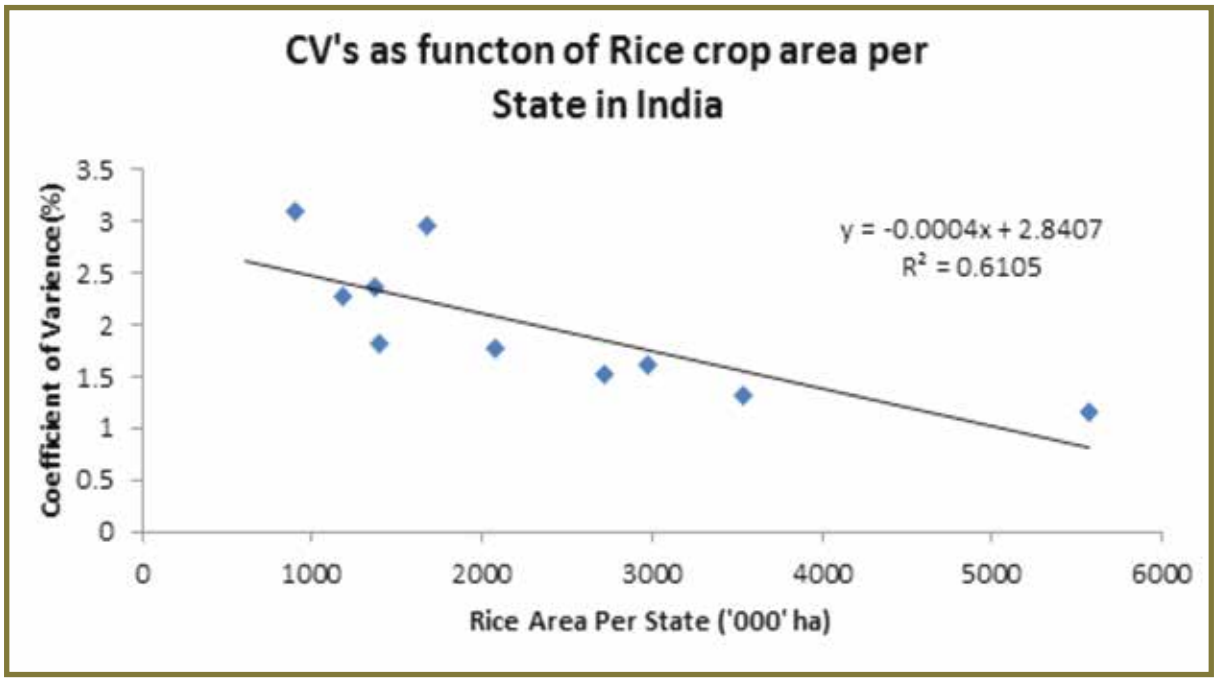

5.2.1.1 Direct estimation or pixel counting

In this approach, the satellite image is classified using the ground truth collected from sample locations. The number of pixels under each crop within an administrative boundary is multiplied by the pixel size to obtain the area of the crop.

The image analysis is carried out in sample segments or on whole scenes (complete enumeration). In the case of sample segments, the area under each segment is estimated and statistically aggregated to obtain the total area. In complete enumeration, the image is overlaid with the administrative boundary (district/state/county/province), and the total crop pixels are counted and multiplied with the pixel size to obtain the crop area. Additionally, under complete enumeration, a crop map is available, which can be used for several other purposes, such as yield sampling.

The classification can be either supervised (where classes are defined based on the ground truth) or unsupervised (and therefore based on the exploitation of the inherent tendency of different classes to form clusters in the feature space). Minimum-Distance-to-Means, Parallelepiped, and Maximum Likelihood (ML) are the common algorithms used for supervised classification; ISODATA and K-Means are the examples of classifiers used in unsupervised classification. The other newer approaches for crop classification include Hierarchical (Decision Tree) classifiers, Support Vector Machines, Artificial Neural Networks and Fuzzy-set classifiers. Prasad *et al*. (2015) have provided a survey of techniques that may be used for image classification.

Classification is carried out using multitemporal moderate-resolution satellite data (MODIS, Resourcesat AWiFS or SPOT VGT) or single-date high-resolution data (Landsat OLI, Resourcesat LISS III or Sentinel 2 MSI). The costs of the various optical satellite data generally used for crop classification are presented in Table 3.

TABLE 3. EXAMPLES OF THE COSTS OF VARIOUS OPTICAL AND MICROWAVE SATELLITE DATA USED FOR CROP AREA ESTIMATION.

Satellite	Sensor	Product Specification	Price (in euros)*
EO1	MODIS (Terra and Aqua)	250 m/500 m/1 km products	Free
SPOT 5	HRS VEGETATION 2	20 m MS, 60 x 60 km 10 m MS, 60 x 60 km 5 m MS, 60 x 60 km 1 km products	1 900 2 700 5 400 Free
Landsat 8	OLI		Free
Resourcesat-2@	AWiFS LISS III LISS IV	56 m MS, 740 x 740 km 24 m MS, 140 x 140km 5.8 m MS, 70 x 70 km	222 96 147
Sentinel 2	MSI		Free
Rapide Eye	Multispectral	Basic/Ortho, Contiguous 3 500 km2	3 325
RISAT 1@	C-Band SAR	MRS, 18 m, 115 x 115 km2	69
Sentinel 1	C-Band SAR		Free
Radarsat 2	C-Band SAR	Wide 30 m; 150 x 150 km2	2 590
COSMO-SkyMed	X-Band SAR	ScanSAR Wide 30 m; 100 x 100km2	1 650

Source: http://www.e-geos.it/products/ pdf/prices.pdf. Prices are for new acquisitions
N.B. Readers are referred to chapter 1 for the detailed information on sensor characteristics

5.2.1.2. Multidate data analysis

Multidate data analysis is based on the concept of using the differences in the phenology (growing patterns) of different crops grown in the same area. Generally, a moderate spatial resolution with high temporal frequency data is used, such as MODIS (250 m, daily or eight-day products), SPOT VGT (1 km, daily or ten-day products) or Resourcesat 2 AWiFS (56 m, five-day products). Seven to ten dates of coregistered data covering the major part of the crop growing period is used for crop classification. A decision-rule (hierarchical) classification approach is used on multidate Normalized Difference Vegetation Index (NDVI) products to classify different crops based on their growth cycle.

Figure 3 illustrates an example of fortnightly composite NDVI products, derived from Resourcesat 2 AWiFS data, for Uttar Pradesh State, India, during the rabi (winter) season (November/December to March/April). This data set is used to classify its major crops, which are wheat, rapeseed & mustard, potato and pulses. Temporal NDVI profiles for all of these crops are shown in figure 4. For potato, the NDVI increases sharply and peaks in end-December and during the first fortnight of January. For mustard, NDVI increases from end-December and decreases towards end-February. The temporal profile for wheat shows an increase in the NDVI from January which continues throughout the growing period, which goes from December to April. For pulses, the different temporal signatures are comparable to those of other major crops.

5.2.2. Single-date data analysis

Single-date data analysis is based on the criterion that, during the maximum vegetative growth of the target, with a sufficient amount of ground information, it can be discriminated from other crop and land use/land cover classes. In this case, higher-resolution satellite data (such as from Resourcesat 2 LISS III, Landsat 8 OLI, or Sentinel 2 MSI) are used. Ground truth information is used for crop signature generation. Supervised classification (such as the ML Classifier) approach is followed for classifying the pixels under a particular crop. The pixel area is multiplied with the number of pixels to obtain the crop area under an administrative boundary. Figure 5 shows an example of mustard and wheat classification using Landsat data.

FIGURE 3. WEEKLY/FORTNIGHTLY COMPOSITE NDVI IMAGES FOR UTTAR PRADESH STATE, INDIA.

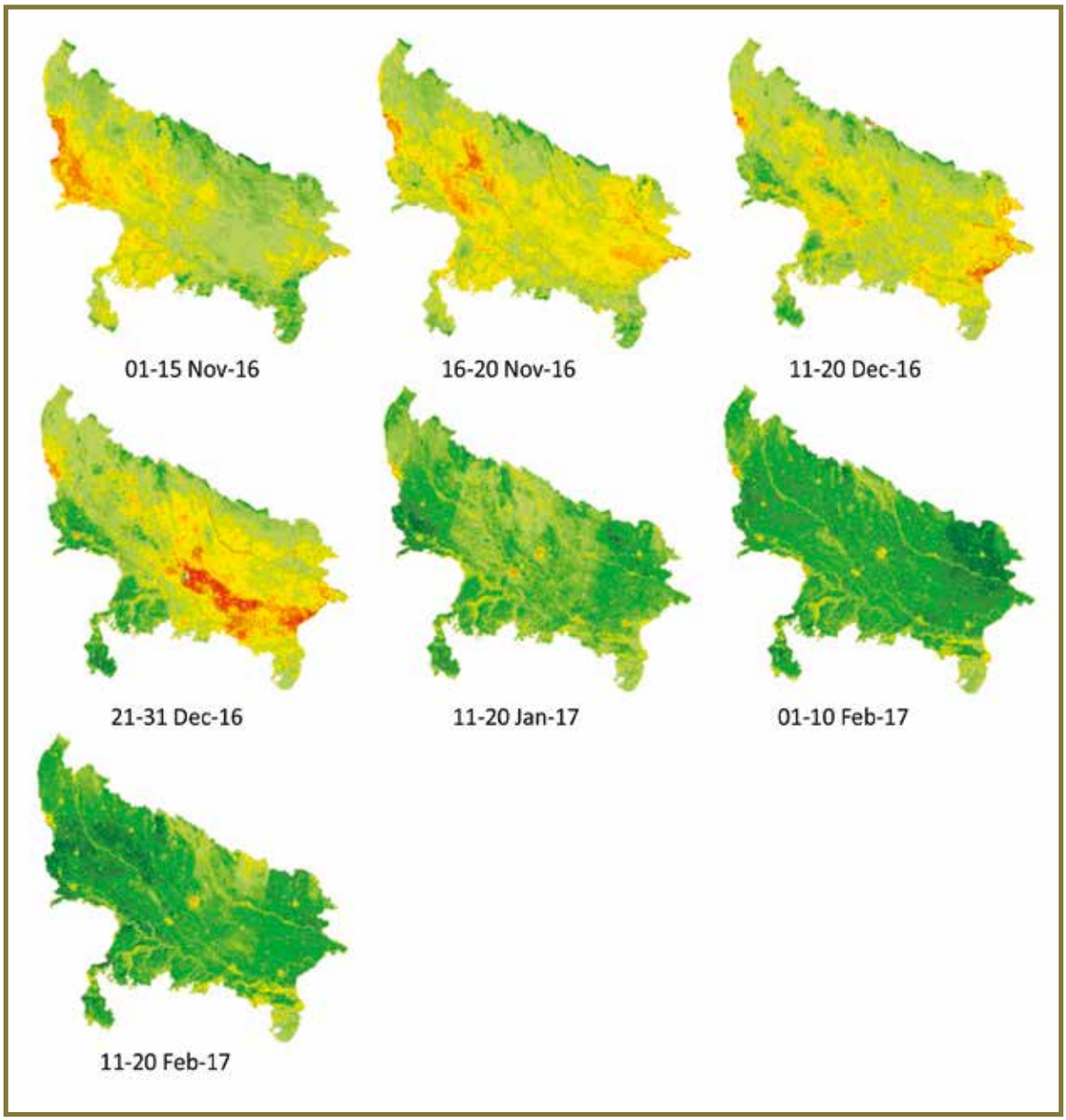

FIGURE 4. TEMPORAL NDVI (SCALED) PROFILE OF VARIOUS CROP CLASSES FOR UTTAR PRADESH STATE, INDIA.

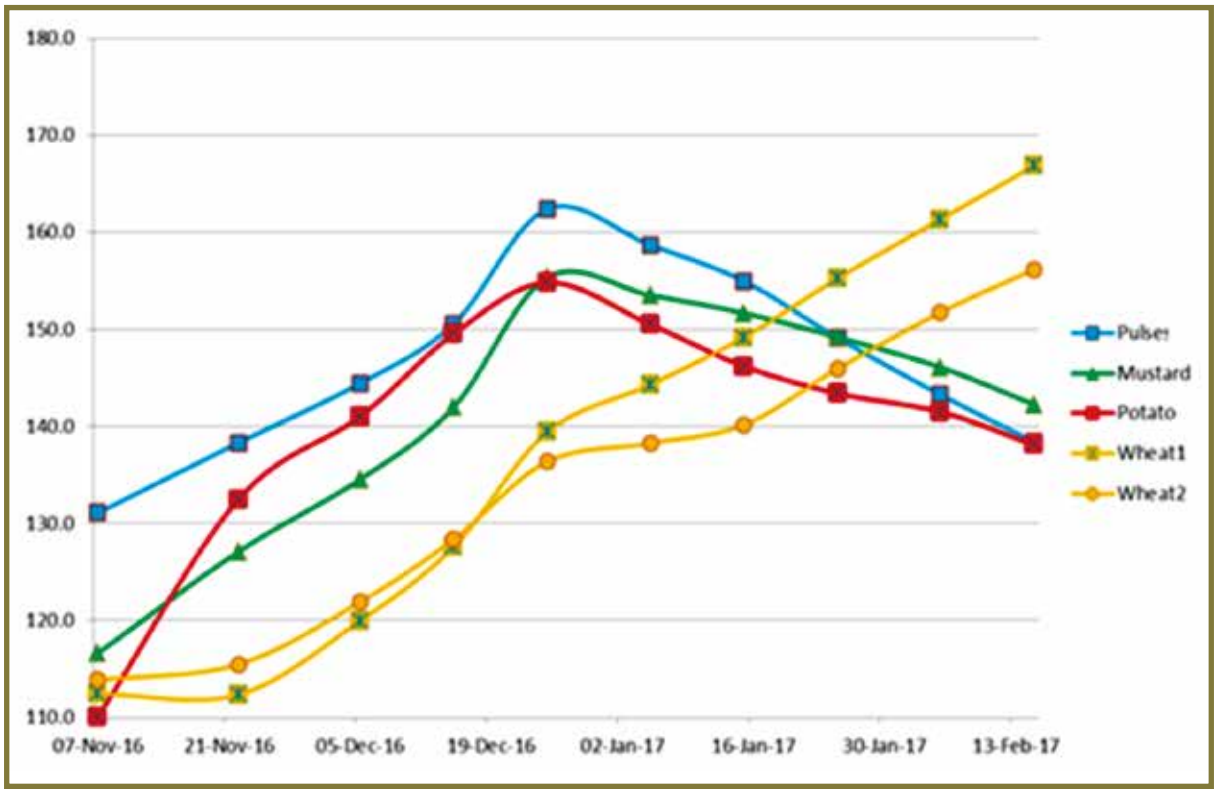

FIGURE 5. LANDSAT FCC (LEFT) AND CLASSIFIED (WHEAT AND MUSTARD, RIGHT) IMAGES FOR BHIWANI DISTRICT, HARYANA STATE, INDIA.PRADESH STATE, INDIA.

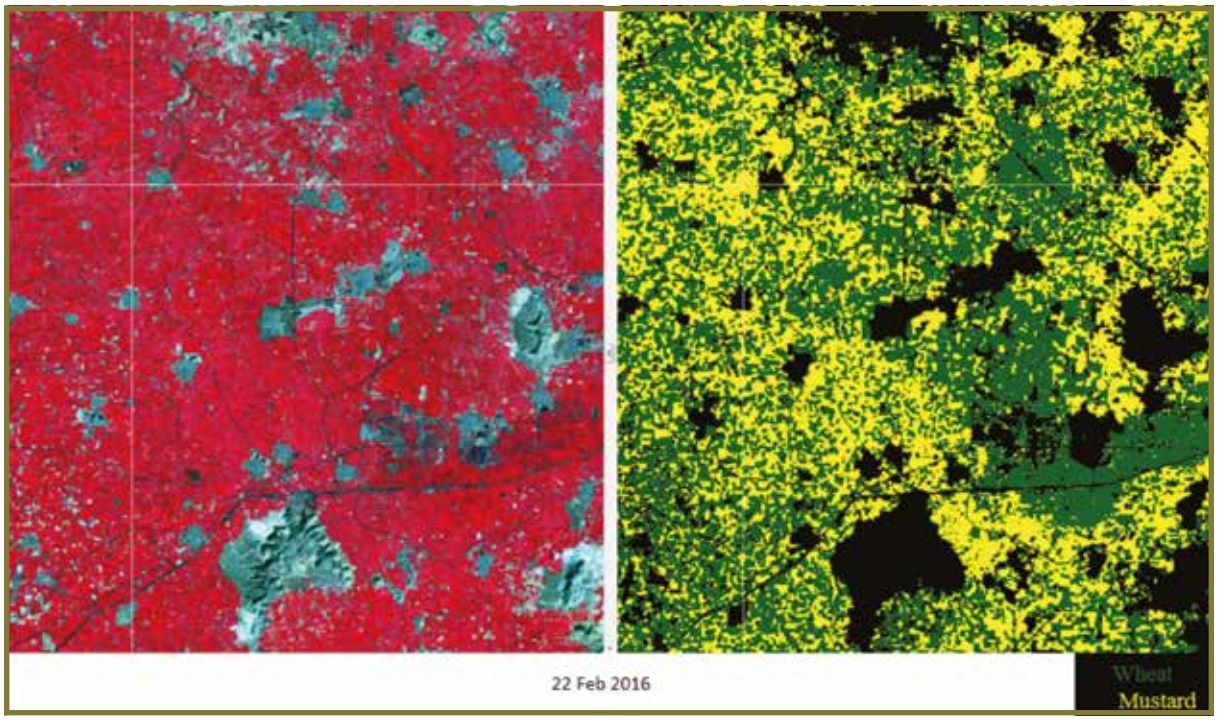

5.2.3. Use of SAR data for crop area estimation

In most South Asian and Southeast Asian countries where paddy rice is grown, it is difficult to obtain optical data during the rainy season (the major rice-growing season) due to persistent cloud cover. The issue of cloud cover can be addressed by using microwave SAR data. SARs are sensitive to surface roughness. Rice is generally grown through transplanting in flooded fields. Freshly transplanted rice plants provide a very low backscatter value due to specular reflection from standing water in the field (Choudhury and Chakraborty, 2006; Suga and Konishi, 2008). As the plant grows and develops tillers, the radar backscatter increases until the plant reaches the reproductive stage. This is due to volume scattering from the vegetation and multiple reflections between the plants and water surface (Chakraborty *et al*., 2006; Nelson *et al*., 2014). Beyond this stage, the radar backscatter remains nearly constant (Chkraborty *et al*., 1997). Therefore, typically, for rice area estimation using SAR data, data from at least three different dates is required: before planting, during planting and after planting, with a gap of approximately 20–25 days between each date.

The general steps for processing SAR data for rice crops are the following:

- Image georeferencing;
- Image calibration and speckle removal using a predefined adaptive low-pass filter;
- Multidate (three dates) image coregistration and data set preparation;
- Conversion of pixel digital numbers to backscatter values;
- Overlaying of ground truth sites and identification of rice sites;
- Development of a decision rule based on the temporal profile of backscatter values for the rice crop (figure 6); and
- Rice crop classification and area estimation.

FIGURE 6. TEMPORAL PROFILE OF VARIOUS RICE CLASSES FOR MIRZAPUR DISTRICT, UTTAR PRADESH STATE, INDIA.

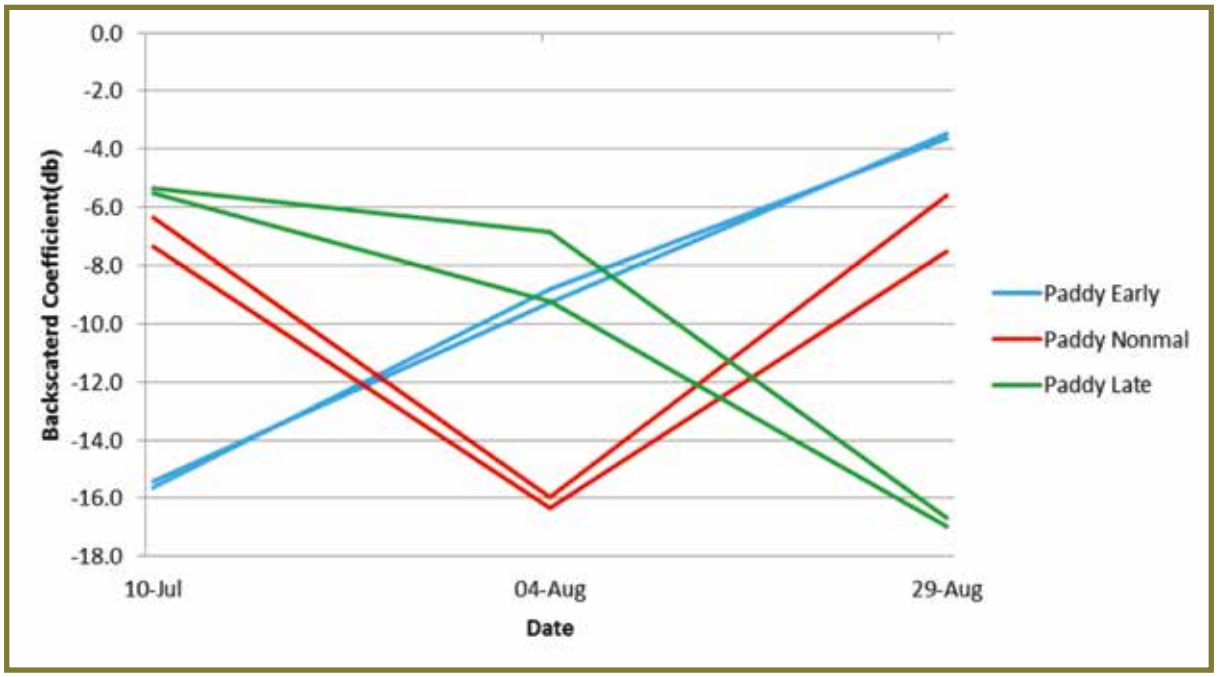

The typical example of decision rule for rice classification is given in the box below.

BOX 2.

- Urban: L1 > -6.0 AND L2 > -6.0 AND L3 > -6.0
- Water: L1 < -17.0 AND L2 < -17.0 AND L3 < -17.0
- Early transplanted rice: (-18.0 <= L1<=-14.0) AND (-12.0 < L2 <=-8.0) AND (-6.0 < L3 <= -2.0) AND (L2>L1+1.0) AND (L3>L2+1.0)
- Normal transplanted rice: (-10.0 <= L1<=-4.0) AND (-18.0 < L2 <-12.0) AND (-10.0 < L3 <=-3.0) AND (L1>L2+1.0) AND (L3>L2+1.0)
- Late transplanted rice: (-8.0 <= L1 <=-3.0) AND (-11.0 < L2 <-5.0) AND (-18.0 < L3 <=-14.0) AND (L2>L3+1.0)

Where
L1 = Backscatter Coefficient (dB) at first date
L2 = Backscatter Coefficient (dB) at second date
L3= Back scatter Coefficient (dB) at third date.

5.2.4. Ground truth data

Ground truth is an essential component for crop classification, either as an input for building a classification algorithm or as validation of the classification. The ground truth is collected with respect to land use and land cover. Typically, ground truth for crop classification includes geographical location, the village, district or state, the name of the crop, the coverage, the condition, the stage, whether it is irrigated or rainfed, the expected yield, the sowing and harvesting dates, etc., along with two photographs (close view and wide view) of the field. The ground truth is collected from selected sample locations spread over the entire study region, covering all types of diversity. Various Android apps for smartphones have been developed for field data collection. The data collected through smartphones can be uploaded in real time to a central server for use by the analysts working on image analysis. In India, ground truth is collected by officials of the agriculture department of the individual state governments, and is then uploaded to the Bhuvan server (a geoportal of the Indian Space Research Organisation, or ISRO; see figure 7).

FIGURE 7. GROUND TRUTH DATA COLLECTED USING SMARTPHONES, AVAILABLE ON THE BHUVAN GEOPORTAL.

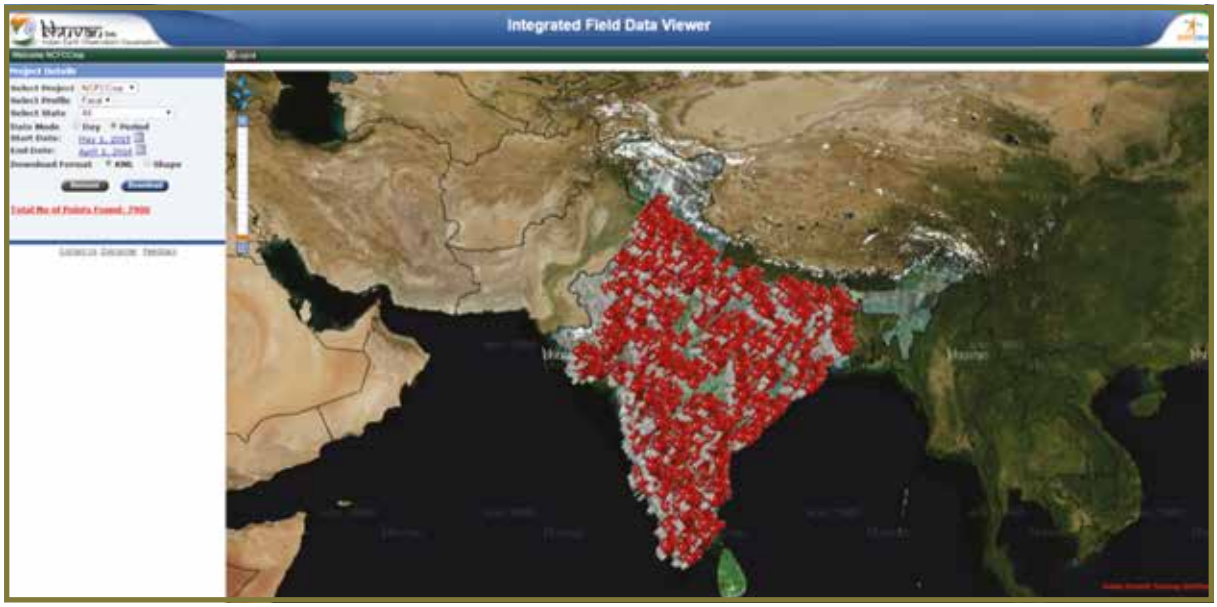

5.2.5. Accuracy estimation: confusion matrix and relative deviation

The confusion matrix, which is also known as the error matrix, represents the visualization of the performance of a classification. In table 4, the two dimensions show the actual or reference class and the predicted or classified pixels in columns and rows respectively. The confusion matrix summarizes the results and enables further inspection of the classification.

Examples of confusion matrices for two classification scenarios (total area of crops and individual crops) are presented in tables 4 and 5 below. In the pilot study conducted in Kazakhstan, Gallego showed that the total area of crops (cereals and fallow) can be estimated by pixel counting with a subjectivity margin of approximately 5 percent, while in India, the individual crop classification accuracy ranged between 70 and 90 percent, with an overall accuracy of 81.09 percent and Kappa statistics of 0.7606. Clauss *et al*. (2016), when mapping paddy rice in China using MODIS time series data, found an overall accuracy of 0.90 and a user accuracy of 0.90 for the no_rice and 0.89 for the rice class.

TABLE 4. EXAMPLE OF CONFUSION MATRIX FOR A PILOT STUDY IN KAZAKHASTAN.

		Reference			
Classification		Cereals + fallow	Grass + abandon	Total	Producer Accuracy
	Crop	1 470 + 152	57	1 679	96.6%
	Grass + abandon	39 + 68	353	460	76.7%
	Total	1 729	410	2 139	
	User Accuracy	93.8%	86.1%		

Source: Gallego, J. 2008. Crop Area Estimation with Remote Sensing: Some considerations and experiences for the application to general agricultural statistics, presentation prepared for the Workshop on measurement of cultivation and production of coca leaves, 25–27 November 2008, Bogotá. Available at: https://www.unodc.org/documents/crop-monitoring/Workshop_coca_leaves/Javier_Gallego1.pdf
Satellite data used: MODIS (250 m resolution)

TABLE 5. EXAMPLE OF CONFUSION MATRIX FOR MADHYA PRADESH STATE, INDIA.

	Reference data									
Classified data	**Gram**	**Wheat**	**Mustard**	**Potato**	**Pea**	**Fallow**	**Settle**	**Lentil**	**Row Total**	**User accuracy**
Gram	153	28	0	3	6	5	2	0	197	78%
Wheat	1	474	62	4	43	2	1	0	587	81%
Mustard	0	56	525	6	27	1	4	2	621	85%
Potato	0	25	28	334	48	0	0	0	435	77%
Pea	0	30	23	11	323	2	2	0	391	83%
Fallow	0	0	3	12	9	102	3	2	131	78%
Settle	3	2	0	1	6	4	112	5	133	84%
Lentil	0	12	9	0	1	0	1	99	122	81%
Column Total	157	627	650	371	463	116	125	108	2 617	
Producer Accuracy	97%	76%	81%	90%	70%	88%	90%	92%	81.09	

Overall classification accuracy = 81.09 %
Kappa statistics =0.7606
Satellite data used: Resourcesat 2 LISS III (23.5 m resolution)

While confusion matrices show the internal accuracy of classification, the accuracy with respect to a standard estimate (such as a ministry of agriculture's estimates) is evaluated using various parameters such as relative deviation, the Root Means Square Error (RMSE) and the correlation coefficient.

In India, the correlation coefficient between remote-sensing-based estimates and Ministry estimates for the state-level area of four crops ranged between 0.986 and 0.999. When mapping paddy rice in China using MODIS time series data, Clauss *et al*. (2016) found a coefficient of determination between 0.91 and 0.93 with the Government's estimates.

5.3. REGRESSION ESTIMATOR

Methods such as regression, calibration and small area estimators combine exhaustive but inaccurate information from satellite images with accurate information on a sample, most often from ground surveys (Gallego, 2006).

Regression estimators are described in standard statistical texts (see for example Cochran, 1963).

The estimator at regional level is (Sud *et al*., 2015):

$$\hat{Y}_R = \sum_{i=1}^{L} N_h \bar{y}_{h(Reg)}$$

where $\bar{y}_{h(Reg)} = \bar{y}_h + \hat{b}_h (\bar{X}_h - \bar{x}_h)$

$\bar{y}_h$ = average ground-reported crop area per sample segment of stratum *h*, that is

$$\bar{y}_h = \frac{1}{n_h} \sum_{j=1}^{n_h} y_{hj}$$

$\hat{b}_h$ = regression coefficient of ground-reported area on remote sensing-derived area based on n_h segments for stratum *h*

$\bar{X}_h$= average remote-sensing-based area for all frame units of stratum *h* (thus, the entire area must be classified to obtain this mean of the population, namely,

$$\bar{X}_h = \frac{1}{N_h} \sum_{j=1}^{N_h} X_{hj})$$

$\bar{x}_h$= average remote-sensing-based crop area per sample segment of stratum *h*,

$$\bar{x}_h = \frac{1}{n_h} \sum_{j=1}^{n_h} x_{hj}$$

Many countries, such as the United States of America, Brazil and China, use a regression estimator for crop area estimation from remote sensing data. FAO (2017) followed a hybrid approach based on the integration of the area frame with image classification to enhance the accuracy of crop statistics. This approach was followed for rice area estimation in Afghanistan. The area frame was developed using satellite imagery from Sentinel-2 and SPOT-5 (having a spatial resolution of 10 m). The agricultural land within the pilot project area was stratified and systematic random segments were visually interpreted together with the ground information to estimation the crop statistics based on the area frame. Visual interpretation of the satellite imagery was used as a training sample in the supervised image classification algorithm to extract the pixel based crop estimates. The R2 in the linear regression in the variables of rice pixels and rice area in segments was 0.96. This showed a very high accuracy between these two systems.

In China, under the CAERSS project, crop area is estimated using a similar approach. First, by using multisource and multitemporal remote sensing, an area frame is constructed and updated for crop sample design. Second, a strategy for sample selection is developed to conduct a reasonable stratification and to select samples to be surveyed as ground truth. Finally, combining the ground survey data with the classified grain acreage from remote sensing imagery as auxiliary data, a linear model is adopted to produce the crop acreage estimation with satisfactory precision. The planted acreage estimation for major crops at provincial and county levels are thus generated. More details on the methodology and procedure are given by Zhou (2013). The CV of estimates by linear regression for three major crops (corn, rice and soybean) ranged between 4.2 percent and 7.0 percent.

5.4. CALIBRATION ESTIMATOR

Calibration estimators incorporate auxiliary information, represented by remotely sensed data, into the estimation process (Benedetti *et al*., 2015). The commission and the omission errors of a confusion matrix can be used to correct the bias. Stehman (2009) indicated that the reference information from a sample used to construct the confusion matrix can also be used to infer the area of the target, directly or via model-assisted inference. The direct estimator and inverse estimator are two approaches that utilize the confusion matrix to adjust the pixel count area. The difference between these two estimators is that the former employs the user's accuracy, and the latter employs the producer's accuracy. The main note of caution is that the confusion matrix must be computed using ground information on a statistical sample of points or segments (area elements) and that the extrapolation is correctly made, taking into account the sampling plan (Gallego *et al*., 2008).

To improve the accuracy of area estimation from classification, Zhu *et al*. (2014) explored the performance and stability of several model-assisted estimators. They used the confusion matrix calibration direct estimator, the confusion matrix calibration inverse estimator, the ratio estimator and the simple regression estimator to infer the areas of several land cover classes, using simple random sampling without replacement. Their comparison showed that confusion matrix calibration estimators, ratio estimators and simple regression estimators were capable of providing more accurate and stable estimates than the simple random sampling estimator.

5.5. SMALL AREA ESTIMATOR

Small area estimation is important in survey analysis when domain (subpopulation) sample sizes are too small to provide adequate precision for direct domain estimators. In remote-sensing-based estimates, the accuracy may be good for large areas (country and states or provinces), because of the higher sample size; however, this may not be the case for smaller areas (districts or counties). To improve the accuracy of estimation for smaller areas, the Small Area Estimation (SAE) technique is followed. Various alternative methodologies have emerged to carry out the SAE; these can be grouped broadly into statistical approaches and spatial microsimulation approaches, each with multiple differing approaches within them (Whitworth, 2013). The statistical approach is based on the regression model that enables the relationship between a characteristic of interest and explanatory variable(s) to be formally assessed. Zhou (2016) used a combination of crop classification from satellite images with field survey data and SAE techniques to generate county- and town-level estimations of rice and corn.

5.6. EXAMPLES OF NATIONAL, REGIONAL AND GLOBAL CROP AREA ESTIMATION PROGRAMMES

5.6.1. National-level programmes

5.6.1.1. USDA/NASS's CDL

The USDA/NASS provides timely, accurate and useful statistics for agriculture in the United States of America. The NASS conducts a large number of surveys to collect information about various aspects of agricultural activity. In 2010, the NASS CDL Program played an important role towards fulfilling this mission, using remote sensing techniques to provide operational in-season acreage estimates to the NASS Agricultural Statistics Board (ASB) and Field Offices (FOs) for 27 states and 16 crops (Baily and Boryan, 2010). The NASS has experimented with many pioneering programmes, including LACIE and AgRISTARS, to show the use of remote sensing data for crop acreage estimation. The NASS started the CDL programme in1997, with in-house software and Landsat data. In 2006, the CDL underwent a major change, with the introduction of the use of commercial software and Resourcesat 1 AWiFS data. The CDL product is a raster-formatted, georeferenced, crop-specific, land cover map (Boryan *et al*., 2011). In 2009, the CDL program played an important role towards providing operational in-season acreage estimates for 15 crops in 27 states. Boryan *et al*. (2001) provide an overview of the CDL program, describing various input data, processing procedures, classification and validation, accuracy assessment, CDL product specifications, dissemination venues and the crop acreage estimation methodology. Using the CDL as the foundation, NASS runs a regression estimator to produce crop acreage estimates.

FIGURE 8. 2009 CROPLAND DATA LAYERS.

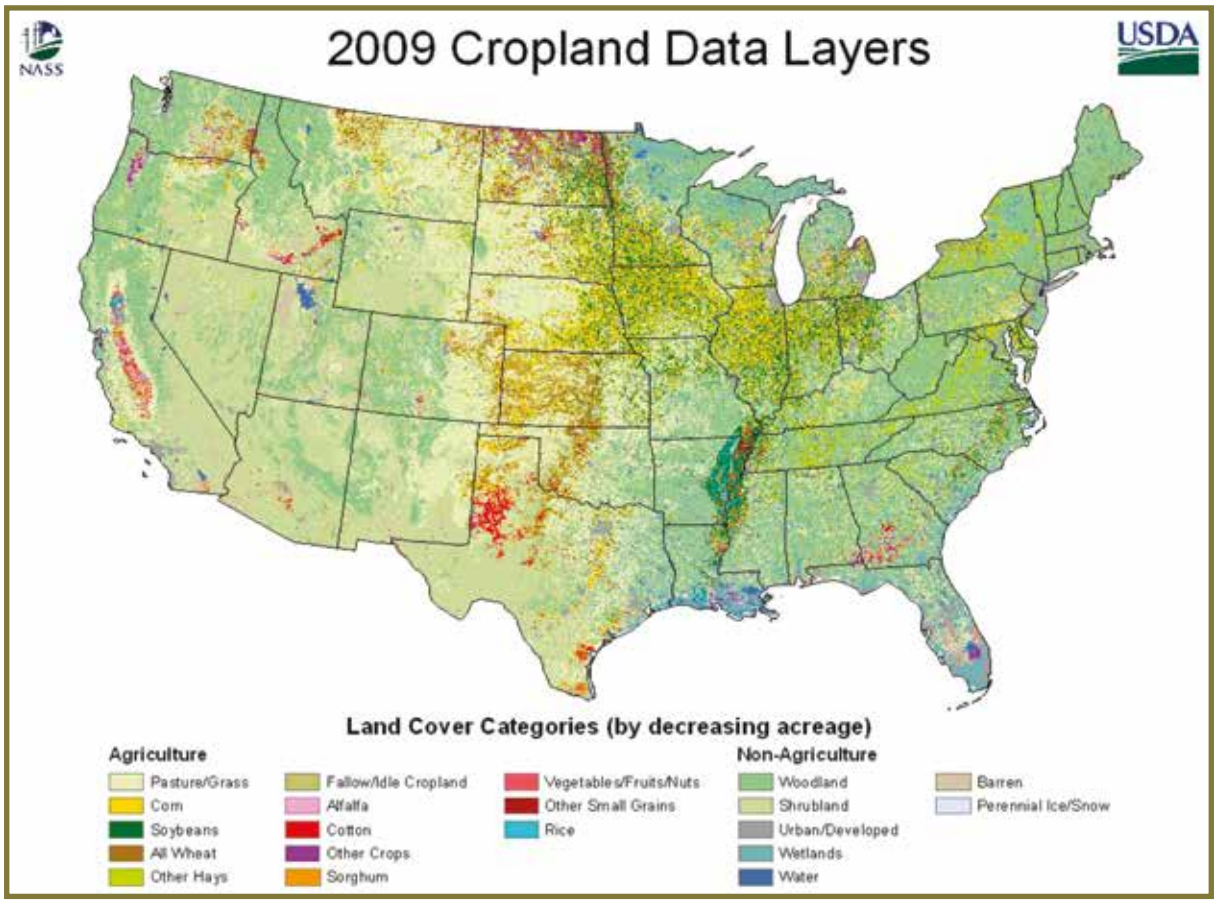

Source: USDA/NASS. (https://nassgeodata.gmu.edu/CropScape/)

5.6.1.2. India's FASAL programme

In India, crop estimation using remote sensing data started in the late 1970s, with a systematic study on crop inventory using Colour Infrared (CIR) aerial data carried out jointly by the ISRO and the Indian Council of Agricultural Research (ICAR) under the Agricultural Resource Inventory and Survey Experiment (ARISE) project (Sahai *et al*., 1977). Subsequently, many experimental studies were conducted using airborne data and, later, Landsat-1 data. These early studies using aerial and Landsat data are documented in Bhavsar (1980), Navalgund and Sahai (1985) and Sahai and Dadhwal (1990). With the launch of IRS 1A, a major national-level programme was launched for Crop Acreage Production Estimation (CAPE), under which the area and production estimation of major crops in district and state level was carried out. The research studies carried out under the CAPE programme helped to develop an optimum sampling plan, sensor specifications, accuracy figures, an optimum analysis procedure and in-house software for crop assessment (Dadhwal *et al*., 2002). Simultaneously, methodologies were developed for using SAR (initially from ENVISAT and later from Radarsat) data for rice area estimation, to overcome the problem of cloud cover during kharif (rainy season) (Patel *et al*., 1995; Panigrahy *et al*., 2000). Based on the experience gained under the CAPE project and various other pilot studies carried out, and on the requirements of the Indian Ministry of Agriculture, a comprehensive crop inventory project was developed – the FASAL programme.

The FASAL programme, which was officially launched in 2007, aimed at providing multiple pre-harvest district-, state- and national-level production forecasts using multiple approaches (econometric, remote sensing and agrometeorological), multiple satellite data (optical and microwave) for 11 major crops of the country (Parihar and Oza, 2006). After the methodologies were developed and optimized for crop production forecasting at the ISRO's Space Applications Centre, the programme was operationalized at the MNCFC, which was established under the Ministry of Agriculture (Ray *et al*., 2015). The approaches followed in FASAL for crop production forecasting are illustrated in figure 9.

FIGURE 9. APPROACHES FOLLOWED FOR CROP PRODUCTION FORECASTING UNDER THE FASAL PROJECT.

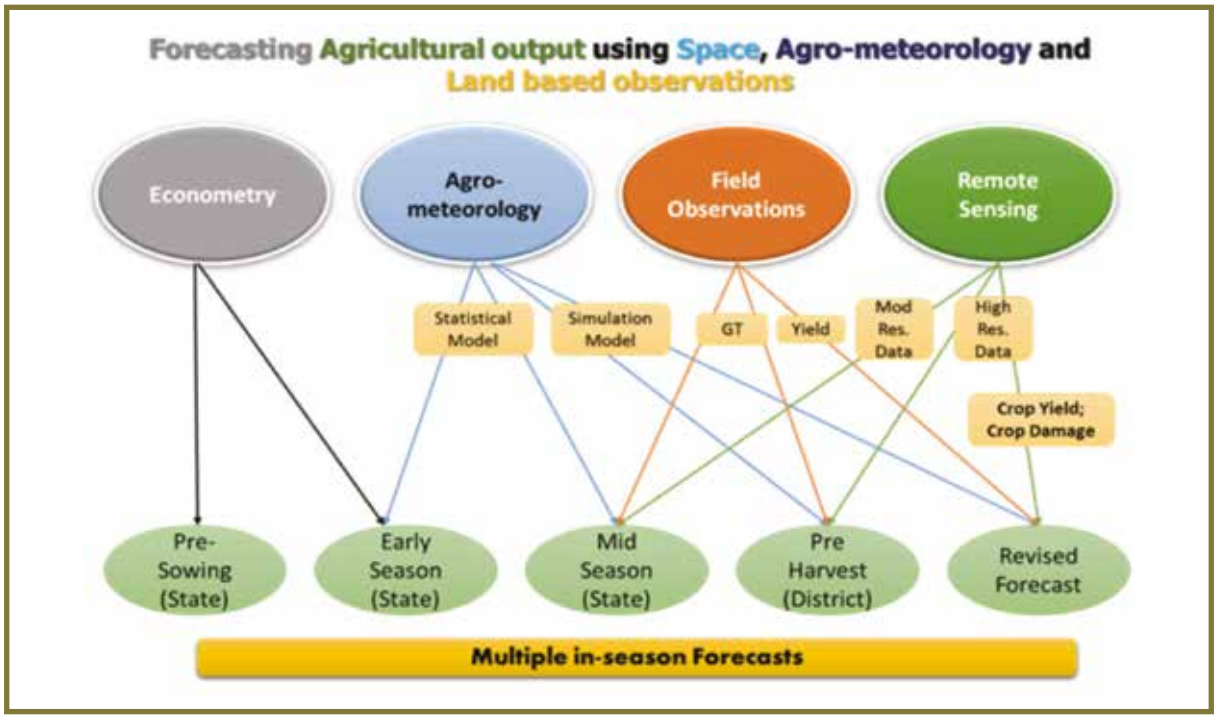

The methodology adopted by FASAL for area estimation uses remote sensing data to: (i) design the sampling plan and (ii) to generate estimates through image classification, using single-date high-resolution data or multidate medium-resolution data. For rice and jute, RISAT-1 SAR data is used, while for other crops (wheat, rapeseed and mustard, sorghum, cotton, and sugarcane) Resourcesat-2 AWiFS, LISS III, Landsat OLI or Sentinel 2 MSI data are used. The rice and jute crops are analysed using a sample segment approach with a 5 x 5 km sample size and a 15 percent sampling fraction with four strata (the stratification is based on crop coverage in each segment). For other crops, a complete enumeration approach is followed. The ground truth data is collected using smartphone-based Android apps. The yield is estimated using agrometeorological models (empirical and crop simulation), remote-sensing-based models and sample crop cutting experiment (CCE) data, where the CCE is done using a remote-sensing-based sampling plan. The estimates generated under the FASAL programme form one of the inputs for generating the final estimates of the MA&FW. A detailed discussion on the approach, results and accuracy of estimates of the FASAL programme is available in Ray *et al*. (2016). Based on the success of remote-sensing-based crop production, the MA&FW has launched a new programme for the Coordinated Horticulture Assessment and Management using geoinformatics (CHAMAN), for the inventorying of horticultural crops (mango, banana, citrus, potato, tomato, chilli and onion) and horticultural developmental planning (Ray *et al*., 2015).

5.6.2. Regional programmes

5.6.2.1. The EU/JRC's MARS Programme

The MARS project was conceived to develop large-scale operational tools in the field of agricultural information for satellite image analysis and related fields, such as area frame sampling and agrometeorological models (Gallego, 2000). In the first period of the MARS project (1988–97), crop area estimation played a central role and envisaged two major components: (1) regional crop inventories and (2) rapid estimates of crop area change at EU level. Gallego (2000) summarizes the progress made during this period. The regional crop inventories combined high-resolution satellite images and ground surveys in a classical statistical scheme based on area frame sampling and ground visits, providing the main estimation variable through a regression estimator. The rapid estimates of crop area change attempted to provide an early estimate of crop area change at EU level on the basis of a sample of 60 sites of 40 x 40 km each, without ground information. Both programmes were later abandoned, the first because it had almost reached the cost-efficiency threshold and the second due to its wide margin of subjectivity.

Currently, the MARS's AGRI4CAST sampling programme focuses on the Land Use/Cover Area-frame Survey (LUCAS) (Gallego and Delincé, 2010). Estimates of the area occupied by different land use or land cover types are computed on the basis of observations taken at approximately 2,70,000 points sample points throughout the EU, rather than mapping the entire area under investigation. By repeating the survey every few years, changes to land use can be identified[1]. LUCAS is a two-phase systematic stratified sampling process: in the first phase, the sample is photointerpreted; in the second phase, field data is collected from the samples. The latest LUCAS survey was carried out in 2012 in 27 EU countries, where total crop land constitutes 24.7 percent of the total area.

1 http://esdac.jrc.ec.europa.eu/projects/lucas.

5.6.3. Global programmes

5.6.3.1. CropWatch (China)

CropWatch was developed by the Institute of Remote Sensing and Digital Earth (RADI) of the Chinese Academy of Sciences (CAS). CropWatch has four assessment levels: global (65 homogeneous crop Monitoring and Reporting Units MRU); regional (seven Major Production Zones or MPZs); national (31 key countries); and subnational (subdivisions of nine large countries) (Wu *et al*., 2015). Different indicators are selected at different levels to best characterize the environmental and agricultural information at the corresponding scale. The various indicators used at different levels of assessment include rainfall, air temperature, photosynthetically active radiation, agroclimatic biomass production potential, cropping intensity, cropped arable land fraction, vegetation health index, maximum vegetation condition index and crop type proportion. CropWatch adopts different crop area estimation methods for different countries. For China, remotely sensed estimates of arable land area and Cropped Arable Land Fraction (CALF) are combined with field-survey-based estimates of crop type proportion (Wu and Li, 2012).

For other 30 key countries and provinces or states of nine large countries, CALF is used to estimate individual crop area using the following equation:

Crop area = a x b x CALF

where *a* and *b* are linear regression coefficients between the cropped area from FAOSTAT or, preferably, subnational data when available from the website of China's Ministry of Agriculture or National Bureau of Statistics.

5.6.3.2. USDA FAS (United States of America)

The USDA FAS provides monthly crop condition assessments, monitoring and crop estimates for 17 global commodities; 159 countries; 1 020 country-crop pairs (for example, Australia-Wheat); and three attributes: area, yield and production (Hoffman, 2016). FAS uses various information, such as satellite imagery, attaché reports, crop travel, official data and news reports to conduct global crop assessment and monitoring. The USDA FAS uses data from eight of 18 of NASA's Earth Observing fleet. FAS uses additional satellites from the European Space Agency (ESA), ISRO and private organizations. The FAS Crop Explorer Web Portal displays numerous weather and vegetation condition data sets over major crop regions every ten days.

5.6.3.3. GEOGLAM

Following the global food price hikes in 2007–2008 and 2010, as part of the Action Plan on Food Price Volatility and Agriculture, the heads of state of the G20 countries endorsed, in their 2011 Declaration, both the GEOGLAM and the Agricultural Market Information System (AMIS) initiatives. GEOGLAM provides a framework that strengthens the international community's capacity to produce and disseminate relevant, timely and accurate forecasts of agricultural production at national, regional and global scales through the use of Earth Observations (EO), including satellite and ground-based observations . Within this framework, GEOGLAM developed the Crop Monitor reports, which provide global crop condition assessments in support of the AMIS market monitoring activities[2]. Asia-Rice is the work of an ad hoc team of stakeholders with an interest in the development of an Asian Rice Crop Estimation & Monitoring (Asia-RiCE) component for the GEOGLAM initiative. In Phase 1 (2013–2015), Asia-Rice developed Technical Demonstration Sites (TDSs) in Chinese Taipei, Indonesia, Japan, Malaysia, Thailand and Viet Nam. Phase 2 of Asia-RiCE is intended to prepare rice growth outlooks for Indonesia, the Philippines, Thailand and Viet Nam, and provide them to AMIS (Asia-Rice, 2016).

2 https://cropmonitor.org/.

5.7. COST-EFFECTIVENESS OF REMOTE-SENSING-BASED AREA ASSESSMENT

Analysing the cost-effectiveness of a system requires its comparison with the cost that would be required pursuant to the use of alternative systems (such as traditional agricultural data collection systems) to achieve the same end result (Radhakrishnan *et al*., 1991). For remote-sensing-based area estimation, the costs include satellite data cost, ground truth collection cost and analysis cost. The benefits may consist not only in direct cost savings (achieving the same estimate in the reduced cost), but also in the improving the timeliness and accuracy of estimates. The accuracy can be assessed in terms of reduction in variance and increases in efficiency (for sampling designs using remote sensing). According to Carfagna (2001), the cost-effectiveness of remote sensing for agricultural statistics has long been debated and depends on several parameters, such as the level of fragmentation of the landscape, the weather conditions, the level of optimization and automation of the project, and the cost structure. Thus, different results have been obtained in different experiences.

Delincé (2015) has studied in detail the cost-effectiveness of the remote-sensing-based agricultural statistics of four national systems. These include Haiti (point area frame sampling), Morocco (area frame sampling), China (area frame sampling and regression analysis) and India (area frame sampling and pixel counting). His findings may be summarized as follows:

- For Haiti, the CNIGS's point frame survey was analysed. The cost of stratification reflected the increased field survey costs of 3 percent; however, decreases in the variances of as much as 50 percent at regional level were obtained.
- In Morocco, the stratification based on land-cover maps of 66 000 km2 derived from expensive SPOT imagery increased annual survey costs by 30 percent. However, in view of the efficiencies obtained, the investment is worthwhile.
- In China, remotely sensed stratification covered 1.65 million km2. The cost increase was only 3 percent, but in Anhui province, relative stratification efficiencies of 2.8 for rice and 1.4 for corn were obtained.
- In India, radar and optical imagery is used to monitor 90 percent of the production of the eight major crops. A stratification efficiency for rice between 1.2 and 3.3 was achieved, and bias induced by pixel counting could be evaluated.

For USDA/NASS, which runs most important operational applications based on area frame surveys and remote sensing for agricultural statistics, the cost-efficiency analysis has yielded positive conclusions (Carfagna, 2013). According to Carfagna (2013), "remote sensing applications to agricultural statistics can be sustainable if their total cost fits in the budget without endangering the feasibility of surveys that cannot be substituted by satellite technology".

However, considering the availability of a great volume of free satellite data (from Landsat, Sentinel, etc.) and the significant reduction in the prices of Indian satellite data, the cost-effectiveness of remote sensing for crop statistics dramatically improves.

5.8. ISSUES AND LIMITATIONS

MacDonald and Hall (1980), while providing a summary of LACIE, wrote that "[a]gricultural information should have the qualities of objectivity, reliability, timeliness, adequacy of coverage, efficiency and effectiveness. Production statistics in many important agricultural countries do not meet any of these standards". This may remain true in many countries today. Although – as seen in the examples shown above – remote sensing data from various satellites have been successfully used for different components (area sampling plan design, estimation by classification or regression) of agricultural statistics collection, there are still many issues which limit the use of remote sensing data for operational crop area assessment. These include:

- Small field size, especially in many countries in Asia and Africa (table 6), which requires high-resolution remote sensing data for crop identification.
- Persistent cloud cover during rainy season. Clouds strongly limit the usefulness of optical imagery for agricultural applications (Eberhardt *et al*., 2016). SAR data is required to overcome the cloud problem. However, the usefulness of SAR data for estimation of crops other than rice is yet to be established.
- Diverse cropping and agronomic practices.
- Mixed and intercropping systems.
- Large varieties of crops grown in a small area, which occurs especially in the context of horticultural crops.

Other technical issues arising in the analysis and use of remote sensing data include the availability of sufficient amount of quality ground truth data describing the variability existing in the field; the computing power, sophisticated software and data storage facilities required to analyse multitemporal high-resolution data; and the availability of satellite data with a low turnaround time.

Despite these issues, several studies have demonstrated the cost-efficiency of using remote sensing data for area estimation (Delincé, 2015; Gallego *et al*., 2014).

With the current and proposed availability of many high-resolution remote sensing satellite constellations, the temporal frequency of satellite data and classification accuracy are expected to increase. There is a need to develop methodologies for the use of SAR data in the area estimation of crops other than rice.

Various opinions have been expressed as to the methods to be used for area estimation, that is, the regression estimator or pixel counting. Carfagna and Gallego (2005) maintain that at the estimator level, classified satellite images should be used as auxiliary variables in a regression estimator or for estimators based on confusion matrices. They also mention that in general, classified or photointerpreted images should not be directly used to estimate crop areas because the proportion of pixels classified into specific crops is often strongly biased.

However, for many applications, in addition to crop area, classified crop maps are also essential, such as for planning CCEs for crop yield. Furthermore, qualified staff are required if better execution for regression-based estimation needs is to be assured; however, such staff are not necessarily available, even in many official organizations (Gallego, 2006). Craig and Atkinson (2013) opined that pixel counting estimates consistently underestimate the actual area under crop, a problem that can be remedied through regression. Therefore, it is necessary to adopt an integrated approach, which is a combination of sampling frame design, pixel counting and regression.

TABLE 6. AVERAGE SIZE AND FRAGMENTATION OF AGRICULTURAL HOLDING, 1995–2005.

Countries by continent (Number of reporting countries is given in parenthesis)	Average area per holding (hectare)	Average number of parcels per holding
World Total (114)	5.5	3.5
Africa (25)	11.5	3.0
America, North & Central (14)	117.8	1.2
America, South (8)	74.4	1.2
Europe (29)	12.4	5.9
Asia (29)	1.0	3.2

Source: FAO, 2010.

5.9. REFERENCES

Ahmad, I., Ghafoor, A., Bhatti, M.I., Akhtar, I.H., Ibrahim, M. & Rehman, O. 2015 *Satellite remote sensing and GIS-based crops forecasting & estimation system in Pakistan*. In Srivastava, M.K. (ed.), *Crop Monitoring for Improved Food Security: Proceedings of the Expert Meeting. Vientiane, Lao People's Democratic Republic, 17 February 2014*. RAP Publication 2014/28. Joint publication of the Food and Agriculture Organization of the United Nations (FAO) and the Asian Development Bank (ADB): Rome – Manila.

Asian Rice Crop Estimation and Monitoring Component (Asia-RiCE). 2016. *Asia-RiCE Phase 2 Work Plan*. Asia-RiCE Publication.

Bailey, J.T. & Boryan, C.G. 2010. *Remote Sensing Applications in Agriculture at the USDA National Agricultural Statistics Service*. Vol. 22030. USDA/NASS Publication: Fairfax, VA, USA.

Bauer, M.E., Cary, T.K., Davis, B.J. & Swain, P.H. 1975. *Crop Identification Technology Assessment for Remote Sensing (CITARS): Results of CITARS Experiments Performed by LARS*. NASA CR 147389, LARS Information Note 072175. Publication of the Laboratory for Applications of Remote Sensing (LARS): West Lafayette, IN, USA.

Benedetti, R., Piersimoni, F. & Postiglione, P. 2015. *Sampling Spatial Units for Agricultural Surveys*. Springer-Verlag: Berlin.

Bhavsar, P.D. 1980. Demonstrated Applications in India of Earth Resources Survey by Remote Sensing. *Proceedings of the National Academy of Sciences, India*, 46, A(3): 275–285.

Boryan, C. 2012. *A Review of Four Area Sample Designs*. Paper prepared for Course GGS796 at George Mason University. Available from Research Division, USDA/NASS: Fairfax, Virginia, USA.

Boryan, C., Yang, Z., Mueller, R. & Craig, M. 2011. Monitoring US agriculture: the US Department of Agriculture, National Agricultural Statistics Service, Cropland Data Layer Program. *Geocarto International*, 26(5): 341–358.

Brisbane, J. & Mohl, C. 2014. *The Potential Use of Remote Sensing to Produce Field Crop Statistics at Statistics Canada*. In *Beyond traditional survey taking: adapting to a changing world. Proceedings of Statistics Canada Symposium 2014*.

Bryan, E.R. 1974. *The ERTS-1 Investigation (ER-600). Volume I - ERTS-l Agricultural Analysis*. NASA Technical Memorandum X-58117.

Carfagna, E. 2001. *Cost-effectiveness of Remote Sensing in Agricultural and Environmental Statistics*. Invited Paper prepared for *Caesar: Conference on Agricultural and Environmental Statistical Applications in Rome*. 4–8 June 2001. Rome, Istituto nazionale di statistica (Istat). Volume III, pp. 617–627.

Carfagna, E. 2013. *Evaluating the Cost-Efficiency of Remote Sensing in Developing Countries*. Presentation prepared for the first Scientific Advisory Committee of the Global Strategy – Improving AG-Statistics. 18–19 July 2013. Rome, FAO.

Carfagna, E. & Gallego, F.J. 2005. Using Remote Sensing for Agricultural Statistics. *International Statistical Review*. 73(3): 389–404.

Chakraborty, M., Patnaik, C., Panigrahy, S. & Parihar, J.S. 2006. Monitoring of wet season rice crop at state and national level in India using multi-date synthetic aperture radar data. In Kuligowski, R.J., Parihar, J.S. & Saito, G. (eds), *Proceedings of SPIE Volume 6411, Agriculture and Hydrology Applications of Remote Sensing*. SPIE Publication: Goa, India.

Chakraborty, M., Panigrahy, S. & Sharma, S.A. 1997. Discrimination of rice crop grown under different cultural practices using temporal ERS-1 Synthetic aperture radar data. *ISPRS Journal of Photogrammetry and Remote Sensing*, 52: 183–191.

Choudhury, I. & Chakraborty, M. 2006. SAR signature investigation of rice crop using RADARSAT data. *International Journal of Remote Sensing*, 27(3): 519–534.

Clauss, K., Yan, H. & Kuenzer, C. 2016. Mapping Paddy Rice in China in 2002, 2005, 2010 and 2014 with MODIS Time Series. *Remote Sensing*, 8: 434

Cochran, G.W. 1963. *Sampling Techniques*. John Wiley & Sons: New York, USA.

Craig, M. & Atkinson, D. 2013. A Literature Review of Crop Area Estimation. FAO Publication: Rome.

Csornai, G., Wirnhardt, C., Suba, Z., Nádor, G., Tikász, L., Martinovich, L., Kocsis, A., Zelei, G., László, I., Bognár. E. 2006. CROPMON: Hungarian Crop Production Forecast by Remote Sensing. In Baruth, B., Royer, A. & Genovese, G. (eds), *ISPRS Archives Volume XXXVI-8/W48 Workshop proceedings: Remote sensing support to crop yield forecast and area estimates* (pp. 65–70). ISPRS Publication: Stresa, Italy.

Dadhwal, V.K., Singh, R.P., Dutta, S. & Parihar, J.S. 2002. Remote sensing based crop inventory: A review of Indian experience. *Tropical Ecology* 43(1): 107–122.

Delincé, J. 2015. *Technical Report on Cost-Effectiveness of Remote Sensing for Agricultural Statistics in Developing and Emerging Economies*. Technical Report Series GO-09-2015. Global Strategy Technical Report: Rome.

Dhanju, M.S. & Shankaranarayana, H.S. 1978. *Agricultural Resources Inventory and Survey Experiment (ARISE)*. ISRO-SAC-TR-11-78. ISRO Publication: Bangalore, India.

Eberhardt, I.D.R. *et al*. 2016. Cloud Cover Assessment for Operational Crop Monitoring Systems in Tropical Areas. *Remote Sensing*, 8(3): 219.

Food and Agriculture Organization of the United Nations (FAO). 2010. *Characterisation of Small Farmers in Asia and the Pacific*. Paper prepared for the Twenty-third Session of the Asia and Pacific Commission on Agricultural Statistics (Agenda item 10), 26–30 April 2010. Siem Reap, Cambodia.

FAO. 2017. *Afghanistan: Monitoring of Rice Crop using Satellite Remote Sensing and GIS Technologies*. FAO Publication: Rome.

Ferreira, S.L., Newby, T. & du Preez, E. 2006. Use of Remote Sensing In Support of Crop Area Estimates in South Africa. In Baruth, B., Royer, A. & Genovese, G. (eds), *ISPRS Archives Volume XXXVI-8/W48 Workshop proceedings: Remote sensing support to crop yield forecast and area estimates* (pp. 51–52). ISPRS Publication: Stresa, Italy.

Fontana, D.C., Melo, R.W., Wagner, A.P.L., Weber, E. & Gusso, A. 2006. Use of Remote Sensing For Crop Yield and Area Estimates in the Southern of Brazil. In Baruth, B., Royer, A. & Genovese, G. (eds), *ISPRS Archives Volume XXXVI-8/W48 Workshop proceedings: Remote sensing support to crop yield forecast and area estimates* (pp. 53–58). ISPRS Publication: Stresa, Italy.

Gallego, F.J. 2000. Statistical aspects of area estimates in MARS. Paper prepared for the *MARS Conference: 10 years of demand-driven technical support*, 22–23 April 1999. Brussels.

Gallego, F.J. 2006. Review of the Main Remote Sensing Methods for Crop Area Estimates. In Baruth, B., Royer, A. & Genovese, G. (eds), *ISPRS Archives Volume XXXVI-8/W48 Workshop proceedings: Remote sensing support to crop yield forecast and area estimates* (pp. 65–70). ISPRS Publication: Stresa, Italy.

Gallego, F.J., Craig, M., Michaelsen J., Bossyns B. & Fritz S. (eds). 2008. *Best practices for crop area estimation with Remote Sensing*. GEOSS Community of Practice Ag 0703a. European Communities Publication: Luxembourg.

Gallego, F.J. & Delincé, J. 2010. The European Land Use and Cover Area-frame statistical Survey (LUCAS), in Benedetti, R., Bee, M., Espa, G. & Piersimoni, F. (eds), *Agricultural Survey Methods* (Ch. 10, pp. 151–168). John Wiley & Sons: Chichester, UK.

Gallego, F.J., Kussul, N., Skakunb, S., Kravchenko, O., Shelestov, A. & Kussul, O. 2014. Efficiency assessment of using satellite data for crop area estimation in Ukraine. *International Journal of Applied Earth Observation And Geoinformation*, 29: 22–30.

Gallego, F.J., Peedell, S. & Carfagna, E. 1999. The use of CORINE Land Cover to improve area frame survey estimates in Spain. *Research in Official Statistics*, 2(2): 99–122.

Hanuschak, G.A., Allen, R.D. & Wigton, W.H. 1982. Integration of Landsat data into the crop estimation program of USDA's statistical reporting service (1972-1982). In *Proceedings of 8th International Symposium on Machine Processing of Remotely Sensed Data with Special Emphasis on Crop Inventory and Monitoring*. Joint publication of LARS and Purdue University: West Lafayette, IN, USA.

Hoffman, S. 2016. *Preparation of the USDA World Ag Supply & Demand Estimates (WASDE) Report*. Paper presented at the International seminar on approaches and methodologies for crop monitoring and production forecasting, 25–26 May 2016. Dhaka.

Holmes, Q.A., Horvath, R., Cicone, R.C., Kauth. R.J. & Malila, W.A. 1979. *Development of Landsat-Based Technology for Crop Inventories*. NASA Technical Report SR-E9-00404. NASA Publication.

Husak, G.J., Marshall, M.T., Michaelsen, J., Pedreros, D., Funk, C. & Galu, G. 2008. Crop area estimation using high and medium resolution satellite imagery in areas with complex topography. *Journal of Geophysical Research*, 113: D14112.

Justice, C. & Becker-Reshef, I. 2007. *Developing a Strategy for Global Agricultural Monitoring in the Framework of Group on Earth Observations (GEO) Workshop Report,* 16–18 July 2007. Rome, FAO.

Li, Y., Zhu, X., Pan, Y., Gu, J., Zhao, A. & Liu, X. 2014. A Comparison of Model-Assisted Estimators to Infer Land Cover/Use Class Area Using Satellite Imagery. *Remote Sensing*, 6(9): 8904–8922.

Lillesand, T.M, Kiefer, R.W. & Chipman, J. 2015. *Remote Sensing and Image Interpretation*. 7th edition. John Wiley & Sons: New York.

MacDonald, R.B., Hall, F.G., & Erb, R.B. 1975. *The Use of LANDSAT Data in a Large Area Crop Inventory Experiment (LACIE)*. Paper 46. From the *Symposium on Machine Processing of Remotely Sensed Data*, 3–5 June 2017. West Lafayette, IN, USA, Laboratory for Applications of Remote Sensing and Purdue University.

MacDonald, R.B. & Hall, F.G. 1980. Global crop forecasting. *Science*, 208: 670–679.

MacDonald, R.B. 1984. A summary of the history of the development of automated remote sensing for agricultural applications. *IEEE Transaction on Geoscience & Remote Sensing*, GE-22: 473–481.

Medina, V. del Blanco & García, D.A. Nafría. 2015. *Mapa de cultivos y superficies naturales de Castilla y León*. Paper prepared for the *XVI Congress of the Spanish Association of Remote Sensing*, 21–23 October 2015. Seville, Spain.

Navalgund, R.R. & Sahai, B. 1985. Remote sensing applications in agriculture - Indian experience and plans. In: Proceedings of the Fourth Asian Agricultural Symposium (pp. 329–343), 28 February–1 March 1985. Kumamoto, Japan, Kyushu Tokai University.

Nellis, M.D., Price, K.P. & Rundquist, D. 2009. *Remote Sensing of Cropland Agriculture*. Papers in Natural Resources. Paper 217. University of Nebraska–Lincoln Publication: Lincoln, NE, USA.

Nelson A. *et al*. 2014. Towards an Operational SAR-Based Rice Monitoring System in Asia: Examples from 13 Demonstration Sites across Asia in the RIICE Project. *Remote Sensing*, 6(11): 10773–10812.

Nelson, A. *et al*. 2014. Towards an operational SAR-based rice monitoring system in Asia: examples from 13 demonstration sites across Asia in the RIICE project. *Special Issue of Remote Sensing in Food Production and Food Security, Remote Sensing*, 6(11): 10773–10812.

Pan, Y., Zhang, J., Zhou, W., Zhao, J. & Yu, X. 2012. *Methodology of the Crops Acreage Estimation Using Remote Sensing and Survey Sampling in National statistical system of China*. Paper prepared for the First International Conference on Agro-Geoinformatics, 2–4 August 2017. Shanghai, China.

Panigrahy, S., Chakraborty, M., Manjunath, K.R., Kundu, N. & Parihar, J.S. 2000. Evaluation of Radarsat ScanSAR synthetic aperture radar data for rice crop inventory and modeling. *Journal of Indian Society of Remote Sensing*, 28: 59–65.

Parihar, J.S. & Oza, S.R. 2006. FASAL: An integrated approach for crop assessment and production forecasting. In Kuligowski, R.J., Parihar, J.S. & Saito, G. (eds), *Proceedings of SPIE Volume 6411, Agriculture and Hydrology Applications of Remote Sensing*. SPIE Publication: Goa, India.

Patel, N.K., Medhavv, T.T., Patnaik, C. & Hussain, A. 1995. Multi-temporal ERS-1 SAR data for identification of rice crop. *Journal of Indian Society of Remote Sensing*, 23: 33–39.

Potgieter, A.B., Apan, A., Dunn, P.K. & Hammer, G.L. 2007. Estimating crop area using seasonal time series of Enhanced Vegetation Index from MODIS satellite imagery. *Crop and Pasture Science*, 58(4): 316–325.

Prasad, S.V.S., Satya Savithri, T., Murali Krishna, I.V. 2015. Techniques in Image Classification; A Survey. *Global Journal of Researches in Engineering: Electrical and Electronics Engineering*. 15(6): 17–32.

Radhakrishnan, K., Jayaraman, V. & Nageswara Rao, P.P. 1991. The Economics of Remote Sensing. *Current Science*. 61(3&4): 272–277.

Ray, S.S., Mamatha, S, Manjunath, K.R., Uday, R., Seshasai, M.V.R., Singh, K.K., Kimothi, M.M., Parihar, J.S. & Saxena, M. 2016. CHAMAN: A National Level Programme for Horticultural Assessment & Development. *Bulletin of the National Natural Resources Management System, NNRMS (B)*, 40: 1–6.

Ray, S.S., Neetu, Mamatha, S. & Gupta, S. 2015. Use of Remote Sensing in Crop Forecasting and Assessment of Impact of Natural Disasters: Operational Approaches in India. In Srivastava, M.K. (ed.), *Crop Monitoring for Improved Food Security: Proceedings of the Expert Meeting. Vientiane, Lao People's Democratic Republic, 17 February 2014* (pp. 111–122). RAP Publication 2014/28. Joint publication of the Food and Agriculture Organization of the United Nations (FAO) and the Asian Development Bank (ADB): Rome – Manila.

Ray, S.S., Neetu, Manjunath, K.R. & Singh, K.K. 2016. *Crop Production Forecasting using Space, Agro-meteorology and Land based Observations: Indian Experience*. Paper presented at the International seminar on approaches and methodologies for crop monitoring and production forecasting, 25–26 May 2016. Dhaka.

Sahai, B. & Dadhwal, V.K. 1990. Remote sensing in agriculture. In Verma, J.P. & Verma, A. (eds), *Technology Blending and Agrarian Prosperity* (pp. 83–98). Malhotra Publishing House: New Delhi.

Sahai, B., Chandrasekhar, S., Barde, N.K. & Nag Bhushna, S.R. 1977. Agricultural resources inventory and surveys experiment. In Rycroft, M.J. & Stickland, A.C. (eds), *COSPAR Space Research* (pp. 3–8). Pergamon Press: Oxford, UK.

Sharman, M.J. 1993. The agriculture project of the joint research centre: Operational use of remote sensing for agricultural statistics. In *Proceedings of the ITC International Symposium Operationalization of Remote Sensing* (pp. 46–57), 19–23 April 1993. Enschede, The Netherlands.

Sharples, J.A. 1973. *The Corn Blight Watch Experiment: Economic Implications for Use of Remote Sensing for Collecting Data on Major Crops*. LARS Technical Report, Paper 121. Purdue University Publication: West Lafayette, IN, USA.

Stehman, S.V. 2013. Estimating area from an accuracy assessment error matrix. *Remote Sensing of Environment*, 132: 202–211.

Suga, Y. & Konishi, T. 2008. Rice crop monitoring using X-, C- and L-band SAR data. In Neale, C.M.U., Owe, M. & d'Urso, G. (eds), *Proceedings of SPIE Volume 7104, Remote Sensing for Agriculture, Ecosystems, and Hydrology X*. SPIE Publication: Cardiff, Wales, UK.

Temnikov, V. & Sergey, I. 2007. *Use of Geo-informational Systems for the Russian Agriculture Census*. Paper prepared for the *International Conference on Agricultural Statistics IV: Advancing Statistical Integration and Analysis*, 22–24 October 2007. Beijing.

Vogel, F. & Bange, G. 1999. *Understanding USDA Crop Forecasts*. Miscellaneous Publication No. 1554. Joint USDA/NASS and WOAB Publication: Washington, D.C.

Whitworth, A. (ed.). 2013. *Evaluations and improvements in small area estimation methodologies*. Discussion Paper. National Centre for Research Methods (NCRM), University of Sheffield Publication: Sheffield, UK.

Wu, B. & Li, Q. 2012. Crop planting and type proportion method for crop acreage estimation of complex agricultural landscapes. *International Journal of Applied Earth Observation*, 16: 101–112.

Wu, B., Gommes, R., Zhang, M., Zeng, H., Yan, N., Zou, W., Zheng, Y., Zhang, N., Chang, S., Qiang Xing, Q. & van Heijden, A. 2015. Global Crop Monitoring: A Satellite-Based Hierarchical Approach. *Remote Sensing*, 7: 3907–3933.

Zhou, W. 2013. *Remote Sensing Application in China's Crop Acreage Estimation*. Paper prepared for the 2013 World Statistics Congress, 25–30 August 2013. China, Hong Kong SAR.

Zhou, W. 2016. *Small Area Estimation for Crop Acreage in Remote Sensing Assisted Crop Survey – A Case of Major Crop Acreage Estimation in Liaozhong County*. Paper prepared for the Seventh International Conference on Agricultural Statistics (ICAS VII), 26–28 October 2016. Rome.

6

Chapter 6

Early Warning Systems and crop yield estimation

Oscar Rojas, Natural Resources Officer, FAO SLM/CBC

6.1. INTRODUCTION

This chapter reviews the fundamental concepts relating Early Warning Systems (EWS) to crop yield forecasting, to better address climatic risks that have an impact on food security. System-based dissemination of timely alerts and specifications of the probability of hazard occurrence are fundamental components of Early Warning Information (EWI), and systematic linkages to early-action options and possibilities would go a long way towards saving lives and livelihoods.

Forecasting crop yields and aggregate production is significant in EWSs that seek to assess the food supply and demand situation of a given country or region. Accurate analyses of market conditions and identification of the surplus and deficit areas in a given country or region will contribute greatly towards the design of appropriate policy responses to food security problems – an important objective the achievement of which is greatly advanced by robust and accurate agricultural statistics. In this context, information derived from remote sensing plays a vital role in improving the production of agricultural statistics by introducing independent verifying mechanisms, particularly when area frame or multiple frame sample designs are used. Remotely sensed data and information can be introduced at both design and estimator levels.

6.2. EARLY WARNING SYSTEMS (EWS)

An EWS is an integrated system for monitoring, data collection and analysis, and communication to enable making early decisions to protect peoples and the environment (Davies et al., 1991). EWS focusing on agriculture and food security[1] monitor people's access to food, to provide timely notice of an impending food crisis and thus to elicit an appropriate response. Whether an EWS succeeds in its goal of eliciting an appropriate response depends on numerous factors, most of which are beyond the control of the EWS itself (Buchanan-Smith, 2000). Normally, a EWS for food security should continuously monitor food production, stocks, prices, trade and consumption, and any extreme event, including climatic and market disruptions that could affect the food supply and demand situation. Box 1 presents a historic background to food security information systems. The precise form of an EWS will depend upon a variety of factors, including the data environment, the communication infrastructure, the intended users and the nature of the hazard (Bailey, 2013). Nevertheless, all EWS – for food shortage or other hazards – share some common elements: they collect early warning data, analyse it to produce EWI and communicate the latter to decision-makers (figure 1).

FIGURE 1. ELEMENTS OF AN EWS.

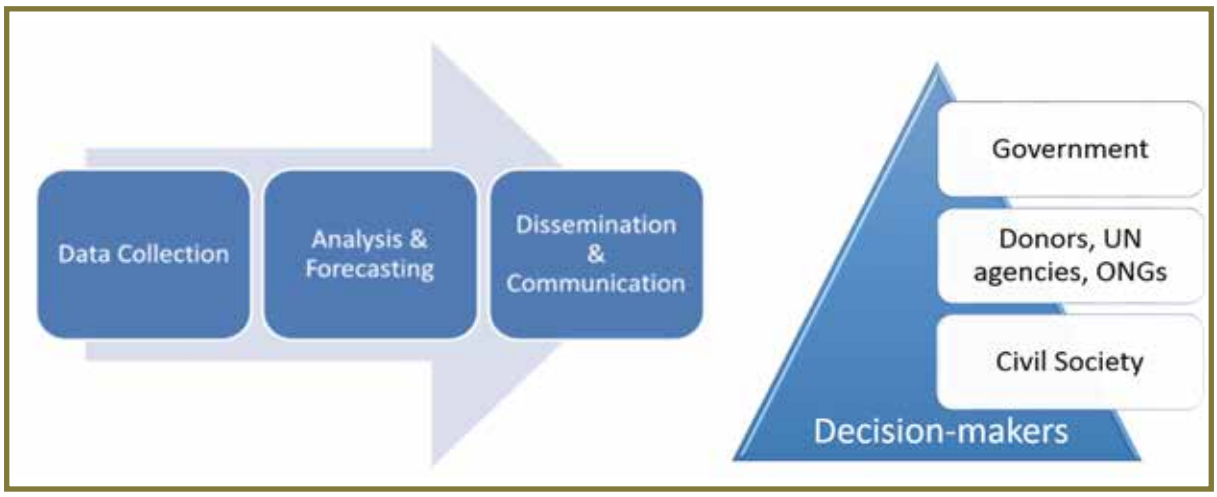

Data collection refers to the process by which the early warning data are gathered and collated. Important considerations include the appropriateness, timeliness and reliability of the data. **Analysis & Forecasting** refers to the technical activities of monitoring and generating EWI. In this respect, significant factors include the parameters monitored, the methodology employed, the specific variables forecast and the level of confidence that may be attached thereto. **Dissemination & Communication** refers to the provision of EWI to relevant stakeholders. Key considerations relate to the channels through which warnings are disseminated, the stakeholders to which warnings are communicated and the format in which EWI is presented.

In many EWS, there exists a fundamental tension between timeliness and confidence. Inevitably, confidence in the accuracy of EWI will increase with time as more data are gathered and analysed, while the amount of warning time available will decrease. A second fundamental tension relates to the richness of EWI. Providing stakeholders with as much EWI as possible should help them to make better informed decisions. However, in practice, this is often not the case: stakeholders may lack the capacity to properly interpret the information, with the result that the key message is lost.

1 "Food security exists when all people, at all times, have physical and economic access to sufficient, safe and nutritious food to meet their dietary needs and food preferences for an active and healthy life." World Food Summit, 1996.

The ideal food shortage EWS should therefore be able to anticipate both livelihood crises and humanitarian emergencies, and recognize them as different phases of the same process. By monitoring key risk factors such as weather, harvest data and market data alongside household economic data, it should identify livelihood stresses and shocks. This, in turn, should inform interventions to shore up livelihoods and avoid destructive coping strategies. EWS should detect whether the crisis appears likely to evolve into a full-blown emergency, thus enabling actors to prepare for a humanitarian response. At each stage of the process, early action should seek to prevent the crisis from escalating and to mitigate its impact on lives and livelihoods. Crisis calendars provide a means to identify when particular interventions are most appropriate (Bailey, 2013).

Sivakumar (2014), referring to the context of contemporary droughts, calls for proactive future actions to be able to cope with their associated imperatives. Despite the repeated occurrences of droughts throughout human history and their large-scale effects on various socio-economic sectors, no concerted efforts have ever been made to initiate a dialogue on the formulation and adoption of national drought policies. The absence of a clear national drought policy implies that governments at the national, state and community levels will continue with the status quo, reacting to the impact of droughts with little coordination between national, state and local agencies. Bailey (2013) suggests that changing the status quo requires governments to anticipate political reward from acting to reduce shortage risk and to expect to be penalized for failing to do so.

A drought (hazard) alone does not trigger an emergency. Whether it becomes an emergency or a disaster depends upon its impact on local communities and the environment. This, in turn, depends on the vulnerability of people and the environment to such a "shock".

6.2.1. Plant pests and diseases

An estimated 30 to 40 percent of crops are lost each year to pests. Reducing this loss by only 1 percent could allow millions more people to receive adequate food. Over one-third of the world's population – which is set to reach 9 billion by 2050 – is supported by 500 million smallholder farmers. Therefore, supporting farmers in their fight against pests is a global food security emergency. In 1994, the Food and Agriculture Organization of the United Nations (FAO) established Locust Watch[2], which exploits the capabilities of current satellites to provide continuous estimates of rain-producing clouds and ecological conditions – such as vegetation development – that are important factors for monitoring desert locust habitats and forecasting locust development. Another recent development is the SATCAFE[3], a system for monitoring potential climatic conditions that foster the proliferation of coffee rust (Hemileia vastatrix; see figure 2). Using mobile technology, SATCAFE collects the degree of infection at coffee-plantation level. Coffee rust is the most economically significant coffee disease in the world, while in monetary terms, coffee is the most important agricultural product in international trade. Therefore, even a very limited reduction in coffee yields or a modest increase in production costs caused by the rust has a great impact on coffee producers, related support services, and even banking systems in those countries the economies of which depend on coffee exports.

2 http://www.fao.org/ag/LOCUSTS/en/activ/DLIS/satel/index.html.
3 http://www.siatma.org/.

FIGURE 2. CLIMATIC CONDITIONS FAVOURABLE TO THE DEVELOPMENT OF COFFEE RUST IN PANAMA.

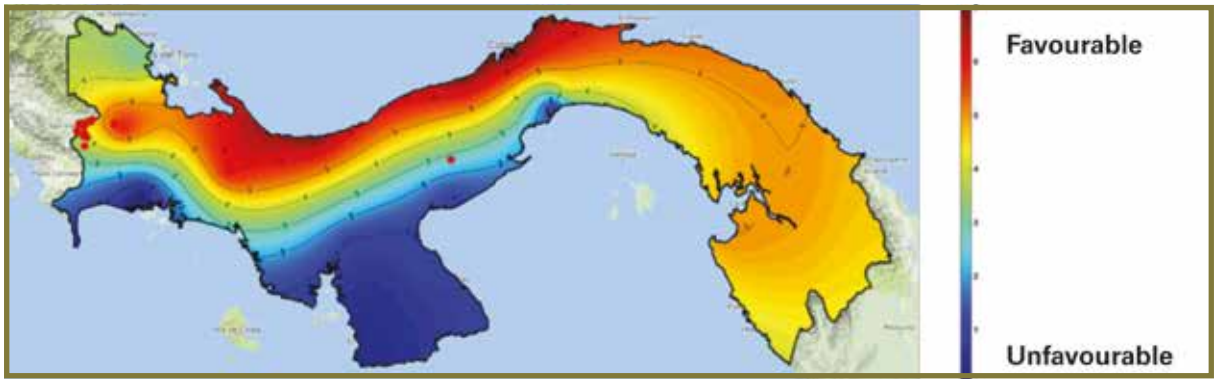

6.2.2. The phenology model for monitoring vegetation

Vegetation phenology (the study of recurring vegetation cycles and their connection to climate) is an important variable in a wide range of Earth and atmospheric science applications. In particular, as interest in global change research grows, accurate phenology models will become increasingly vital tools, as they enable researchers to monitor and predict vegetation responses to interannual climatic variability. Early in the history of satellite phenology research, Justice et al. (1985) used the Normalized Differenced Vegetation Index (NDVI) (see section 4.2 below) to qualitatively assess the global phenology of numerous land cover types. Goward et al. (1985) demonstrated that the NDVI corresponds to known seasonality in the continental United States of America. Satellites were later used to interpret phenology as an indicator of land cover changes in South America (Stone et al., 1994) and to detect phenological dynamics in shrublands (Duncan et al., 1993). Vrieling et al. (2011), focusing on the cumulated NDVI over the season (which is a proxy for net primary productivity), characterize the vegetation phenology for sub-Saharan Africa and assess the variability and trends of phenological indicators based on NDVI time series from 1982 to 2006 (figure 3).

FIGURE 3. MEAN START OF SEASON (LEFT); σ_t OF SOS (MIDDLE; IN DAYS); AND SPEARMAN TREND OF SOS (RIGHT), BASED ON AVHRR NDVI TIME SERIES. THE LOWER PART SHOWS THE VALUES FOR THE SECOND SEASON FOR LOCATIONS WHERE A SECOND SEASON OCCURS.

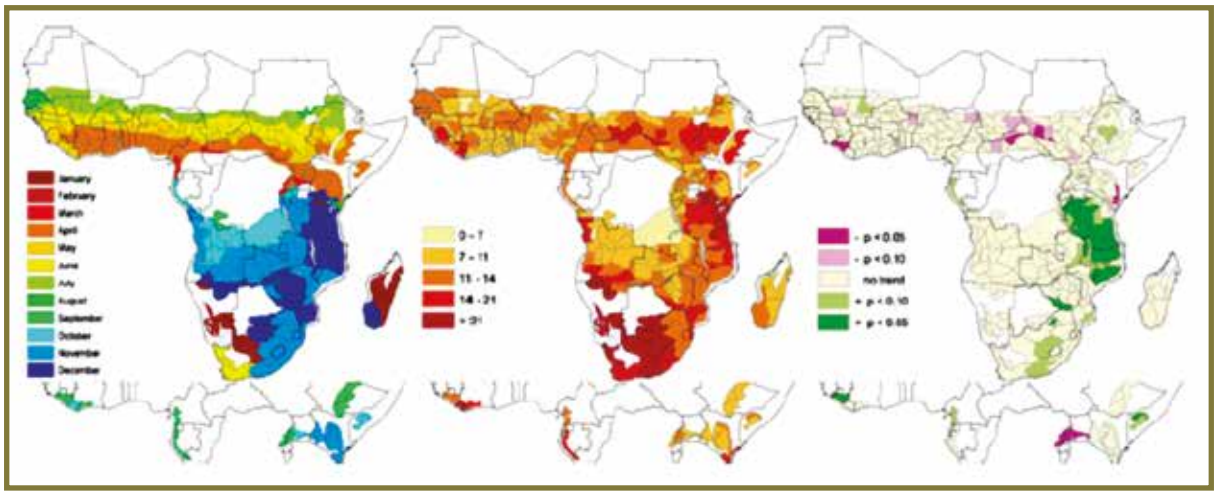

6.2.3. How early is "early" warning?

Figure 4 shows the current warning times for climatic hazards. It may be seen that EWS can provide seconds of available warning time for earthquakes, to months of warning for droughts, which are the quickest and slowest onset hazards, respectively. Specifically, EWS provide tens of seconds of warning for earthquakes, days to hours for volcanic eruptions, and hours for tsunamis. Tornado warnings provide minutes of lead-time for response. Hurricane warning time varies from weeks to hours. The warning time increases to years or even decades of lead-time available for slow-onset threats (El Niño, global warming, etc.). Drought warning time is in the range of months to weeks.

Slow-onset (or creeping) changes may cause serious problems to the environment and society, if preventive measures are not taken when necessary. Such creeping environmental changes require effective early warning technologies due to the high potential impact of incremental cumulative changes on society and the environment (UNEP, 2012).

FIGURE 4. HOW EARLY IS "EARLY" WARNING? THE GRAPH SHOWS THE TIMELINESS OF EWS FOR HYDROMETEOROLOGICAL HAZARDS AND THE AREA OF IMPACT (BY SPECIFYING THE DIAMETER OF THE SPHERICAL AREA) FOR DIFFERENT CLIMATIC HAZARDS. SOURCE: GOLNARAGHI, 2005.

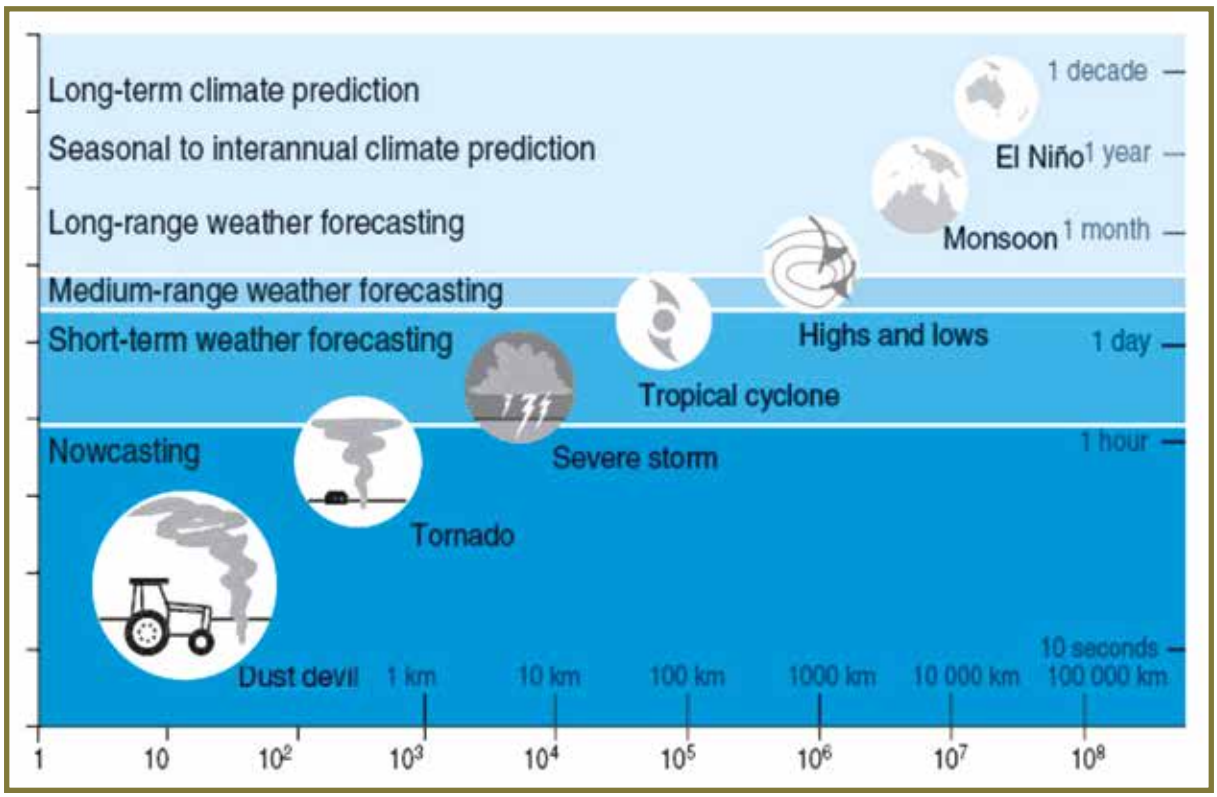

6.3. EARLY WARNING EARLY ACTION

The Red Cross (2008) defines Early Warning-Early Action (EWEA) as routinely taking humanitarian action before a disaster or health emergency occurs, making full use of scientific information on all timescales. It is much more effective to evacuate people before a flood than to rescue people during the flood, or to provide relief to its victims. It is also much more effective to support farmers in finding alternative livelihood options than to provide food aid when the harvest has failed. Remarkable advances in science and technology have enabled access to a wide range of EWS. General circulation models and satellite images, regional centres of expertise, national meteorological offices and other government agencies, local field reports and community observations all allow for a better comprehension of phenomena, and of their likely consequences. This, in turn, enables a much better anticipation of climate-related threats. At the shortest timescales, warnings of impending storms can help communities to prepare and take immediate actions, such as evacuation, to reduce loss of life. At intermediate timescales, a seasonal forecast based on El Niño may indicate that the upcoming storm season may be particularly severe, or that a continuing drought may result in food scarcity. At the longest timescales, future climate change scenarios present an early warning of increasing hazards which, along with trends such as urbanization and population growth, provide a new analysis of risk.

At each end of this temporal scale, disaster risk is the interaction between hazards (cyclones, storms, droughts, etc.) and the vulnerability of communities. Both of these elements are constantly changing. Climate change causes the frequency, intensity and location of hazards to change. Phenomena such as urbanization, poverty, population growth and disease continuously alter the nature of vulnerability. Disaster risk reduction is not only an effort to produce detailed risk maps, but rather a means to continually understand the evolving nature of hazards and vulnerabilities and to take action against vulnerability and its underlying causes.

Early warnings are ineffectual without corresponding early action. Numerous examples illustrate how reliable information about expected threats was insufficiently acted upon to avert a disaster, including Cyclone Nargis, Hurricane Katrina, and the food crisis in Niger. At the shortest timescales, the action could be evacuation. On the longest timescales, early action means working closely with local communities to assess and address the root causes of the changing risks that they face. Constructing houses on stilts, planting trees against landslides, conducting dengue awareness and prevention campaigns, installing water catchment systems and millions of other risk reduction measures can be taken. Early action also includes updated contingency planning and volunteer mobilization. In terms of geographic range, early action can take various forms: if a large flood is expected, at the local scale, the most a community is to protect its main water well from contamination. At country level, a government may update its contingency plans. On a global scale, international institutions can mobilize human and financial resources ahead of the disaster to assist national societies in reducing the impact of such hazards and even preventing loss of life completely. The more action is taken in response to warnings on the longest timescales – by identifying communities at risk, investing in disaster risk reduction, and enhancing preparedness to respond – the more lives and livelihoods can be salvaged at the shortest timeframes when a flood does arrive. Similarly, better links to global and regional knowledge centres and standardized procedures to deliver information to the correct locations will facilitate more effective action at the local level.

A few hours in advance, it is usually possible to identify rather well where and when a large storm will hit. However, for such a warning to be actionable, an investment must be made well in advance to create a comprehensive emergency management system. With a warning period of a few days, a storm forecast leads to the possibility to take immediate disaster preparedness action – identifying evacuation routes, evacuation centres, protecting assets and mobilizing community organizers for immediate response. However, a longer-term warning (months or years in advance) of the changing nature of the storm risk makes it possible to expand disaster risk reduction actions, to include measures such as helping communities plant trees to stabilize hillsides, self-organizing to respond better to warnings, building storm-resistant houses or advocating for the construction of storm shelters. Awareness that a

risk is higher than normal demands a higher level of investment in preparing the capacity to take early actions that will be useful regardless of when and where disaster strikes.

Using such risk information may also mean that "wrong" decisions may be made – for instance, when a forecast predicts an 80 percent likelihood that there will be hurricane-force winds in a certain time and place. While it is very likely to happen, there is no certainty. Indeed, in 20 percent of these cases, the predicted condition is actually expected to not happen. When promoting early action, such uncertainty should not be hidden: an honest description of what is and is not known about the future should be a key component of communication to all stakeholders, and an important consideration in how risks are assessed and addressed.

There is a need to transform scientific information – which is often complex and takes the form of maps or percentages – into simple and accessible messages that enable those at risk to make sensible decisions on how to respond to an impending threat. For instance, Rojas (2016) proposes using the Agricultural Stress Index System (ASIS) as a trigger to activate drought mitigation activities in agriculture (figure 5).

FIGURE 5. FROM THE AGRICULTURAL DROUGHT EWS TO EARLY ACTION. THE MAP ILLUSTRATES THE PERCENTAGE OF AGRICULTURAL AREA AFFECTED BY DROUGHT (AGROCLIMATIC INFORMATION SYSTEM, OR ASI) IN 2006.

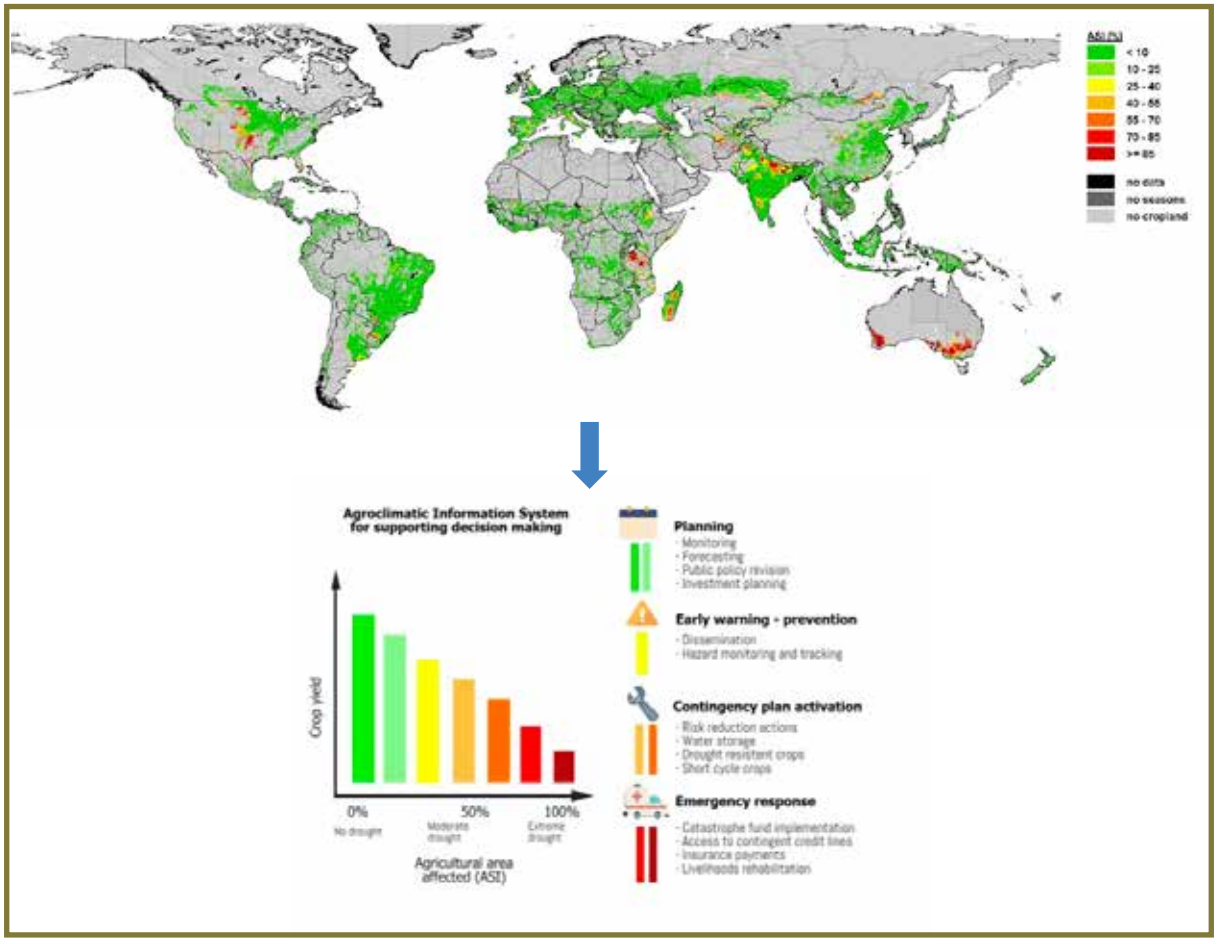

The bar graph links the ASI to the drought mitigation activities. Source: Rojas, O., 2016.

Continuing advances in remote sensing technology, improvements in weather forecasting and meteorological models, new possibilities from information and communication technologies (ICT) and major opportunities to expand the coverage and capacity of EWS in vulnerable countries and regions point towards an ever-improving predictive capacity. There is much that governments, agencies and early warning providers can do to facilitate these advances. However, without meaningful reforms in other areas, comparable improvements in early action will not follow (Bailey, 2013).

6.4. CROP YIELD FORECASTING

Forecasting is the foundation of all warning systems. It must be applied to the four areas of food security (availability, stability, access and biological utilization) to give decision-makers enough time to react to warnings, and with a sufficiently high degree of reliability (as a general rule, the more long-term the forecasts, the less reliable they are) to avoid false alarms from being raised. All forecasts have a probability rating (which may or may not be calculable), which is a good indicator of their reliability.

Basso et al. (2015) reviewed methods for crop yield forecasting, establishing that the process requires crop simulation models (CSMs). CSMs are computerized representations of crop growth, development and yield that are simulated through mathematical equations as functions of soil conditions, weather and management practices (Hoogenboom et al., 2004). CSMs are divided into statistical models, mechanistic models and functional models. Crop models are only an approximation of the real world, and many do not account for important factors such as weeds, diseases, insects, tillage and nutrients (Jones et al., 2001). Nevertheless, CSMs have played important roles in the interpretation of agronomic results, and their application as decision support systems for farmers is increasingly common. Models range from simple to complex. Simple models are often used for yield estimation across large land areas based on statistical information related to climate and historical yields, and include little detail about the soil-plant-system. Most simple models are used in National Early Warning Systems (NEWS).

Analysis of meteorological and climatic data allows providing near real-time information about the crop state, in quality and quantity, with the possibility of early warning on alarm/alert situations so that timely interventions can be planned and undertaken (Gommes et al., 2006). Crop forecasting philosophy is based on various types of data that are collected from different sources: meteorological data, agrometeorological (phenology, yield) data, soil (water holding capacity) data, remotely sensed data and agricultural statistics. Based on meteorological and agronomic data, several indices are derived which are deemed to be relevant variables in determining crop yield, such as crop water satisfaction, surplus and excess moisture, average soil moisture, etc.

The outputs are empirically related to crop yield through standard regression techniques. This procedure is known as “model calibration”. The result of the calibration is a mathematical expression – known as “yield function” – that is used to calculate yield estimates on the basis of model outputs. Available crop statistics at administrative level are used to calibrate the regression models; therefore, the latter’s ultimate accuracy depends, to a great extent, on the quality of those input statistics.

As noted by Pulwarty (2007), the timing and form of climatic information input (including forecasts and projections), and access to trusted guidance and capability to interpret and implement information and projections in decision-making processes, are as important to individual users as are improvements in prediction skill.

6.4.1. The agrometeorological model

Agricultural statistics show an interannual variability of crop yields due to three sources: (a) trends; (b) direct weather factors; and (c) indirect effects of the weather, pests, diseases, weed competition, etc. However, it must also be considered that the spatial variability of crop yield is dominated by soil fertility. The issue of the impact of the weather on food availability is further complicated by the fact that the weather plays a part at several levels of the food chain (Gommes, 2002). The relative importance of the listed sources of the variability of food production depends largely on the general socio-economic setting. In many developing countries, the technology component is not particularly marked, and some of the poorest countries may show no yield trend at all. This is a situation where the impact of weather can have dramatic conditions and threaten the food security of millions of people. When the same farmers are gradually forced by circumstances to adapt to more commercial farming, they will experience a transition phase, during which their vulnerability to weather vagaries will increase. In countries where the agricultural sector is more advanced (because of mechanization, irrigation, improved varieties, advanced on-farm decision-making, etc.), the trend accounts for a large proportion of yield variability (over 80 percent). If the trend is removed from the time series, it can therefore be assumed that the largest proportion of the residual variability is due to weather. Balaghi et al. (2013) propose a crop yield function based on meteorological data (rainfall), which is used as an explicative variable of crop yield variation in Morocco (figure 6). The authors consider that the slope of the regression line represents Rain Water Productivity (RWP, g/l), defined as the ratio of yield (kg/ha) to the cumulated rainfall (mm) during the cropping season (September to April). In semi-arid regions, a single meteorological variable such as rainfall is capable of explaining most of the crop yield variation; however, in tropical countries, an integration of other meteorological and soil moisture content should be performed. To forecast rice yield in Bangladesh, Gommes (2001) uses a simple water model and principal component analysis to identify actual evapotranspiration (ETA) and maximum temperature in August (Tx8) as independent variables (figure 7).

FIGURE 6. COUNTRY-LEVEL RELATIONSHIP BETWEEN DURUM WHEAT (KG/HA) AND RAINFALL DURING THE CROPPING SEASON (MM) (DATA FROM 1988 TO 2011).

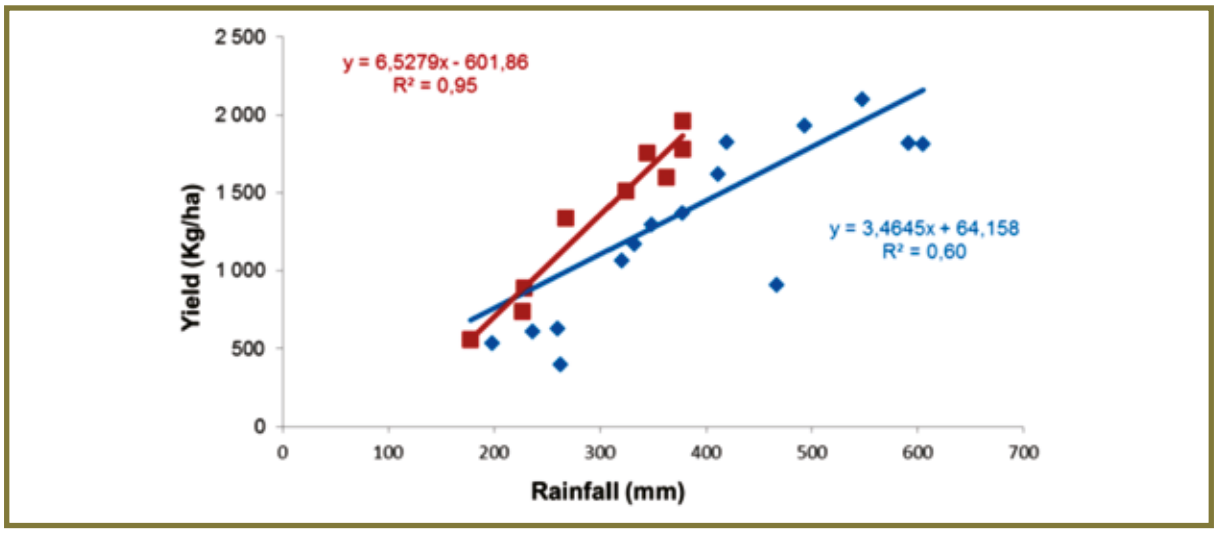

The slope of the blue regression line represents the RWP of soft wheat in Morocco, which is 0.346 g/l. The slope of the red regression line denotes the maximum RWP that is manageable in optimum conditions (0.653 g/l).
Source: Balaghi *et al.*, 2013.

FIGURE 7. RELATIONSHIP BETWEEN OBSERVED AND CALCULATED YIELD FOR HIGH RICE VARIETIES IN RAJSHAHI, BANGLADESH (1983-1998).

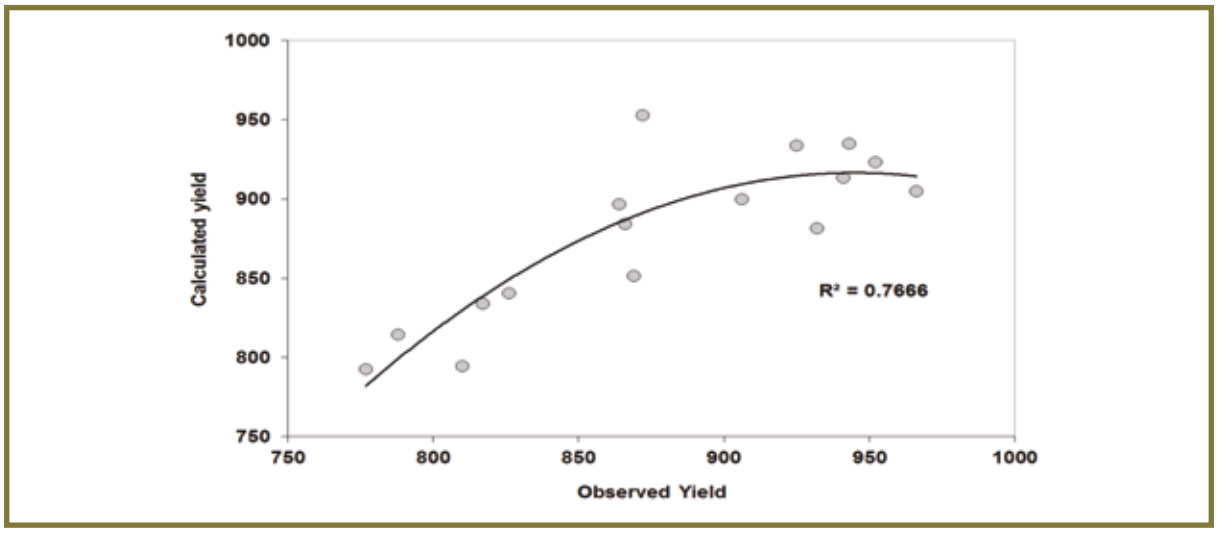

The regression model is based on actual evapotranspiration (ETA) and maximum temperature in August (Tx8).
Source: Gommes, 2001.

Most authors relate the weather variables to explain crop yield variation; however, if the area planted is kept relatively constant in a specific country, the weather could directly explain any fluctuations in production.

The European Commission's Joint Research Centre (JRC) provides near-real-time crop growth monitoring and yield forecasting information for the European Union (EU) and neighbouring countries, and is extending these activities to the main producing regions of the world. It also assesses the impact of climate change on agriculture through the simulation of the impact of different climate change scenarios in crop models. The JRC constitute an example of the operational use of complex crop models; to simulate the impact of climate change on agriculture and to evaluate potential adaptation strategies, the JRC uses its Biophysical Models Applications (BioMA) framework. A suite of model components implemented in this modelling framework help to carry out simulations of various crops in agricultural systems under present and future climate change scenarios.

Since 2012–2013, Statistics Canada has been collaborating with Agriculture and Agri-Food Canada (AAFC) and Environment Canada (EC) on a model that can derive crop yield estimates for the principal crops grown in Canada. Statistics Canada recognized the opportunity to make new estimates available with these modelled yields. These estimates could eventually replace collected data and reduce the response burden on crop producers[4]. The model utilizes data from low-resolution satellite imagery, historical field crop survey estimates, and agroclimatic information.

In Australia, Potgieter et al. (2014) propose a methodology that uses remote sensing information to predict aggregated field scale wheat yields (with a deviation of approximately 2.6 percent) (figure 8). The results of the first application in the country could be used by the insurance industry.

4 http://www.23.statcan.gc.ca/imdb/p2SV.pl?Function=getSurvey&SDDS=5225.

FIGURE 8. SIMULATED LONG-TERM MEDIAN OF SHIRE WHEAT YIELD (1901–2015).

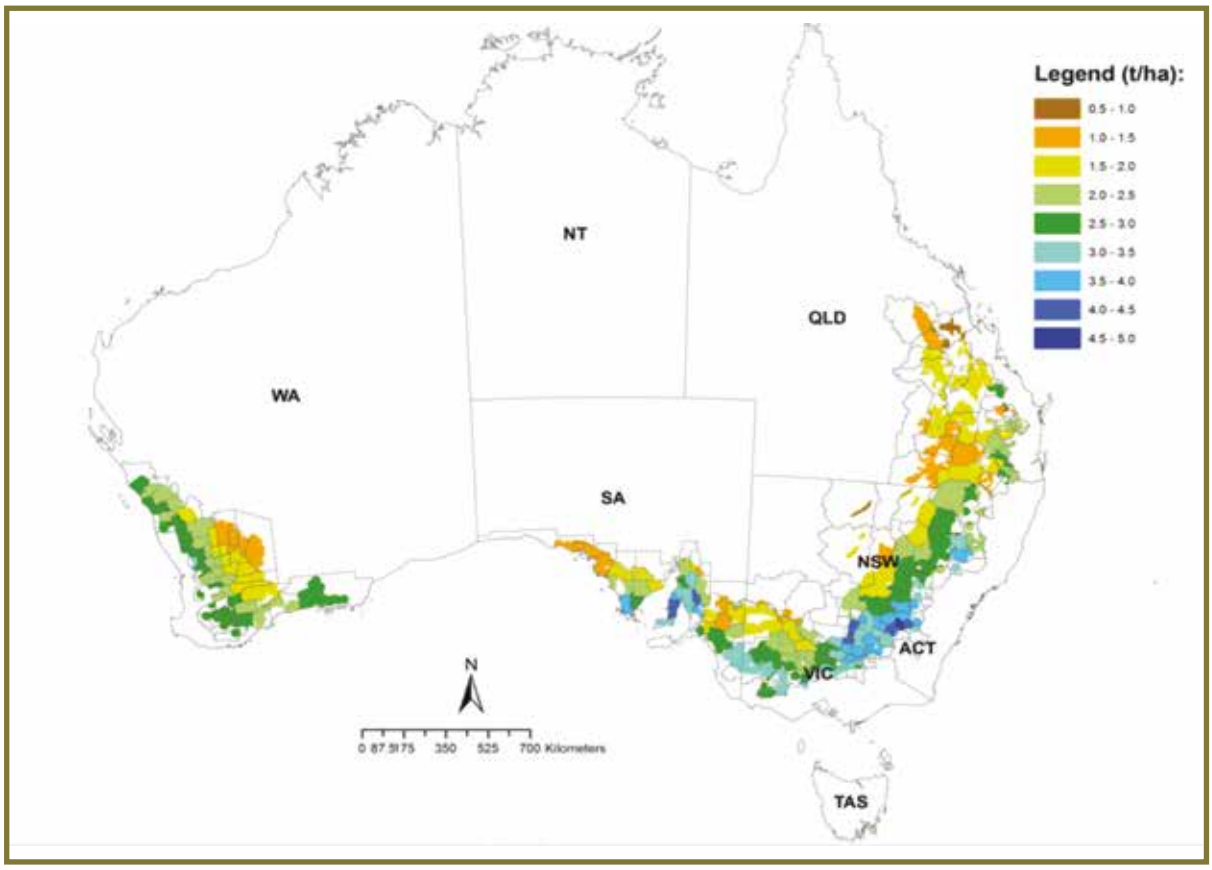

Source: Potgieter et al., 2014.

Crop yield forecasting provides the opportunity to prepare for the consequences of shortages in production by taking action to reduce vulnerability to climatic risks. Therefore, it is a valuable tool for decision-making in agriculture, enabling the planning in advance of actions as aids to agricultural insurance company (Balaghi et al., 2013).

6.4.2. The remote sensing model

Remote sensing is the science of acquiring information about an object through the analysis of data obtained by a device that is not in contact with that object (Lillesand and Keifer, 1994). Such data can be obtained from a variety of platforms, such as satellites, airplanes, unmanned aerial vehicles (UAVs), and handheld radiometers. They may be gathered by different devices, for example sensors, film cameras, digital cameras and video recorders. The instruments used for measuring electromagnetic radiation are called sensors. Sensors are passive when they do not have their own source of radiation and are sensitive only to radiation from a natural origin; they are active when they have a built-in source of radiation.

Field studies and airborne scanner experiments (Tucker, 1979) demonstrate that the spectral reflectance properties of vegetation canopies, and in particular combinations of red and near infrared (NIR) reflectance (also called "vegetation indices" or VIs), are useful for monitoring green vegetation. Vegetation indices are mathematical combinations or ratios of mainly red, green and infrared spectral bands, designed to identify functional relationships between crop characteristics and remote sensing observations (Wiegand et al., 1990). Vegetation indices are strongly modulated by the interaction of solar radiation with crop photosynthesis and are thus indicative of the dynamics of

biophysical properties related to crop status. Box 2 notes the most commonly used vegetation indices for vegetation monitoring. One of the different VIs based on these two spectral channels, is the NDVI. The NDVI was proposed by Deering (1978), and remains the most popular indicator for studying vegetation health and crop production (MacDonald and Hall, 1980; Sellers, 1985). Research in vegetation monitoring has shown that the NDVI is closely related to the Leaf Area Index (LAI) and to the photosynthetic activity of green vegetation. The NDVI is an indirect measure of primary productivity through its almost linear relation with the Fraction of Absorbed Photosynthetically Active Radiation (fAPAR) (Los, 1998; Prince, 1990). The NDVI does present certain well-known limitations, such as the effects of soil humidity and surface anisotropy. Composite products used in most applications tend to limit these effects; however, they cannot be completely ignored. Rojas (2007) proposes a yield function based on remote sensing and agrometeorological data for forecast maize yield in Kenya. The model's NDVI and ETA explain 79 percent of the maize crop yield variance, with a root square mean error (RMSE) of 0.3766 t/ha (figure 9). The agrometeorological models display information on solar radiation, temperature, air humidity and soil water availability, while the spectral component contains information about crop management, varieties, and stresses that were not taken into consideration by the agrometeorological models (Rudorff and Batista, 1990).

FIGURE 9. RELATIONSHIP BETWEEN OBSERVED AND ESTIMATED MAIZE YIELD IN KENYA.

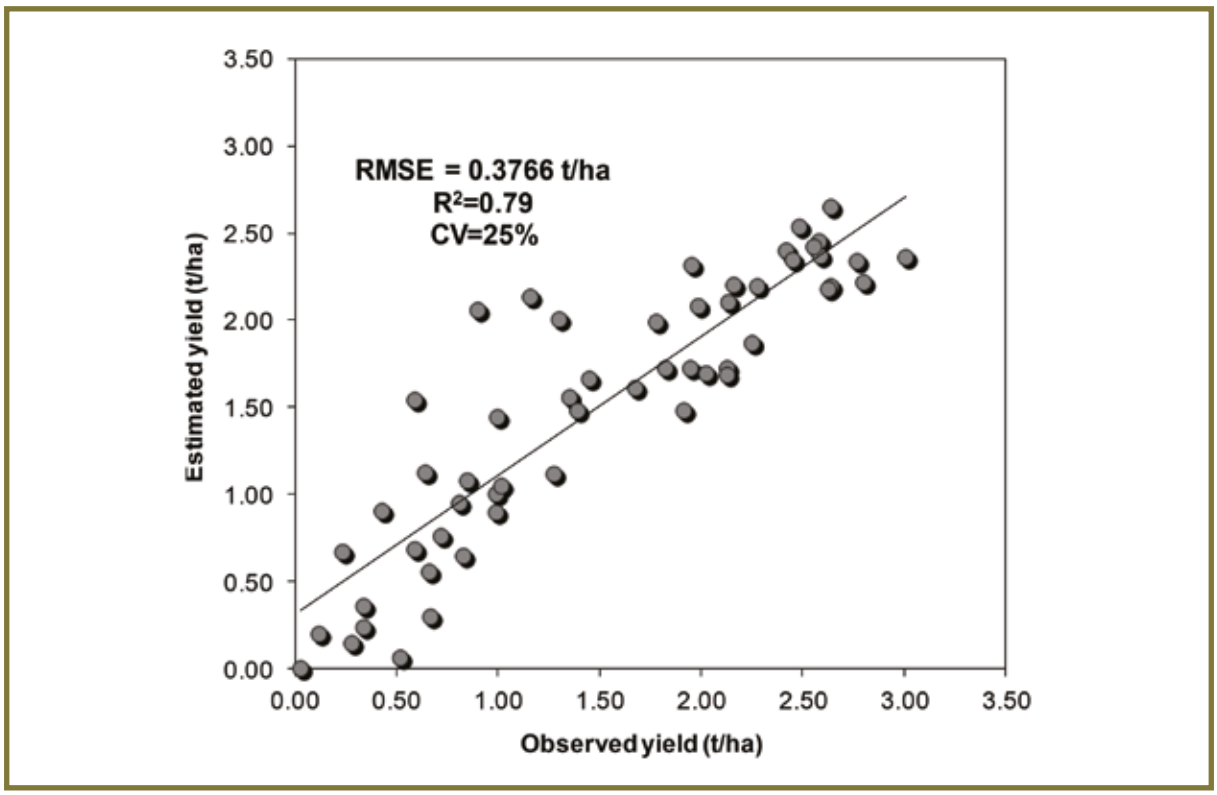

Regression model based on ETA and NDVI data for years from 1985 to 2003.
Source: Rojas, 2007.

To detect agricultural areas with a high likelihood of water stress (drought) at the global level, FAO has developed the Agriculture Stress Index System (ASIS). ASIS uses the Vegetation Health Index (VHI), a composite index joining the Vegetation Condition Index (VCI) and the Temperature Condition Index (TCI). The VCI (Kogan, 1994) is derived from the NDVI. The TCI algorithm is similar to the VCI, but relates to the brightness temperature T estimated from the AVHRR's thermal infrared band (channel 4). Kogan (1995) proposed this index to remove the effects of cloud contamination in the satellite assessment of vegetation condition because the AVHRR channel 4 is less sensitive to

water vapour in the atmosphere than the visible light channels. High mid-season temperatures indicate unfavourable or drought conditions, while low temperatures indicate mostly favourable conditions (Kogan, 1995).

The first step in ASIS is to elaborate a temporal average of the VHI, to assess the intensity and duration of the dry period(s) occurring during the crop cycle at pixel level. ASIS is based on ten-day (dekadal) satellite data of vegetation and land surface temperature from the METOP-AVHRR sensor at a resolution of 1 km.

The second step is to calculate the percentage of agricultural area affected by drought (pixels with a VHI lower than 35 – a value identified as critical in previous studies) to assess the extent of the drought. Finally, the entire administrative area is classified according to the percentage of area affected. ASIS assesses the severity (intensity, duration and spatial extent) of the agricultural drought and indicates the final results at administrative level, given the possibility to compare it with the agricultural statistics of the country (Rojas et al., 2011; Van Hoolst et al., 2016). Rojas (2016) proposes a yield function based on the Agricultural Stress Index (ASI) and wheat yield in Syria (figure 10).

FIGURE 10. RELATIONSHIP BETWEEN AGRICULTURAL STRESS INDEX (ASI) AND WHEAT YIELD IN SYRIA (1985-2012).

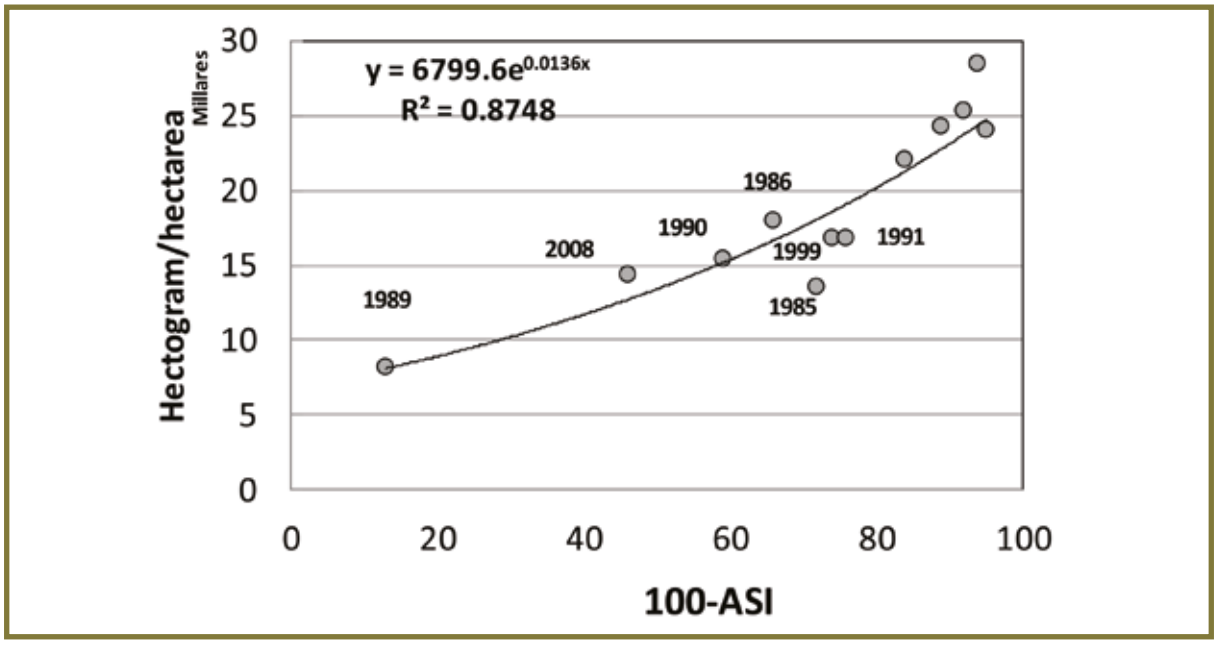

Source: FAO, GIEWS

India's Mahalanobis National Crop Forecast Centre (MNCFC) combines agrometeorological models with remote sensing data to provide multiple preharvest production forecasts of crops at national, state and district levels[5]. The MNCFC releases six production forecasts during the crop cycle: Pre-season, Early-season, Mid-season, Pre-Harvest (state level), Pre-Harvest (district level) and a Revised Assessing Damage. The MNCFC uses conventional tools, such as econometry and agrometeorology during pre- and early-season forecasts, medium- to high-resolution remote sensing products during mid-season forecasts and high-resolution imagery during preharvest at district level. Another of the strengths of this approach lies in the remote-sensing-driven crop cutting experiments (CCEs) that the MNCFC conducts every crop season to train the different agrometeorological models and remote sensing products.

5 http://www.nrsc.gov.in/Agriculture.

Brown et al. (2009) suggest the crop yield forecasting model as a methodology to forecast the price of food staples using NDVI information. They use the NDVI as a proxy for local millet supply in the model, for which no appropriate market-level data is available. Linking the NDVI with information on the planted area is likely to increase the predictive power of the NDVI; however, regrettably, comprehensive information on the area in cultivation is not readily available at local level in West Africa. The model accounts for 85 to 90 percent of the observed price variation, and the error of the four-month-ahead forecast is in the range of 13.4 percent (Niger) to 19.5 percent (Burkina Faso) on average using in-sample observations, or 18.8 percent (Burkina Faso) to 21.9 percent (Mali) on average using out-of-sample observations. Figure 11 shows an example of the relationship between millet production, the NDVI, actual millet prices and predictions.

FIGURE 11. LEFT: RELATIONSHIP BETWEEN THE NDVI AND MILLET PRODUCTION IN BURKINA FASO IN THE YEARS FROM 1982 TO 2006.
RIGHT: AVERAGE PRICES AND FOUR-MONTH PREDICTIONS FOR BURKINA FASO.

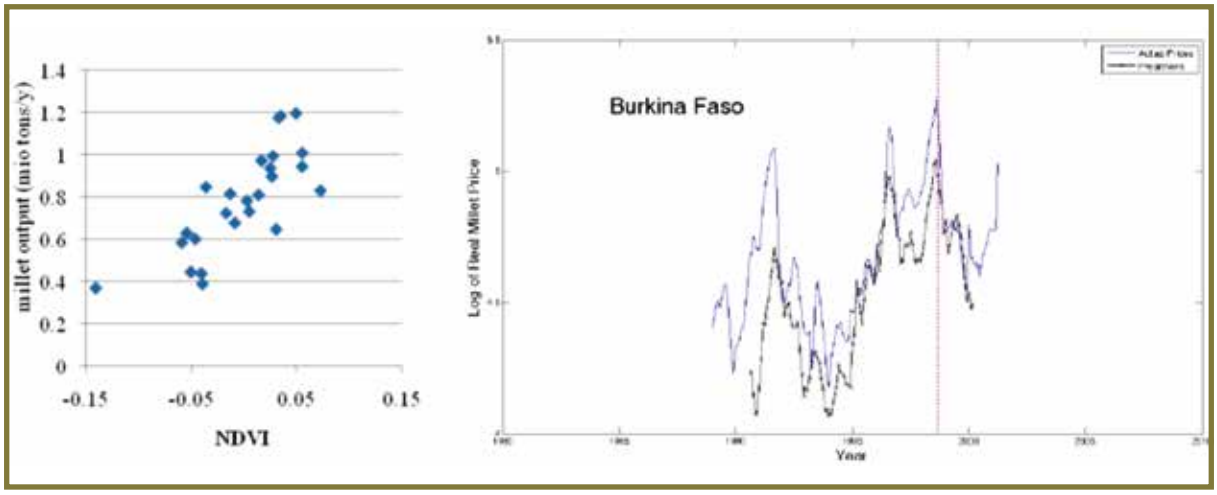

Source: Brown *et al.*, 2009.

Finally, using a general circulation model (GCM), Hansen et al. (2004) forecast regional wheat yields in northeast Australia. The model's prediction accuracy was generally better at state level than at the smaller district level. Although the wheat simulation model accounted for approximately 75 percent of the variance of de-trended state average wheat yields, correlations for individual districts were generally lower, accounting for an average of 58 percent of the variance weighted by the area under wheat in each district. The authors compared the results of the GCM model with predictions based on climatology alone, phases of the El Niño-Southern Oscillation (ENSO) and phases of the Southern Oscillation Index (SOI). Figure 12 shows a correlation between the district wheat yields observed in Queensland and GCM-based wheat hindcasts.

FIGURE 12. CORRELATION BETWEEN OBSERVED DISTRICT WHEAT YIELDS IN QUEENSLAND AND GCM-BASED WHEAT HINDCASTS CAPTURED ON (A) 1 MAY (B) 1 JUNE, (C) 1 JULY AND (D) 1 AUGUST, FROM 1975 TO 1993, ADJUSTED TO THE 2001 TECHNOLOGICAL TREND.

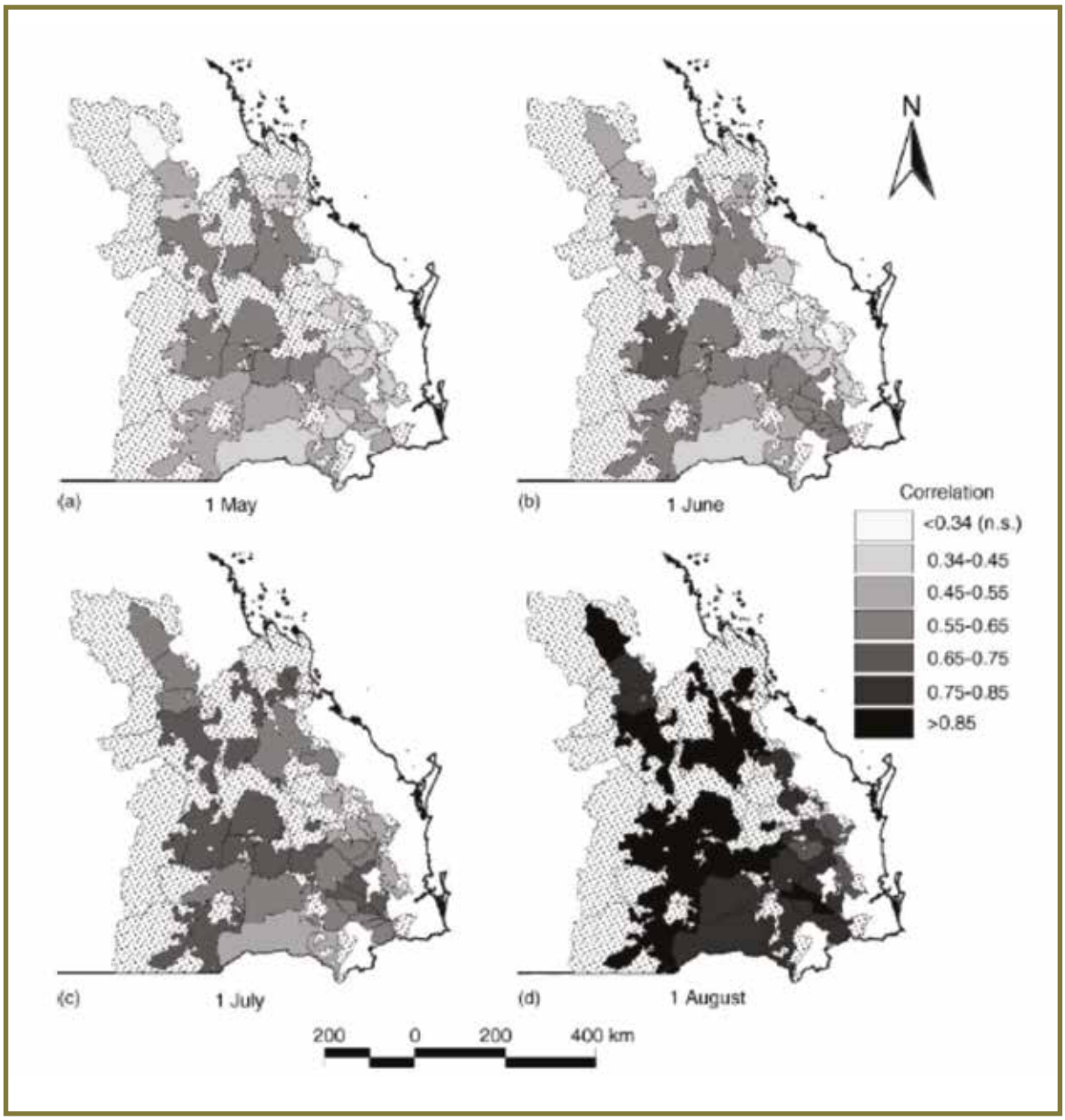

Source: Hansen et al., 2004.

United States Department of Agriculture's National Agricultural Statistics Service (USDA/NASS) has researched and used remote sensing technology for acreage estimation since the early 1970s. Significant advancements in recent years have enabled NASS to transition the use of remote sensing, from serving primarily a research function to performing an integral role in the agency's crop acreage estimation programme, covering all major crops grown in high-producing states in the United States of America. This accomplishment was largely achieved pursuant to (1) enhanced data partnerships; (2) improved methodologies; (3) increased availability of commercial software;, and (4) improved imagery and ancillary data. With acreage estimation now operational, the USDA is focusing its efforts to transition yield estimation too from the research to the operational context. Currently, corn and soybean yield estimates for ten major producing states are provided in-season to the Agricultural Statistic Board (ASB) and to NASS field offices. Although the yield estimates are currently solid, additional experience and research are expected to bring further improvements. Looking to the future, NASS has begun conducting research to quantitatively measure crop progress and condition using remote sensing and intends to expand the use of remote sensing into the mapping of soil moisture and improving of disaster assessments and monitoring.

6.5. CONCLUSION

This chapter has reviewed the concept and importance of the EWS, mainly supporting food security and nutrition aspects. The main conclusion is that to be effective, any EWS should be within the framework of national mitigation plans for disaster risk reduction of the hazard(s) monitored. Warnings of any hazard risk can help communities to prepare and take immediate action; however, the alert cannot, in itself, mitigate the potential impact of the eventual disaster. Consequently, the concept of Early Warning-Early Action was introduced, as highly relevant philosophy that governments and society should implement to defend communities, save lives and protect assets. In terms of agricultural production (mainly evaluating the availability of the four areas of food security, but indirectly affecting other two through the impact of local markets: stability and access), crop yield forecasting techniques may be of assistance by providing the opportunity to prepare for the consequences of any shortage in production by taking action to reduce vulnerability to climatic risks. A variety of models, with different level of complexity, are proposed to estimate crop yields at regional level, from simple regression between climate variables to more elaborate yield functions, introducing remote sensing products and general circulation models. The model selected depends on the data access and quality available in individual countries and the ultimate purpose of the forecasting. Currently, remote sensing performs a central role within statistical programs in the estimation of crop area and yields. Advances in imagery and Information Technology (IT) capabilities have enabled remote sensing to transition from a research effort to a production process. Future developments are expected to include a more rapid advance of remote sensing applications from research to operational status and to achieve benefits with reduced respondent burden, the expansion of additional spatially rich data, and savings from data collections in traditional surveys having the ultimate purpose of improving agricultural statistics.

BOX 3. HISTORICAL BACKGROUND TO FOOD SECURITY INFORMATION SYSTEMS.

- Until the 19th century, population fluctuations were linked to three main factors (war, famine and epidemics) and were often correlated with fluctuations in food production. Commercial and industrial development gradually modified this tendency in industrialized countries, as people became less dependent on subsistence farming. Until then, population monitoring gave an idea (ex post) of food insecurity.
- Until the beginning of the 20th century, subsistence farming remained the principal source of food in countries that were not industrialized. The successive waves of colonization and decolonization of the poorest countries were based on policies of food self-sufficiency, to preserve political independence. The food monitoring systems of the time were based mainly on knowledge of basic agricultural production.
- The major food crises that occurred in the 1970s illustrated the importance of world public opinion and of the need to inform the public at large of food crises. The nutritional monitoring of young children was developed during this time, as the basis for gathering information on, and providing assistance to, the most needy.
- At the World Food Conference held in 1974 in Rome, over one hundred countries adopted the Universal Declaration on the Eradication of hunger and malnutrition. At this time, analyses of the causes of hunger abounded and the modern notion of "food security" was developed with the creation, in 1975, of the World Food Security Committee (FSC). Although governments were urged to introduce "national food policies", the results were poor. Emphasis was placed on seeking to balance the supply and demand of staple foods. During this period, food-supply monitoring systems were gradually developed.
- Public marketing offices (for cereals in particular) were given powers to supervise these supplies in many countries, and efforts were made to create national or regional food security stocks (particularly in dry areas) to be used in the event of food crises. In this setting, information regarding production, national supplies, stocks and imports could theoretically be controlled by the same national body.
- Statistical systems and national accounts have recorded ever-increasing demands for information, especially in planning and economic monitoring. Statistical systems have tended to be highly compartmentalized (whether entrusted to a ministry or to a separate national body) and geared to their own internal requirements. Therefore, the information supplied has not been particularly useful for monitoring food security (for example, the statistics may be unreliable or that take a long time to be published; otherwise, the areas covered may be incompatible, making it difficult to compare data gathered from different systems). Some development partners have thus preferred to establish – in sub-Saharan Africa especially – parallel information systems that they finance and supervise themselves, and that provide the information they need to target their food security aid and assistance.
- Subsequently, structural adjustments and privatization radically changed the economies of developing countries and their trajectories, having major repercussions on food security. Donors decided to combine their economic aid with targeted interventionist policies to avoid major food or social crises. It became apparent that the problem of access to staple foods (poverty) would have to be examined more closely and that specific information was required to organize social aid.
- The diminishing world grain surplus and some negative experiences with large-scale distribution led the international community to reduce aid and question its use: when unsuitable or mismanaged, such aid could have a negative effect on food security. The existing information systems were then redirected to better target and monitor the distribution of aid. The development and use of satellite images offered a way to estimate the vegetation in each country, especially for rain-fed crops. This made information on global production available to the major donors.

▸▸ ▸▸

- The globalization of trade is now linked to the fast pace of modern communication (possible through Internet, fax, satellite telephone, etc.) and management (computer) systems. Today, it is much easier to manage databases, make forecast and disseminate results. Food security monitoring and forecasting systems have become – at least in theory – easy to manage in national contexts, and donors support the training of managers to use these modern tools and media.
- The speed at which developing countries undergo urbanization also has an effect on food security data, in that it becomes essential to monitor food security and vulnerable groups at urban and rural levels.
- Parallel to the development of faster information channels, it has become necessary to introduce decentralized decision-making and widen the area of concerted action to include the various actors in food security (public, private and civil society). Food security information systems have gradually become centres for the exchange of information at all levels throughout the country.
- The need to reduce the number of undernourished people has indicated the need for decentralization and concerted action among all the actors in food security. This requirement was clearly noted by all participants in the World Food Summit held in November 1996, at which government representatives decided to take all necessary measures to reduce by half the number of undernourished people (estimated at 800 million at the time) by 2015. Since then, efforts have been made to complete information system databases by developing concrete indicators for monitoring the undernourished.
- Most recently, on 25 September 2015, countries adopted a set of goals to end poverty, protect the planet and ensure prosperity for all as part of a new sustainable development agenda. Each goal has specific targets to be achieved over the next 15 years. The proposal contained 17 goals with 169 targets, covering a broad range of sustainable development issues. These included ending poverty and hunger, improving health and education, making cities more sustainable, combating climate change, and protecting oceans and forests.

TABLE 1. LIST OF THE COMMON VIS, MATHEMATICAL FORMULAE, SCALE OF THEIR DEVELOPMENT AND PARAMETER THEY ESTIMATE.

Index	Formula	Reference	Scale	Parameter
NDVI	$\frac{(NIR - \mathrm{Re}d)}{(NIR + \mathrm{Re}d)}$	Rouse *et al.*, 1974	Canopy	Biomass; Vegetation fraction
Green Normalized Difference Vegetation Index (GNDVI)	$\frac{(NIR - Green)}{(NIR + Green)}$	Gitelson *et al.*, 1996	Canopy	Chlorophyll; Vegetation rraction
Photochemical Reflectance Index (PRI)	$\frac{(R570 - R531)}{(R570 + R531)}$	Gamon *et al.*, 1992	Canopy	Photosynthesis efficiency/ RUE
Normalized Difference Red Edge (NDRE)	$\frac{(R790 - R720)}{(R790 + R720)}$	Barnes *et al.*, 2000	Canopy	Chlorophyll/nitrogen
Canopy Chlorophyll Content Index (CCCI)	$\frac{(NDRE - NDRE_{\min})}{(NDRE_{\max} - NDRE_{\min})}$	Fitzgerald *et al.*, 2006	Canopy	N Status/chlorophyll
Ratio Vegetation Index (RVI)	$\frac{NIR}{\mathrm{Re}d}$	Jordan, 1969	Leaf	Biomass
Enhanced Vegetation Index (EVI)	$2.5 * \frac{(NIR - \mathrm{Re}d)}{(NIR + C1 * \mathrm{Re}d - C2 * Blue + L)}$ $[C1 = 6; C2 = 7.5; L = 1]$	Huete *et al.*, 2002	Canopy/ regional	Biomass/vegetation cover
Enhanced Vegetation Index 2 EVI 2)	$G * \frac{NIR - \mathrm{Re}d}{NIR + \left(6 - \frac{7.5}{c}\right) * \mathrm{Re}d + 1}$ $\mathrm{Re}d = c * Blue$ $G = f(c)$	Jiang *et al.*, 2008	Canopy/ regional	Biomass/vegetation cover
Visible Atmospherically Resistant Index (VARIgreen)	$\frac{(Green - \mathrm{Re}d)}{(Green + \mathrm{Re}d + Blue)}$	Gitelson *et al.*, 2002	Canopy/ regional	Vegetation fraction/LAI
Visible Atmospherically Resistant Index; 700 nm (VARI700)	$\frac{(R700 - 1.7 * \mathrm{Re}d - 0.7 * Blue)}{(R700 + 2.3 * \mathrm{Re}d - 1.3 * Blue)}$	Gitelson *et al.*, 2002	Canopy/ regional	Vegetation fraction/LAI
Triangular Vegetation Index (TVI)	$0.5 * [120 * (R750 - R550) - 200 * (R670 - R550)]$	Brodge and Leblanc, 2000	Canopy	Chlorophyll
Modified Triangular Vegetation Index 1 (MTVI 1()	$1.2 * [1.2 * (R800 - R550) - 2.5 * (R670 - R550)]$	Haboudane *et al.*, 2004	Canopy	Chlorophyll
Modified Triangular Vegetation Index 2 (MTVI 2)	$\frac{1.5 * [1.2 * (R800 - R550) - 2.5 * (R670 - R550)]}{\sqrt{(2 * R800 + 1)^2 - (6 * R800 - 5 * \sqrt{R670}) - 0.5}}$	Haboudane *et al.*, 2004	Canopy	Chlorophyll

Index	Formula	Reference	Scale	Parameter
MERIS Terrestrial Chlorophyll Index (MTCI)	$\frac{R735.75 - R708.75}{R708.75 - R681.25}$	Dash and Curran, 2007	Canopy	Chlorophyll
Chlorophyll Absorption Reflectance (CAR)	$\frac{\lvert(a*670 + R670 + b)\rvert}{\sqrt{(a^2+1)}}$ $\begin{bmatrix} a = (R700 - R550)/150 \\ b = R550 - (a*550) \end{bmatrix}$	Kim *et al.*, 1994	Canopy	Chlorophyll
Chlorophyll Absorption Reflectance Index (CARI)	$\frac{\lvert(a*670 + R670 + b)\rvert}{\sqrt{(a^2+1)}} * \frac{R700}{R670}$	Kim *et al.*, 1994	Canopy	Chlorophyll
Modified Chlorophyll Absorption Reflectance Index (MCARI)	$[(R700 - R670) - 0.2*(R700 - R550)] * \frac{R700}{R670}$	Daugthry *et al.*, 2000	Leaf/ canopy	Chlorophyll/LAI/soil reflectance
MCARI 1	$1.2*[2.5*(R800 - R670) - 1.3*(R800 - R550)]$	Haboudane *et al.*, 2004	Canopy	Chlorophyll/LAI/soil reflectance
MCARI 2	$\frac{1.5*[2.5*(R800 - R670) - 1.3*(R800 - R550)]}{\sqrt{(2*R800+1)^2 - (6*R800 - 5*\sqrt{R680}) - 0.5}}$	Haboudane *et al.*, 2004	Canopy	Chlorophyll/LAI/soil reflectance
Transformed Chlorophyll Absorption Reflectance Index (TCARI)	$3*[(R700 - R700) - 0.2*(R700 - R550)*(R700/R670)]$	Haboudane *et al.*, 2002	Canopy	Chlorophyll/LAI/soil reflectance
Weighted Difference Vegetation Index (WDVI)	$NIR - a * \mathrm{Re}\,d$	Clevers, 1989	Canopy	LAI/biophysical parameters
Perpendicular Vegetation Index (PVI)	$\frac{1}{\sqrt{a^2+1}*(NIR - a*\mathrm{Re}\,d - b)}$	Richardson and Wiegand, 1977	Canopy	Canopy biophysical parameters
Soil-Adjusted Vegetation Index (SAVI)	$\frac{(1+L^a)*(R800 - R670)}{(R800 + R670) + L}$	Huete *et al.*, 1988	Canopy	Canopy biophysical parameters
Transformed Soil-Adjusted Vegetation Index (TSAVI)	$\frac{a^b*(R800 - a*R670 - b^c)}{[a*R800 + R670 - a*b]}$	Baret *et al.*, 1989	Canopy	Canopy biophysical parameters
Optimized Soil-Adjusted Vegetation Index (OSAVI)	$\frac{(1+0.16)*(NIR - \mathrm{Re}\,d)}{(NIR + \mathrm{Re}\,d + 0.16)}$	Rondeaux *et al.*, 1996	Canopy	Canopy biophysical parameters
Modified Soil-Adjusted Vegetation Index (MSAVI) Vegetation Health Index (VHI)	$\frac{(1+L^e)*(R800 - R670)}{(R800 + R670 + L)}$ VHI= a*VCI + b*TCI	Qi *et al.*, 1994 Kogan, 1995	Canopy Canopy	Canopy biophysical parameters Biomass, biophysical parameters

[a] L is a soil-adjustment factor and is set at 0.5.
[b and c] a and b are soil-line coefficients derived from the following equation: $NIR_{soil} = a * RED_{soil} + b$.
[d] χ is an adjustment factor for minimizing the soil background effects. It is set at 0.08.
[e] L is a self-adjustment factor derived from the following equation: $L = 1 - 2*a*NDVI*WDVI$.

6.6. REFERENCES

Bailey, J. & Boryan, C. 2010. *Remote Sensing Applications in Agriculture at the USDA National Agricultural Statistics Service*. USDA/NASS Publication.

Bailey, R. 2013. *Managing Famine Risk. Linking Early Warning to Early Action*. Chatham House Report. Chatham House Publication: London.

Balaghi, R., Jlibene, M., Tychon, B. & Eerens, H. 2013. *Agrometeorological cereal yield forecasting in Morocco*. National Institute for Agronomic Research Publication: Rabat.

Basso, B., Cammarano, D. & Carfagna, E. 2013. *Review of Crop Yield Forecasting Methods and Early Warning Systems*. FAO Publication: Rome.

Brown, M., Higgins, N. & Hintermann, B. 2009. *A Model of West African millet prices in rural markets*. CEPE Working Paper No. 69. CEPE Publication: Zurich.

Buchanan-Smith, M. 2000. *Early Warning Systems for Drought Preparedness and Drought Management: Proceedings of an Expert Group Meeting held 5–7 September, 2000, in Lisbon, Portugal*. World Meteorological Organization (WMO) Publication: Geneva, Switzerland.

Cammarano, D. 2010. *Spatial integration of remote sensing and crop simulation modelling for wheat nitrogen management*. University of Melbourne, Victoria, Australia. (Ph.D. Thesis)

Campbell, J.B. 1996. *Introduction to Remote Sensing*. Second edition. Guilford Press: New York, NY, USA.

Golnaraghi M. 2005. Early warning systems, UNEP/GRID-Arendal Maps and Graphics Library. http://maps.grida.no/go/graphic/early_warning_systems.

Davies, S., Buchanan-Smith, M. & Lambert, R. 1991. *Early warning in the Sahel and Horn of Africa: The state of the art. A review of the literature*. Vol. 1, Research report No. 20. IDS Publication: Brighton, UK.

Deering, D.W. 1978. *Rangeland reflectance characteristics measured by aircraft and spacecraft sensors*. Texas A&M University, College Station, TX, USA. (Ph.D. Thesis)

Duncan, I., Stow, D., Franklin, I. Hope, A. 1993. Assessing the relationship between spectral vegetation indices and shrub cover in the Iornada Basin, New Mexico. *International Journal of Remote Sensing*, 14: 3395–3416.

Food and Agriculture Organization of the United Nations (FAO) & Global Information and Early Warning System (GIEWS). 2014. *Syrian Arab Republic: Continued conflict and drought conditions worsen 2014 crop production prospects*. GIEWS-Update. FAO Publication: Rome.

Gommes, R., Bernardi, M. & Petrassi, F. 2001. *Agrometeorological Crop Forecasting*. FAO Publication: Rome. Available at: http://www.fao.org/nr/climpag/agromet/index_en.asp. Accessed 10 June 2017.

Gommes, R. 2002. *Agrometeorological models and remote sensing for crop monitoring and forecasting in Asia and the Pacific*. FAO Publication: Rome.

Gommes, R. 2001. *An introduction to the art of agrometeorological crop yield forecasting using multiple regressions*. FAO Publication: Rome.

Goward, S.N., Tucker, C.J. & Dye, D.G. 1985. *North American vegetation patterns observed with the NOAA advanced very high resolution radiometer*. *Vegetation*, 64: 3–14.

Hansen, J.W., Potgieter, A. & Tippett, M.K. 2004. Using a general circulation model to forecast regional wheat yields in northeast Australia. *Agricultural and Forest Meteorology*, 127:77–92.

Hoogenboom, G., White, J. & Messina, C. 2004. From genome to crop: integration through simulation modelling. *Field Crop Research*, 90: 145–163.

Jones, J., Keating, B. & Porter, C. 2001. Approaches to modular model development. *Agricultural Systems*, 70: 421–443.

Justice, C.O., Townshend, J.R.G., Holben, B.N. & Tucker, C.J. 1985. Analysis of the phenology of global vegetation using meteorological satellite data, International Journal of Remote Sensing, 6: 1271–1318.

Kogan, F. 1994. Droughts of the late 1980s in the United States as derived from NOAA polar-orbiting satellite data. *Bulletin of the American Meteorological Society*, 76(5): 655–668.

Kogan, F. 1995. Application of vegetation index and brightness temperature for drought detection. *Advances in Space Research*, 15: 91–100.

Lillesand, T. & Kiefer, R. 1994. *Remote sensing and Image Interpretation*. Third edition. John Wiley & Sons: New York, USA.

Los, S.O. 1998. Linkages between global vegetation and climate. An analysis based on NOAA Advanced Very High Resolution Radiometer data. Vrije Universiteit, Amsterdam – Goddard Space Flight Centre, Greenbelt Maryland. (Ph.D. Thesis)

MacDonald, R. B. & Hall, F.G. 1980. Global crop forecasting. *Science*, 208(4445): 670–679.

Potgieter, A., Power, B., Mclean, J., Davis, P. & Rodríguez, D. 2014. Spatial estimation of wheat yields from Landsat´s visible, near infrared and thermal reflectance bands. *International Journal of Remote Sensing Applications*. 4(3): 134–143.

Pulwarty, R. 2007. Communicating agroclimatological information, including forecasts for agricultural decisions. In: World Meteorological Organization (WMO), *Guide to Agrometeorological Practices* (ch. 17). WMO Publication: Geneva, Switzerland. Available at http://www.wmo.ch/ web/wcp/agm/RevGAMP/. Accessed on 10 June 2017.

International Federation of Red Cross and Red Crescent Societies. 2008. *Early warning Early action*. Publication of the International Federation of Red Cross and Red Crescent Societies: Geneva, Switzerland.

Prince, S.D. 1990. High temporal frequency remote sensing of primary production using NOAA AVHRR. *Applications of remote sensing in agriculture*, 4: 169–183.

Rojas, O. 2007. Operational maize yield model development and validation based on remote sensing and agro-meteorological data in Kenya. *International Journal of Remote Sensing*. 28(17): 3775–3793.

Rojas, O. Vrieling, A. & Rembold, F. 2011. Assessing drought probability for agricultural areas in Africa with remote sensing. *Remote Sensing of Environment* 115: 343–352.

Rojas, O. 2016. *Protocol for country-level ASIS: calibration and national adaptation process*. FAO Publication: Rome.

Rudorff, B. & Batista, G.T. 1990. Yield estimation of sugarcane based on agrometeorological-spectral models. *Remote Sensing of Environment*, 33: 183–192.

Sellers, P.J. 1985. Canopy reflectance, photosynthesis and transpiration. *International Journal of Remote Sensing*, 6(8): 1335–1372.

Sivakumar, M., Stefanski, R., Bazza M., Zelaya, S., Wilhite D. & Rocha, A. 2014. High Level Meeting on National Drought Policy: Summary and Major Outcomes. *Weather and Climate Extremes*, 3: 126–132.

Stone, T.A., Schlesinger, S., Houghton, R.A. & Woodwell, G.M. 1994. A map of the vegetation of South America based on satellite imagery. *Photogrammetric Engineering & Remote Sensing*, 60: 541–551.

Tucker, C.J. 1979. Red and photographic infrared linear combinations for monitoring vegetation. *Remote Sensing of Environment*, 8: 127–150.

UN Environment Programme (UNEP). 2012. *Early Warning Systems: A State of the Art Analysis and Future Directions*. UNEP Publication: Nairobi.

Van Hoolst, R., Eerens, H., Haesen, H., Royer, A., Bydekerke, L., Rojas, O., Li, Y. & Racionzer, P. 2016. FAO's AVHRR-based Agricultural Stress Index System (ASIS) for global drought monitoring. *International Journal of Remote Sensing*, 37(2): 418–439.

Vrieling, A., de Beurs, K. & Brown, M. 2011. Variability of African farming systems from phenological analysis of NDVI time series. *Climatic Change*, 109: 455–477.

Wiegand, C.L., Gerbermann, A.H., Gallo, K.P., Blad, B.L. & Dusek, D. 1990. Multisite analyses of spectral-biophysical data for corn. *Remote Sensing of Environment*, 33: 1–16.

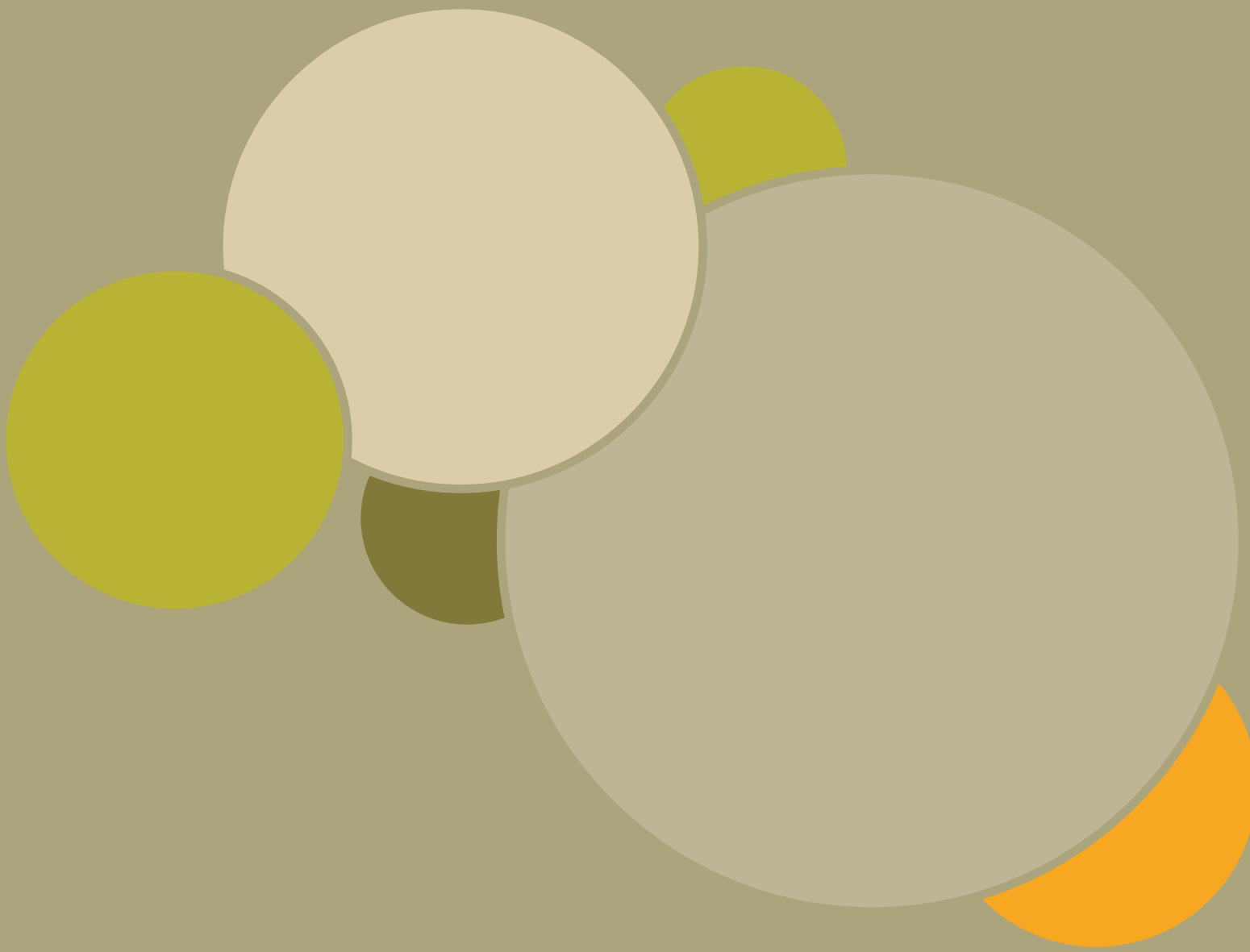

7

Chapter 7

Monitoring forest cover and deforestation

Frédéric Achard, Yeda Maria Malheiros de Oliveira and Danilo Mollicone

7.1. INTRODUCTION AND MAIN OBJECTIVES

Forests provide a range of goods and services that benefit peoples' livelihoods and wellbeing and that play an important role in economies around the world. It is widely acknowledged that reliable and timely information on forest resources are essential to assess the full benefits of forests, as well as facilitate governments and other stakeholders in assessing and monitoring the effectiveness of policies and programs related to forestry and other land uses (MacDicken, 2015).

Moreover, global demand for agricultural products such as food, feed, and fuel is a major driver of cropland and pasture expansion across much of the developing world (DeFries *et al*., 2010). Whether these new agricultural lands replace forests, degraded forests, or grasslands greatly influences the environmental consequences of expansion. Across the tropics, between 1980 and 2000, over 55 percent of new agricultural land was obtained at the expense of intact forests, and another 28 percent of disturbed forests (Gibbs *et al*., 2010). Recently, deforestation driven by commercial cropland has significantly increased, with hotspots occurring in South America (de Sy *et al*., 2015).

Poor information and statistics on forest resources may lead to insufficient or inaccurate knowledge of the country's forest resource utilization, impede successful planning and policy decisions regarding forestry and other land uses, mislead donors in identifying targeted priorities and projects, and hinder proper assessment of the progress being made towards Sustainable Forest Management (MacDicken *et al*., 2015) and other development goals.

The Reduction of Emissions from Deforestation and forest Degradation (REDD+) activities held under the United Nations Framework Convention on Climate Change (UNFCCC) are expected to offer results-based payments to developing countries for reducing greenhouse gas emissions from forested lands (UNFCCC, 2014). It is necessary

to determine reference data on forest carbon losses against which future rates of change can be evaluated, and to establish reliable methods for monitoring, reporting and verifying such changes. Most developing countries must yet develop forest monitoring systems at national level in the framework of REDD+.

Although some national agencies (in particular, those of Brazil, India and Mexico) are making great progress at country level from, in the past, several tropical countries had limited capacity to implement such monitoring systems. Capacity-building efforts are now being made to strengthen the technical skillsets necessary to implement national forest monitoring at institutional levels (Romijn *et al*., 2015). It is highly desirable to help developing countries to foster and enhance their own statistical capacity to produce statistics on forest resources.

The last few decades have seen great progress in producing and disseminating information on global forest cover resources among major international agencies such as the Food and Agriculture Organization of the United Nations (FAO; see FAO, 2015a) or the World Resources Institute. Robust examples advancing such approaches, applied on the full tropical belt, and examples of good practices adopted at national scale are also included in this review.

Advances in measuring approaches and techniques based on satellite remote sensing are of tremendous interest (Achard and Hansen, 2012). Data and methods are no longer an obstacle to the implementation of REDD+ within the Paris Agreement (UNFCCC, 2016). Moreover, the global community of Earth Observation and carbon experts have prepared technical guidelines on methodological issues relating to the integration of remote sensing and ground-based observations to estimate emissions and removals of greenhouse gases in forests: the GOFC-GOLD REDD sourcebook (GOFC-GOLD, 2016), and the GFOI Methods and Guidance Documentation (GFOI, 2014). These guidelines are intended to be instruments to assist countries in identifying data gaps in their national forest inventory systems and to provide operational guidance on developing national forest monitoring systems. Countries are encouraged to incorporate the international standards into their forest monitoring program to promote international comparability.

Improvements in national monitoring capacities to produce forest area estimates ultimately benefit policy-makers, economic entities and the livelihoods of forest-dependent people, enhancing the availability and quality of data on forest resources, and thus ensuring better policy and investment decisions.

The purpose of this chapter is to provide guidelines on the use of remote sensing for forest cover statistics and to present the existing approaches to the use of remote sensing for assessing forest cover and evolution, from global to national scales. This review seeks to support the development of national REDD+ interventions and forest monitoring systems.

7.2. THE USE OF REMOTE SENSING TO MONITOR FOREST COVER – BACKGROUND INFORMATION

Technically, it became possible to rely upon remote sensing imagery to monitor forest area change from the 1990s. The feasibility and accuracy of such monitoring depends largely upon national circumstances (in particular, with regard to data availability); that is, potential limitations relate more to definitions, resources and data availability than to methodologies (GOFC-GOLD, 2016).

7.2.1. Definition of forests, deforestation and degradation

Several terms, definitions and other elements relevant to REDD+ activities are not formally established (including terms such as "deforestation" and "forest degradation"). As decisions regarding REDD+ are based on the current modalities prescribed by the UNFCCC and the Kyoto Protocol, the definitions provided in those two documents will be used in this chapter, and are set out below (see GOFC-GOLD, 2016, for further details).

Forest land – Under the UNFCCC, forest land includes all land with woody vegetation consistent with thresholds used to define forest land in the national greenhouse gas inventory. It also includes systems with a vegetation structure that does not, but that in situ could potentially reach, the threshold values used by a country to define the forest land category. Moreover, the presence of other uses that may be predominant should be taken into account.

Estimations of deforestation are affected by the definitions of 'forest' versus 'non-forest' land, as these may vary widely in terms of tree size, area and canopy density. There are myriad definitions of forest. However, most definitions share certain threshold parameters, including for the minimum area, minimum height and minimum level of crown cover. In its 2015 forest resource assessment, FAO (FAO, 2015a) uses a minimum cover of 10 percent, a minimum height of 5 m and a minimum area of 0.5 ha, adding that forest use should be the predominant use. Most remote sensing studies, on the other hand, use a land cover definition (Magdon *et al*., 2014), because land use cannot be determined by remote sensing alone.

For the purposes of the Kyoto Protocol, parties select a single value for crown area, tree height and area to define forests within their national boundaries (UNFCCC, 2006). The selection is made from within the following ranges, with the understanding that young stands that have not yet reached the necessary cover or height are included as forest:

- Minimum forest area: 0.05 to 1 ha
- Potential to reach a minimum height at maturity *in situ* of 2 to 5 m
- Minimum tree crown cover (or equivalent stocking level): 10 to 30 percent

The definition of forest allows some flexibility to countries when designing a monitoring plan, because the analysis of remote sensing data can adapt to different minimum tree crown cover and minimum forest area thresholds. However, consistency in forest classifications for all REDD+ activities is critical for integrating different types of information, including remote sensing analysis. The use of different definitions affects the technical requirements for Earth Observation and may influence cost, availability of data, and the ability to integrate and compare data through time.

Deforestation – Most definitions characterize deforestation as the long-term or permanent conversion of land from forest use to other non-forest uses. Under Decision 16/CMP.1, the UNFCCC defined deforestation as: "the direct, human-induced conversion of forested land to non-forested land." (UNFCCC, 2006).

In practical terms, this definition entails a reduction in crown cover from above to below the threshold for the forest definition. Deforestation causes a change in land use, usually in land cover. Common changes include conversion of forests to annual cropland, to pasturelands, to perennial plants (such as oil palm or shrubs), and to urban lands or other human infrastructure.

Forest degradation – Forest degradation occurs due to various processes, including unsustainable logging, shifting cultivation, firewood collection or burning. It leads to a reduction of biomass, opening of forest canopies and changes in the structure of forests. It also modifies species composition, thus affecting ecosystem services, including future potential for carbon capture and storage.

A report authored by the Intergovernmental Panel on Climate Change (IPCC, 2003) presents five different potential definitions for degradation, along with their respective pros and cons. The report suggested the following characterization for degradation:

"A direct, human-induced, long-term loss (persisting for X years or more) or at least Y percent of forest carbon stocks [and forest values] since time T and not qualifying as deforestation".

In practice, it is likely to be difficult to agree upon the values for X, Y and T. Therefore, it is also possible that no specific definition is necessary, and that any "degradation of forest" will be reported simply as a net decrease of carbon stock in the category of "Forest land remaining forest land" at national or subnational level. The GFOI Methods and Guidance Document (GFOI, 2014) does not attempt to formally to define degradation, although it does set out steps for estimating degradation using IPCC methods.

7.2.2. Specifications for monitoring deforestation from remote sensing

Tropical forest mapping and monitoring is a key application domain for Earth Observation (EO) because of the need for recurrent and frequent data to produce annual information on forest cover in humid and seasonal domains, and regular information on forest disturbance processes. It benefits from long-term consistent archives of Landsat imagery for forest area change, for instance supporting various mature and operational applications such as the Global Forest Watch (GFW) platform[1] of the World Resources Institute and the PRODES project[2] of the Brazilian National Space Agency. Previous attempts to integrate moderate to fine-resolution EO imagery into operational forest degradation mapping and monitoring have largely failed because of inadequate technical parameters, high costs and uncertain long-term prospects. Currently, the EO community mostly uses Landsat sensors (30 m), with products having global coverage and an annual frequency. Today, the use of such imagery (approximately 30 m) leads mainly to the creation of tree cover percentages or forest/non-forest binary maps, which are released at yearly intervals (Hansen *et al*., 2013).

The remote sensing techniques to monitor changes in forest areas (e.g. deforestation) provide high-accuracy area estimates and may also allow for the spatial mapping of the main forest ecosystems (GOFC-GOLD, 2016). As a minimum requirement, it is recommended to use Landsat-type remote sensing data (30-m resolution) or finer-resolution imagery (e.g. Sentinel-2 data at 10 m resolution) to monitor forest cover changes, with the Minimum Mapping Unit (MMU) measuring between 1 to 5 ha. These data will allow to assess changes in forest areas (in particular, to derive the area deforested and forest regrowth for the period considered). A hybrid approach combining automated digital segmentation and classification techniques with visual interpretation and/or validation of the resulting classes/polygons should be preferred, as this constitutes a simple, robust and cost-effective method.

Different spatial units may be used to detect forest and forest change. Current national and regional remote sensing monitoring systems provide several examples of MMU: Brazil's PRODES system[3] for monitoring deforestation in the Brazilian Legal Amazon region (initially 6.25 ha, today 1 ha for digital processing); India's national forest monitoring system (1 ha); the EU-wide CORINE land cover/land use change monitoring system (5 ha); the Peruvian Ministry of Environment's deforestation monitoring programme (0.1 ha); and the Global Forest Watch deforestation monitoring system (0.1 ha).

Currently, there are two main sources of free global mid-resolution (30 m × 30 m to 10 m × 10 m) remote sensing imagery: NASA (Landsat satellites), for data acquired since the early 1980s; and the European Space Agency, or ESA (Sentinel satellites, through Copernicus programme) for data acquired since the mid-2010s, although some quality issues arise with respect to certain parts of the tropics (resulting from clouds, seasonality, etc.). All Landsat

1 http://www.globalforestwatch.org/.
2 http://www.obt.inpe.br/prodes/index.php.
3 The PRODES project of the Brazilian Space Agency (INPE) has been producing annual rates of gross deforestation since 1988. PRODES has quantified approximately 750 000 km2 of deforestation in the Brazilian Amazon through 2010, a total that accounts for approximately 17 percent of the original extent of the forest.

data from archives of the United States of America (in particular, the United States Geological Service, or USGS) are available for free. Brazilian/Chinese remote sensing imagery from the CBERS satellites is also freely available. CBERS-4 is part of the second phase of this Sino-Brazilian cooperation. The imagery is now used in important projects involving deforestation control and environmental monitoring in the Amazon Region. Other areas, such as water resources monitoring, urban growth, soil occupation and education, are also benefitting from CBERS-4 imagery. In fact, it is currently fundamental for large-scale national and strategic projects. Two important examples are the aforementioned PRODES[4] project and CANASAT[5] (monitoring of sugar-cane areas). Data fusion between CBERS-4 and Sentinel-2 are already being considered.

TABLE 1. CHARACTERISTICS OF LANDSAT-8 OLI AND SENTINEL-2 SENSORS.

Country	Satellite and sensor	Resolution and coverage	Cost for data (archive)	Feature
United States of America	Landsat-8 OLI	15 m – 30 m 180 × 180 km²	All data archived at USGS may be accessed free of charge	Data are systematically acquired since June 2013
EU	Sentinel-2	10 m- 20 m Swath 290 km	All data archived at ESA may be accessed free of charge	Data are systematically acquired since July 2016

Optical mid-resolution data (such as Landsat data) have been the primary tool for deforestation monitoring. Other, newer, types of sensors, such as radar (ERS1/2 SAR, JERS-1, ENVISAT-ASAR and ALOS PALSAR 1/2) and LiDAR, are potentially useful and appropriate (De Sy *et al*., 2012). Radar, in particular, alleviates the substantial limitations of optical data in persistently cloudy parts of the tropics. Data from LiDAR and radar have proven to be useful in project studies; however, to date, they are not widely used operationally for forest monitoring over large areas. In the future, the utility of radar may increase depending on data acquisition, access and scientific developments.

7.2.3. Specifications for monitoring forest degradation from remote sensing

Most forest degradation can be detected by means of remote sensing methods; however, optimal approaches and methodologies for monitoring forest degradation are likely to vary depending on the type and location of the degradation, as well as on the forest types concerned. Robust methods to monitor forest degradation (and forest regrowth) remain under development. As stated in the GOFC-GOLD REDD+ Sourcebook (2016), measuring forest degradation or forest regrowth and related changes in forest carbon stock is more challenging than measuring deforestation, because such forest changes are not easily detectable through remote sensing, but require more frequent and better imagery and processing.

4 http://www.obt.inpe.br/prodes/.
5 http://www.dsr.inpe.br/mapdsr/.

Monitoring forest degradation is limited by the technical capacity to sense and record the change in canopy cover: small changes are unlikely to be apparent unless they produce a systematic pattern in the satellite imagery. Many activities cause the degradation of carbon stocks in forests; however, not all of them can be monitored well with a high degree of certainty, and not all of them must be monitored using remote sensing data (Miettinen *et al*., 2014). To develop a monitoring system for degradation, it is first necessary to identify the causes of degradation and assess their likely impact on carbon stocks:

- The areas of forests undergoing selective logging – with the presence of gaps, roads, and log decks – are likely to be observable in remote sensing imagery, especially the network of roads and log decks. Gaps in canopy caused by harvesting of trees have been detected in imagery such as that captured by Landsat, using more sophisticated analytical techniques to process frequently collected imagery (Grecchi *et al*., 2017).
- The degradation of carbon stocks caused by forest fires may be more difficult to monitor with existing satellite imagery (Miettinen *et al*., 2016). Almost all fires in tropical forests have anthropogenic causes.
- Degradation resulting from over-exploitation for fuelwood or other local uses of wood is often followed by animal grazing, that prevents regeneration – a situation more common in drier forest areas. This situation is unlikely to be detectable from satellite image interpretation unless the rate of degradation was intense, thus causing larger changes in the canopy.

7.2.4. Availability of Landsat data

In 1972, NASA launched the first Landsat satellite with a mid-resolution sensor that was capable of collecting land information at a landscape scale. This satellite was the first in a series of (seven, to date) Earth-observing satellites that have enabled continuous coverage since 1972. Subsequent satellites were launched every two to three years. Still in operation, Landsat 7 covers the same ground track repeatedly every 16 days. To continue the series, the Landsat Data Continuity Mission (Landsat 8) was launched in 2013.

Almost complete global coverage captured by these Landsat satellites since the early 1990s may be downloaded free of charge from the USGS web portals[6]: in particular, such imagery consists in the Global Land Survey (GLS) data sets. These data serve a key role in establishing historical deforestation rates, although in some parts of the humid tropics (such as Central Africa), persistent cloudiness is a major limitation to using them. The full Landsat 8 OLI (since June 2013) and Landsat 7 ETM+ (since 1999) USGS archives, and all USGS archived Landsat 5 TM data (since 1984), Landsat 4 TM (1982-1985) and Landsat 1-5 MSS (1972-1994) may be ordered at no charge from the USGS.

To date, given its low cost and unrestricted license use, Landsat has been the workhorse source for mid-resolution (10–50 m) data analysis. Key limitations in the use of Landsat sensors consist in the mixed nature of the measured signal, and the difficulties in identifying forest cover disturbances. The latter aspect is especially important in areas where small-scale processes are significant. Alternative sources of data include ASTER, SPOT, IRS, CBERS, DMC, AVNIR-2 or Sentinel-2.

7.2.5. Availability of Sentinel-2 data

Sentinel-2A (S2A) was launched in 2015 and provides wide-area optical imagery with resolutions of 10 m (visible and near-infrared, or NIR), 20 m (red-edge, NIR and short-wave infrared, or SWIR) and 60 m (visual to short-wave infrared for atmospheric correction) from October 2015 onwards.

6 http://glovis.usgs.gov/.

The S2A has a wide swath width (290 km) and a 10-day revisit frequency. S2A coverage is global (capturing land masses). The launching of the S2's identical B unit is scheduled for 2017, and will increase the S2's revisit capacity to five days. The Copernicus programme already envisages C and D versions of these Sentinels to guarantee data availability until at least 2027.

The Sentinel 2 sensors – together with Landsat 8 – will provide core capacity upon which a viable set of globally consistent services in the forestry domain can be based, thus setting the stage for a number of innovative and challenging applications, and for the redesign of monitoring systems for a more accurate monitoring of forest degradation.

Sentinel-2 Product Level 2A is the standard level for which a processing tool will be made available through the Copernicus program (on the ESA Sentinel-2 Toolbox)[7]. Level-1C products contain applied radiometric and geometric corrections (including orthorectification and spatial registration in a fixed cartographic geometry). Level-2A products are at the bottom of atmosphere reflectance in cartographic geometry. Currently, Level-2A products must be processed by the user. A higher level of processing of satellite imagery data (Level 3) would be required for REDD+ countries. Level 3 should consist in adequate image mosaics (that minimize cloud coverage) from the Sentinel-2 satellite time series, composed every 30 days or every three months over the tropical belt. The specifications for a standard Sentinel-2 Level 3 core product, to be made systematically and freely available through a free and open distribution platform, were prepared by the Copernicus programme in 2017.

The technical quality of the Sentinel sensors significantly enhances the separation of land cover classes in forest land use, both for forest land (that is, forest types) and the complex domain of mosaics of agriculture and forest (including shifting cultivation). The 10 to 20 m spatial resolution of S2A (and S2B), combined with a ten-day (or five days with both S2A and S2B) revisit frequency will resolve the forest cover status and small-scale disturbances delineation at plot and log level detail. Slower forest conversion changes – in particular, the progressive removal of fuel wood or agricultural land abandonment leading to forest regrowth – will benefit from the high level of spatial details and the possibility to select the most relevant seasonal acquisitions. The complementarity of visible, NIR and SWIR channels (from S2) is unique in this respect too. Furthermore, the spectral compatibility of S2 with Landsat-8 and much improved atmospheric correction will greatly expand intersensor consistency and the potential for data fusion.

The finer spatial resolution (10 m) and the higher temporal frequency (a revisit time of five to ten days) of Sentinel-2 acquisition will enable more accurate and regular detection and quantification of forest degradation in tropical countries than is possible from current medium-resolution satellite imagery. Consequently, in the near future, satellite imagery from the Sentinel-2 satellite sensor will provide potential for incremental change in the assessment of forest conditions.

The introduction of Sentinel-2 will potentially lead to a diffusion of forest monitoring capacities to national and regional government levels in the next five to ten years, for instance, as an extension or a component of National Forest Inventory (NFI) systems. This will require significant capacity building efforts, which should be, insofar as possible, directed towards anchoring a robust methodological framework. To the greatest extent possible, this should lead to standardized forest area estimates and map products at national level with an agreed level of accuracy and quality that can be integrated into regional and global applications.

In summary, Landsat-type data are most suitable for assessing historical rates and patterns of deforestation. The availability of free and open Landsat-8 and Sentinel-2 data has increased for recent years; therefore, more detailed assessments of coverage periods lesser than five years may be possible in several parts of the world.

7 http://www.esa.int/Our_Activities/Observing_the_Earth/Copernicus/Sentinel-2/Data_products.

7.3. THE FAO GLOBAL FOREST RESOURCES ASSESSMENT'S REMOTE SENSING SURVEY

7.3.1. Background on statistical sampling designed to estimate deforestation from optical sensors having moderate spatial resolution

It would be ideal to conduct an analysis that covers the full spatial extent of the forested areas with imagery having moderate spatial resolution (Landsat-type), termed "wall-to-wall" coverage; however, this may not be practical over large and heterogeneous areas. In addition, it would place commensurate constraints on the resources available for analysis. For digital analysis with moderate-resolution satellite images at pan-tropical or continental levels, several approaches have been successfully applied by sampling within the total forest area, to reduce the costs and time required to conduct the analysis.

A sampling procedure that adequately represents deforestation events can capture deforestation trends (Achard *et al*., 2002; Richards *et al*., 2000). Since deforestation events are not randomly distributed in space, particular attention is required to ensure that the statistical design is adequately sampled within areas of potential deforestation (figure 1), for example through a high-density systematic sampling when resources are available (Mayaux *et al*., 2005).

FIGURE 1. LOCATION OF SAMPLE UNITS OF THE TREES-II SURVEY

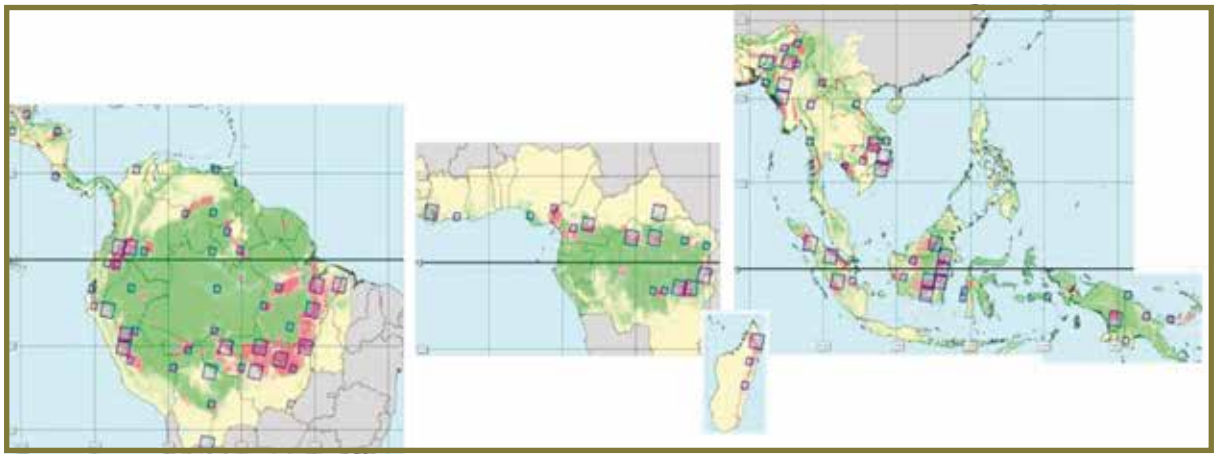

Achard *et al.*, 2002; Richards *et al.*, 2000

For its global Forest Resources Assessment 2010 programme (FRA 2010), FAO continued to develop its monitoring of forest cover changes at global to continental scales to complement national reporting. Technological improvements and better access to remote sensing data made it possible to expand the scope of the survey, compared to FRA 2000. The findings of the FRA 2000 tropical Remote Sensing Survey (RSS) (figure 2) were included as a chapter in the FRA 2000 Main Report (FAO, 2001) and reported upon in Drigo *et al*. (2009).

FIGURE 2. LOCATION OF SAMPLE UNITS OF THE FOREST RESOURCES ASSESSMENT 2000 PROGRAMME

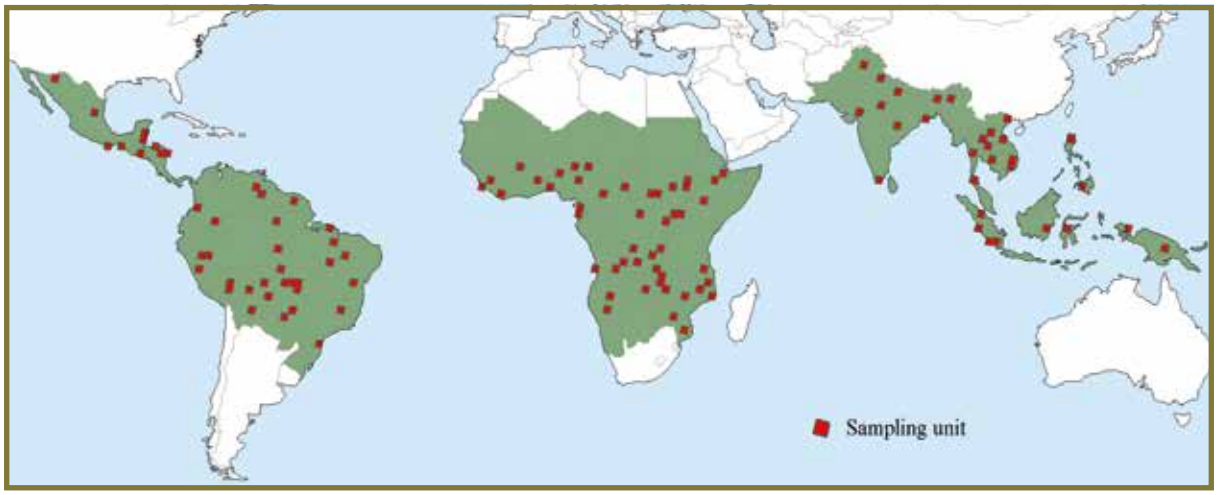

FAO, 2001; Drigo *et al.*, 2009

7.3.2. General sample approach selected for the Global Remote Sensing Survey

The remote sensing surveys of FRA 2010 and FRA 2015 have been extended to all lands (not only the pan-tropical zone). These surveys aimed to estimate forest change based on a sample of moderate-resolution satellite imagery, and were designed to provide consistent and comparable estimates of tree cover and forest land-use changes over two decades at global and regional scales, to complement the increasing number of national statistics in FRA main reports that are based on national remote sensing surveys.

In a coordinated effort, FAO and the Joint Research Centre (JRC) of the European Commission produced estimates of forest land use change from 1990 to 2005 for RSS 2010 (FAO and JRC, 2012). This global survey was then extended to the year 2010 (to cover the period from 1990 to 2010) for the FRA-2015 (Achard *et al*., 2014; Keenan *et al*., 2015).

The FRA 2010 RSS is based on a much higher number of smaller sample units than the previous FRA exercises, with a systematic grid – sample units are located at each intersection of the 1° × 1° lines of latitude and longitude that falls over land. This global systematic sampling scheme was developed jointly by FAO and the JRC to estimate the rates of deforestation at global or continental levels at intervals of five to ten years (Mayaux *et al*., 2005).

Each sample unit has a core size of 10 km × 10 km with an external 5-km buffer for forest cover contextual information (that is, the full size of sample units is 20 km × 20 km for land cover information). These dimensions were chosen to allow for spatially explicit monitoring at a scale relevant to land management.

This sampling scheme leads to approximately 13 500 sample units for the terrestrial part of the globe, or approximately 9 000 sample units when excluding desert areas, and represents approximately 1 percent of the land surface (0.8 percent along the Equator) with the geographical grid (figure 3).

FIGURE 3. LOCATION OF SAMPLE UNITS OF THE REMOTE SENSING SURVEY (RSS) OF THE FRA-2010 OVER THE TROPICS.

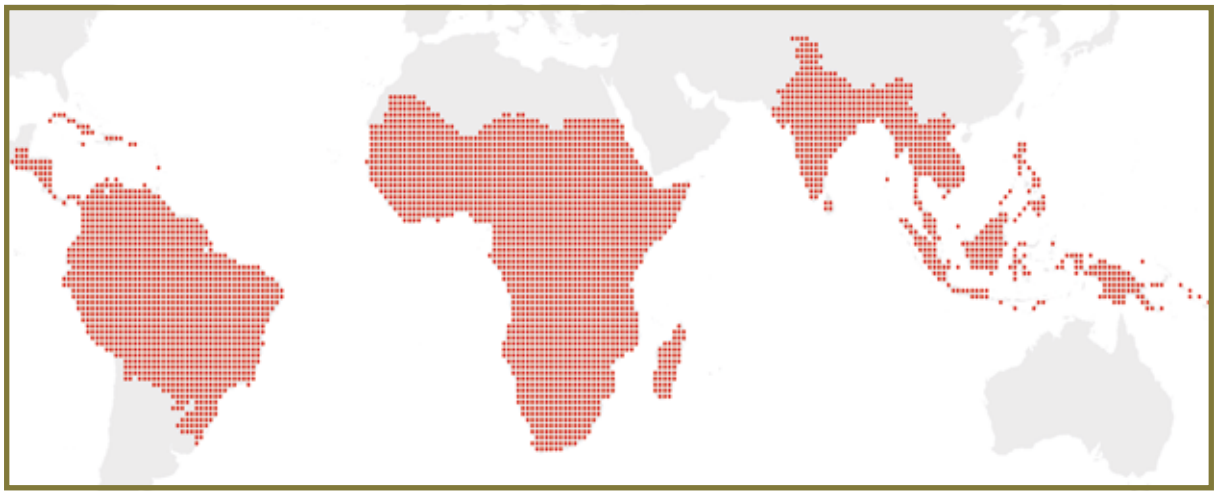

7.3.3. Selection and preprocessing of satellite imagery

The FAO FRA RSS 2010 is a global study with consistent methods and time series that can be extended to include more recent periods. Time series of moderate-resolution remote sensing data are attached to each sampling location through a quality-controlled, standardized and decentralized process. The following paragraphs briefly describe the satellite data set and preprocessing steps used for the FAO FRA RSS 2010 over the tropical regions.

For each sample unit, orthorectified Landsat (E)TM Landsat images were acquired at no cost from the GLS archives, which are created and made available by the USGS (Gutman *et al*., 2013). For each sample unit, four images were selected with the lowest possible cloud cover and as close as possible to the target dates of 30 June for the years 1990, 2000, 2005 and 2010. Where GLS data was unavailable, of bad quality (such as Landsat 7 SLC-off data) or cloudy for the area of the sample units (Potapov *et al*., 2010), alternative satellite scenes were acquired from the Landsat archives of the USGS or of other space agencies, such as Brazil's INPE (Beuchle *et al*., 2011). The range of image acquisition dates was 1986–1993, 1999–2003, 2004–2007, and 2009–2011 for the years 1990, 2000, 2005 and 2010 respectively.

The selected images underwent an extensive preprocessing, including an image geolocation check, conversion to top-of-atmosphere reflectance, cloud-masking, de-hazing and image normalization on the basis of pseudo-invariant features (Bodart *et al*., 2011). For multitemporal image analysis, a good geometric match of the images is fundamental. In this context, the geolocation of some images required enhancement. For this purpose, the Landsat ETM image (from the year 2000) was determined to be the "master image". Consequently, the "slave image", consisting mostly in Landsat 5 imagery, was shifted until a correct overlay with the master image was achieved.

7.3.4. Processing and analysis of satellite imagery

This section describes the analysis carried out over the tropical regions.

After preprocessing, the satellite imagery was used in an automated multidate image segmentation to subdivide the sample unit (10 000 ha) into delineated areas (polygons) with similar spectral and structural attributes. The target MMU was 5 ha. On the segmented imagery, a supervised automated land cover classification was carried out, which was later converted to a land use classification with the help of expert human interpretation.

For each sample unit, the preprocessed images from the four "epochs" (that is, the years 1990, 2000, 2005 and 2010) were subjected to a multistep segmentation using eCognition software (Trimble©), followed by an object-based classification process based on membership functions defined by a collection of spectral signatures taken from across the tropical belt (Raši *et al.*, 2011 and 2013). An MMU of 5 ha (or 50 pixels at 30 m × 30 m resolution) is considered for the interpretation of the satellite imagery to identify the forest cover changes. A finer "detection unit level" at approximately 1 ha was used in a first automated segmentation and labelling step before aggregation to 5-ha objects for the interpretation phase.

Objects were classified into five land cover classes: Tree Cover, Tree Cover Mosaics, Other Wooded Land, Other Land Cover and Water (see table 2 for a description of each class). The Tree Cover class was defined in compatibility with the FAO definition of forest (FAO, 2010).

TABLE 2. LAND COVER CLASSES USED BY THE JRC.

Class name	Class description
Tree cover (TC)	Objects covered by 70–100 percent of trees, where trees are defined as plants higher than 5 m and with a wooden stem, and tree canopy density is greater than 30 percent
Tree cover mosaic (TCM)	Objects covered by 30–70 percent of trees
Other wooded land (OWL)	Objects covered with more than 50 percent of plants lower than 5 m with one or more wooden stem(s)
Other land cover (OLC)	Land not covered by the TC, TCM or OWL classes, comprising natural grassland, agricultural land, built-up areas, bare soil and rock
Water (W)	Rivers and lakes

The resulting classified objects, with an MMU of 5 ha, underwent an intensive process of correction of the land cover information assigned for each target year (Eva *et al.*, 2012).

The JRC and FAO scientists collaborated with more than 100 remote sensing and forestry experts from tropical countries, including largely forested countries such as Brazil, India, Indonesia and the Democratic Republic of Congo.

It must be noted that for the FRA 2010 RSS reporting (FAO and JRC, 2012), FAO employs a land use classification (FAO, 2010b), including a "Forest" land use class[8]; this is better suited to assessing drivers than a land cover classification, such as that used by the JRC (de Sy *et al.*, 2015). A young forest plantation is considered as "Forest" in the FAO survey (trees able to reach more than 5 m), but is classified as "Other land cover" according to the JRC legend if the trees are not visible or lower than 5 m.

8 The "Forest" class of the FAO FRA 2010 report is defined as: "Land spanning more than 0.5 hectares with trees higher than 5 meters and a canopy cover of more than 10 percent, or trees able to reach these thresholds in situ. It does not include land that is predominantly under agricultural or urban land use."

7.3.5. Statistical analysis

The land cover and land cover change information available for all sample units is used to produce statistical estimates for the entire area of interest. Considering that very few satellite images were acquired at the exact same date of their respective epochs, the land cover (change) information of each sample unit is first linearly "normalized" (as a best approximation) to the target dates of 30 June for the years 1990, 2000, 2005 and 2010 to produce land cover statistics. For this purpose, we assume that the land cover changes detected occurred linearly over time.

Areas lacking data due to clouds, poor satellite coverage or low-quality imagery in any of the reference years were considered as an unbiased loss of data, and assumed to have the same proportions of land cover as non-cloudy areas within the same site. This is achieved by converting the 1990–2000 and 2000–2010 land-cover change matrices to area proportions relative to the total cloud-free land area of the sample units. For the missing sample units (4, 39 and 3 for 1990–2000 and 3, 39 and 3 for 2000–2010, from totals of 1 230, 2 045, and 741 sample units, for South America, Africa and Southeast Asia, respectively) a local average was used from surrounding sample sites as surrogate results. The following weights ($\delta_{jj'}$) were applied to obtain the local average of missing sites:

$$\delta_{jj'} = 1/d(j,j') = 1/\left(dif(lat)\right)^4 + \left(dif(long)\right)^4 \quad [1]$$

where d(j,j') is the distance between two sites.

For the statistical estimation phase, the sample units are weighted in relation to their statistical probability of selection. Indeed, although the sampling frame is systematic, it does not give equal probability to all sample units because the distance between sample units along a parallel is not the same as the distance along a meridian. All sample units are given a weight, which is equal to the cosine of the latitude to account for this unequal probability. The impact of these weights is moderate in tropical areas. The selected sample units that contain a proportion of sea compensate for those non-selected sample units that contain a proportion of land (when the centre of the sample unit is located in the sea), because they were considered as full sites.

The proportions of land cover changes were then extrapolated to the study area using the Horvitz-Thompson Direct Expansion Estimator (Särndal *et al*., 1992). The estimator for each land cover class transition is the mean proportion of that change per sample unit, given by Equation 2:

$$\bar{y}_c = \frac{1}{m}\sum_{i=1}^{n} w_i . y_{ic} \quad [2]$$

where y_{ic} is the proportion of land cover change for a particular class transition in the *i*th sample unit. The weight of the sample unit is w_i and m is the sum of the sample weights.

In case of systematic sampling, the usual "random case" estimator is positively biased (Stehman *et al*., 2011). Alternative estimators based on a local estimation of the variance enable a partial solution of the problem, that is, to reduce the bias. Here, an estimator of the standard error based on local variance estimation is used:

$$s^2 = (1-f)\frac{\sum_{j \neq j'} w_{jj'}\delta_{jj'}\left(y_j - y_{j'}\right)^2}{2\sum_{j \neq j'} w_{jj'}\delta_{jj'}} \quad [3]$$

where f is the sampling rate, the weight $w_{jj'}$ is an average of the weights w_j and $w_{j'}$ and $\delta_{jj'}$ is a decreasing function [1] of the distance between j and j' (note that if it is determined to set $\delta_{jj'} = 0$, the usual variance estimator is obtained). The standard error (se) is then calculated as:

$$se = \frac{s}{\sqrt{n}} \quad [4]$$

where n is the total number of available sample sites (that is, not accounting for the missing sites even if these are replaced by a local average).

Land cover changes were estimated by assessing the matrices of change (see table 3), for the decades 1990–2000 and 2000–2010. An object labelled as Tree Cover Mosaic (TCM) was considered as 50 percent forest cover, defined by the average of the upper and lower percent limit. Consequently, forest cover loss was calculated as being 100 percent of the tree cover converted to Other Wooded Land (OWL), Other Land Cover (OLC) or Water (W) plus 50 percent of the tree cover converted to TCM and 50 percent of the TCM converted to OL, OWL or W.

7.3.6. Accuracy/consistency assessment of estimates of forest cover changes

The observations (source data sets) used to produce the results given in this chapter are derived from satellite interpretations. These surrogates to ground observations may be subject to error or uncertainty (bias) (Foody, 2010); however, these issues were not addressed in this assessment. The use of such surrogate data for assessing area change is inevitable in many areas of the tropics where no ground observations exist and where large areas of inaccessible forests can only be monitored at affordable costs by exploiting satellite data. However, an independent assessment was performed over 1 185, 1 552 and 830 points (for a total of 3 567 points) distributed systematically within a random subsample of 240, 338 and 166 sample units in South America, Africa and Southeast Asia, respectively (a central point plus four points in the corners taken in each sample unit). In addition, from a 9 x 9 systematic grid (81 points taken at a distance of 1 km in each sample unit), all points identified as change in land cover during the decade from 1990 to 2000 were selected, resulting in 1 663, 1 194 and 1 425 points (for a total of 4 282) respectively for the three subregions. The corresponding polygons were carefully visually reinterpreted by independent experts using any available ancillary information (such as imagery from Google Earth, with due attention to the date of image capture). This enables an assessment of the "consistency" of the results of the interpretation.

To complement this consistency assessment, the results were also compared to the INPE interpretations for the decade from 1990 to 2000 (INPE, 2013) for a random selection of 34 sample units among the 411 sample units falling in the Brazilian Legal Amazon (Eva *et al*., 2012).

7.3.7. Results for the tropics

Results of the FRA 2010 RSS have been published at global level for 1990–2000 and 2000–2005 (FAO and JRC 2012) and at tropical or regional scales for 1990–2000 and 2000–2010 (Achard *et al*., 2014; Beuchle *et al*., 2015; Bodart *et al*,. 2013; Eva *et al*., 2012; Mayaux *et al*., 2013; Stibig *et al*., 2014). This section briefly reports the main results for the tropical region, to illustrate the outcomes of this RSS.

In 1990, there were 1 635 million ha of tropical forest and 964 million ha of other wooded land. By 2010, the forest area had fallen to 1 514 million ha, with an overall net loss over the two decades of 56.9, 30.9 and 32.9 million ha in South and Central America and the Caribbean, sub-Saharan Africa and South and Southeast Asia, respectively. Other

wooded land increased in that period to 975 million ha, mainly due to the increase of 18.6 million ha in Southeast Asia. In 2010, humid tropical forests accounted for approximately 64 per cent of the tropical forest cover, that is, 972 million ha from a total of 1 514 million ha, with the following regional distribution: 599 million ha in South America, 210 million ha in Africa and 163 million ha in Southeast Asia.

At global level, the gross loss of tropical forests was of 8.0 million ha y-1 during the 1990s (0.497 per cent annually), with a slight decrease of 7.6 million ha y-1 during the 2000s (0.494 per cent annually), mainly due to reduced deforestation rates in the humid forests of Africa and Southeast Asia (from 0.70 to 0.36 million ha y-1 and from 1.70 to 1.22 million ha y-1, respectively) (Achard *et al*., 2014). Large non-forest areas were also reoccupied by forests, reaching 1.9 million ha y-1 in the 1990s and 1.6 million ha y-1 in the 2000s.

7.3.8. Precision of the estimates for the tropics

The estimates of forest area changes (gross loss, gross gain and net loss) have small statistical standard errors due to the large sample size: from 4 percent to 10 percent at global level, and from 11 percent to 19 percent on average at regional level. A dedicated accuracy assessment was carried out for the land cover maps of the tropical sample units for the 1990–2000 period. The overall agreements between the RSS results and the reinterpretations considered as reference information are of 92.9 percent for the forest labels and 85.5 percent for the forest change labels. The potential bias in these results (due to errors of interpretations) were assessed by comparing estimates derived from our sample to estimates derived from the reference data set. The relative difference is of -8.9 percent for the global forest area estimate – that is, a lower forest area estimate is derived from the RSS study compared to the reference data set – and of 11.2 percent for the global gross deforestation estimate; in other words, larger deforestation estimates were obtained from the RSS study. Comparison to the INPE interpretations for the 1990–2000 period for a random selection of 34 sample sites displays a good correspondence between the INPE interpretations and the RSS results, both for the forest area of the year 1990 and for deforestation in the 1990–2000 period, with slopes close to 1 (1.017 and 1.008 respectively) and an R2 close to 1 (0.986 and 0.978 respectively) (Eva *et al*., 2012).

7.3.9. Intensification of the sampling scheme for forest cover change estimation at national scale

The global systematic sampling scheme described above can be intensified to produce results at the national level. Deforestation estimates derived from two levels of sampling intensity have been compared with estimates derived from the official inventories for the Brazilian Amazon and for French Guyana (Eva *et al*., 2010).

By extracting nine sample data sets from the official wall-to-wall deforestation map derived from satellite interpretations produced for the Brazilian Amazon for the year-long period from 2002 to 2003 (INPE, 2016), the global systematic sampling scheme estimate gives 2.8 million ha of deforestation with a standard error of 0.1 million ha. This compares with the full population estimate from the wall-to-wall interpretations of 2.7 million ha deforested. The relative difference between the mean estimate from the sampling approach and the full population estimate is of 3.1 percent and the standard error represents 4 percent of the full population estimate. The testing of the systematic sampling design within the Brazilian Amazon resulted in a low standard error of less than 5 percent of forest cover change rate.

To intensify the sampling intensity of this global survey over French Guyana, Landsat-5 TM data were used for the historical reference period (1990) and a coverage of SPOT high-resolution visible sensor imagery at a resolution of 20 m × 20 m was used for 2006. The estimates of deforestation between 1990 and 2006 from the intensified global sampling scheme over French Guyana are compared with those produced by the national authority to report

on deforestation rates for its overseas department under the rules established by the Kyoto Protocol rules (Stach *et al*., 2009). The latter estimates derive from a sampling scheme of almost 17 000 plots derived from the traditional forest inventory methods carried out by the country's *Inventaire Forestier National* (IFN) and analysed from same spatial imagery acquired between 1990 and 2006. The intensified global sampling scheme leads to an estimate with a relative difference from the IFN of 5.4 percent. These results, as well as other studies (Steininger *et al*., 2009), demonstrate that the intensification of the global sampling scheme can provide forest area change estimates that are close to those achieved by official forest inventories with precisions of less than 10 percent, although only the estimated errors from sampling are considered and not errors from the use of surrogate data.

7.3.10. The future of the Global Forest Resources Assessment: towards FRA 2020

The FAO FRA is a continuously improving process: each assessment is an upgrade of the former one as information needs change, new and better data become available and new methods and technologies can be applied. Due to recent developments in the international forestry and policy arena, such as the Paris Agreement and the Sustainable Development Goals (SDGs), FRA must adapt to respond to evolving information needs, in terms of both scope and reporting periodicity.

The FRA has received technical guidance and support from international specialists through expert consultations organized at regular intervals by FAO and the United Nations Economic Commission for Europe (UNECE) over the last 30 years. The first consultation on the FRA was held in 1987; subsequent consultations took place in 1993, 1996, 2002 and 2006 (Kotka I-V) in Kotka, Finland and 2012 in Ispra, Italy. The latest expert consultation was held in June 2017 in Joensuu, Finland.

The objectives of the expert consultation include the provision of recommendations on the scope of the next global assessment, including the country reporting process and the remote sensing component, and discussion of the frequency of reporting on core variables and annual reporting on SDG indicators.

7.4. OTHER EXAMPLES OF RSS USED FOR FORESTRY STATISTICS

7.4.1 Deforestation statistics from the Global Tree Cover product, University of Maryland

More recently, a new approach that employs recommended IPCC good practices and a combination of remote sensing data (De Sy *et al*., 2012) to quantify tropical forest above-ground carbon (AGC) losses from 2000 to 2012 was presented by the University of Maryland (Tyukavina *et al*., 2015). This study is an important extension of earlier studies applied to the Democratic Republic of Congo and Peru (Tyukavina *et al*., 2013; Pelletier and Goetz, 2015).

More specifically, Tyukavina *et al*. (2015) use a sample-based approach combined with a wall-to-wall tree cover loss data set (Hansen *et al*., 2013) to estimate tropical forest area losses.

The Global Tree Cover data set from the University of Maryland (Hansen *et al*., 2013) provides wall-to-wall data starting from the year 2000. Hansen *et al*. (2013) divide world land area into four "tree cover" classes – 0–25 percent, 26–50 percent, 51–75 percent and 76–100 percent – when undertaking wall-to-wall mapping using Landsat images. The authors found that in the tropics, the 76–100 percent tree cover class, which broadly corresponds with tropical moist forest, covered 1 324 million ha in the year 2000, while the area having above 25 percent tree cover, of 2 094 million ha, was of the same order of magnitude as the FRA 2015 figure for all tropical forest, a figure that was based on a threshold tree cover of 10 percent (Keenan *et al*., 2015).

Tyukavina *et al*. (2015) produced an unbiased estimate of forest area loss using a stratified random sample of 3 000 pixels (each approximately 0.1 ha in size) distributed in tropical forested regions. Furthermore, Tyukavina *et al*. distinguished "'natural forests" (primary and mature secondary forests, and natural woodlands) from "managed forests" (plantations, agroforestry systems and areas of subsistence agriculture with tree cover rotation). Tyukavina *et al*. confirmed that a sample-based approach can provide more accurate and significantly higher estimates of forest cover losses than a wall-to-wall approach: the higher estimate is explained by small-scale forest dynamics that were not depicted in the wall-to-wall tree cover loss map. Ensuring that these small-scale dynamics are captured correctly can be very important for individual countries' efforts to set accurate reference levels.

The use of different definitions and methods can lead to very different estimates of forest area losses: for example, Tyukavina *et al*. define forests as areas where the tree canopy cover is greater than 25 percent, while FAO reporting is based on a tree cover threshold of 10 percent and a definition of land use. Moreover, Tyukavina *et al*. account only for gross forest losses, while FAO reports net forest loss (including afforestation and forest regrowth) (Keenan *et al*., 2015).

Tyukavina *et al*. (2015) illustrate the current capabilities of satellite data with a sample-based approach for estimating forest cover losses in the tropics and related carbon losses.

7.4.2. Example at national level: the Landscape Units of the Brazilian National Forest Inventory

Brazil occupies approximately 8.5 million km2, of which 4.9 million are covered by forests (FAO, 2015b). These forests are of enormous importance for the country, in environmental and socio-economic terms, and because of the contribution they make globally by delivering forest services, such as biodiversity conservation and carbon retention. The National Forest Inventory (NFI) of Brazil is compiled by the Brazilian Forest Service (BFS)[9] of the Ministry of the Environment, in partnership with other institutions such as Embrapa, state environmental agencies, universities, research institutions and specialized herbaria. The NFI is one of the most important components of the National Forest Information System (Freitas *et al*., 2010), and therefore a key step in producing reliable and regular information on forest resources (Brazilian Forest Service, 2016).

The main purpose of the Brazilian NFI is to generate information on forest resources, both natural and plantation, based on a five-year measurement cycle, to support the formulation of public policies aiming at the use and conservation of forest resources. For some Brazilian states, information on the second cycle is being collected; however, for the majority of the 27 states, data collection is still in the first cycle.

The Brazilian NFI is based on a systematic sampling design, with the distribution of clusters (Field Sample Units, or FSUs) on a national network of sample points that are 648 seconds equidistant from each other, corresponding to approximately 20 km × 20 km between sample points at the Equator line. The cluster is composed by four subunits of 20 m × 50 m each. Field data collection comprises biophysical variables for forest and environment condition assessment, as well as socio-economic variables (interviews) to characterize how people living in nearby forests use and perceive the forest resources (Freitas *et al*., 2010). In addition, for some states, the NFI preliminary results present information on forest stocks, composition, and health and vitality. The assessment of patterns of change in time is possible by comparing estimates from successive inventory cycles.

In addition to field data collected every 20 km × 20 km over the entire territory, the NFI also includes a Geospatial Component, which provides information at landscape level through Landscape Sample Units (LSUs), Land Use/Land Cover (LULC) mapping and spatial analysis (Luz *et al*., 2015b). The Geospatial Component LSU methodology was developed as a joint effort between the FAO/BFS team[10] and the Embrapa Forestry team[11]. As stated by Freitas *et al*. (2006), the sampling design to collect data at landscape level must be based on the same systematic grid used for the fieldwork, although using a systematic subsample with an interval of 40 km × 40 km (figure 4). The size of each LSU is of 10 km × 10 km (100 km2), the geometric centre of which corresponds to the location of a field cluster.

9 The Brazilian National Forest Inventory is led by Joberto Veloso de Freitas and Claudia Melo Rosa.
10 Naissa Batista da Luz and Jessica Maran.
11 Maria Augusta Doetzer Rosot, Marilice Cordeiro Garrastazú and Yeda Maria Malheiros de Oliveira.

FIGURE 4. LOCATION OF THE LANDSCAPE SAMPLE UNITS OF THE BRAZIL NFI FOR THE STATE OF PARANA.

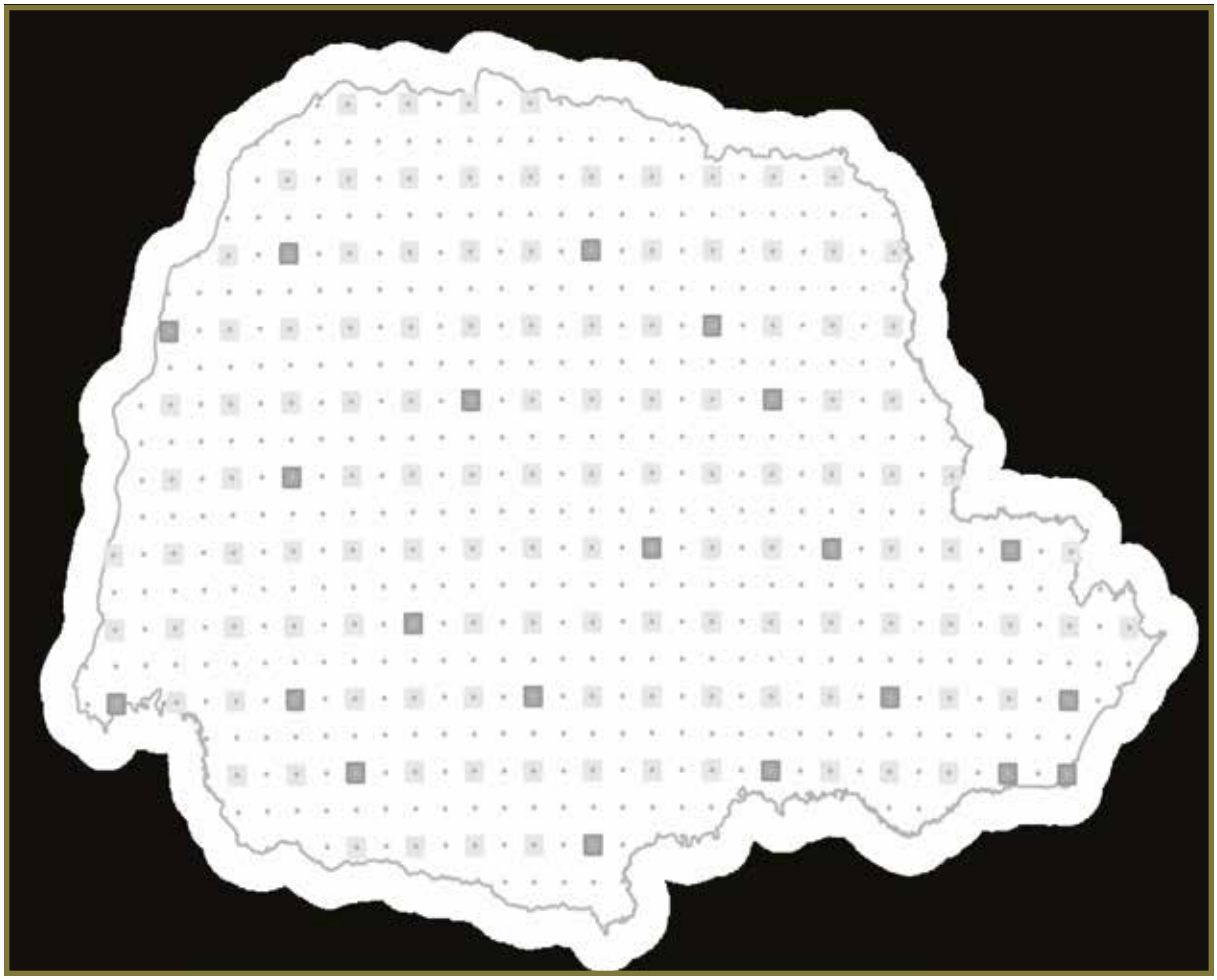

Recently, the Brazilian Government has issued a recent regulation on the use of and changes to natural resources, under the umbrella of the new Brazilian Forest Law. The Rural Environmental Cadastre (CAR) is one element of this legislation. To implement this new regulation, the Ministry of the Environment acquired RapidEye (RE) imagery covering the entire country, annually, since 2011. As this imagery is available to other governmental agencies, in 2013, the Embrapa Forestry team, BFS and FAO initiated the NFI Landscape Study as a pilot project, using the available RapidEye and Landsat 8 (L-8) imagery. RapidEye orthorectified imagery was used as the basis for an object-based image analysis approach (implemented in Definiens software). Polygons generated from RapidEye segmentation were then classified with the aid of several ancillary layers, such as enhanced vegetation indices, temporal series statistical layers (one year mean, minimum, maximum, and standard deviation) and information derived from the Global Forest Change (GFC; such as tree cover percentage for 2013) and processed using the Google Earth Engine Code Editor. Pixel-based RapidEye and L-8 unsupervised classification, performed using the IMPACT Toolbox software (developed by the JRC), were also included as ancillary information for RapidEye polygon classification (Luz *et al*., 2015b).

Within the Brazilian NFI, landscape can be considered as a heterogeneous group of ecosystems embodied in different LULC types interacting with one another (Luz *et al*., 2015a). The mosaic of LULC classes – in which natural and anthropogenic components contribute to the quality of existing forest resources – were defined as: (a) tree/shrub cover; (b) planted forest; (c) natural grasslands; (d) agriculture and pasture; (e) urban areas; (f) bare soil; and (g) water bodies.

After the first phase concerning the LULC mapping involving the aforementioned classes, a second step is performed, the landscape structural analysis of each LSU. The methodology, which is tailored specifically to the NFI's LSUs envisages innovative aspects relating to landscape spatial patterns, LULC mosaics and habitat fragmentation, connectivity and interface. The design incorporates traditional indicators, such as landscape composition, but also addresses fragmentation in a different manner, adopting a normalized and comparable index based on the habitat's overall Euclidean distance. Another approach involves the quality assessment of riparian zones, based on the structural connectivity of these environments such as vegetation corridors, the degree of anthropogenic pressure and scenario simulations for riparian protection zones, as well as their ranking (Clerici and Vogt, 2012) with reference to conservation priorities. This is especially important in light of recent changes occurring in the Brazilian Forest Law concerning the extent of forest vegetation to be restored along rivers and water bodies. Trees Outside Forest (TOFs) are a specific theme within LSU analysis, and different approaches were tested to discriminate between and classify them using RapidEye imagery. The relevant definitions and premises were established by FAO, in partnership with the *Institut de Recherche pour le Développement* (IRD) (De Foresta *et al*., 2013).

A group of landscape indicators (and respective indices) is currently being calculated. These are the following:

- Landscape composition (proportion of tree/shrub cover that includes natural forest, other wooded lands and TOFs) and proportion of other natural/seminatural areas, which include natural grasslands and planted forest;
- Landscape taxonomy defined by the degree (percentage) of the presence of each LULC class;
- Habitat morphological spatial pattern analysis (MSPA) implemented by Soile and Vogt (2008) in the Guidos Toolbox software (Vogt *et al*., 2007; Saura *et al*., 2011), which encompasses possible categories or classes, as core, edge, perforation, bridge, loop, branch and islets;
- Forest landscape mosaic, which envisages various classes and indices (and classifies a given location according to the surface of intensive agriculture and urbanized areas surrounding it) and is implemented in the Guidos Toolbox.
- Edge interface model, which generates various indices and considers the importance of fragmentation related to the change of LULC in the forest edges, and is implemented in the Guidos Toolbox;
- Landscape connectivity encompasses landscape connections priorities, based on the MSPA and Conefor[12] software (Saura and Torné, 2009); a ranking of the structural corridors under pressure in the landscape is also presented;
- Landscape fragmentation, an indicator that introduced innovative concepts to quantify forest fragmentation (in the Guidos Toolbox); it enables comparison of the degree of fragmentation in different locations, the measurement of changes in fragmentation and its monitoring over time;
- Riparian zones analysis, based on the structural connectivity of those environments as vegetation corridors, on the degree of anthropogenic pressure acting upon them and on scenario simulation for riparian protection zones based on the concepts elucidated by Clerici *et al*. (2011) and Ivits *et al*., (2009).

The LSUs' structural quality is assessed against these indicators, represented by groups of indices. The linear weighted combination of selected indices generate a single score by LSU, which allows for analyses and comparisons between them, aiming to restore and monitor certain aspects of the landscape.

The efforts made by the Brazilian NFI constitute an essential contribution to the Brazilian Government's commitment to sustainability. In 2010, Brazil voluntarily committted to reduce emissions by 80 percent in the Amazon and 40 percent in the Cerrado (Savannah region) by 2020. The country plans to integrate existing instruments and to promote coordination and synergies between them to maximize the REDD+ results. The NFI provides tools that can contribute to those decisions. The NFI programme can also benefit the implementation and monitoring of other national policies on planted forests and on the integration of agriculture, livestock and forestry (iLPF-agroforestry), among others.

12 http://www.conefor.org.

Brazil's intended Nationally Determined Contribution – or iNDC – is considered a highly ambitious project. Regarding the spheres of forestry and LULC, it was proposed to strengthen compliance with the new Brazilian Forest Law at all levels; strengthen policies and measures to achieve, in the Brazilian Amazon, zero illegal deforestation by 2030 and compensation of greenhouse gas emissions from legal removal of vegetation by 2030; restore and plant 12 million ha of forest by 2030 for multiple uses; expand the range of sustainable management systems of native forests through georeferencing and traceability systems applicable to the management of native forests, to discourage illegal and unsustainable practices. Additionally, the commitment relating to the agricultural sector was to strengthen the Low-Carbon Agriculture Plan (ABC Plan) as the main strategy to ensure sustainable development in agriculture, including the further restoration of 15 million ha of degraded pastures by 2030 and the increment by 5 million ha of iLPF-agroforestry projects, by the same year. Therefore, the Brazilian NFI will play an important role in the fulfillment of country goals and targets by providing valuable data sets on forest resources, LULC and landscape quality.

The landscape analysis complements the other two components of the IFN-BR, which consist in a field data collection exercise and a socio-economic survey. The adopted strategy has been to develop the methodology of all Brazilian NFI components, aiming at their integration and subsequent joint analysis. Thus, aspects of the physical and biological environment obtained in the field survey (ecosystem approach), integrated with spatialized information on LULC and the socio-economic environment may conform that which in contemporary terms is known as the landscape approach.

7.4.3. The FAO Global Forest Survey project

Objectives of the Global Forest Survey project

The main objective of the Global Forest Survey (GFS) project is to provide global and regional estimates of forest inventory data for specific forest ecosystems. Forest inventory data is to be collected through a global network of field plots. The project is intended to be implemented on a global scale.

The specific objectives of the GFS project are to:

- develop a global network of permanent field sample plots, which will utilize existing field plots where possible, but will also include new field sample plots as required;
- Produce detailed, georeferenced global estimates of forest carbon, forest health, and other forest characteristics based on the field sample plots and remote sensing data;
- Develop an information portal and data sharing policy to make all data and results freely available; and
- Demonstrate the value of a single, permanent, freely available, web-based repository.

The data collection exercise is intended to be based on a multiscale sampling design and measurement protocols will be developed to assess forests, from basic (for example, tree cover percentage) to complex (such as land use types) parameters Data will be collected by partner organizations, local authorities and communities and, where necessary, by FAO staff directly. All of the data collected in the context of the GFS will be freely available and accessible through a web-based GIS-enabled portal.

The first Global Drylands Assessment

The Global Drylands Assessment (FAO, 2016) is a pilot action within the World Forest Open Data project that focuses solely on drylands and on the use of satellite images from publicly available repositories (such as Google Earth Engine and Bing Maps). For the first Global Drylands Assessment, more than 200 experts with knowledge of the land and land uses in specific dryland regions were involved.

The global assessment draws on information from 213 795 sample plots in the world's drylands. Each plot measured 70 m x 70 m (approximately 0.5 ha), a size corresponding to the smallest patch that qualifies as forest according to the forest definition used by the FAO Global FRA (FAO, 2015a).

In locating sample plots in a grid across the drylands, each aridity zone was treated as an independent stratum. The relative sampling intensity assigned to each aridity zone was as follows: hyperarid = 0.5; arid = 1; and semiarid and dry subhumid = 1.5. The results are reported at the global and regional levels (FAO, 2016). The statistical sampling error for the estimate of the total forest land area for all drylands is about 1 percent.

FIGURE 5. ILLUSTRATION OF SAMPLING INTENSITY OF THE FIRST GLOBAL DRYLANDS ASSESSMENT

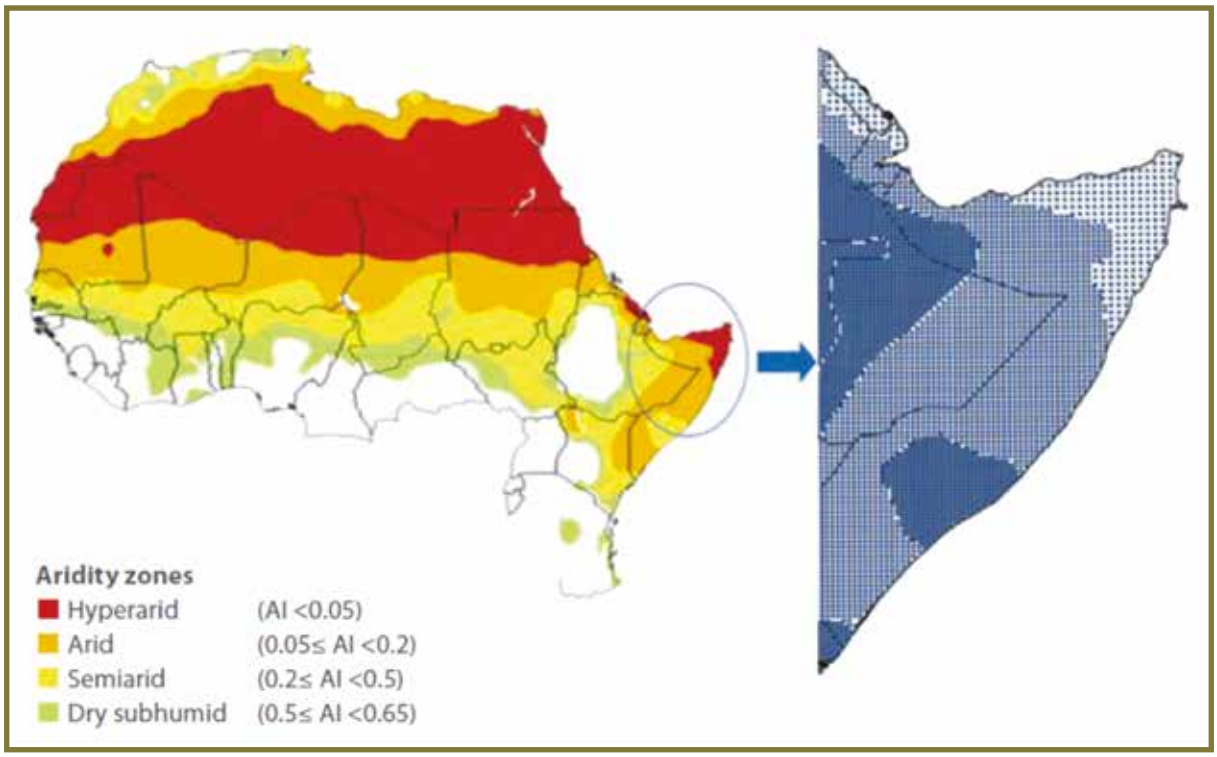

FAO, 2016

Data and tools used for the Global Drylands Assessment

The survey was set up using Collect, a software tool available in the Open Foris suite[13] and then embedded in Collect Earth, which was developed in cooperation with Google Earth Outreach (Bey *et al*., 2016).

Sample plot data were collected from online libraries of satellite images using Collect Earth. Typically, each plot was overlaid onto several images obtained through Google Earth Engine and Bing Maps. Collect Earth is capable of visualizing reflectance values and user-defined indices such as the Normalized Difference Vegetation Index (NDVI) based on Landsat and MODIS satellite images. The visual interpretation exercise was facilitated by the temporal profiles of interannual vegetation indices, which were derived from lower-resolution satellite data (the ground resolution ranging from 30 to 250 m).

13 Open Foris is a suite developed by the FAO Forestry Department to facilitate flexible and efficient data collection, analysis and reporting; see http://www.openforis.org/.

Landsat imagery (having a resolution of 30 m) was available for all plots, and 89 percent of plots were also covered by finer-resolution images, more than half of which consisted in images from Digital Globe and having a spatial resolution finer than 1 m. The proportion of satellite image types was similar for all land-use categories.

Collect Earth projected each sample plot as a frame containing a grid of 49 control points, enabling users to make precise estimates of the proportion of plots taken up by trees, shrubs and other land elements. In the visual interpretation exercise, each expert used his or her knowledge of the location and information provided by remote sensing data to support the survey process.

Land use image interpretation

For each sample plot, data on over 70 characteristics were collected and recorded for the most recent point in time for which satellite images were available. The variables were selected to characterize land cover, land use, land use change and other significant land dynamics (such as desertification and greening), along with biophysical indicators. The year 2000 is used as the reference year, because it is considered to be first year for which consistent global coverage of satellite data (Landsat 7) is available.

The simultaneous use of low-resolution and very-high-resolution (VHR) satellite imagery facilitates the detection of land use and land-use change. For certain land elements (for example, distinguishing between trees and shrubs), satellite data and local knowledge sometimes proved to be insufficient; therefore, a decision rule based on the crown diameter of trees and shrubs was adopted. Elements with a crown diameter larger than 3 m were considered trees; elements with smaller diameters were considered shrubs. Collect Earth does not allow for the direct measurement of tree height; therefore, tree shadows (where visible) were used in addition to the crown diameter threshold to determine whether elements were sufficiently tall (in other words, 5 m or taller, consistently with the definition of forests used in the Global Drylands Assessment) to be considered trees.

Land use is assessed on the basis of the six land-use categories established by the IPCC (IPCC, 2006): forest, cropland, grassland, wetlands, settlements, and other land. A predominant land use is assigned to each sample plot, based on the presence of key land-use indicators interpreted according to a hierarchical rule (Martinez and Mollicone, 2012). For example, a sample plot with a crown cover greater than 10 percent is not classified as forest unless the prevailing land use can also be identified as forest. Only one land use per sample plot can be assigned.

Results and lessons learned during the first Global Drylands Assessment

FAO has used this approach to produce a global assessment of the drylands (FAO, 2016) by analysing approximately 214 000 sample plots (Bastin *et al*., 2017). This survey is the first statistical sampling-based assessment of land use, including the assessment of forests and tree cover, in the global drylands. Therefore, it provides a baseline for monitoring changes in dryland forests, tree cover and land use, globally, regionally and by aridity zone.

According to the first Global Drylands Assessment, the world's drylands contain 1.11 billion ha of forest. More than half of these (specifically, 566 million ha) are in the dry subhumid zone, mostly in the northeastern part of southern Africa and the western (pre-Andean) part of South America. Approximately two thirds of dryland forests (742 million ha) can be considered closed forests, because they have a crown cover density of more than 40 percent. More than half of these forests (most of which are in Europe and South America) have a crown cover of 90 percent or more.

The Global Drylands Assessment uses data from publicly and freely available online libraries of satellite images using a simple visual interpretation tool, and it engages people with land-use expertise in a systematic data collection exercise. This approach has the following advantages:

- A statistics-based assessment of a basic set of variables can be conducted rapidly and inexpensively to complement other methods, because sample plots are assessed using satellite images rather than in the field; and
- A large number of people can be engaged in the assessment process, thanks to the ease of use of the interpretation and because the software and data are both available free of charge.

The first Global Drylands Assessment produced results (FAO, 2016; Bastin *et al*., 2017) in less than one year from conception, in a participatory and collaborative manner. The Global Drylands Assessment provided an opportunity to test the approach developed at a global scale. However, the methodology must be further developed for non-dryland areas, in particular to reduce interpretation errors.

A potential source of error is inconsistency: more than 200 people were engaged in the visual interpretation of satellite images, and the supply of images was not the same for all 213 795 sample plots assessed. The risk of inconsistency was mitigated by ensuring that all experts used the same training modules and tools. Additional measures to reduce inconsistencies and errors in interpretation will be implemented in a pilot assessment of all lands worldwide.

The methodology can be adapted to accommodate more intensive sampling for specific regional, national and landscape-scale needs, if required by countries and other users. For example, it is used at the regional scale for the baseline assessment of the Great Green Wall area over more than 20 countries both north and south of the Sahara, building on data already collected in North Africa, the Sahel and the Horn of Africa.

Future prospects

The results of the Global Drylands Assessment were reported in early 2017 (Bastin *et al*., 2017), following supplementary ground measurements and analyses. The results were made publicly available. It is expected that the Global Drylands Assessment will be repeated every two years.

The use of Collect Earth and other relevant tools for baseline assessments and monitoring must be further promoted through capacity-development events and workshops at regional and national levels. These tools provide a new and economically feasible way of assessing trees, forests, land use and land-use change in all areas of the world, as shown by the first Global Drylands Assessment.

FAO intends to apply the methodology in a global pilot assessment of all types of land by adding approximately 250 000 sample plots to be visually interpreted through Collect Earth. Global estimates of forest areas will be produced from a total of approximately 500 000 sample plots each about 0.5 ha in size. These results will be integrated into the Global Forest Survey's project database.

7.5. COMPLEMENTARITY BETWEEN ESTIMATES OF CHANGES IN FOREST AND AGRICULTURE

The complementarity between estimates of changes in forest and agriculture areas is illustrated by the analysis carried out by VITO, IIASA, HIVA and IUCN NL in the study entitled "Comprehensive analysis of the impact of EU consumption on deforestation", funded by the European Commission, hereafter EC Technical Report (European Commission, 2013).

Worldwide gross deforestation from FAO Forest Resources Assessment 2010 for 1990–2008

For the period from 1990 to 2008, worldwide gross deforestation is estimated at 239 million ha (Mha), or about 13 Mha on average per year, with substantial regional variations, as reported in the FAO Forest Resources Assessment 2010. During the same period, gross deforestation was partially compensated by afforestation and by the natural expansion of forests, together counting for 115 Mha. Thus, net deforestation was of 124 Mha (FAO, 2010a).

In the EC Technical Report (2013), using FRA 2010 (FAO, 2010a) and FAOSTAT land use domain databases (FAOSTAT, 2011), gross deforestation is attributed to five main sectors: Agricultural Expansion, Logging (prior to agricultural expansion), Urban Areas Expansion, Natural hazards (especially wildfire), and Unexplained. Using a transition model, the land use changes reported in FAOSTAT for the above sectors are linked to the deforestation areas identified in the FRA 2010. Moreover, a fraction of the agricultural land expansion allocated to deforestation is reallocated to "logging for industrial round wood extraction", to account for wood extraction preceding the conversion of forest land for agriculture.

Unexplained deforestation

When gross deforestation cannot be explained by agriculture, logging, built-up area increases or natural hazards, it is termed Unexplained in the EC Technical Report (2013). Of the 239 Mha of worldwide gross deforestation, approximately 58 Mha (24 percent) of reported deforestation cannot be conclusively linked to the conversion of forests for clear consumption purposes or other reported deforestation causes. The largest source of uncertainty relates to the data on deforestation. However, FAO considers even the 9 percent difference in forest area between the FRA 2010 assessment and the FRA 2010 RSS as a good result, considering the differences in the methods adopted (FAO and JRC, 2012). Furthermore, an accurate assessment of tree cover at lower canopy densities (from 10 to 30 percent) is difficult with both the country-level FRA 2010 assessment and the RSS. Therefore, uncertainties are particularly significant in dry regions and for degraded forests. Unlike the situation in Africa, no large discrepancies were found between the RSS survey and FRA 2010 with regard to the deforestation rates for South America. Agricultural production statistics and trade data were considered to be relatively reliable.

Unexplained deforestation can be partially attributed to erroneous deforestation figures (overreporting) and agricultural area data at the national level (underreporting), as demonstrated by the recent results of the FRA 2010 RSS. Second, the Unexplained category can be partially interpreted as the result of long-term degradation effects ensuing from several informal practices being carried out in forests, such as illegal logging and unsustainable fuelwood gathering. As consistent global data and clear cause-consequence relationships on the latter are non-existent, their impact is assumed to be taken into consideration in this category. Third, the conversion of forests into agricultural land may encompass more conversion than will actually result in productive (and reported) agricultural land.

Drivers of deforestation

For the remaining 182 Mha of worldwide gross deforestation, approximately 41 Mha (17 percent) were caused by natural hazards (mainly natural or man-made fires) that failed to result in reported agricultural land expansion (EC, 2013). The country of Indonesia alone lost 9 Mha of forest because of the 1997–1998 El Niño Southern Oscillation (ENSO). Furthermore, approximately 9 Mha (4 percent) were turned into built-up land and infrastructure. The remaining 132 Mha, or 55 percent of worldwide gross deforestation, can be clearly attributed to the conversion of forest land to land for crop production, ruminant livestock production and industrial round wood production (logging).

Of the 132 Mha (55 percent) of deforestation linked to the global production of agricultural and forestry products, only 4.5 Mha (or 2 percent) of deforestation was attributed to logging, representing only the impact of logging which precedes conversion into agricultural land (EC, 2013).

Additionally, within the overall impact of the agricultural sector (128 Mha or 53 percent), 69 Mha (or 29 percent) of forests were directly or indirectly cleared for cropland to meet the global human demand for food, feed for livestock, fuel and fibres from crops. Approximately 58 Mha (24 percent) of forests were cleared for pastures to raise livestock.

7.6. REFERENCES

Achard, F., Beuchle, R., Mayaux ,P., Stibig, H.-J., *et al*. 2014. Determination of tropical deforestation rates and related carbon losses from 1990 to 2010. *Global Change Biology* 20: 2540–54.

Achard, F. & Hansen, M.C. (eds). 2012. *Global Forest Monitoring from Earth Observation*. CRC Press, Taylor & Francis Group: Boca Raton, FL, USA.

Achard, F., Eva, H.D., Stibig, H.-J., Mayaux, P., Gallego, J., Richards, T. & Malingreau, J.P. 2002. Determination of Deforestation Rates of the World`s Humid Tropical Forests. *Science*, 297: 999–1002.

Bartalev, S.S., Kissiyar, O., Achard, F., Bartalev, S.A. & Simonetti, D. 2014. Assessment of forest cover of Russia by combining a wall to wall coarse resolution land cover map with a sample of 30m resolution forest maps. *International Journal of Remote Sensing*, 35: 2671–2692.

Bastin, J.F., Berrahmouni, N., Grainger, A. *et al*. 2017. The extent of forest in dryland biomes. *Science*, 356, 635–638**.**

Beuchle, R., Grecchi, R.C., Shimabukuro, Y.E., Seliger, R., Eva, H.D., Sano, E., Achard, F. 2015. Land cover changes in the Brazilian Cerrado and Caatinga biomes from 1990 to 2010 based on a systematic remote sensing sampling approach. *Applied Geography* 58: 116–127.

Beuchle, R., Eva, H.D., Stibig, H.-J. *et al*. 2011. A Satellite Data set for Tropical Forest Change Assessment. *International Journal of Remote Sensing*, 32: 7009–7031.

Bodart, C., Eva, H.D., Beuchle, R. *et al.* 2011. Pre-processing of a Sample of Multi-scene and Multi-date Landsat Imagery used to Monitor Forest Cover Changes over the Tropics. *ISPRS Journal of Photogrammetry and Remote Sensing*, 66: 555–563.

Bodart, C., Brink, A., Donnay, F., Lupi, A., Mayaux, P. & Achard, F. 2013. Continental estimates of forest cover and forest cover changes in the dry ecosystems of Africa for the period 1990-2000. *Journal of Biogeography*, 40: 1036–1047.

Brazilian Forest Service (BFS). (2016) *National Forest Inventory of Brazil*. Available at: www.florestal.gov.br. Accessed on 21 June 2017.

Bey, A., Sánchez-Paus Díaz, A., Maniatis, D. *et al.* 2016. Collect Earth: Land Use and Land Cover Assessment through Augmented Visual Interpretation. *Remote Sensing*, 8: 807.

Brink, A.B. & Eva, H.D. 2009. Monitoring 25 years of land cover change dynamics in Africa: a sample based remote sensing approach. *Applied Geography*, 29: 501–512.

Clerici, N., Weissteiner, C.J., Paracchini, M.L. & Strobl, P. 2011. *Riparian zones: where green and blue networks meet—Pan-European zonation modelling based on remote sensing and GIS. JRC Scientific and Technical Report*. Publication of the European Communities: Luxembourg.

De Foresta, H., Somarriba, E., Temu, A., Boulanger, D., Feuilly, H. & Gaulthier, M. 2013. *Towards the assessment of trees outside of forests. A thematic report prepared in the framework of the global forest resources assessment*. Forest Resources Assessment Working Paper 183. FAO Publication: Rome.

DeFries, R.S., Rudel, T.K., Uriarte, M. & Hansen, M.C. 2010 Deforestation driven by urban population growth and agricultural trade in the twenty-first century. *Nature Geoscience*, 3: 178–181.

De Sy, V., Herold, M., Achard, F., Asner, G.P., Held, A., Kellndorfer, J. & Verbesselt, J. 2012. Synergies of multiple remote sensing data sources for REDD+ monitoring. *Current Opinion in Environmental Sustainability*, 4: 696–706.

De Sy, V., Herold, M., Achard, F., Beuchle, R., Clevers, J.G.P.W., Lindquist, E. & Verchot, L. 2015 Land use patterns and related carbon losses following deforestation in South America. *Environmental Research Letters*, 10: 124004.

Drigo, R., Lasserre, B. & Marchetti, M. 2009. Patterns and trends in tropical forest cover. *Plant Biosystems*, 143: 311–327.

European Commission (EC). 2013. *The impact of EU consumption on deforestation: Comprehensive analysis of the impact of EU consumption on deforestation*. Technical Report 2013 – 063. European Union Publication: Luxembourg.

Eva, H.D., Achard, F., Beuchle, R., de Miranda, E.E., Carboni, S., Seliger, R., Vollmar, M., Holler, W., Oshiro, O.T. & Barrena Arroyo, V. 2012. Forest cover changes in tropical South and Central America from 1990 to 2005 and related carbon Emissions Removals. *Remote Sensing*, 4: 1369–1391.

Eva, H.D., Carboni, S., Achard, F., Stach, N., Durieux, L., Faure, J.-F. & Mollicone, D. 2010. Monitoring forest areas from continental to territorial levels using a sample of medium spatial resolution satellite imagery. *ISPRS Journal of Photogrammetry and Remote Sensing*, 65: 191–197.

Food and Agriculture Organization of the United Nations (FAO) & Joint Research Centre of the European Commission (JRC). 2012. *Global forest land-use change 1990–2005*. FAO Forestry Paper No. 169. FAO Publication: Rome. Available at: http://www.fao.org/forestry/fra/remotesensingsurvey/en/. Accessed on 10 June 2017.

FAO. 2016. *Trees, forests and land use in drylands – The first global assessment*. FAO Publication: Rome.

FAO. 2015a. *Global Forest Resources Assessment 2015: How are forests changing?* FRA-2015 Synthesis report. FAO Publication: Rome.

FAO. 2015b. *Country Report Brazil – Global Forest Resource Assessment 2015*. FAO Publication: Rome. Available at: http://www.fao.org/documents/card/en/c/6261857f-c0da-4f72-98fd-a18e9ca50509/. Accessed on 10 June 2017.

FAO. 2010a. *Global Forest Assessment 2010: Main Report*. FAO Publication: Rome.

FAO. 2010b. *Global Forest Assessment 2010: terms and definitions*. FAO Working Paper 144/E. FAO Publication: Rome.

FAO. 2001. *Global Forest Resources Assessment 2000*. FAO Forestry Paper No. 140. FAO Publication: Rome.

FAOSTAT. 2011. *Time-series and cross sectional data relating to food and agriculture*. FAO Publication: Rome. Available at: http://faostat.fao.org/default.aspx. Accessed in 2011 for EC report (2013).

Freitas, J.V., Oliveira, Y.M.M., Brena, D.A., Gomide, G.L.A., Silva, J.A., Collares, J.E., Mattos, P.P., Rosot, M.A.D., Sanquetta, C.R., Vencatto, M.F., Barros, P.L.C., Santos, J.R., Ponzoni, F.L. & Shimabukuro, Y.E. 2008. The New Brazilian National Forest Inventory. In: McRoberts, R.E., Reams, G.A., Van Deusen, P.C. & McWilliams, W.H. (eds), *Proceedings of the Eight Annual Forest Inventory and Analysis Symposium, Monterey, CA, October 16-19, 2006* (pp. 9–12) USDA Forest Service Publication: ; Washington, D.C.

Freitas, J.V., Oliveira, Y.M.M, Rosot, M.A.D., Gomide, G.L.A. & Mattos, P.P. 2010. Brazil National Forest Inventory Report. In: Tomppo, E., Gschwantner, T., Lawrence, M. & McRoberts, R.E. (eds), *National forest inventories: pathways for common reporting (*pp. 89–95). Springer-Verlag: Heidelberg Germany.

Foody, G.M. 2010. Assessing the accuracy of land cover change with imperfect ground reference data. *Remote Sensing of Environment*, 114: 2271–2285.

Global Forest Observations Initiative (GFOI). 2014. *Integrating remote-sensing and ground-based observations for estimation of emissions and removals of greenhouse gases in forests: Methods and Guidance from the Global Forest Observations Initiative*. Group on Earth Observations Publication: Geneva, Switzerland. Available at: http://www.gfoi.org/methods-guidance/. Accessed on 10 June 2017.

Gibbs, H.K., Ruesch, A.S., Achard, F., Clayton, M., Holmgren, P., Ramankutty, N. & Foley, J.A. 2010. Tropical forests were the primary sources of new agricultural land in the 1980s and 1990s. *Proceedings of the National Academy of Sciences USA*, 107: 16732–16737.

GOFC-GOLD. 2016. *A sourcebook of methods and procedures for monitoring and reporting anthropogenic greenhouse gas emissions and removals associated with deforestation, gains and losses of carbon stocks in forests remaining forests, and forestation* GOFC-GOLD Report version COP22-1. Publication of the GOFC-GOLD Land Cover Project Office – Wageningen University: Wageningen, The Netherlands. Available at: http://www.gofcgold.wur.nl/redd/index.php. Accessed on 10 June 2017.

Grassi, G., Federici, S. & Achard, F. 2013. Implementing conservativeness in REDD+ is realistic and useful to address the most uncertain estimates. *Climatic Change*, 119: 269–275.

Grecchi, R., Beuchle, R., Shimabukuro, Y.E., Aragão, L.E, Arai, E., Simonetti, D. & Achard, F. 2017. An integrated remote sensing and GIS approach for monitoring areas affected by selective logging: a case study in northern Mato Grosso, Brazilian Amazon. *International Journal of Applied Earth Observation and Geoinformation*, 61: 70–80.

Gutman, G., Huang, C., Chander, G., Noojipady, P. & Masek J.G. 2013. Assessment of the NASA/USGS global land survey (GLS) datasets. *Remote Sensing of Environment*, 134: 249–265.

Hansen, M.C., Potapov, P.V., Moore, R. *et al.* 2013. High-resolution global maps of 21st-century forest cover change. *Science*, 342: 850–853.

Hansen, M.C., Stehman, S.V. & Potapov, P.V. 2010. Quantification of global gross forest cover loss. *Proceedings of the National Academy of Sciences USA*, 107: 8650–8655.

Instituto Nacional de Pesquisas Espaciais (INPE). 2016. *Monitoramento da Floresta Amazônica Brasileira por Satélite*. INPE Publication: São José dos Campos, Brazil. Available at http://www.obt.inpe.br/prodes/index.html. Accessed on 10 June 2017.

Penman, J., Gytarsky, M., Krug, T. *et al*. (eds). 2003. *Definitions and Methodological Options to Inventory Emissions from Direct Human induced Degradation of Forests and Devegetation of Other Vegetation Types*. Intergovernmental Panel on Climate Change (IPCC) Publication: Kanagawa, Japan.

IPCC. 2006. Consistent representation of lands. In: *Guidelines for GHG inventories. Volume 4: agriculture, forestry and other land use* (Chapter 3). IPCC Publication: Kanagawa, Japan.

Ivits, E., Cherlet, M., Mehl, W. & Sommer, S. 2009. Estimating the ecological status and change of riparian zones in Andalusia assessed by multi-temporal AVHHR datasets. *Ecological Indicators*, 9(3): 422–431.

Keenan, R.J., Reams, G.A., Achard, F., de Freitas, J., Grainger, A. & Lindquist, E. 2015. Dynamics of global forest area: results from the FAO Global Forest Resources Assessment 2015. *Forest Ecology and Management*, 352: 9–20.

Luz, N.B., Oliveira, Y.M.M., Rosot, M.A.D., Garrastazú, M.C., Franciscon, L., Mesquita, H.N. Jr & Freitas, J.V. 2015a. *Classificação híbrida de imagens Landsat-8 e RapidEye para o mapeamento do uso e cobertura da terra nas Unidades Amostrais de Paisagem do Inventário Florestal Nacional do Brasil*. Anais XVII Simpósio Brasileiro de Sensoriamento Remoto - SBSR, João Pessoa-PB, Brazil, 25–29 April 2015. INPE Publication: São José dos Campos, Brazil. Available at: http://www.dsr.inpe.br/sbsr2015/files/p1606.pdf. Accessed on 10 June 2017.

Luz, N.B., Oliveira, Y.M.M., Rosot, M.A.D., Garrastazú, M.C., Franciscon, L., Mesquita, H.N. Jr, Freitas, J.V. & Costa, C.R. 2015b. Developments in forest monitoring under the Brazilian National Forest Inventory: multi-source and hybrid image classification approaches. Paper prepared for the XIV World Forestry Congress, 7–11 September 2015. Durban, South Africa. Available at: http://foris.fao.org/wfc2015/api/file/5547d6d115ae74130aee6a2f/contents/e09e6ff0-e135-48d6-82e7-28466b86f63d.pdf. Accessed on 10 June 2017.

MacDicken, K.G., Sola, P., Hall, J.E., Sabogal, C., Tadoum, M. & de Wasseige, C. 2015. Global progress toward sustainable forest management. *Forest Ecology and Management*, 352: 47–56.

MacDicken, K.G. 2015. Global Forest Resources Assessment 2015: What, why and how? *Forest Ecology and Management*, 352: 3–8.

Magdon, P., Fischer, C., Fuchs, H. & Kleinn, C. 2014. Translating criteria of international forest definitions into remote sensing image analysis. *Remote Sensing of Environment*, 149: 252–262.

Martinez, S. & Mollicone, D. 2012. From land cover to land use: a methodology to assess land use from remote sensing data. *Remote Sensing*, 4: 1024–1045.

Mayaux, P., Pekel, J.-F., Desclée, B. *et al.* 2013. State and evolution of the African rainforests between 1990 and 2010. *Philosophical Transactions of the Royal Society B: Biological Sciences*, 368: 20120300.

Mayaux, P., Holmgren, P., Achard, F., Eva, H.D., Stibig, H.-J. & Branthomme, A. 2005. Tropical forest cover change in the 1990's and options for future monitoring. *Philosophical Transactions of The Royal Society B*, 360: 373 – 384.

Miettinen, J., Shimabukuro, Y.E., Beuchle, R., Grecchi, R.C., Velasco-Gomez, M., Simonetti, D. & Achard, F. 2016. On the extent of fire-induced forest degradation in Mato Grosso, Brazilian Amazon, in 2000, 2005 and 2010. *International Journal of Wildland Fire*, 25: 129–136.

Miettinen, J., Stibig, H.-J. & Achard, F. 2014. Remote sensing of forest degradation in Southeast Asia - aiming for a regional view through 5-30 m satellite data. *Global Ecology and Conservation*, 2: 24–36.

Pelletier, J. & Goetz, S.J. 2015. Baseline data on forest loss and associated uncertainty: advances in national forest monitoring. *Environmental Research Letters*, 10: 021001.

Potapov, P., Hansen, M.C., Gerrand, A.M. *et al.* 2010. The global Landsat imagery database for the FAO FRA remote sensing survey. *International Journal of Digital Earth*, 4:2–21.

Raši, R., Bodart, C., Stibig, H.-J. et al. 2011. An automated approach for segmenting and classifying a large sample of multi-date Landsat imagery for pan-tropical forest monitoring. *Remote Sensing of Environment*, 115: 3659–3669.

Richards, T.S., Gallego, J. & Achard, F. 2000. Sampling for forest cover change assessment at the pan-tropical scale. *International Journal of Remote Sensing*, 21:1473–1490.

Romijn, E., Herold, M., Kooistra, L., Murdiyarso, D. & Verchot, L. 2012. Assessing capacities of non-annex I countries for national forest monitoring in the context of REDD+. *Environmental Science Policy*, 20: 33–48.

Romijn, E., Lantican, C.B., Herold, M., Lindquist, E., Ochieng, R., Wijaya, A.,Murdiyarso, D. & Verchot, L. 2015. Assessing change in national forest monitoring capacities of 99 tropical countries. *Forest Ecology and Management* 352: 109–123.

Saura, S. & Torné, J. 2009. Conefor Sensinode 2.2: a software package for quantifying the importance of habitat patches for landscape connectivity. *Environmental Modelling & Software,* 24: 135–139.

Stach, N., Salvado, A., Petit, M., Faure, J.F., Durieux, L., Corbane, C., Joubert, P., Lasselin, D. & Deshayes, M. 2009. Land use monitoring by remote sensing in tropical forest areas in support of the Kyoto Protocol: the case of French Guiana. *International Journal of Remote Sensing*, 30: 5133–5149.

Särndal, C.E., Swensson, B. & Wretman, J. 1992. *Model Assisted Survey Sampling*. Springer-Verlag: New York, USA.

Stehman, S.V., Hansen, M.C., Broich, M., Potapov, P.V. 2011. Adapting a global stratified random sample for regional estimation of forest cover change derived from satellite imagery. *Remote Sensing of Environment*, 115: 650–658.

Steininger, M.K., Godoy, F. & Harper, G. 2009. Effects of systematic sampling on satellite estimates of deforestation rates. *Environmental Research Letters*, 4: 034015.

Stibig, H.-J., Achard, F., Carboni, S., Raši, R. & Miettinen, J. 2014. Changes in tropical forest cover of Southeast Asia from 1990 to 2010. *Biogeosciences*, 11: 247–258.

Tyukavina, A., Baccini, A., Hansen, M.C., Potapov, P.V., Stehman, S.V., Houghton, R.A, Krylov, A.M., Turubanova, S. & Goetz, S.J. 2015. Aboveground carbon loss in natural and managed tropical forests from 2000 to 2012. *Environmental Research Letters* 10: 074002.

Tyukavina, A., Stehman, S.V., Potapov, P.V., Turubanova, S.A., Baccini, A., Goetz, S.J., Laporte, N.T., Houghton, R.A. &d Hansen, M.C. 2013. National-scale estimation of gross forest aboveground carbon loss: a case study of the Democratic Republic of the Congo. *Environmental Research Letters*, 8: 044039.

United Nations Framework Convention on Climate Change (UNFCCC). 2016. *Report of the Conference of the Parties on its twenty-first session, Decision 1/CP.21: Adoption of the Paris Agreement*. UNFCCC Publication: Bonn, Germany.

UNFCCC. 2014. *Key decisions relevant for reducing emissions from Deforestation and forest degradation in developing countries (REDD+)*. Decision Booklet REDD+. UNFCCC Publication: Bonn, Germany. Available at: http://unfccc.int/files/land_use_and_climate_change/redd/application/pdf/compilation_redd_decision_booklet_v1.1.pdf. Accessed on 10 June 2017.

UNFCCC. 2006. *Report of the Conference of the Parties serving as the meeting of the Parties to the Kyoto Protocol on its first session, Decision 16/CMP.1 Land use, land-use change and forestry*. UNFCCC Publication: Bonn, Germany.

Verhegghen, A., Eva, H.D., Desclée, B. & Achard, F. 2016. Review of recent forest cover and forest cover change assessments in Cameroon. *International Forestry Review* 18: 14–25.

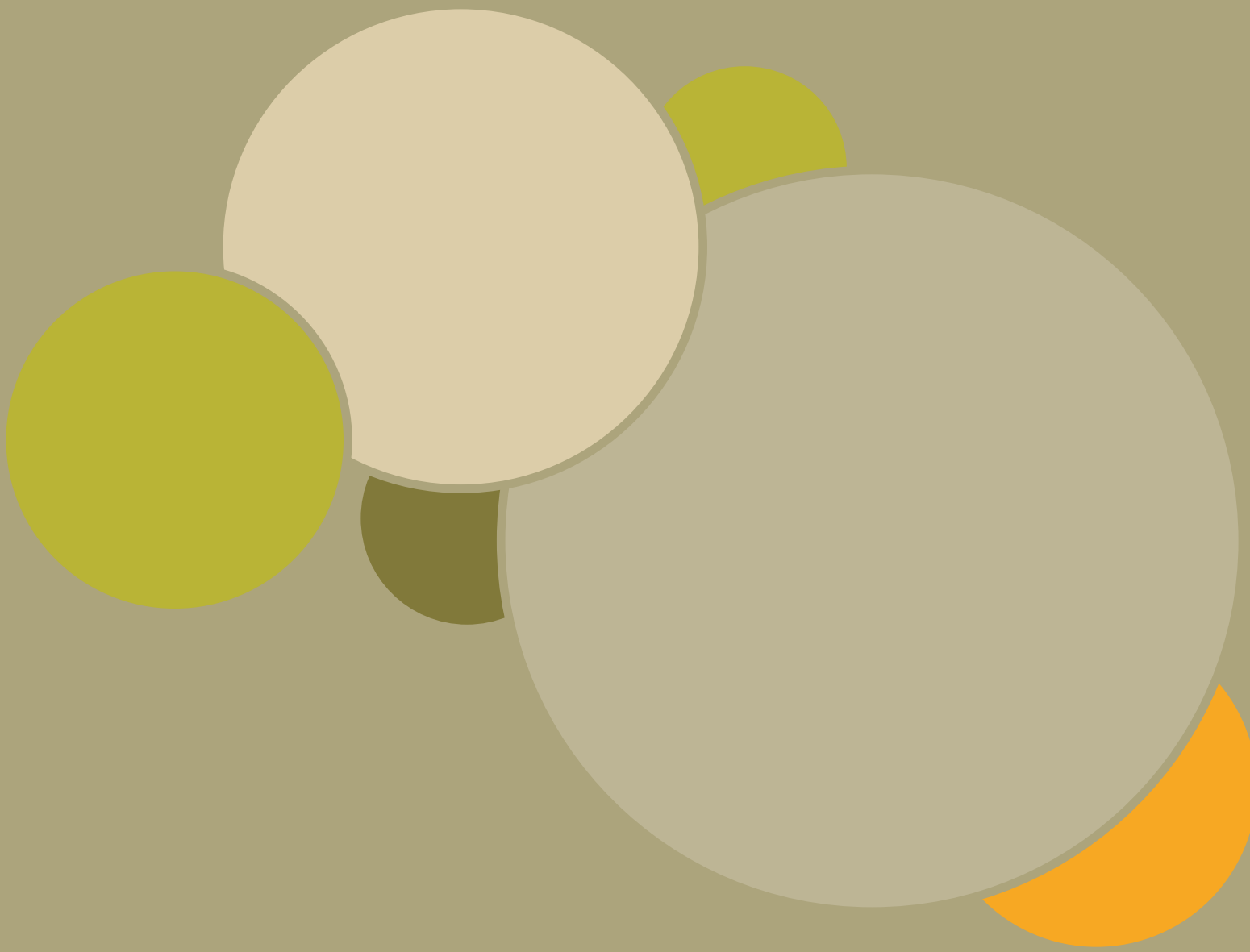

8

Chapter 8

Organization, resources and competences for adopting remote sensing in agricultural statistics

John Latham

8.1. BACKGROUND

Timely and accurate temporal information on crops during the growing period, and estimates at harvest, provide important inputs into reliable estimates for food security, planning, policy formulation and agriculture marketing strategies. Experience has shown that the quality of available agricultural data (agricultural censuses, crop monitoring and yield estimations) is generally inconsistent and erratic. Therefore, an improvement in data collection and reporting techniques is warranted. Recent developments in geospatial data and remote sensing processing, together with reductions in cost and increases in the cover, frequency and resolution of satellite imagery offer robust new data and methods for strengthening data systems (Bell and Dalton, 2007; Murray, 2010). A paradigm shift has now taken place, such that remote sensing data systems now offer robust primary estimates of agricultural production and are no longer surrogates of purely ancillary data sets for validation.

Traditional methods of predicting crop yields focus on models that integrate climate, soils and fertilizers, irrigation water and agrometeorology as response functions to describe crops yields and production assessment (Wiegand and Richardson, 1990). These techniques are generally based on strong physiological and physical concepts. However, they suffer from limitations when delivering reliable outputs under conditions of extensive spatial variability in soils, stress factors or poor management practices (Wiegand and Richardson, 1984 and 1990). However, geospatial technologies (remote sensing and geographic Information systems (GIS)) have been promoted as potentially valuable tools for agricultural monitoring because of their synoptic coverage and ability to monitor temporally (Hinzman et al., 1986; Quarmby et al., 1993). There has been an emphasis on developing fast-track and reliable procedures to provide crop forecasts early in the season, and estimations at the end of the season.

Agricultural censuses are increasingly employing geospatial technologies and satellite remote sensing, or using land cover products derived for other purposes to support area sample frame (ASF) based approaches based on area sample frames (ASFs) over list frame sampling. Remote sensing and other GIS data sets also support the development and maintenance of Master Sample Frames (MSFs; see Carfagna, 2013) that integrate multiple geospatial data layers (such as census enumeration areas, field boundaries and crop coverages), that allow for the effective reuse of the sample frame (Carfagna and Gallego, 2005). While remote sensing techniques have not replaced the need for agricultural enumeration, integrating remote sensing and GIS into these sampling and survey procedures has the purpose of increasing the accuracy, practical efficiency, repeatability and cost-effectiveness by reducing the time required to create sampling frames. Currently, GPS, GIS and imagery are used together to support more efficient field-based agricultural surveys and censuses (Carfagna et al., 2013).

However, the use of remote sensing within agricultural monitoring, estimation and reporting requires both data and technical resources capable of addressing the big data analytics in which the new generation of geospatial modellers must be well versed. The above situation promotes the use of satellite remote sensing for monitoring of crops and agricultural systems, enhanced skill sets and training for image processing and use within the field operations. Despite the inherent challenges, these approaches have been extensively developed within other sectors; therefore, the use of remote sensing within agriculture can often capitalize on data sourcing and processing for other objectives and with significant options for institutional sharing.

The following sections specify the technical and practical requirements to support the use of remote sensing and GIS within agricultural statistics and provide examples of the integration of remote sensing within agricultural statistics and reporting.

8.2. ORGANIZATION

Generally, public-sector organizations are the main producers of agricultural statistics. However, in recent years, private-sector organizations have increasingly been conducting these assignments. Business enterprises, and particularly industries such as sugar mills, feed and beverages, tend to outsource their temporal requirements, to improve their working efficiency and manage industrial operations. In the conventional system, manual methods have predominated and the data would only become available at the end of the season, moreover lacking a temporal and broad perspective at a specific time.

Satellite-based organizations must necessarily be multidisciplinary in nature, capable of simultaneously integrating information from satellite remote sensing, GIS, statistics, agronomy, agrometeorology, economics and software development. Additional subject-matter specialists can be dovetailed into programmes to address the specific requirements of a particular industry or to study issues of consumption patterns, food security, and import and export regimes. Organizations should hire technical staff for data entry, basic maintenance work for data development and for conducting field surveys, although crowdsourcing has considerably changed the nature and modalities for these types of work too. Maintaining the representativeness of crowd sourced data and ensuring that it is unbiased are current challenges.

8.3. RESOURCES

The resources required by organizations to begin producing agricultural statistics may be broadly divided into the following categories:

- Qualified staff;
- Laboratories (hardware and software; however, these are becoming increasingly limited due to cloud-based storage and processing analytics);
- Input data determination (multi-sensor is often preferred);
- Work planning;
- Training; and
- Funds.

Agricultural statistics can benefit from the use of remote sensing data and geospatial processing in multiple ways, depending on a number of criteria and resource requirements. These vary with the objectives and purpose of the surveys, and range from:

i. Availability of baseline data for identifying the ASF's most appropriate characteristics, given the specificities of the territory;
ii. Construction and maintenance of the ASF;
iii. Stratification of the ASF, for example by using land cover data on the cropped area or on specific or seasonal crops;
iv. Geospatial mapping of specialist and minor crop distributions, large- and medium-scale commercial farms for selective sampling frames;
v. Support for crop field survey procedures and logistics;
vi. Provision of additional variables in regression or a calibration estimator and small area estimation;
vii. Crop yield monitoring and forecasting; and
viii. Mapping of condition factors (such as pests and diseases) and natural hazards and derived indices of seasonal crop productivity (such as the Normalized Difference Vegetation Index or NDVI).

The multiple applications of remote sensing beyond its direct application in agricultural statistics may also be relevant in related domains. For example, imagery is widely used within livestock pasture and rangeland assessment, natural resource management, monitoring sustainable agriculture and rural development, land degradation, human impact assessments and hazard and vulnerability mapping. These distinct uses may affect the selection of the appropriate image resources and characteristics (such as the seasonality, date, resolution, return interval, and spectral bands) supporting multi-use submissions. The uses will also require different levels of ancillary geospatial data, funding support, equipment and training.

8.3.1. Qualified staff

Statistics on crop production are based on two major components: crop area estimation and yield forecasting. The area can be estimated using Area Frame Sampling (AFS) or image classification of the complete coverage of a region. Remote sensing and GIS analysts are traditionally responsible for the image processing and construction of Area Frames, while statisticians are responsible for sample design, extrapolation and making estimates, together with their respective coefficient of variations. Image analysts often calculate the area based on pixel- or object-based classification. Field staff are responsible for conducting the field survey and crop signature collection. There may be an overlap in the skill requirements, for example where certain sampling and listing processes require both geospatial inputs and statistical sampling procedures (such as serpentine sampling).

A wide range of disciplines must be combined and collaborate with one another to support the improvement of agricultural statistics (table 1).

TABLE 1. SUMMARY OF THE DISCIPLINES REQUIRED TO OPERATE REMOTE SENSING WITHIN AGRICULTURAL STATISTICS AND REPORTING.

Thematic areas and expertise	Description of requirements
Remote sensing and GIS analysis	Satellite-extracted products (such as NDVI and NDWI (Normalized Difference Water Index)). Land cover, land use data sets, image processing (image enhancement, pixel- and object-based image classification, features interpretation and extraction, generation of thematic maps, spectral signatures of crops, remotely sensed phenological crop calendars and crop maps), geospatial inputs into sampling and area frame construction
Statistician	Construction of sample frame design, area frame development, random segments selection, questionnaire design for field data collection, field data correction, crop area estimates, statistical analysis for crop yield forecasting
Agronomist	Crop calendar, satellite acquisition time frame, crop condition assessment using satellite and ground-based information
Agrometeorologist	Collection and updating of meteorological parameters
Software developer	Development of desktop and web applications for field data collection and automation of data processing
Field staff	Field staff for ground data collection using GPS, validation, listing and agricultural sampling or cutting
Support staff	Data entry, digitization, printing

8.3.2. Laboratories: hardware and software requirements

Laboratories are required to accommodate the necessary manpower and equipment. The space to be allocated for the laboratory may depend upon the size of the operation that the particular organization is to carry out. Large analytical facilities can now be compact, given the availability of cloud-based computing and analytics technologies.

The hardware resources required for a geospatial agricultural statistics laboratories are shown in table 2.

TABLE 2. SUMMARY OF REQUIREMENTS FOR A GEOSPATIAL AGRICULTURAL STATISTICS LABORATORY (HARDWARE).

Item	Description/purpose
Workstation	Processor: core i7, Xeon RAM: >32 GB RAM Graphic card: 2–6 GB Hard disk size: 2–4Tb For image processing
Laptop/tablet	Field data collection
GPS	To capture field coordinates
Smartphone/tabs	Field data collection and near-real-time transmission
Camera	Digital cameras for validation and verification of classifications
Printer/plotter	Colour printer A4 and A3 size, plotter of A0 size to print reports and maps
Scanner	A3 or larger-size scanning for historical maps
Storage/backup server	Data storage: 16Tb
Network	To connect workstations

Modern mobile devices may integrate GPS tagging for photographs, data communications and storage for offline applications, thus reducing the number of systems used in the field.

The software requirements for a geospatial agricultural statistics lab are shown in table 3.

TABLE 3. SUMMARY OF REQUIREMENTS FOR A GEOSPATIAL AGRICULTURAL STATISTICS LABORATORY (SOFTWARE).

Discipline	Software
Statistical	SPSS: statistical analysis
	Excel Stat: area and yield calculation
	R (Open Source statistical software)
GIS/remote sensing	ArcGIS 10.x: development of GIS, spatial queries and analysis
	QGIS (Open Source): development of GIS, spatial queries and analysis
	ERDAS Imagine 9.x: image processing, Classification
	ENVI: image processing, classification
	E-Cognition: image processing, object-based classification
	FME (conversion, transformation and workflow automation in geospatial domain)
Mobile survey applications and Computer-Assisted Personal Interviewing (CAPI)	ODK (Open Data Kit) etc./bespoke Android applications for field geospatial survey (e.g. MAGIS)
	CAPI software – e.g. Survey Systems (World Bank / Area Frame Survey System (AFSS), Collect mobile (FAO)
Metadata/data dissemination	GeoNetwork – geospatial metadata, data download and display Web mapping applications – for information dissemination (MapStore, GeoServer, Leaflet, Arc Server, etc.)

8.3.3. Input data

A key component of the implementation process is the input Earth Observation data and the ancillary geospatial data required for agricultural statistics generation. A number of factors determine the suitability of different image sources (spatial and temporal resolution, frequency of coverage, spectral resolution and sensor type), with consequent implications for the sourcing and costs of acquisition and processing. Image resolution is a critical parameter in the selection criteria; however, it is balanced against a range of related factors, such as the size of the field, the revisit frequency, and practical factors such as costs and processing. The increasing availability of high-resolution (over 1 m and lower than 5 m) and very-high-resolution (or VHR; lower than 1 m) data, combined with larger swath widths (such as that obtainable from Sentinel 2 (9 to 10 m), free of charge and at medium-resolution – between 5 and 30 m in resolution – with a swath width of 290 km), is changing the availability and suitability of imagery resolutions. Delincé (2017) has examined image suitability in relation to the size of field systems and plots, emphasizing the predominance of small and very small fields within agriculture, particularly in Africa and Asia, where over 80 per cent of the fields fall within such definitions as determined by the IIASA 1-km2 global cropland data (Fritz, 2015). The implication of such smallholder dominance is that imagery suitability favours higher-resolution data in those agricultural settings where increased numbers of pixels are contained within a plot boundary (that is, reduced mixed pixels). However, this is an evolving situation, and new sensors with wider swaths and higher resolutions are enhancing the options available. Additional constellations of satellites and use of mixed sensors (for example, Demos 1 and 2/UrtheDaily, OptiSar, Pangeo Alliance and Planet Labs) provide new capabilities, frequencies and data resolutions that open up new possibilities for application.

Data inputs also include remote sensing validation and field survey data. Imagery can also be used for "pseudo-field" verification, using higher-resolution imagery and aerial photography to replace on-site surveys. While VHR imagery enables the straightforward identification of objects at the ground level, it is important to understand the specific needs and applications for which the imagery is proposed. Generally, not only the cost of the procurement of the images increases with the spatial resolution, but also the ability to store, process and analyse these images. However, the capacity to conduct big data analytics in cloud computing is rapidly reducing these considerations.

8.3.4. Work plan

The workflow for the integration of remote sensed data and derived land cover data into the crop area and yield estimation procedures include the following steps:

i. selection and acquisition of imagery or existing classified data;
ii. preprocessing and image processing;
iii. integration of ancillary data and field validation data to generate classifications that can be integrated into the Area Sampling Frame; and
iv. ASF construction, stratification and calculation

The acquisition time period of the satellite imagery depends upon the crop's phenological stages; however, the image selection may depend on the survey's specific objective (table 4).

TABLE 4. SAMPLE CROP CALENDAR FOR ASIA TO SUPPORT IMAGE ACQUISITION WINDOWS AND MEET SAMPLING OBJECTIVES.

Task	Month											
	Jan	Feb	Mar	Apr	May	Jun	Jul	Aug	Sep	Oct	Nov	Dec
Acquisition												
Pre Processing												
Field survey												
Image classification												
Validation												
Crop estimates												

Winter (Rabi) Crops Summer (Kharif) Crops

Third-party evaluation is always useful to identify any shortcomings and deficiencies in proposed or approved systems. It is appropriate to engage experts of repute from an independent organization or source to validate the procedures and findings. A technical audit of the data can also help to improve data quality.

8.3.5. Training requirements

The technical requirements for use of remote sensing and GIS call for investment in training and capacity development to support implementation. This, in turn, requires adequate training, e-learning materials and support to the application of crop area and yield estimation. Regular training from specialized national and international organizations is necessary to further support the use of new technologies, although much of the specialist remote sensing processing and geospatial analysis can be run nationally by more specialized sensors (such as the Synthetic Aperture Radar, or SAR), which may require further capacity development.

The following training curricula for integrating and supporting the application of remote sensing and GIS are envisaged:

i. Basic concepts of
   a. Remote sensing
   b. GIS
   c. Statistics
   d. Agronomy
ii. Remote sensing and image preprocessing, processing, classification, analysis and reporting;
iii. GIS data creation, editing, geodatabase development and geospatial tools for analysis;
iv. Land cover classification approaches, image segmentation, photo-interpretation, automated and manual classification, field verification and accuracy assessment, including use of pseudovalidation;
v. Integration of agro-environmental parameters derived from remote sensing data (crop calendars, phenology and plant response) and ground-based information for yield forecasting;
vi. Remote sensing and GIS for ASFs, stratification, sample selection, design of questionnaire, using information derived from remote sensing, and probability sampling;
vii. GIS software for constructing area sample design, stratification, probability-based sample selection, design of questionnaire, control sampling and non-sampling errors;
viii. GPS operation and field data collection for enumerators;
ix. Statistical sampling techniques for strata base point and interval estimation of parameters and accuracy of their estimates.

The extent, scope and periodicity of training are to be determined according to the team's requirements and/or composition.

8.3.6. Funding

Integrating remote sensing into agricultural statistics necessitates allocation of appropriate funding levels. The costs for national statistical purposes may be defrayed by using imagery for multipurpose applications, and ensuring multiple-use licensing is important. However, with the availability of Sentinel-1 and -2 and Landsat-8 medium-resolution imagery reduces the data proportion of the costs and supports shifting from imagery to processing and field data collection and validation activities. Such costs must be set against the increased efficiency of the resulting statistics, the efficiency gains in the practical and logistical execution of field operations and the potential to share costs with other applications.

The costs of verification using high- and VHR data may reduce the costs of field validation; however, it does not eliminate the field survey components, although it can make these more efficient by removing the need for field-based measurements where the field enumeration is supported by GIS and contemporary image products for field area measurements.

Hardware and software are mostly one-time costs. The distribution of the costs among resources for operating an agricultural monitoring system based on remote sensing or GIS is illustrated in figure 1.

FIGURE 1. DISTRIBUTION OF COSTS WITHIN AN AGRICULTURAL MONITORING SYSTEM BASED ON REMOTE SENSING OR GIS.

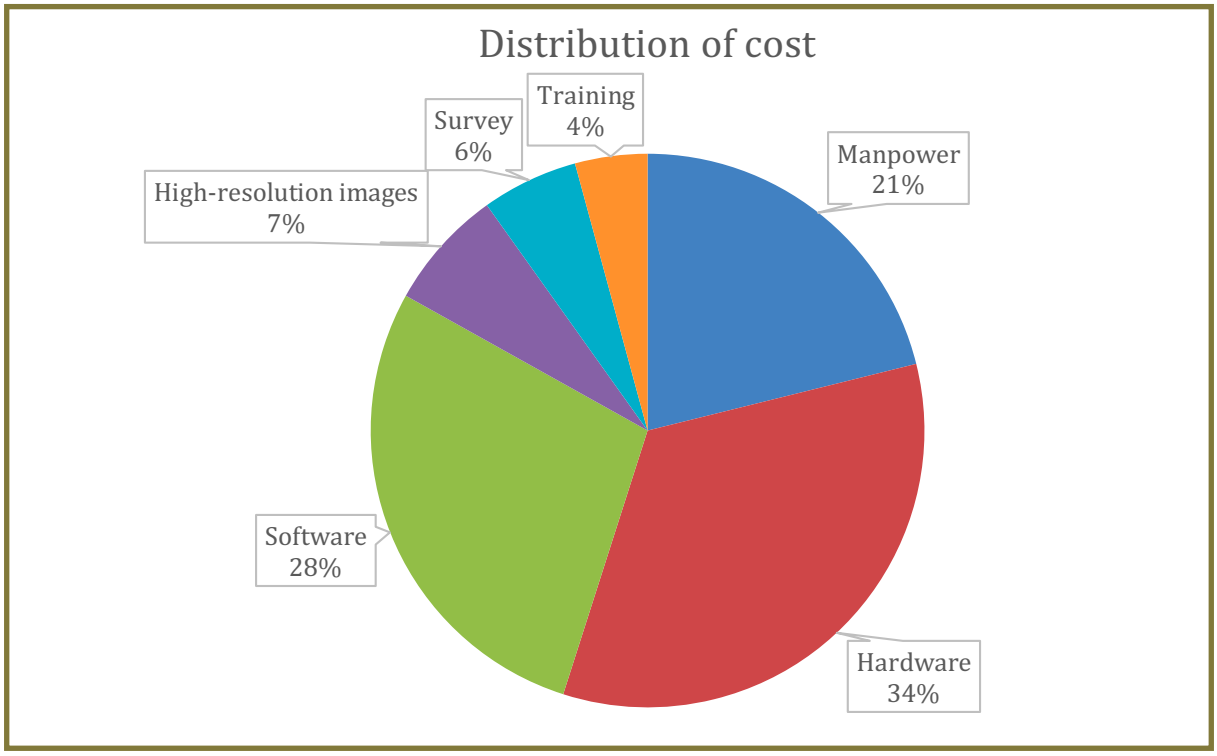

This distribution may vary from country to country, crops to crops, and by season and project area.

The United Nations (UN) has developed a series of purchase agreements with key image providers, including MacDonald Dettwiler (MDA, for QuickBird, IKONOS, WorldView-1, WorldView-2, GeoEye-1, WorldView-3, KOMPSAT-2, KOMPASAT-3, ZY-3 and RADARSAT-2) and Airbus DS Geo (the images of which are derived from TerraSAR-X, SPOT 6/7 and Pleiades). In the context of humanitarian actions, the image sources are also available through the International Charter for Space and Major Disasters[1]. Integrating national agricultural monitoring with the FAO/WFP CFSAM (*Crop and Food Security Assessment Mission*) assessment missions provides technical assistance to crop production forecasts.

8.4. IMPLEMENTATION OF THE PROGRAM: CASE EXAMPLES

FAO programmes supporting land cover mapping provide examples of the application of multiple scales of remotely sensed data to agricultural statistics. Applications in Ethiopia, Pakistan, Afghanistan, and Bangladesh have created national land cover databases from high-resolution imagery and supported the integration of products into agricultural surveys, capacity development, training and IT systems development. An example from Rwanda illustrates the use of VHR aerial orthophotographs as the basis for multiple frame surveys. Recent FAO Land Cover Classification (LCCS) standardized land cover mapping in Pakistan (in particular, in the Sindh and Punjab, Khyber Pakhtunkhwa, Baluchistan and FATA provinces) and in Afghanistan provide the relevant inputs to area frame development. However, even with existing land cover data, it is necessary to evaluate the suitability of the data to support the stratification (for example, based on crop percentage classes). Existing land cover data may only be suitable for stratification if it is of a suitable resolution, maintains certain classes and is relatively recent compared to the rate of change within the landscape.

8.4.1. Example 1: Ethiopia – application of area frame stratification

A key use of geospatial and remotely sensed data within agricultural statistics occurs at the design level: that is, area frame and stratification and sample selection (Carfagna, 2013). The Central Statistical Agency (CSA) of Ethiopia has used traditional list frame sampling (based on the list of Enumeration Areas, or EAs) as the basis for field- and household-based agricultural surveys. It was recognized that this approach has limitations: the raising factors rely on the number of households (HHs) rather than on the cultivated areas, and there are non-sampling errors of missing fields. The CSA conducted a comparative evaluation of list- and area-frame-based approaches in the 2008–2009 meher season (the rainy season from June to October). The area frame was based on EAs as the Primary Sampling Units (PSUs) and were the same as those used for population census surveys conducted with approximately 150 to 200 HHs, which were digitized in GIS. Stratification of the PSU was undertaken on the basis of the percentage of cropped area that was created by the manual interpretation of the remotely sensed data (National Statistical Methods Programs for Agriculture in Ethiopia, 2008).

The EAs were categorized into five classes (zero cropped areas and four equal interval classes up to 100 per cent cropped); the stratum comprising zero cropped areas was excluded from the survey, although this may introduce bias in cases where there is marginal production (such as in forest cropping or urban agriculture). The initial evaluation (conducted in West Shewa) used manual interpretation of images to derive the cropped area within each

1 https://www.disasterscharter.org/web/guest/home;jsessionid=E8C6DFA7B8CEDD1D3C1622415CA623C6.jvm1.

EA. Although the process did not initially use image segmentation and full land cover mapping, subsequent tests (held in Oromiya) employed a land cover classification system using the FAO LCCS (Di Gregorio et al., 2005) methods. The LCCS-based approaches offer repeatability, a level of automation and consistency resulting from the adoption of ISO standards (19144-2).

GIS technology was used to develop the Secondary Sampling Units (SSUs). These were derived by splitting the EAs into land units of 40 ha each based on the image interpretation of boundaries to match the assigned number of SSUs.

Sample selection was based on a two-stage process: PSUs (EAs) were proportionally allocated to strata and sample EAs were then selected in each stratum on the basis of probability proportional to size (PPS; that is, the assigned number of SSUs in the EA). SSUs were only generated within the selected PSU. For the 2009 survey, in the chosen EA, two "segments" were selected by random sampling. Image maps of the selected segments were produced to support the ground survey conducted by the enumerators.

8.4.2. Example 2: Pakistan – Crop Reporting Services

The Crop Reporting Service (CRS) of Pakistan provides an example of a comprehensive service working under the Secretary of Agriculture to provide crop information to the Pakistani Federal Government and Federal Bureau of Statistics, provinces, the Punjab Bureau of Statistics, universities, agricultural researchers, the Agriculture Extension Food Department, and other bodies. The approach has evolved, from being originally based on revenue surveys to the current conduction of area frame surveys supported by geospatial processing and remote sensing. The CRS was organized at the provincial level and supported by statistical officers at tehsil level, with statistical assistants and crop reporters working in area frame villages. The service employs 1 611 professional staff with degrees in statistics, economics and mathematics and operates in Punjab, Sindh, Khyber Pakhtunkhwa and Baluchistan. The CRS receives proportional provincial normative finance based on the size of the individual provinces in which it is active; this is supplemented by project-level activities.

Capacity development is part of the programme, with refresher courses at the beginning of the rabi and kharif seasons provided by the former Ministry of Food and Agriculture or by the federal and provincial bureaus of statistics.

The methods, tools and techniques have evolved since the early opinion surveys run by the Revenue Department, which were conducted until the mid-1950s. Subsequently, crop cutting was used as the basis for estimation of crop yields. The Ministry of Food and Agriculture and the Federal Bureau of Statistics developed a statistics-based sample frame for crop area and yield estimation. This was based on land revenue records for 1973–1974 acquired from the Land Revenue Department in 1978. This data provided the basis for stratification, with administrative boundaries as the PSUs stratified by village size classes. From 20 to 40 villages were selected in each district in wheat producing areas to provide the Wheat Frame. This approach was subsequently extended to other cropped areas as the Village Master Sample. The sampling structure was developed by the Federal Bureau of Statistics and subsequent surveys were undertaken by the CRS within the province.

This system was applied to cover cotton (550 villages), sugarcane (450 villages) and rice (550 villages). One crop reporter (frontline person) was stationed in one or more area frame villages to carry out seasonal field surveys and report the crop area sown under crops from these surveys. The crop yield was estimated from three random samples, each of which was replicated twice. These estimates were used to work out crop area and yield at district level. The area for the initial crop production forecast was taken from the CRS. However, for final estimation, the crop area was acquired from the Revenue Department and the yield was taken from the CRS.

Currently, the overall system presents a combination of objective and subjective techniques. Subsequent development of the sample frame in 2004 by the FBS (Federal Bureau of Statistics) was based on a multiple cropping area frame that included wheat, cotton, rice, sugarcane and maize. A sample frame for small-acreage crops (such as mango, citrus, potato, gram, moog lentil and mash) was developed with the former Federal Ministry of Food and Agriculture in the late 1990s.

TABLE 5. TECHNIQUES FOR IDENTIFICATION OF CROP COVERAGE.

Technique Type	Season	Crop covered
Objective	Rabi	Wheat, gram, potato, lentil, onion, oilseeds, maize spring, citrus
	Kharif	Cotton, rice, sugarcane, maize autumn, sesamum, guarseed, moong, mash, groundnut, mango
Subjective	Rabi	Barley, matter pulses, tobacco, garlic, chillies, tomato, turnip, banana, guava, dates, grapes, rabi, fodders, rabi condiments and other rabi fruits, vegetables and pulses
	Kharif	Bajra, jowar, turmeric, oilseeds, other Kharif pulses, lady finger, Kharif fodders, other Kharif fruits and vegetables

8.4.3. Example 3: Pakistan – the SUPARCO/FAO operative geospatial unit

FAO and SUPARCO have been jointly developing a new integrated Agricultural Information System (AIS) at federal level, supported by remote sensing and geospatial technologies and dissemination tools. The objective is to develop a consolidated, reliable and timely method of delivering a unified official set of agricultural statistics. The programme has developed a robust system for crop area estimation, area frame development and procedures for distributing agricultural statistics to stakeholders and decision-makers.

Crop area estimation is based on the image processing of satellite data acquired for a specific time, the conduction of ground truth surveys during cropping season, the collection of crops signature, the execution of laboratory processing, and an assessment of accuracy assessment. These activities are supported by the SUPARCO receiving station facilities. Countrywide acquisition of satellite imagery is undertaken done for rabi (spring) and kharif (autumn) crops, twice at the following stages:

- First, at four weeks after the completion of sowing (June–July for kharif crops and December–January for rabi crops);
- Second, at eight weeks after completion of sowing (August for kharif crops and February for rabi crops).

Extensive groundtruthing was undertaken with the support of real-time GPS navigation. Field sample classifications were used to supervise the maximum likelihood classification of the multidate imagery acquired using ERDAS image processing software.

Area frame development was based on remote sensing and GIS processing from imagery acquired from February and September, and was used to develop the strata based on vegetation intensity and visual interpretation of land cover into ten classes. Pakistan was divided into ten zones, of which 4 were in Punjab, 2 in Sindh & Khyber Pakhtunkhwa and 1 in Baluchistan. The sampling strategy assigned PSUs and SSUs. The SSUs were assigned serpentine numbering and used to ensure spatial distribution across the zones identified. Twenty to thirty segments of 30 ha approximately each were selected across each stratum, for a total of 379 segments in each region.

Based on the area frame sample design, Raising Factors (RFs) were developed to estimate the crop area sown in each stratum in each zone. The RF values helped to determine the crop area sown under various crops, by means of a statistical design. A critical examination of the data generated was made by a team of experts in the fields of agronomy, remote sensing and statistics to standardize the technique through image classification and historical trend lines. Dissemination of information is a key component of the SUPARCO/FAO satellite-based crop monitoring system, with monthly crop bulletins including information on VIs depicting crop growth pattern, fertilizers and irrigation availability, the agro-meteorological situation during the cropping seasons and crop yield and production forecasts or estimates for different seasons. Bulletins are distributed in paper and online[2]. Within the scope of the programme, four distribution mechanisms and tools have been developed: the Crop Information Portal; the satellite-driven Global Agricultural Monitoring for Pakistan (GLAM); the Mobile Agricultural Geo-Tagging Information System (MAGIS) and the Area Frame Sampling System (AFSS).

CROP INFORMATION PORTAL

The Crop Information Portal is a web-based, open-source platform developed to support the analysis and dissemination of Pakistan's crop data and related climatic, agronomic, hydrologic and economic variables.

The Portal allows for the advanced filtering of the data archive based on a combination of user-defined spatial and temporal parameters, to focus on specific crops, agronomic or environmental factors, which are stored into the system to produce standard outputs such as summary tables, maps, charts and user-defined reports. The portal integrates other records for water, fertilizer, agrometeorological information, market prices and crop status modules to support the broader agricultural information system.

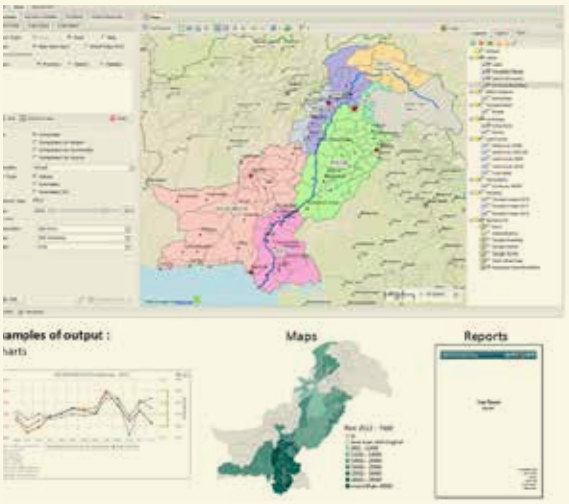

GLAM

Pakistan's GLAM is a MODIS-based web portal designed and implemented by the University of Maryland (United States of America) for direct access to web-based MODIS vegetation conditioning and anomalies analysis at different spatial and temporal scales. GLAM aims to enhance the capacity of the provincial CRS to issue improved timely forecasts on crop conditions and production.

The system includes the definition of different input parameters, image visualization and graphical interpretation of vegetation conditions. Input parameters include a MODIS composite product which is 8-day and 16-day angular normalized product. This portal is integrated with vector data layers to carry out vegetation condition monitoring at provincial, divisional and district level. Moreover, it provides tool for AOI-based rectangular grid analysis of vegetation anomalies ranging from 0.25 km2 to 4 900 km2. Another crucial feature of Pakistan's GLAM is its capacity to automatically generate NDVI and NDWI profile graphs from MODIS and its histogram analysis.

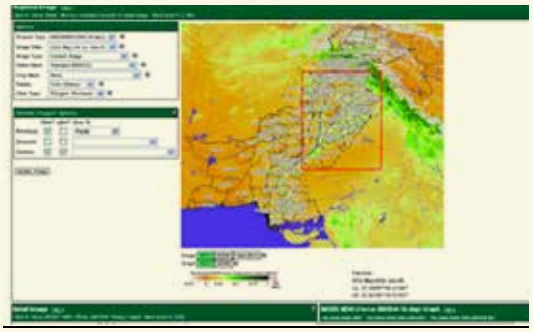

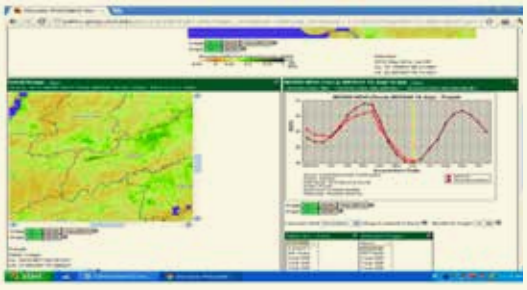

2 http://suparco.gov.pk/webroot/pages/pak-scms.asp.

MAGIS
MAGIS is a mobile-based application developed to support Pakistan's CRSs and their crop reporters in improving data collection efficiency as related to the list frame.
MAGIS enables the collection of digital and georeferenced data in the field and relays these data via cellular phone network or the Internet to the central MAGIS server at the CRS head office, and makes it accessible to statisticians for further analysis and reporting.

AFSS
The CRS gathers information on crops and other related parameters within segments for both rabi and kharif cropping seasons. The AFSS GPS-enabled smartphone application replaces past paper-based forms, allowing for validation of records in the field, ground photography and combination with RS imagery for the spatial data capture of areas. The AFSS has been trialled for field data capture in the AFS in Punjab and Sindh provinces, and has been proven to enhance the efficiency and accuracy of data capture and syncing with backend databases for effective record management.

The benefits of implementing a remote-sensing-supported crop estimation system include:

i. The creation of rigorous agricultural and rural survey methods and tools, which increase the quality (timeliness, precision, accuracy, reliability and cost-effectiveness) of the sampling effort and results in Pakistan at the provincial level and which improve the overall national estimation of crop acreage, yield and production.
ii. The development of human resources and technical capacities in four regional CRS units and two major agricultural universities in the utilization of new remote sensing and geospatial technologies, and statistical methods for data collection and for production of agricultural statistics and dissemination of crop information. The CRS provincial units are capable of operating effective crop monitoring services.
iii. Integration of mobile applications into the crop monitoring workflow, which provides significant new capacities for in-field data capture and measurement improvements, data validation and CAPI interviewing capabilities. The back-end synchronization of data allows for remote operation and rapid record validation and postprocessing.
iv. Development of a customized web-based information analysis and data delivery system and creation of a single relational database for crop assessment, for use by CRS crop analysts.
v. Demonstration of how cooperative use and sharing of field data, imagery data, and derived data enhance crop estimation and forecasting to serve as a knowledge base for other entities in Pakistan contemplating the integration of remote sensing, GIS, area frame, and related practices into their agricultural statistics.
vi. Development of protocols and procedures to address potential future decommissioning or introduction of new satellite platforms, as well as modifications to data configurations to ensure the continuity of operations or reasonable transition or migration.

8.4.4. Example 4: Bangladesh – an operational geospatial unit

This example illustrates the multiple possible uses of data created for purposes other than crop monitoring, which – through collaborative actions – make available a satellite-derived national land cover map suitable for area frame construction and support to crop reporting. Such initiatives enhance the cost-effectiveness of the crop reporting activities.

FAO, together with private organizations, governmental institutions and universities in Bangladesh, is developing a national land cover data set to be used as a baseline product for several applications, including environmental monitoring and assessment of potential agriculture productivity within the context of research on the impact of various climatic scenarios.

The stages to create a land cover data set include the development of technical and human resources:

- Capacity-building
- Team definition and roles
- Legend definition
- Satellite image selection and acquisition
- Image preprocessing
- Object-based segmentation
- Interpretation
- Quality control and final release

8.4.4.1. Training

Training and capacity development, supported by FAO, included the development of a new land cover legend using the Land Cover Meta Language (LCML) ISO standard and the Land Cover Classification System (LCCS3) tool, as well as a workshop to produce a National Reference System against which to define the overall reference land cover classes and attributes necessary to identify the land cover legend for Bangladesh. Professionals from various local institutions participated in the workshop, including representatives of the Bangladesh University of Engineering and Technology (BUET), the Center for Environmental and Geographic Information Services (CEGIS), the RIMS unit of the Forestry Department of Bangladesh, the Bangladesh Society of Geoinformatics (BSGI) and the Bangladesh Space Research and Remote Sensing Organization (SPARRSO).

8.4.4.2. Team definitions

National land cover mapping is a complex task that requires the establishment of a number of groups with specific competences and skills. The list of units that have been identified are the following:

i. A geospatial (GIS) unit;
ii. Photointerpreters;
iii. A technical support unit; and
iv. A quality

The **GIS unit** is responsible for all activities relating to the management, storage, analysis and dissemination of the geospatial information requested and produced during the development of the land cover product. It provides support to the photointerpreters for editing and other GIS-related tasks and for managing the ancillary information required for image analysis, including support on the available satellite imagery.

The **photointerpreters** undertake the majority of the land cover mapping. Supervised by a technical leader, they are responsible for the visual or semiautomatic classification of the imagery, to code it to the land cover polygons generated by the segmentation process.

The **technical support team** is responsible for providing training and support to the technical supervisor and to the photointerpreters. The team provides technical solutions and workflow productivity.

The **quality control team** is responsible for critically reviewing the interpretation of the land cover. It can comment upon or reject the interpretation.

In addition to these units, **IT support** is required to manage the hardware, software, backups, licenses and any other related issues.

8.4.4.3. Legend definition

Legend definition is a critical component of the process and is based on a number of criteria:

i. Availability and quality of satellite imagery procured, and ability of photointerpreters to distinguish individual classes;
ii. Availability of ancillary information (such as field surveys and data sets from other mapping projects);
iii. Representativeness of the classes in the country; and
iv. Requirements of the specific classes for the product's overall objectives and intended applications.

The land cover classes have been identified from an analysis of the diagram of the National Reference System. The classes identified are then described using the LCML ISO standard.

8.4.4.4. Satellite image selection and acquisition

The selection of the image satellites to be used for land cover mapping requires a number of factors to be balanced: the available budget, the quality of images across the year, and the land cover classes to be identified. For Bangladesh, the main cropping season occurs during the monsoon season, which is heavily affected by clouds. Interpretation of the drier season facilitates the interpretation of natural and cultivated woody vegetation, which clearly stands out from bare non-vegetated land. For this reason, a combination of high-resolution optical imagery (SPOT6/7 at a spatial resolution of 6 m) in the dry season and multitemporal radar imagery (Sentinel-1) SAR data for the rainy season have been selected, as they are unaffected by meteorological conditions.

8.4.4.5. Image preprocessing

Image preprocessing was required to prepare the images accessed for further analysis. This includes band composition, image mosaicking, re-projection, format changes, and changes in pixel depth. It also includes techniques for image enhancement and cloud and noise removal. The processing requirements for SAR imagery were different from those for optical sensors, thus requiring extended processing skill sets.

8.4.4.6. Object-based segmentation

The preprocessed images were segmented with a multiresolution algorithm to generate a layer with unclassified vector polygon objects. In this step, the most critical factor was the selection of the segmentation parameters used by the algorithm to apportion and segment the input images. There were no specific settings to suggest, because these depend on many factors and require several tests to be conducted until the objects to be identified have been segmented to provide the level of resolution and discrimination associated with the classification legend.

8.4.4.7. Interpretation

Interpretation is the phase during which photointerpreters assign land cover codes to the polygons. This time-consuming task was carefully planned and monitored to ensure standardized interpretation in case manual techniques are applied. A preliminary automatic interpretation based on the spectral and shape characteristics of the objects and on training data sets of classified areas may be used to run supervised classifications. A multitemporal analysis was conducted to extract averages values within each object (such as NDVI values) that can be used in statistical clustering techniques to select similar vegetation patterns.

8.4.4.8. Quality control and final release

The accuracy assessment was based on a series of checkpoints at which the classification and quality control procedures were verified across the entire interpretation process, to ensure that the land cover data set met the quality results and consistency expected. The final structuring of the data set was applied, including metadata and data documentation.

8.4.5. Example 5: Rwanda – multipurpose probability sample surveys

Based on VHR (0.25m) orthophotographs, the National Institute of Statistics of Rwanda (NISR) has designed and implemented multiple frames for the country (spanning an area of 26 000 km2), combining an area frame and a list frame to support the national agricultural statistics. The multiple frame accommodates 560 specialized farms producing commodity crops that are significant in terms of national economic agricultural estimates. The specialized farms are added as a list frame and are fully enumerated, and therefore do not contribute to sample errors; they are also included in the area frame. The importance of standardized terms (such as “farm”, “farm parcel”, “field”, “farmer”, “hired manager” and “respondent”) are emphasized in terms of consistent agricultural surveys and have employed FAO ontologies (FAO, 2015).

The first stage in the survey design is to define the objectives of the agricultural survey, to ensure that the required levels of accuracy may be reached. Typically, questions that support the design include:

i. What are the objectives and expectations of the survey?
ii. What definition of “farm” is used?
iii. Which agricultural variables should be surveyed, and over which time scales and periodicity (for example, seasonality)?
iv. Which agricultural commodities surveys are considered inadequate and therefore the focus of the new survey?
v. What are the required levels of accuracy?
vi. At what level will the data be summarized: country, state, region, watershed, etc.?

The objective of the Rwandan survey was to provide a national, seasonal and multipurpose (crop, livestock, forest and commodities) agricultural survey, covering a range of variables for each farm:

i. Planted and harvested area, area intended for planting, potential and actual crop yield of each crop or variety of crop, crop production and number of trees;
ii. Livestock and poultry inventories (for example, number, type, age, sex, breed and use);
iii. Production of milk, eggs, honey and seeds;
iv. Number and types of farming methods and agricultural inputs, including labour, type and quantity of seeds, fertilizers and pesticides, source of irrigation water, drainage, extent of shifting cultivation, stocks, machinery, equipment and agricultural buildings;
v. Number and types of farms (for example, number, location, legal status and land tenure);
vi. Costs of production and value of sales;
vii. Population involved in agriculture (such as the basic demographic characteristics of the farmer, farmer's household members working on the farm, hired workers on the farm, and days of work).

The area frame was based on the land use strata within the 30 districts; the strata were subdivided into non-overlapping "segment" sampling units (SUs), each of which was subdivided into non-overlapping tracts. A tract was defined as the land area of a farm inside a segment, or the land area that does not belong to any farm. The total survey area was entirely subdivided into non-overlapping tracts. The segments and tracts used recognizable physical boundaries or fields to support unambiguous identification by the enumerators. The survey reporting unit for each variable consisted in the farm tractor non-farm tracts. The Rwandan probability sample survey was based on a stratified cluster sample survey that used a systematic sample drawn from PSUs combining an area frame and a list frame of specialized farms (a multiple frame). Enumeration was by interview, using paper forms to collect the abovementioned variables. The interview covers selected tracts, disregarding those of non-agricultural land (for example, wasteland or water); it is intended to add CAPI survey tools and GPS to support data collection.

Area frame construction can be based on different land use strata (proportion of cultivated land, special agricultural practices, predominance of certain crops, and average size of cultivated fields) with boundaries that can be located on the ground. Within each stratum, the PSUs are ordered by similarity and selected on the basis of PPS; within the PSU, segments are selected with equal probability. The measured area of each PSU was used to determine the total number of SSUs in each stratum and in the entire frame, without the need to map each segment. Orthorectified photographs (printed at a scale of 1:1 000) for each segment selected were used to identify and measure agricultural areas by the enumerators; however, they are not currently used in digital format in the field. The areas of the fields within the questionnaire surveys may be provided by farmers during interviews or drawn on the photographs, although more accurate assessments of the field areas may be achieved by mapping against the orthophotography combined with mobile GIS technology. The supervision of the survey was facilitated by the area calculations based on the imagery.

The design of the area sampling frame was used to provide formulae for the direct expansion and variance calculations for the closed, weighted and open segment estimators. The area sample design ensured that the total number of segments was known for each strata and PSUs and that the probability of selection of each segment was equal to its conditional probability in two-stage sampling. The direct expansion sample estimate of a total for each survey variable was based on the formula:

$$Y_c = \sum_{h \in S} \sum_{j \in B_h} \sum_{k \in G_{hj}} e_{hjk} \sum_{m \in T_{hjk}} t_{hjkm}$$

where:

Y_c = sample estimate of a total for the survey variable y
S = set of all land-use strata
B_h = set of all substrata in stratum h
G_{hj} = set of all segments in substratum j of land-use stratum h
T_{hjk} = set of all tracts in segment k of substratum j or land-use stratum h
e_{hjk} = expansion factor for all tracts in segment k
t_{hjkm} = tract value for the variable y associated with tract m

8.5. CONCLUSION

Remote sensing applications and their integration with GIS have made crop monitoring operations simpler, quicker and more accurate. The integration of these techniques and data into area sampling frame construction, stratification, and field data collection procedures is changing the way in which crop estimation tasks are executed. The multipurpose use of remotely sensed imagery and the generation of derived products within agricultural statistics, such as land cover maps, enables effective and cost-efficient processes to integrate satellite data into crop area and yield estimation activities. The use of such data in agricultural statistics relies on a set of fundamental organizational aspects, resource and thematic image processing efforts, sampling activities, field data collection, and geospatial and statistical competencies. It also relies on collaboration between the agencies responsible for the components that make up the agricultural monitoring and reporting community, including the statistical services, mapping agencies, satellite agencies and thematic user agencies. Integrated programmes such as Pakistan's AIS and related developments, provide examples of coordination of the image processing, sampling and field survey support and dissemination of information to users and comprehensive interfaces for decision-makers. Collaborative programmes with multiple objectives further support the use of satellite imagery and the potential to use image analysis for wider area assessment, also covering conditions such as natural hazards (including floods, drought and landslides) and their impact on crop production.

8.6. REFERENCES

Bell, K.P. & Dalton, T.J. 2007. Spatial Economic Analysis in Data-Rich Environments. *Journal of Agricultural Economics*, 58(3): 487–501, 09.

Carfagna, E. 2013. *Using satellite imagery and geo-referencing technology for building a master sampling frame*, Invited Paper for the 59th World Statistical Congress, Invited Paper Session (IPS110) on "Developing a master sampling frame for integrated survey", pp. 1078–1083, Hong Kong, 25–30 August 2013. International Statistical Institute, The Hague, The Netherlands. Available at: http://2013.isiproceedings.org/Files/IPS110-P1-S.pdf.

Carfagna, E. & Gallego, F.J. 2005. *Using Remote Sensing for Agricultural Statistics*. International Statistics Review 73(3): 389–404.

Carfagna E., Pratesi, M. & Carfagna, A. 2013. *Methodological developments for improving the reliability and cost-effectiveness of agricultural statistics in developing countries*, the 59th World Statistical Congress, Special Topic Session (STS043) "Using geospatial information in area sampling and estimation for agricultural and environmental surveys", pp 1930 – 1935, Hong Kong, 25–30 August 2013. Available at: http://2013.isiproceedings.org/Files/STS043-P1-S.pdf.

Delincé, J. 2017. Cost-effectiveness of remote sensing in agricultural statistics. In Delincé, J. (ed.), *Handbook on Remote Sensing for Agricultural Statistics* (chapter 9), Global Strategy Handbook: Rome.

Food and Agriculture Organization of the United Nations (FAO). 2015. *Implementing the Global Strategy at Country Level: Pilot Experience of Sample Country – Rwanda*. Paper presented at the Twenty-Fourth Session of the African Commission on Agricultural Statistics, 1–4 December 2015. Kigali. Available at: http://www.fao.org/fileadmin/templates/ess/documents/meetings_and_workshops/AFCAS24/en/5d__Eng_.pdf.

Global Strategy to improve Agricultural and Rural Statistics (GSARS). 2015. *Handbook on Master Sampling Frames for Agricultural Statistics: Frame Development, Sample Design and Estimation*. GSARS Handbook: Rome. Available at: http://gsars.org/wp-content/uploads/2016/02/MSF-010216-web.pdf.

Hinzman, L.D., Bauer, M.E. & Daughtry, C.S.T. 1986. Effects of Nitrogen fertilization on eflectance Characteristics of Winter Wheat. *Remote Sensing of Environment,* 19: 47–61.

Ishimwe, R. & Manzi, S. 2015. *Current and Future Activities to Improve Stratification for Seasonal Agriculture Surveys in Rwanda*. National Institute of Statistics of Rwanda (NISR) Publication. Available at: https://www.geotechrwanda2015.com/wp-content/uploads/2015/12/186_Roselyne-Ishimwe.pdf.

Manzi, S. 2013. *Seasonal Agricultural Survey (SAS): The Overview of the Multiple Frame Survey in Rwanda*. Presentation. Available at: http://www.fao.org/fileadmin/templates/ess/documents/afcas23/Presentations/AFCAS_5b2_WCA2010_Rwanda.pdf.

Murray, H., Lucieer, A. & William, R. 2010. Texture-based Classification of sub-Antartic Vegetation Communities on Heard Island. *International Journal of Applied Earth Observation and Geoinformation*, 12(3): 138–149.

Quarmby, N.A., Milnes, M. & Hindle, T.T. 1993. The use of multi-temporal NDVI measurements from AVHRR for crop estimation and prediction. *International Journal of Remote Sensing*, 14(2): 199–210.

Wiegand, C.L. & Richardson, A.J. 1984. Leaf Area, Light Interception, and Yield Estimates from Spectral Components Analysis. *Agronomy Journal*, 76(4): 543–548.

Wiegand, C.L. & Richardson, A.J. 1990. Use of Spectral Vegetation Indices to Infer Leaf Area, Evapotranspiration and Yield: II Results. *Agronomy Journal*, 82: 630–636.

9

Chapter 9

The cost-effectiveness of remote sensing in agricultural statistics

Jacques Delincé

The cost-efficiency of using remote sensing in agricultural statistics is best evaluated by comparing the gains obtained (usually expressed as a reduction of sampling variance) to the additional costs involved (cost of imagery, data analysis, staff training, and investment in hardware and software). Noteworthy solutions in this respect are suggested by Carfagna (2001, 2013), Nelson *et al*. (2007), Tenkorang and Lowenberg-DeBoer (2008), Miller *et al*. (2012), Gallego (2014) and Delincé (2015).

9.1. THE ISSUE OF COSTS

The costs relating to the use of remote sensing can be broadly divided into two categories: the costs of image purchase and the costs arising from data treatment (purchase and maintenance of hardware and software, recruitment of staff, and training). Hardware and software costs have drastically decreased in recent years because open-access software is now widely available. With cloud-based image analysis having become a standard, low-cost personal computers and disk storage allow for the analysis of very large image data sets. However, attention must be paid to staff availability and competence (Latham, 2017). Expertise in Geographic Information Systems (GIS), image analysis, statistics, yield modelling, agrometeorology, soil science and crop science will require a team of specialists possessing the relevant multidisciplinary qualifications, training and experience. The majority of costs will be incurred in this respect.

Currently, high-, medium- and low-resolution imagery is freely available in raw format and as derived products, such as geometrically (RMS 1.5 pixels) and radiometrically (top of atmosphere) rectified imagery, vegetation indices, regional or country mosaics, and periodic cloud-free coverage. Thanks to initiatives undertaken by the National Oceanic and Atmospheric Administration (NOAA), the U.S. Geological Survey (USGS) and the European Space Agency (ESA), vast real-time freely accessible depositories allow for downloading or online processing of what the United Nations Security Council considers to be the Big Data challenge (2015). The most important websites are:

- Google Earth Engine (GEE), at https://earthengine.google.com/, for real-time data from MODIS, Landsat, Sentinel-1, 2 and 3, as well as archive Globeview/Airbus very high resolution (VHR) imagery
- USGS Earth Explorer, at http://earthexplorer.usgs.gov/, for Landsat/MODIS data
- USGS WELD, at https://landsat.usgs.gov/WELD.php, for archive Landsat 7 and 5 data
- Australian Geoscience Datacube (AGDC), at http://www.datacube.org.au/, covering Australia only
- ESA data hub, at https://scihub.copernicus.eu/, from which Sentinel 1, 2 and 3 data can be downloaded
- JRC-SPIRIT database, at http://spirits.jrc.ec.europa.eu/download/downloaddata/, containing worldwide ten-daily agrometeorological data from ECMWF, CHIRPS and TAMSAT
- FAO-GIEWS METOP/AVHRR indicators – in particular, the Agricultural Stress Index (ASI), at http://www.fao.org/giews/earthobservation/asis/index_1.jsp?lang=en

Only VHR imagery with a ground sampling distance (GSD) lower than 5 m should be purchased. The offers of the following three providers are based on a satellite constellation: Rapideye, with a resolution of 5 m and four bands at a price of US$1/km2; AIRBUS-SPOT with a resolution between 2 m and 8 m, and five bands at a price of US$3.5/km2; and Worldview, with a resolution of 31 cm and eight bands at a price of US$20/km2. In addition, since 2010, newcomers to the market such as Terra bella, Planet, Satellogic and Blacksky Global have been operational with flocks of "microsatellites" targeting a multispectral resolution of 1 to 2 m; however, to date, they have not succeeded in offering sufficiently competitive prices.

Readers seeking a more detailed description of the characteristics and prices of sensors may find a complete review in Delincé (2015, chapter 6).

9.2. THE DOMAINS OF APPLICATION AND THE RELATIVE GAINS

Bearing in mind that remote sensing is capable of making various contributions to agricultural statistics, the cases to be examined will first be described briefly.

9.2.1. Optimization of sampling design

The major and cheaper use of remote sensing occurs in the improvement of the sampling design of agricultural censuses or surveys. In these cases, the natural approach is to use recent imagery (Global Strategy, 2015) or even land cover maps derived from imagery (Waldner *et al*., 2015). At the outset, the material obtained through remote sensing will at least enable the creation of reference maps upon which administrative limits can be univocally located.

- In a census approach, the work usually begins with a pre-enumeration mapping (the Enumeration Areas, or EAs, are the Primary Sampling Units – PSUs – of the census) and the identification, within the field, of households or holdings per EA sampled (the holdings or households are the Secondary Sampling Units, or SSUs). An efficient method to define EAs is the use of imagery (having a resolution from 0.5 m to 2 m) in a GIS environment, seeking to subdivide the entire territory into entities with physical limits corresponding to 50–100 holdings, such that one enumerator can collect the data relating to a subset of EAs during the census period (Geospace, 2007). Based on projects carried out in Lesotho, Namibia, the Seychelles and the United Republic of Tanzania (Loots, 2015), the significant savings that may be achieved in terms of time and fieldwork largely repay the costs of adopting the required technology (that is, imagery, GIS, expert consultancies and training). The general quality of the census also improves, because of the better planning, transparency and traceability of the work; in addition, all of the infrastructure created can easily be reused in subsequent efforts, which is of particular interest if a Master Sampling Frame (MSF) approach is adopted (Global Strategy, 2015b).
- In a regional survey approach, the two major paths available are: (1) to define four or five strata that are as internally homogeneous as possible, while being as different as possible from one another, or (2) to define the PSUs of a two-stage plan that are as similar as possible to one another, with a minimum of internal homogeneity. Design complexity can be enhanced by using probability-proportional-to-size (PPS) sampling or by adding further stages. Regardless of the master frame selected (list, area, point or multiframe), imagery is of the utmost help to achieve the intended goals, because it will provide up-to-date detailed information that is suitable for modern digital treatment. Additionally, even a rough image classification will enable obtaining a proxy for cropping intensity that can be used to optimize the sizes of the sampling unit (based on spatial correlation) and variable sampling fractions (based on the relation between sampling variance and agricultural intensity; see Benedetti *et al*., 2015).
- A first case to be examined is the Area Sampling Frame (ASF) of the June Agricultural Survey (JAS) of the National Agriculture Statistical Service of the United States Department of Agriculture (USDA/NASS). Traditionally, the frame consists of stratified PSUs which are composed of SSUs called "segments" (Cotter *et al*., 2010). First, all the territory is divided in PSUs with physical boundaries, through visual interpretation of satellite imagery (with each PSU being composed of six to eight segments). The PSUs are then stratified into agricultural classes intensity by photointerpretation. Finally, after samples have been extracted from the PSUs, the PSUs selected are subdivided into segments (the size of each being comprised within 2.5 to 21 km2). One segment is randomly selected per PSU sampled; therefore, the final JAS sample consists of approximately 11 000 segments (with the sampling fraction being of 0.2 percent). This approach, which Boryan *et al*. (2016) call "traditional", requires a total of 30 man-months of work per state. Recently, NASS has adopted an automated approach based on PSU delineation and stratification by automatic classification of the previous year's Crop Data Layers (CDLs). Therefore, the automatic approach now requires only 12 man-months of work per state, thereby decreasing the cost by a factor of 2.5. Computed on the 2013 South Dakota survey (which comprised 578 segments and a coverage of 199 730 km2), the traditional JAS frame has been compared to the automated frame, the survey data of which were simulated in two ways: first by extracting the segment land use from the declared Farm Service Agency's Common Land Unit (FSA-CLU); second, by extracting the land use from the CDL 2013 (Common Land Unit Crop Data Layers, or CLU-CDL).

TABLE 1. 2013 SOUTH DAKOTA TRADITIONAL STRATIFICATION (TS) VERSUS AUTOMATED (AS) STRATIFICATION: CROP ESTIMATES COMPARISON.

Crop	NASS Estimate (million ha)	Acreage Difference TS and AS CLU-FSA (%)	TS JAS CV (%)	AS CLU-FSA CV (%)	AS CLU-CDL CV (%)
Corn	6 200 000	6.74	4.9	4.3	3.9
Soybean	4 600 000	19.03	5	6.0	5.2
Spring wheat	1 190 000	47.10	17.6	14.3	13.3
Winter wheat	1 400 000	46.34	17.9	16.8	19

Boryan *et al.*, 2016

In both cases, the resulting sampling variances were of the same order of magnitude. However, it should be recalled that the costs of building the frame were divided by 2.5.

- This could be compared with the costs to be sustained in less developed countries when the traditional NASS methodology is used. For example, Morocco renewed its area frame over 66 900 km2 using SPOT 5 imagery at a resolution of 2.5 m. For a subset of 18 provinces (covering an area of 49 000 km2), access was available to a sample of 810 segments the sizes of which ranged from 4 to 30 ha (for a sampling fraction of 0.1 percent), leading to a relative precision of 1.8 percent for the acreages of cereals (1 950 000 ha), 4.1 percent for fallow land (650 000 ha) and 16.3 percent for pasture land (120 000 ha). It must first be noted that with a lower sampling fraction, the survey conducted in Morocco presents CVs that are two times lower than those of NASS for a similar crop extent. NASS uses imagery with a resolution ranging from 20 to 56 m, while in Morocco, the resolution is of 2.5 m and the total stratification efficiency for cereals amounted to 3, it may be seen that the type of imagery can be an important factor to consider when building a frame. From the point of view of costs, the stratified area frame construction amounted to US$7/km2 for the creation of the land use maps (50 percent for SPOT imagery, 15 percent for photointerpretation and 35 percent for field validation). The sample extraction costs were marginal because the dedicated GIS software cost US$20 000 and the time required amounted to ten days per province.
- Another comparison can be drawn with the area frame used by China's National Bureau of Statistics in ten provinces (covering 1 652 083 km2) using a stratified two-stage sampling design with PPS selection in the first stage (the size of each PSU ranging between 1 km2 and 5 km2) and random selection in the second stage (each SSU having a size between 2 ha and 5 ha, with a total sampling fraction in the order of 0.2 percent). For Anhui province (139 400 km2), a sample size of 6 000 segments leads to a CV of 1.3 percent for wheat (2 200 000 ha), of 0.9 percent for middle rice (1 900 000 ha) and of 3 percent for corn (1 000 000 ha). The good level of precision obtained results from the stratification and from the PPS sampling, based on the classification of GF1 and ZY3 Chinese satellite imagery (with a resolution of 2 m). The associated costs amount to US$75 000 per province, and therefore approximately US$0.5/km2.
- Frame creation and stratification can also be based on a Point Sampling Frame, making use of the satellite imagery available:
    - The Land Use and Cover Area Frame Survey (LUCAS), which was initiated over Europe in 2001, provides the opportunity to evaluate the advantages of stratification over imagery by comparing the initial systematic plan with the stratified plan used in 2006 (Gallego, 2007). For the area of EU cereals, the relative efficiency gain (resulting from the stratification itself and from the varying sampling fractions) amounted to 1.76; for common wheat and for barley, 1.64; for corn, 1.70; for potato, 1.44; for sugar beet, 1.60; and for sunflower, 2.01. Considering that the stratification was based on imagery available free of charge (aerial orthophotographs created for the Integrated Administrative Control System's Land Parcel Identification System (IACS LPIS) and the photointerpreter was able to analyse

approximately 500 points per day (1 million for the entire EU, which at the time comprised 25 Member States), it may be considered that the costs of the stratification amounted to approximately US$200 000 for a survey the annual cost of which was in the order of €3.5 million. Even if the multiannual use of the frame is not considered, dedicating 5 percent of project expenditure to image analysis is largely repaid by the reduction in the variances, ranging from 30 percent (potato) to 50 percent (sunflower).

- Haiti is another case study in which it is possible to evaluate the costs and benefits of using 50-cm resolution archive aerial photographs for establishing a point area frame. Approximately 1.7 million points located on a 125-m grid were photointerpreted (in 3 400 working days), enabling the creation of a stratified sample of 25 000 points (each representing approximately 1 km2). Conceived to be used for ten years, the additional cost of using imagery-based stratification amounted to 2 percent. However, it provided a decrease in variance by 8 to 38 percent for major crops, which illustrates the cost-efficiency of remote sensing for stratification in Haiti.

9.2.2. Crop Data Layers (CDLs)

CDLs were created by USDA/NASS 20 years ago. Described as costing US$75 000 per state in 1997, it has drastically improved over time in terms of the number of crop categories, map accuracy, dissemination tools and elaboration costs. Muller and Harris (2013) describe in detail the 2011 CropScape portal in terms of coverage (48 states), technical aspects (imagery and ground reference data) and the list of products, as well as the user community. Approximately 5 000 Landsat, Resourcesat and DMC scenes (available for free or at a low cost, lesser than US$0.10/km2) are classified every year and result in a CDL (with a scale of 1:100 000) which is distributed draft in August and frozen in February after harvest. The image processing and integration is based on ERDAS, See5, ArcGIS and SAS. CropSpace was developed externally (Yang, 2014) requiring 15 man-months for its development. It runs on two servers (32 GB and 1 TB of disk space respectively) under Apache, Tomcat, Mapserver, GDAL and PostgreSQL software. Although NASS does not release much information on the project's running costs, it clarifies that this public good meets the needs of the private agribusiness sector (in particular, relating to insurance, decision support and financial services).

9.2.3. Improved estimators

At estimation level, merging data from the ground survey and from satellites is usually achieved through regression or calibration estimators (Global Strategy, 2015a). Gallego *et al*. (2014) present detailed results for a northern region (78 500 km2) of Ukraine, containing 2.45 million ha of cropland. Ninety 4 km x 4 km square segments were field-surveyed in 2010 (with a sampling fraction of 1.8 percent and a field size up to 250 ha). Later, the entire region was covered with MODIS, Landsat5, AWiFS, LISSIII and Rapideye imagery. Image classification was trained on data collected along the road, independently of the area frame segments. For the major crops (wheat, barley, maize and soybean), the respective mean efficiencies amounted respectively to 1.59, 1.54, 1.48, 1.50 and 1.50; therefore, the sensors' performance was approximately equal. Comparing the cost of the field survey and the cost of imagery (today, the cost of image classification is so low that it can be set aside), the situation changes drastically, because only the two free-of-charge sensors (MODIS and Landsat TM) remain cost-effective, as the purchase price of the other three sensors make them inefficient (AWiFS 0.92, LISIII 0.43 and Rapideye 0.18). Some comments should be made to provide a general context to the study. First, field size in Ukraine tends to be large, allowing for coarse-resolution sensors to compare with finer-resolution ones in terms of classification accuracy. This would not hold in most African or Asian countries, where fields tend to be small. Second, this study relied only on the Maximum Likelihood Classification (MLC) method. Today, the USDA relies on the decision-tree classification method (See5); ESA, after testing various algorithms (support vector machines, decision trees, gradient-boosted trees and random forests) on 12 sites around the world (Inglada *et al*., 2015) will apply a random forest algorithm to its Sentinel-2

data delivery services. Finally, the availability of freely accessible imagery is increasing: not only are MODIS (250-500m) or Landsat 8 (15-30m) rectified or classified products (with resolutions in the range of 250 m to 500 m, and 15 m to 30 m, respectively) freely downloadable in near-real-time; also Sentinel 1 (SAR-GRD, 9-m resolution), Sentinel 2 (10-m resolution) and Sentinel 3 (300-m resolution) are now available from the ESA hub or Google Earth Engine.

9.2.4. Crop monitoring and yield forecast

Crop monitoring and yield forecast is usually performed using a recognized crop modelling system, such as DSSAT[1], BIOMA[2], APSIM[3], ORYZA[4], STICS[5], CERES[6], CROPSYST[7] or EPIC[8], many of which form part of the AGMIP[9] project (Rosenzweig *et al*., 2013). The choice of model depends mainly on the crops of interest, the region concerned and the open-access nature of the model. In any case, all models rely on the availability of:

- Administrative limits (GADM, at http://www.gadm.org/);
- Agro-ecological zoning (GAEZ, at http://gaez.fao.org/Main.html#);
- Cropland masks (Global Food Security Area Database at a resolution of 1 km: http://e4ftl01.cr.usgs.gov/provisional/MEaSUREs/GFSAD/; a Unified Cropland Layer at 250m: http://maps.elie.ucl.ac.be/geoportail/);
- Crop parameters (ECOCROP at http://ecocrop.fao.org/ecocrop/srv/en/home);
- Soil database (http://www.fao.org/soils-portal/soil-survey/soil-maps-and-databases/harmonized-world-soil-database-v12/en/);
- Real-time and archive agrometeorological databases (temperatures from GSDO: https://data.noaa.gov/dataset/global-surface-summary-of-the-day-gsod; radiation MERRA2 from http://disc.sci.gsfc.nasa.gov/datareleases/merra_2_data_release; rainfall from CHIRPS http://chg.geog.ucsb.edu/data/chirps/, SPIRIT – http://spirits.jrc.ec.europa.eu/download/downloaddata/ – or from FEWS: http://earlywarning.usgs.gov/fews or http://www.isac.cnr.it/~ipwg/data/datasets.html);
- Real-time and archive vegetation indices (METOP at http://www.eumetsat.int/website/home/Data/index.html; MODIS at http://modis.gsfc.nasa.gov/data/dataprod/mod13.php; or SEN3/VEG at http://land.copernicus.eu/global/products/ndvi); and
- Local management practices (available in the AMIS crop calendar, at http://www.amis-outlook.org/ or http://www.usda.gov/oce/weather/pubs/Other/MWCACP/).

Considering that most of the space products for yields monitoring are available free of charge, the costs will mainly derive from the running costs of the monitoring system itself and in the estimation of crop acreages.

Considering India's Mahalanobis National Crop Forecast Centre (http://www.ncfc.gov.in/), it may be seen that to issue periodical forecasts for eight crops, an annual budget of US$1.7 million is necessary to meet the costs relating to the offices, salaries (of 31 staff members), field surveys (10 percent of the total budget), imagery (20 percent of total budget), hardware (19 workstations) and software (ERDAS, ARCGIS, GEOMATICA STAT licenses).

Another example is CROPWATCH (http://www.cropwatch.com.cn/htm/en/index.shtml) of China's RADI. Its annual budget for regional crop monitoring in China and in the major production zones worldwide (covering 31 countries and representing 80 percent of the world production of maize, wheat, rice, and soybean), amounts to US$1.5 million.

1 Decision Support System for Agrotechnology Transfer Model.
2 Biophysical Models Applications Model.
3 Agricultural Production Systems sIMulator Model
4 Further information is available at http://oryza.com/.
5 Simulateur mulTIdiscplinaire pour les Cultures Standard.
6 Crop Environment Resource Synthesis Model.
7 Cropping Systems Simulation Model.
8 Environmental Policy Integrated Climate Model.
9 The Agricultural Model Intercomparison and Improvement Project.

Manpower costs (15 persons) represent approximately 35 percent of this total budget; those resulting from imagery data amounts only to 20 of the budget, thanks to interinstitutional data sharing; the rental cost of computers, networks and software is approximately 10 percent; and the cost of fieldwork missions, academic costs, meeting and travelling costs, logistics, etc. is of approximately 35 percent.

9.3. SENSOR SUITABILITY

Several examples confirm the efficiency of using remote sensing for agricultural statistics. An important factor to verify is whether the available satellites are adapted to the predominant sizes of agricultural fields in the various regions of the world. To answer this question, the data published by Fritz (2015) have been reworked. These data consist in a 1-km2 resolution map of cropland (arable land, permanent crops and permanent grassland) with five categories: no cropland, cropland with very small, small, medium and large field sizes. For cropland, the freely downloadable IIASA database provides a field-size interpolated map with a 1-km2 resolution. By using a country mask, it is thus possible to create a database providing the total number of pixels per country (country area in km2), the total cropland area and the area for each of the four field size classes. As these categories of field sizes are linked to the GEOGLAM recommendation for satellite monitoring of agriculture (see Waldner *et al.*, 2015, table 4), it is easy to derive the agricultural area per country that can be monitored by satellites with a ground sampling distance of 100 to 500 m (MODIS, Sentinel 3), 20 to 100 m (Landsat 5, AWiFS, DMC, DEIMOS)), 5 to 20 m (Sentinel 1 & 2), or less than 5 m (SPOT, Rapideye, LISS4, Worldview).

Agricultural monitoring has various facets (cropland areas, crop type acreages, or yield monitoring at regional or field levels). This enquiry will focus on the regional acreages of major crop categories (such as cereals), of other arable land, of permanent cropland and of permanent grassland.

TABLE 2. AREA (MILLION HA) PER FIELD SIZE BY CATEGORY AND REGION.

Region	Cropland	Very small	Small	Medium	Large
Africa	773.0	242.6	394.1	110.4	25.9
Middle East	107.8	9.0	70.0	26.6	2.2
Asia	1 411.6	472.5	673.1	179.3	86.7
Central and South America	665.8	21.7	154.5	295.9	193.7
Europe	1 165.9	14.0	281.2	532.8	337.9
North America	856.7	1.9	68.0	454.5	332.3
Oceania	130.5	0.0	9.8	34.3	86.4
World	**5 111.3**	**761.6**	**1 650.8**	**1 633.9**	**1 065.0**

As shown in table 2, the vast majority of agricultural land falls into the small- and medium-parcel size categories. The very-small-parcel category occupies only 15 percent of cropland at world level; Asia and Africa are less favoured from this point of view, as one third of the agricultural areas of both regions fall within the very-small-field size category.

Based on the above, it may be deduced that MODIS and Sentinel 3 sensors are adapted to monitoring the acreage of 21 percent of the world's agricultural land, with increased possibilities in Oceania and North America. However, they cannot be used in Asia and Africa. For medium-resolution satellites, such as Landsat 8, half of the world's agricultural acreages can be monitored; however, in this case too, Asia and Africa remain disadvantaged, with less than 20 percent of their agricultural areas being able to benefit from coverage. The situation is dramatically enhanced with the arrival of Sentinel 1 (radar) and 2 (optical). Five of the regions reach a suitability greater than 90 percent and Africa and Asia are close to 70 percent. Total suitability is reached with VHR satellites, although they are unaffordable for all statistical systems under examination.

TABLE 3. SATELLITE RESOLUTIONS AND RELATIVE COMPATIBLE PERCENTAGE OF CROPLAND AREA.

Region	Spot/Rapideye	Sentinel 1&2	Landsat8/ AWiFS	Modis/ Sentinel 3
Africa	100	69	18	3
Middle East	100	92	27	2
Asia	100	67	19	6
Central and South America	100	97	74	29
Europe	100	99	75	29
North America	100	100	92	39
Oceania	100	100	92	66
World	**100**	**85**	**53**	**21**

It is noteworthy that image resolution and cost are not the only limiting factors. In tropical zones, cloud coverage can seriously hamper the percentages reported above, except for Sentinel 1 (high-resolution) and RISAT 1 (medium-resolution). Whitcraft *et al*. (2015) provide a detailed analysis of the cloud cover patterns during the agricultural growing season, showing, that the probability of clear view imagery remains a general concern, particularly in India and Southeast Asia.

In addition, VHR satellites are not designed to obtain wall-to-wall coverage at country level, and the "stamps mosaics" that they deliver are very costly and time-consuming to process. In addition to its suitability scores, Sentinel 2 provides a swath of 290 km and a revisit cycle of five days, as opposed to the swath of 170 km and revisit cycle of 16 days for Landsat 8; therefore, it is necessary to mosaic three times more images with Landsat 8 than with Sentinel 2.

Table 4 ranks African and Asian countries by percentage of cropland per parcel size categories, illustrating the ten easiest and ten most difficult countries in terms of making use of satellite imagery for crop acreage statistics.

TABLE 4. THE MOST DIFFICULT AND EASIEST COUNTRIES IN AFRICA AND ASIA, IN TERMS OF THE PERCENTAGE OF CROPLAND AREA BY FIELD SIZE.

AFRICA				
List of most difficults countries				
	Very Small	Small	Medium	Large
Burundi	99.8	0.2	0.0	0.0
Madagascar	86.3	13.4	0.3	0.0
Eritrea	79.6	18.2	2.2	0.0
Togo	79.2	19.9	0.8	0.0
Rwanda	76.3	21.4	2.2	0.0
Equatorial Guinea	73.1	26.9	0.0	0.0
Mauritania	70.9	28.4	0.7	0.0
Ethiopia	69.7	29.2	1.0	0.1
Guinea-Bissau	65.5	34.5	0.0	0.0
Uganda	65.1	32.8	2.1	0.0
List of most easy counties				
	Very Small	Small	Medium	Large
Gambia	5.1	91.9	2.4	0.7
Senegal	16.7	82.6	0.7	0.0
Somalia	7.1	79.3	13.5	0.0
Angola	10.3	78.5	10.4	0.8
Egypt	20.3	77.6	2.1	0.0
Zimbabwe	10.2	76.8	12.7	0.3
Mali	21.0	76.5	2.5	0.0
Guinea	23.8	74.9	1.3	0.0
Sierra Leone	24.3	74.2	1.6	0.0
Lesotho	9.8	73.9	16.4	0.0

ASIA				
List of most difficult countries				
	Very Small	Small	Medium	Large
Sri Lanka	99.8	0.2	0.0	0.0
Nepal	86.3	13.4	0.3	0.0
Bangladesh	79.6	18.2	2.2	0.0
India	79.2	19.9	0.8	0.0
Republic of Korea	76.3	21.4	2.2	0.0
Pakistan	73.1	26.9	0.0	0.0
Lao People's Dem. Rep.	70.9	28.4	0.7	0.0
China	69.7	29.2	1.0	0.1
Myanmar	65.5	34.5	0.0	0.0
Dem People's Rep of Korea	65.1	32.8	2.1	0.0
List of most easy counties				
	Very Small	Small	Medium	Large
Taiwan	10.1	89.9	0.0	0.0
Armenia	7.5	88.8	3.7	0.0
Bhutan	14.0	86.0	0.0	0.0
Timor-Leste	17.6	82.4	0.0	0.0
Cambodia	15.8	80.8	3.4	0.0
Thailand	12.2	79.2	8.5	0.0
Jammu and Kashmir	19.9	78.7	1.4	0.0
Viet Nam	16.2	76.6	6.6	0.5
Indonesia	19.2	69.6	10.9	0.3
Philippines	14.4	66.0	17.6	2.0

9.4. CONCLUSION

Three main factors support the cost-effectiveness of remote sensing for agricultural statistics. The decrease in image prices, as free-of-charge long-term systems are secured by NASA and ESA at the resolutions required for crop yield monitoring (METOP, MODIS, Sentinel 3) and acreage estimation (Landsat 8, Sentinel 1 & 2). Quality is improving in terms of guaranteed long-term availability, image resolution (up to 10 m), frame size (up to 290 m x 290 m), revisiting time (up to five days) and the number of radiometric channels (above ten). Finally, open-source applications have become the standard in GIS and image analysis, as well as in access to remote cloud processing tools (hardware and software, such as Google Earth Engine).

As crop yield monitoring is essential to food security and market management, it is best served by a remote sensing approach that guarantees the periodic and timely delivery of the yields trend while minimizing the burden of costly fieldwork. Long-established systems exist at national level (consider India's MNCFC, Brazil's CONAB, Morocco's DMN, Mozambique's DSNA, Pakistan's SUPARCO, Senegal's CSE, Tunisia's CNT and VEGA-PRO in Russia) and global level (CropWatch, CropExplorer, JRC-MARS, FEWSNET, FAO-GIEWS, UNEP-DEWA, WFP-VAM, AMIS and GEOGLAM).

Crop acreage estimation with remote sensing has also proven to attain cost efficiency. Current season imagery is used in the United States of America with CropScape, in Canada at AGRIFOOD, in India at the MNCFC, and in Pakistan with SUPARCO. Although field size remains a limiting factor in 70 countries, the opportunity remains for at least 125 countries to envisage a successful use of remote sensing for current-season crop acreage estimation. In addition, the use of archive imagery in sampling design optimization occurs in most national statistical offices, even when a list frame approach (both for censuses and surveys) is adopted.

9.5. REFERENCES

Boryan, C.G., Yang, Z. & Seffrin, R. 2016. Post stratification assessment of the NASS automated stratification method based on the Cropland Data Layer. In Institute of Electrical and Electronics Engineers, Inc. (ed.), *Geoscience and Remote Sensing Symposium (IGARSS), 2016 IEEE International* (pp. 5933–5936). IEEE Publication.

Benedetti, R., Piersimoni, F. & Postiglione, P. 2015. *Sampling Spatial Units for Agricultural Surveys*. Springer-Verlag: Berlin and Heidelberg.

Carfagna, E. 2001. *Cost-effectiveness of remote sensing in agricultural and environmental statistics*. Invited Paper prepared for *Caesar: Conference on Agricultural and Environmental Statistical Applications in Rome*. 4–8 June 2011. Rome, Istituto nazionale di statistica (Istat). Volume III, pp. 617–627.

Carfagna, E. 2013. *Evaluating the cost-efficiency of remote sensing in developing countries*. Presentation prepared for the first Scientific Advisory Committee of the Global Strategy – Improving AG-Statistics. 18–19 July 2013. Rome, FAO.

Cotter, J., Davies, C., Nealon, J. & Roberts, R. 2010. Area Frame Design for Agricultural Surveys, in Benedetti, R., Bee, M., Espa, G. & Piersimoni, F. (eds), *Agricultural Survey Methods*. John Wiley & Sons: Chichester, UK.

Delincé, J. 2015. *Technical Report on Cost-Effectiveness of Remote Sensing for Agricultural Statistics in Developing and Emerging Economies*. Technical Report Series GO-09-2015. Global Strategy Technical Report: Rome.

Fritz, S., See, L., McCallum, I., You, L., Bun, A., Moltchanova, E. *et al*. (2015). Mapping global cropland and field size. *Global Change Biology*, 21(5): 1980–1992.

Gallego, F.J. 2007. *Sampling efficiency of the EU point survey LUCAS 2006*. Paper presented at the 56th ISI session, 22-29 September 2007. Lisbon.

Gallego, F.J., Kussulb, N., Skakunb, S., Kravchenkob, O., Shelestov, A. & Kussuld, O. 2014. Efficiency assessment of using satellite data for crop area estimation in Ukraine. *International Journal of Applied Earth Observation and Geoinformation*, 29: 22–30.

GeoSpace International. 2007. *Census mapping methodology using remote sensing and GIS technology*. Report prepared for the Seychelles National Statistics Bureau. Geospace International Publication: Pretoria, South Africa.

Global Strategy to improve Agricultural and Rural Statistics (GSARS). 2015a. *Spatial Disaggregation and Small-Area Estimation Methods for Agricultural Surveys: Solutions and Perspectives*. Technical Report Series GO-07-2015. GSARS Technical Report: Rome.

_____ 2015b. *Handbook on Master Sampling Frames for Agricultural Statistics: Frame Development, Sample Design and Estimation*. GSARS Handbook: Rome.

Inglada, J., Arias, M., Tardy, B., Hagolle, Valero, O.S., Morin, D., Dedieu, G., Sepulcre, G., Bontemps, S., Defourny, P. & Koetz, B. 2015. Assessment of an Operational System for Crop Type Map Production Using High Temporal and Spatial Resolution Satellite Optical Imagery. *Remote Sensing*, 7: 12356–12379.

Latham, J. 2017. Organization, resources and competences. In Delincé, J. (ed.), *Handbook on Remote Sensing for Agricultural Statistics* (chapter 8). Global Strategy Handbook: Rome.

Loots, H. 2015**.** The use of Hexagon's Smart Client for Census software for the demarcation of census enumeration areas for the 2016 Population and housing census in Lesotho. Paper prepared for *Geomatics Indaba: Conference and exhibition of surveying, geospatial information, GIS, mapping, remote sensing and location-based business*, 11–13 August 2015. Gauteng, South Africa.

Miller, H.M., Richardson, L., Koontz, S.R., Loomis, J. & Koontz, L. 2012. *Users, uses and value of Landsat satellite imagery: results from the 2012 Survey of Users*. USGS Open-File Report 2013-1269. USGS Publication: Washington, D.C.

Muller, R. & Harris, M. 2013. *Reported uses of CropScape and the national cropland data layer program*. Paper prepared for the Sixth International Conference on Agricultural Statistics (ICAS VI), 23–25 October 2013. Rio de Janeiro, Brazil.

Nelson, G.C., Schimmelpfennig, D., Sumner, D. & Buck, J. 2007. *Can satellite-based land imaging data be made more valuable for agriculture?* Report to the USDA.

Rosenzweig, C., Jones, J.W., Hatfield, J.L., Ruane, A.C., Boote, K.J., Thorburn, P., Antle, J.M., Nelson, G.C., Porter, C., Janssen, S., Asseng, S., Basso, B., Ewert, F., Wallach, D., Baigorria, G. & Winter, J.M. 2013. The Agricultural Model Intercomparison and Improvement Project (AgMIP): Protocols and pilot studies. *Agricultural and Forest Meteorology*, 170: 166–182.

Tenkorang, F. & Lowenberg-DeBoer, J. 2008. On-farm profitability of remote sensing in agriculture. *Journal of Terrestrial Observation* 1(1): 50–59.

United Nations Statistical Commission (UNSC). 2015. *Report of the Global Working Group on Big Data for Official Statistics*. Report E/CN.3/2015/4. United Nations Economic and Social Council Publication: New York, USA.

Waldner, F., Fritz, F., Di Gregorio, A. & Defourny, P. 2015. Mapping Priorities to Focus Cropland Mapping Activities: Fitness Assessment of Existing Global, Regional and National Cropland Maps. *Remote Sensing*, 7(6): 7959–7986.

Whitcraft, A.K., Vermote, E.F., Becker-Reshef, I. & Justice, C.O. 2015. Cloud cover throughout the agricultural growing season: Impacts on passive optical earth observations. *Remote Sensing of Environment*, 156: 438–447.

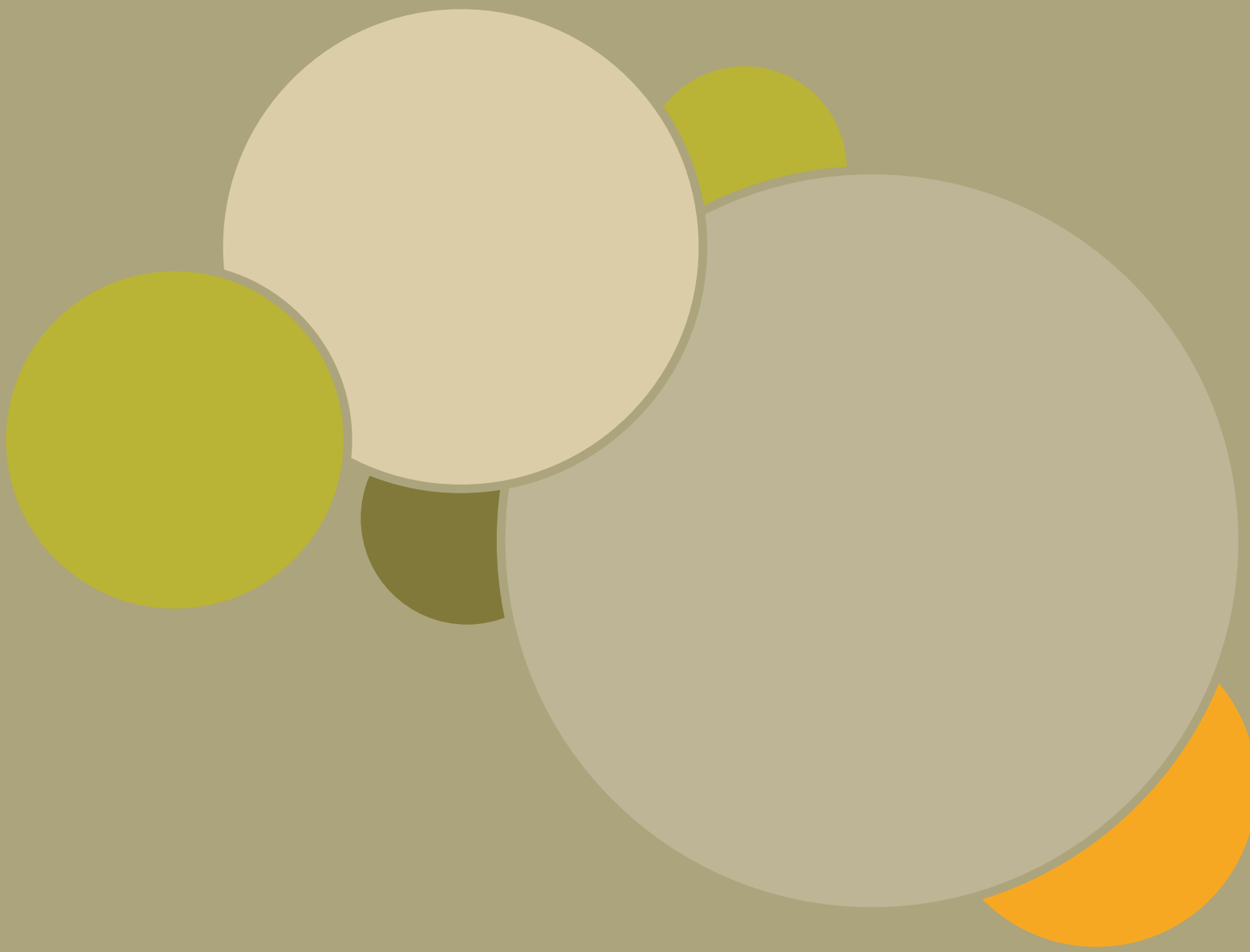

Annex

Estimating and correcting the bias of pixel counting

Javier Gallego

A1. INTRODUCTION

This annex is a complement to chapter 5 for readers seeking further details on the characteristics of the main estimators introduced in that chapter. Additional bibliographic references are also provided, in particular for institutions that would consider the implementation of a system of unbiased crop area estimation with the help of remote sensing.

Remote sensing has a strong potential for several different uses in agricultural statistics (Carfagna and Gallego, 2005). This annex will only explore its use in the final stages of crop area estimation, excluding in particular its use in building a sampling frame.

In the early times of satellite imagery, there was a widespread belief that pixel counting in classified satellite images would be enough to obtain accurate crop area estimates (Mc Donald and Hall, 1980). The initial setup of the USDA LACIE program was based on pixel counting on a sample of image pieces of 6 x 5 nautical miles. After some analysis, the approach was soon substituted with a regression estimator combining field data in a sample of segments with an exhaustive coverage of classified satellite images as covariates (Hanuschak *et al*., 1980). A main target became the cost-efficiency of remote sensing, the attainability of which appeared doubtful in the 1980s (Allen, 1990), but was actually fully achieved in the 1990s (Hanuschak *et al*., 2001).

Later, the European Union (EU) MARS Project followed a different path to reach a similar conclusion. In particular, the "rapid estimates of crop area changes" (called Activity B or Action 4) was an attempt to produce crop area change estimates from pixel counting on a set of 60 sites each extending over 40 km × 40 km. A subsequent assessment of the method indicated that the margin for subjectivity could be in the order of ±10 percent to ±30 percent for major crops (Gallego, 2006).

A number of papers dealing with crop or land cover mapping continue to assume that pixel counting can be used to estimate areas without a specific analysis of the estimator's properties. There are two main sources of error when classified satellite images are used for direct estimation: the presence of mixed (border) pixels; and the misclassification of pure pixels. An additional sampling error also appears if the region of interest is not fully covered but only a sample of images is considered.

The effect of mixed pixels has been widely studied for low-resolution images (Mayaux and Lambin, 1995; Verbeiren *et al*., 2008; Wu, 2009, Atzberger *et al*., 2013). There is also some literature regarding high-resolution images (Chhikara, 1984). Moody and Woodcock (1994, 1996) studied the impact of scale (pixel size) on pixel counting area estimators by simulating coarse image classifications from Landsat TM classifications. They noticed that pixel counting tends to overestimate dominant classes and underestimate marginal classes; however, the importance of this effect can change for different landscapes or classification algorithms. Waldner and Defourny (2017) mainly focus on the bias component due to mixed pixels as a function of image resolution combined with sensor characteristics, and on the Matheron index of landscape complexity. For a large proportion of the South African landscape, Waldner and Defourny find that, using Landsat-8 images, the bias may exceed 10 percent of the crop area, even assuming a classification accuracy of 100 percent for pure pixels. The situation significantly improves when Sentinel-2 images are used.

Initially, remote sensing users may believe that the accuracy of image classification is always better when the image resolution is finer. However, the question is more complex: a number of studies suggest that a high resolution can increase the within-class variability of the radiometric response of pure pixels of the same class, thereby degrading the separability between classes and thus the classification accuracy of pure pixels. On the other hand, a coarse spatial resolution increases the proportion of mixed pixels. The choice of an optimal resolution is a complex problem that requires making a trade-off (Latty *et al*., 1985; Cushnie, 1987; Treitz *et al*., 1992; Atkinson and Curran, 1997; Hsieh *et al*., 2001; Boschetti *et al*., 2004; Duveiller and Defourny, 2010; Löw and Duveiller, 2014). A reasonable rule of thumb might be choosing a resolution for which a large majority of pixels is pure (such as 90 percent), without trying to reach a vast majority (for example, 99 percent). However, this conjecture is far from being verified.

A2. THE BIAS OF PIXEL COUNTING

This section focuses on the impact of misclassification on pixel counting estimates, assuming that the impact of mixed pixels and missing data is negligible. The problem of bias in pixel counting has been well known to the remote sensing community since the late 1970s (Bauer *et al*., 1978; Card, 1982; Hay, 1988; Czaplewski, 1992). Several approaches have been developed to correct it. Here, we outline an expression of the bias in terms of the error matrix (or confusion matrix) and highlight some cautions that must be exercised during the correction.

The relationship between a classified image and the actual land cover can be expressed by a confusion matrix. The confusion matrix A is considered for the entire population of pixels. In practice, A is unknown and must be estimated. Each cell A_{gc} is the area of class g (ground) classified as c or the proportion compared with the total area of the region. A_{cc} is the area correctly classified under class c. A_{+c} is the total area classified as c, A_{c+} is the unknown total area actually belonging to class c. The pixel counting estimator uses A_{+c} to estimate A_{c+}. It has no variance unless it is computed on a sample of images. Its bias is the difference between the commission and the omission error.

$$B = A_{+c} - A_{c+} = \sum_{c' \neq c} A_{c'c} - \sum_{c' \neq c} A_{cc'} = \Phi_c - \Psi_c \qquad (1)$$

Table 1 illustrates the sums to be made to compute the commission error Φ_c and omission error Ψ_c in a confusion matrix, expressed as total areas. In the literature on remote sensing, the confusion matrix is often expressed as a number of sample units; however, this is usually not a good choice because it may be strongly biased if it is considered as an estimator of A.

TABLE A1. CONFUSION MATRIX WITH M CLASSES. YELLOW: COMMISSION ERROR OF CLASS 1 (WHEAT). PINK: OMISSION ERROR FOR THE SAME CLASS.

		Classified				
		1	2		M	Total
Actual class	1 wheat	A_{11}	A_{12}	……	A_{1M}	A_{1+}
	2 maize	A_{21}	A_{22}	…….	A_{2M}	A_{2+}
	….					
	M non-crop	A_{M1}	A_{M2}	……	A_{MM}	A_{M+}
	Total	A_{+1}	A_{+2}	…..	A_{+M}	A_{++}

Unfortunately, there are no theorems for a classification algorithm that ensures that the commission and omission errors will tend to compensate each other. It should be noted that the commission and omission errors are usually expressed as ratios, dividing the errors Φ_c and Ψ_c by A_{+c} and A_{c+} respectively (Congalton and Green, 1999). In this case, the expression of the bias becomes slightly more complicated (Gallego, 2004). It is preferred to express Φ_c and Ψ_c in terms of total areas, to keep the expression of the bias more simple.

In practice, the confusion matrix A is not known. The totals A_{+c} of the columns are known and it is therefore possible to estimate the rest of the matrix and derived indicators, including Φ_c and Ψ_c. If the unbiased estimators ϕ_c and ψ_c can be computed, it will be necessary to obtain an unbiased estimator of the bias and it can be corrected. For this purpose, a few basic rules (listed below) must be observed. Additional details can be found in many works, for example Stehman (2009), Foody (2002) and McRoberts and Walters (2012). The rules are:

- The validation data used to compute the confusion matrix must be selected with a statistical method, such as random stratified sampling, systematic with a random origin, etc. This rule is not always respected in remote sensing because of the cost of field data collection; however, it this is necessary for the correct computation of extrapolation weights. Failing to respect it may lead to a completely wrong bias correction (Gallego *et al*., 2016).
- The validation sample should not include the data used to train the classification algorithm. The cost of field data collection often pushes practitioners to do so, but this is not recommendable
- The validation sample and the training set should not be spatially correlated (Congalton and Green, 1999; Hammond and Verbyla, 1996; Zhen *et al*., 2013). For example, using a two-stage sampling scheme and selecting training and validation sets in the same PSUs may lead to a significant optimistic bias, in particular if the classification algorithm involves a large number of parameters (Gallego and Rueda, 1993). For neural network classifiers, the problem of overfitting that leads to optimistic bias has been widely studied in other fields (Tetko *et al*., 1995; Hawkins, 2004; Piotrowski and Napiorkowski, 2013; Lawrence *et al*., 1997). However, the extent to which it is considered in remote sensing is unclear.
- Boundary pixels should not be excluded. This condition is debatable if only a measure of classification accuracy is required. Remote sensing practitioners often take only pure pixels (far enough from the boundaries) to avoid the pessimistic bias that may derive from misregistration (Verbyla and Hammond, 1995; Foody, 2008). However, if confusion matrices are used to correct the bias of pixel counting, mixed or boundary pixels should also be considered. This requires a generalization of confusion matrices to subpixel or soft classifications (Pontius and Cheuk, 2006; Silván-Cárdenas and Wang, 2008).

In principle, the bias is estimated from a sample of validation data, and its variance must be computed taking into account the sampling plan for the validation data. If the proportion of mixed pixels is negligible (as occurs in landscapes with very large homogeneous patches), binomial distribution in each of the strata used for the sample selection can be used to estimate the variances of ϕ_c and ψ_c. There is no guarantee that their distributions are independent; still, it may be reasonable to sum up both variances to obtain the variance of the bias. The variance of the estimated bias will become the variance of the bias-corrected pixel counting estimate.

A2.1. Calibration estimators

The most frequently used methods to correct the bias of pixel counting probably belong to the calibration estimator family. The way this expression is used in the remote sensing literature is related but not identical to the estimator that is usually called "calibration estimator" in the statistical literature (Brown, 1982; Deville and Särndal, 1992).

Let
A : confusion matrix for the total population. Unknown.
T : column vector with ground truth totals $T_g=A_{g+}$ (T stands for "truth"). Unknown.
R : Column vector with $R_c=A_{+c}$ total area of pixels classified into each class c. Known.
a : known confusion matrix from a sample of test pixels a_{gc} = estimated area of class g classified as c.
t : column vector of ground truth totals in the sample $t_g=a_{g+}$.
r : Column vector with $r_c = \sum_g a_{gc}$ number of pixels classified into each class c in the sample.
D_T, D_R, D_t and D_r are diagonal matrices with elements T_g, R_c, t_g and r_c.

The vector R gives a biased but exhaustive information of the crop area. The objective is to estimate T from the known elements R and the confusion matrix a.

$E_c = A' D_t^{-1}$ and $E_g = A D_R^{-1}$ are relative error matrices (unknown) on the population. E_c gives the probability that a pixel is classified as c knowing that the ground truth is g and E_g gives the probability that the ground truth is g knowing that the pixel is classified as c.

Similar matrices $e_c = a' D_t^{-1}$ and $e_g = a D_r^{-1}$ can be computed from the sample. They are approximately unbiased estimators of E_c and E_g if the sample data are extrapolated with the correct weights, inversely proportional to the sampling probability.

The following expressions are identities derived directly from the definitions above:

$$R = A' D_T^{-1} T = E_c T \qquad T = A D_R^{-1} R = E_g R \qquad T_g = R_g + N\left(\frac{T_g - R_g}{N}\right) \qquad (2)$$

if E_c is square and non-singular, we can write $T = E_c^{-1} R$

This leads to three calibration estimators:

Direct calibration: $$\hat{T}_{dir} = e_g R \qquad (3)$$

which is a maximum-likelihood estimator for a multinomial distribution (Tenenbein, 1972). The matrix *eg* contains estimates of the conditional probabilities *p(g/c)* of each ground class *g* given the class *c* in the classification.

Inverse calibration: $$\hat{T}_{inv} = e_c^{-1} R \qquad (4)$$

this is an asymptotically maximum likelihood (Grassia and Sundberg, 1982). The matrix ec contains estimates of the conditional probabilities *p(c/g)* of each image class *c* given the class g in the ground.
This estimator is presented in slightly different ways by Bauer *et al*. (1978), Priesley and Smith (1987) and Hay (1988). In a comment on the paper by Hay, Jupp (1989) analyses the risk of instability when is nearly singular, that is, when some eigenvalues are very small.

additive correction $$T_{ad}(g) = R_g + n\left(\frac{t_g - r_g}{n}\right) \qquad (5)$$

proposed by Dymond (1992).
Woodcock and Gopal (2000) give an extension of the direct calibration estimator for fuzzy classifications, so that estimations can be computed for any membership level.

A2.2. Computing the variance of some estimators

To assess estimators that combine field data and classified images, it is important to compute the variance of the type of estimator that has been chosen. Computing variances can become complicated in many cases; here, the simplest situations will be seen; in particular, for the direct calibration

$\hat{T}_{dir} = e_g R$. For a given ground class g,

$$\hat{T}_{dir}(g) = \sum_c \frac{n_{gc}}{n_c} R_c \qquad (6)$$

that is, the estimated area from a stratified sampling in which the classes c are the strata with size R_c known from the classified image.

If the sampling is random in each class c and the sample size n_c has been determined a priori in each class, the variance is provided by the usual binomial expression

$$\hat{V}_{dir}(g) = \sum_c \frac{1-f_c}{n_c} \frac{n_{gc}}{n_c}\left(1 - \frac{n_{gc}}{n_c}\right) R_c^2 \qquad (7)$$

where the finite population correction f is usually negligible in remote sensing applications.

A fixed sample size n_c presumes that the image classification is known before sampling. This usually happens for area estimation of land cover (or change) with environmental or forest monitoring purposes. If a previous stratification is available, both the area and variance estimators are computed separately in each stratum h and added later.

If the sample must be prepared before image classification, as may happen for the estimation of the area of annual crops, having a fixed n_c is not possible. The sample size n_c for different classes will have a multinomial distribution, in case of a simple random sampling, and the situation will be one of post-stratification defined by the classification; an additional term in the variance will be required (Cochran, 1977, p. 135).

For the regression estimator reported in chapter 5 that exploits the link between the field proportion of a given crop y and the proportion x of a related class (the stratification sub-index is omitted here too):

$$\bar{y}_{Reg} = \bar{y} + \hat{b}\,(\bar{X} - \bar{x}) \qquad (8)$$

the usual approximation for the computation of the variance is

$$Var(\bar{y}_{Reg}) = Var(\bar{y})\left(1 - r_{xy}^2\right) \qquad (9)$$

When the sample size is not large enough or there is one or more strongly influential observations, a more complex approximation may be necessary (Gallego *et al.*, 2014). It should be highlighted that a reasonable application of the regression estimator requires approximately continuous distributions of x and y between 0 and 1. This means that the sampling units should not be points (that would concentrate both distributions on 0 and 1), but rather area segments that are sufficiently large to contain several crop plots or landscape patches.

A2.3. Confusion matrices expressed as numbers of points

The expressions provided in the previous section refer to the application of direct and inverse calibration estimators using extrapolated confusion matrices, assuming that the matrix has been built on the basis of a sample with known sampling probabilities pi and extrapolated with weights 1/pi . Unbiasedness is only approximate when unbiased estimators appear in denominators; at any rate, the distortions will be minor if the sample is large compared to the number of cells in the confusion matrix.

In the literature on remote sensing, confusion matrices are often expressed in terms of agc , the number of pixels belonging to ground class g that have been classified into class c. At this point, three situations linked to the sampling plan used to select the field sample may be distinguished.

1. If the sampling probability is uniform across the whole region, the confusion matrix a becomes an unbiased estimator of *A* by simply applying a constant extrapolation factor, and can be used for both direct and inverse calibration. This is usually the situation if the sample is selected before the images are acquired and classified. With this sampling strategy, the confusion matrix *a* expressed in terms of a number of points can be used both for direct and inverse calibration.
2. If the sample of points for field observation is selected after the classification of images, the classes c can be used as strata to sample points for field observation. This approach is generally recommended when the field sample is used to validate land cover maps obtained from images and, at the same time, build area estimations that combine field observations with classified images (Stehman, 2009). The sample size n_c is determined by applying an allocation system (Wagner and Stehman, 2015), or simply by rules of thumb such as "at least 50 points per stratum". With this sampling strategy, the direct calibration estimator can be used with a without extrapolating to *A*. Commission errors will be correct because the sampling probability is homogeneous in each classification class *c*; however, omission errors may be strongly biased when the sampling probability changes greatly from class to class (Gallego, 2016). Inverse calibration cannot be used without a correct extrapolation to A.
3. The number of points n_g to be observed in each ground class *g* is determined a priori. This approach is sometimes applied with a purposive sampling that can be referred to as quota sampling: field surveyors will be circulated with the aim of collecting a given number of points. For example, the target may be recording coordinates of 50 points in maize fields, 50 points in wheat fields and 50 points in other land cover classes. Surveyors travel around and choose points that they consider to be "representative", often in the middle of large fields. This is a practical way to collect field data at a low cost; however, the impact on the possible bias of estimators is not well known. Probabilistic sampling methods in which n_g is fixed a priori may be envisaged, although the sampling probabilities are likely to be complex. In any case, the author of this annex is not aware of any application in the context of agricultural surveys. If it is assumed that this sampling strategy can be applied with a uniform probability for each ground class *g*, inverse calibration can be applied on *a*, omission errors will be correct, but the commission errors will be biased. Direct calibration cannot be used without extrapolating to *A*. If the analyst is confident that the conditional probability *p(c/g)* is computed on a quota sample, an inverse calibration estimator based on the confusion matrix a expressed in number of points or pixels may be a cheap solution. From the quota sample, the extrapolation to *A* will not be possible and the direct calibration estimator cannot be used. Commission and omission errors computed from a cannot be compared to assess whether direct pixel counting on the classified images overestimates or underestimates each class *c*.

Generally, probabilistic sampling is recommended for both land cover maps validation and for area estimation combining field data with classified satellite images (Congalton and Green, 1999; Foody, 2002; Stehman *et al*., 2003, 2005; Wagner and Stehman, 2015; Olofsson *et al*., 2013, 2014; Li *et al*., 2014). However, if a survey based on probabilistic sampling cannot be afforded, it is legitimate to seek cheaper systems. The inverse calibration estimator based on a quota field sampling might be a good approach, although the suitability is likely to be related to the share of pure and mixed pixels.

A2.4. Which approach is best to correct the bias?

All calibration estimators encounter problems when dealing with mixed pixels, because the sampling unit is a point or a pixel and the location accuracy is usually in the order of magnitude of a pixel. Thus, a pixel in the image is compared with field data that correspond to a neighboring pixel. When the plot size is small or crops are mixed, as generally happens in less developed agriculture, image classification is not very accurate and the efficiency of calibration estimators is further reduced by co-location inaccuracy. For example, Ceccarelli *et al*. (2016) have found that calibration estimators gave relative efficiencies close to 1 in tests conducted in Senegal and Kenya, despite using RapidEye images with a resolution of approximately 5 m. This means that, for this particular example, the ex post use of classified images did not significantly improve the accuracy of field surveys, although the same study gives a more optimistic assessment of the use of images to improve the sampling frame.

If an inverse calibration estimator is used with a quota sampling of points in the middle of relatively large fields, the problem of misregistration (co-location inaccuracy) will be irrelevant. The impact of nonprobabilistic sampling on the estimations is not well known, even if it is known that it introduces an optimistic bias in the confusion matrix (Hammond and Verbyla, 1996).

The problem of mixed pixels can be formally addressed by considering subpixel land cover proportions; however, there is as yet insufficient knowledge on the behaviour of calibration estimators with subpixel classifiers.

Czaplewski and Catts (1992) and Walsh and Burk (1993) compare $\hat{T}_{dir}$ and $\hat{T}_{inv}$ in different data sets and report a superior performance of the direct estimator against several criteria: feasibility, bias and variance. Yuan (1997) finds that $\hat{T}_{inv}$ gives a slightly smaller variance than $\hat{T}_{dir}$ and poorer results for Dymond's additive correction; according to his results, $\hat{T}_{dir}$ is still preferable from the point of view of bias if the sample is not very large compared to the number of cells in the confusion matrix.

The regression estimator is generally less sensitive to location inaccuracy. The regression estimator is suitable when the sampling units are segments or clusters of points containing a relatively large number of pixels. It can also be seen as a bias correction method, and it does not exclude mixed pixels that are naturally included in the sampling units. If the sampling units are segments with a size at least one order of magnitude larger than the registration inaccuracy, the impact of location uncertainty is minor. For example, if the images have a resolution of 20 m, the location uncertainty is likely to be in the order of 20 m. If the sampling units are square segments of 300 m x 300 m or 500 m x 500 m, they approximately correspond to the same patch in the field data and the image, including mixed pixels. From this point of view, the regression estimator is probably the safest bias correction for crop area estimation, even if it is less frequently applied in the literature on remote sensing than calibration estimators.

Kerdiles *et al*. (2013) and Liu *et al*. (2014) report values between 1.6 and 2.7 for the relative efficiency of the regression estimator in test areas in China with complex landscapes of thin stripes.

Li *et al*. (2014) compare various estimators in three pilot areas in China and obtain better results for regression estimators than for calibration estimators. They also observe a stronger degradation of the inverse calibration when the accuracy of the image classification becomes weaker.

A3. THE PROBLEM OF SUBJECTIVITY IN PIXEL COUNTING ESTIMATION

Pixel counting may pose a dilemma if an a priori belief is available from external information on the area of a given crop c. Suppose, for example, that an area close to 1 000 000 ha is expected. The image analyst will compute a first area estimate with a given setup of the classification. The setup of the classification includes the choice of the algorithm type, the rules to eliminate outliers or fill missing data, and the tuning of specific parameters. A simple example of a specific parameter is the prior probability in the maximum likelihood classifier.

If the area classified as c is far from the expected figure of 1 000 000 ha, a conscientious analyst will probably attempt to improve the classification reviewing the initial setup until a more suitable agreement is found. This approach towards improving the classification, is certainly acceptable, conceived as an answer to the question "Where is the crop c grown?". However, doubts appear as to the objectivity of the estimated area if direct pixel counting is used. This is a major reason to emphasize the importance of rigorous bias correction when estimating areas from classified images.

A4. REFERENCES

Allen, J.D. 1990. A Look at the Remote Sensing Applications Program of the National Agricultural Statistics Service. *Journal of Official Statistics*, 6(4): 393–409.

Atkinson, P.M. & Curran, P.J. 1997. Choosing an appropriate spatial resolution for remote sensing investigations. *Photogrammetric Engineering and Remote Sensing,* 63(12): 1345–1351.

Atzberger, C. & Rembold, F. 2013. Mapping the spatial distribution of winter crops at sub-pixel level using AVHRR NDVI time series and neural nets. *Remote Sensing, 5*(3), 1335–1354.

Bauer, M.E., Hixson, M.M., Davis, B.J. & Etheridge J.B. 1978. Area estimation of crops by digital analysis of Landsat data. *Photogrammetric Eengineering and Remote Sensing,* 44: 1033–1043.

Boschetti, L., Flasse, S.P., & Brivio, P.A. 2004. Analysis of the conflict between omission and commission in low spatial resolution dichotomic thematic products: The pareto boundary. *Remote Sensing of Environment,* 91(3-4): 280–292.

Brown, P.J. 1982. Multivariate calibration, *Journal of the Royal Statistical Society*, B, 44(3): 287–321.

Card, D. 1982. Using Known Map Category Marginal Frequencies to Improve Estimates of Thematic Map Accuracy. *Photogrammetric Engineering and Remote Sensing*, 48: 431–439.

Carfagna, E. & Gallego F.J. 2005. Using remote sensing for agricultural statistics. *International Statistical Review,* 73(3): 389–404.

Ceccarelli, T., Downie, M. & Remotti, D. 2016. *Role of Earth Observations for Crop Area Estimates in Africa. Experiences from the AGRICAB Project*. Paper prepared for the ICAS VII, Rome. 26–28 October 2016.

Chhikara, R.S. 1984. Effect of mixed (boundary) pixels in crop proportion estimation. *Remote Sensing of Environment*, 14: 207–218.

Congalton, R.G. & Green, K. 1999. *Assessing the accuracy of remotely sensed data: principles and practices*, Lewis publishers: Boca Raton, USA.

Cushnie, J.L. 1987. The interactive effect of spatial resolution and degree of internal variability within land-cover types on classification accuracies. *International Journal of Remote Sensing,* 8(1): 15–29.

Czaplewski, R.L. 1992. Misclassification bias in areal estimates. *Photogrammetric Engineering and Remote Sensing,* 58(2): 189–192.

Deville, J.C. & Särndal, C.E. 1992. Calibration estimators in survey sampling, *Journal of the American Statistical Association*, 87: 376–382

Duveiller, G. & Defourny, P. 2010. A conceptual framework to define the spatial resolution requirements for agricultural monitoring using remote sensing. *Remote Sensing of Environment,* 114(11): 2637–2650.

Foody, G. 2008. Harshness in image classification accuracy assessment. *International Journal of Remote Sensing,* 29(11): 3137–3158.

Foody, G.M. 2002. Status of land cover classification accuracy assessment. *Remote Sensing of Environment,* 80(1): 185–201.

Gallego, F.J. 2004. Remote sensing and land cover area estimation. *International Journal of Remote Sensing*. 25(15): 3019–3047.

Gallego F.J. 2006. Review of the Main Remote Sensing Methods for Crop Area Estimates, *Remote Sensing Support to Crop Yield Forecast and Area Estimates*, ISPRS archives, XXXVI, 8/W48, 65–70. Available at: http://www.isprs.org/publications/PDF/ISPRS_Archives_WorkshopStresa2006.pdf.

Gallego, F.J. , Kussul, N., Skakun S., Kravchenko, O., Shelestov, A. & Kussul, O. 2014, Efficiency assessment of using satellite data for crop area estimation in Ukraine. *Internatinal Journal of Applied Earth Observation and Geoinformation*, 29: 22–30.

Gallego, F.J. & Rueda C. 1993, Balanced a Priori Probabilities for Maximum Likelihood Classification of Satellite Images. *Bulletin of the Int. Stat. Inst. 49th meeting. Contributed papers, Book 1* (467–468).

Gallego, J., Sannier, C. & Pennec, A. 2016. Validation of Copernicus Land Monitoring Services and Area Estimation. Paper presented at the *ICAS VII*, 26–28 October 2016. Rome.

Hammond, T.O. & Verbyla, D.L. 1996, Optimistic bias in classification accuracy assessment, *International Journal of Remote Sensing,* 17(6): 1261–1266.

Hanuschak, G., Hale, R., Craig, M., Mueller, R. & Hart, G. 2001, The new economics of remote sensing for agricultural statistics in the United States, in *Proceedings of the Conference on Agricultural and Environmental Statistical Applications in Rome (CAESAR), June 5-7*, vol. 2, pp. 427-437.

Hanuschak, G.A., Sigman, R., Craig, M.E., Ozga, M., Luebbe, R.C., Cook, P.W., Kleweno, D.D. & Miller, C.E. 1980, Crop-Area Estimates from Landsat. Transition from research and development to timely results. *IEEE Transactions on Geoscience and Remote Sensing*, GE-18(2): 160–166.

Hawkins, D.M. The problem of overfitting. *Journal of Chemical Information and Computer Sciences*, 44.1 (2004): 1–12.

Hay, A.M. 1988. The derivation of global estimates from a confusion matrix. *International Journal of Remote Sensing*, 9: 1395–1398.

Hsieh, P., Lee, L. C., & Chen, N. 2001. Effect of spatial resolution on classification errors of pure and mixed pixels in remote sensing. *IEEE Transactions on Geoscience and Remote Sensing,* 39(12): 2657–2663.

Kerdiles, H., Dong, Q., Spyratos, S. & Gallego F.J. 2013: Use of high resolution imagery and ground survey data for estimating crop areas in Mengcheng county, China. In *Proceedings of 35th International Symposium on Remote Sensing of Environment (ISRSE35).*

Latty, R.S., Nelson, R., Markham, B., Williams, D., Toll, D., & Irons, J. 1985. Performance comparisons between information extraction techniques using variable spatial resolution data. *Photogrammetric Engineering & Remote Sensing,* 51(9) 1459–1470.

Lawrence, S., Giles, C.L. & Tsoi, A.C. 1997. Lessons in neural network training: Overfitting may be harder than expected. Paper presented at the *Proceedings of the National Conference on Artificial Intelligence,* 540–545.

Li, Y., Zhu, X., Pan, Y., Gu, J., Zhao, A. & Liu, X. 2014. A comparison of model-assisted estimators to infer land cover/use class area using satellite imagery. *Remote Sensing,* 6(9): 8904–8922.

Liu, J., Chen, Z., Wang, L., Wang, X., Dong, Q. & Gallego, J.F. 2014. Assessing the crop acreage at county level on the north china plain using an adapted regession estimator method. Paper presented at the Third *International Conference on Agro-Geoinformatics, Agro-Geoinformatics 2014*, 11–14 August 2014. Beijing.

Löw, F. & Duveiller, G. 2014. Defining the spatial resolution requirements for crop identification using optical remote sensing. *Remote Sensing,* 6(9): 9034–9063.

Mac Donald ,R.B. & Hall, F.G. 1980, Global crop forecasting. *Science*, 208: 670–679.

Mayaux, P. & Lambin, E.F. 1995. Estimation of tropical forest area from coarse spatial resolution data: a two-step correction function for proportional errors due to spatial aggregation. *Remote Sensing of Environment,* 53: 1–15.

McRoberts, R.E. & Walters, B.F. 2012. Statistical inference for remote sensing-based estimates of net deforestation. *Remote Sensing of Environment,* 124: 394–401.

Moody, A. & Woodcock, C. 1994. Scale-dependent errors in the estimation of land cover proportions: implications for global land-cover datasets. *Photogrammetric Engineering and Remote Sensing,* 60(5): 585–594.

Moody, A. & Woodcock, C.E. 1996. Calibration-based models for correction of area estimates from coarse resolution land-cover data, *Remote Sensing of Environment,* 58: 225–241.

Olofsson, P., Foody, G.M., Herold, M., Stehman, S.V., Woodcock, C.E. & Wulder, M.A. 2014. Good practices for estimating area and assessing accuracy of land change. *Remote Sensing of Environment*, 148: 42–57.

Piotrowski, A.P. & Napiorkowski, J.J. (2013). A comparison of methods to avoid overfitting in neural networks training in the case of catchment runoff modelling. *Journal of Hydrology,* 476: 97–111.

Pontius Jr., R.G. & Cheuk, M.L. (2006). A generalized cross-tabulation matrix to compare soft-classified maps at multiple resolutions. *International Journal of Geographical Information Science,* 20(1): 1–30.

Silván-Cárdenas, J.L. & Wang, L., 2008, Sub-pixel confusion-uncertainty matrix for assessing soft classifications, *Remote Sensing of Environment*, 112: 1081–1095.

Stehman, S.V., Sohl, T.L. & Loveland, T.R. 2003, Statistical sampling to characterize recent United States Land-cover change, *Remote Sensing of Environmen*t, 86: 517–529.

Stehman, S.V. (2009). Sampling designs for accuracy assessment of land cover. *International Journal of Remote Sensing,* 30(20): 5243–5272.

Stehman, S.V. & Foody, G.M. (2008). Accuracy assessment. *The SAGE handbook of remote sensing* (pp. 297-314). SAGE Publications Ltd.: London.

Stehman, S.V., Sohl, T.L. & Loveland, T.R. 2005. An evaluation of sampling strategies to improve precision of estimates of gross change in land use and land cover. *International Journal of Remote Sensing*, 26(22): 4941–4957.

Stehman, S.V., Wickham J.D., Smith J.H. & Yang L. 2003, Thematic accuracy of the 1992 national land-cover data for the Eastern United States: statistical methodology and regional results. *Remote Sensing of Environment* 86: 500–516.

Tetko, I.V., Livingstone, D. J. & Luik, A.I. 1995. Neural network studies. 1. Comparison of overfitting and overtraining. *Journal of Chemical Information and Computer Sciences,* 35(5): 826–833.

Treitz, P. M., Howarth, P. J., Suffling, R. C. & Smith, P. 1992. Application of detailed ground information to vegetation mapping with high spatial resolution digital imagery. *Remote Sensing of Environment,* 42(1): 65–82.

Verbeiren, S., Eerens, H., Piccard, I., Bauwens, I. & Van Orshoven, J. 2008. Sub-pixel classification of SPOT-VEGETATION time series for the assessment of regional crop areas in Belgium. *International Journal of Applied Earth Observation and Geoinformation,* 10(4): 486–497.

Verbyla, D.L. & Hammond, T.O. 1995. Conservative bias in classification accuracy assessment due to pixel-by-pixel comparison of classified images with reference grids. *International Journal of Remote Sensing,* 16: 581–587.

Wagner, J.E. & Stehman, S.V. 2015. Optimizing sample size allocation to strata for estimating area and map accuracy. *Remote Sensing of Environment,* 168: 126–133.

Waldner, F. & Defourny, P. 2017. Where can pixel counting area estimates meet user-defined accuracy requirements? *International Journal of Applied Earth Observation and Geoinformation,* 60: 1–10.

Wu, C. 2009. Quantifying high-resolution impervious surfaces using spectral mixture analysis. *International Journal of Remote Sensing,* 30(11): 2915–2932.

Yuan, D. 1997. A simulation comparison of three marginal area estimators for image classification, *Photogrammetric Engineering and Remote Sensing*, 63(4): 385–392.

Zhen, Z., Quackenbush, L.J., Stehman, S.V. & Zhang, L. 2013. Impact of training and validation sample selection on classification accuracy and accuracy assessment when using reference polygons in object-based classification. *International Journal of Remote Sensing,* 34(19): 6914–6930.